

**NASA TECHNICAL
MEMORANDUM**

NASA TM-73,224

(NASA-TM-73224) FLIGHT TEST RESULTS OF THE
STRAPDOWN HEXAD INERTIAL REFERENCE UNIT
(SIRU). VOLUME 3: APPENDICES A-G (NASA)
104 p HC A06/MF A01 CSCI 17G

N78-20098

Unclas
09225

G3/04

NASA TM-73,224

FLIGHT TEST RESULTS OF THE STRAPDOWN HEXAD
INERTIAL REFERENCE UNIT (SIRU)
VOLUME III: APPENDICES A - G

Ronald J. Hruby and William S. Bjorkman

Ames Research Center
Moffett Field, Calif. 94035

July 1977



FLIGHT TEST RESULTS OF THE STRAPDOWN HEXAD INERTIAL REFERENCE UNIT (SIRU)

VOLUME III: APPENDICES A - G

Ronald J. Hruby and William S. Bjorkman*

Ames Research Center

SUMMARY

Results of flight tests of the Strapdown Inertial Reference Unit (SIRU) navigation system are presented. The fault-tolerant SIRU navigation system features a redundant inertial sensor unit and dual computers. System software provides for detection and isolation of inertial sensor failures and continued operation in the event of failures. Flight test results include assessments of the system's navigational performance and fault tolerance.

This, the third of three volumes, contains 7 appendixes which describe selected facets of the flight tests in detail:

- A. Flight Test Plans and Ground Track Plots
- B. Navigation Residual Plots
- C. Effects of Approximations in Navigation Algorithms
- D. Vibration Spectrum of the CV-340 Aircraft
- E. Modification of the Statistical FDICR Algorithm Parameters for the Flight Environment
- F. SIRU Flight Test System Description
- G. SIRU Inertial Sensors

*Senior Analyst, Analytical Mechanics Associates, Inc., Mountain View, California 94040.

~~PAGE INTENTIONALLY BLANK~~

APPENDIX A

FLIGHT TEST PLANS AND GROUND TRACK PLOTS

This appendix contains the 15 flight test plans and ground track plots of the 33 recoverable segments of the SIRU flight test program derived from the 15 flights. Each plot (figure) shows, as a solid curve, SIRU's best estimate of the trajectory segment which was flown. The dotted paths represent the trajectory or track as computed from DME data, radar data, or SIRU's B-computer when B differs from A. The identities of the dotted paths are given in the figure titles. The flight segments are identified in the figure titles (e.g., SFT530B means "SIRU Flight Test of 5/30, second segment").

The x-axis of each figure is longitude east in degrees. The values shown are negative, indicating longitude west. The y-axis is geodetic latitude north, shown in Mercator projection. Most of the figures show some portions of the California and San Francisco Bay coastlines and some show Lake Tahoe and California's eastern border. DME locations are titled and denoted by "*". Slashes which may be observed on the SIRU trajectory are spaced 300 sec (5 min) apart in time. Times of position fixes (tape marks) are indicated in the legend which appears in the upper right-hand corner of each figure. SIRU's estimated position at the time of a tape mark is indicated in the figures by a letter which appears a half-letter space below and to the left of SIRU's estimated position. The legend which identifies the marks tells time (seconds) of the mark, SIRU's indicated latitude and longitude (degrees), and baro-altitude (feet).

Each ground track plot is preceded by a one-page description of the test objectives and general characteristics of the flight.

PRECEDING PAGE BLANK NOT FILMED

1. TEST OBJECTIVES:

- A. Verify system operation
- B. Flight test crew orientation and indoctrination

2. SYSTEM CONFIGURATION:

A. Computer

- 1. Configuration - A and B identical
- 2. FDI Limits
 - a) Gyro statistical static 4 meru 0.06°/hr
 - b) Gyro statistical maximum dynamic increase 8 meru .12°/hr
 - c) Gyro TSE MASE 18 pulses² .76°/hr
 - d) Gyro TSE maximum dynamic increase 20 pulses² .81°/hr
 - e) Accelerometer 1st failure MASE 72 pulses² .14 cm/sec²
 - f) Accelerometer 2nd failure MASE 57.6 pulses² .13 cm/sec²

B. Inertial components

- 1. Gyros - all operational
- 2. Accelerometers - all operational

3. FAILURES SCHEDULED

- A. Inertial components - none
- B. Computer - none

4. FLIGHT DESCRIPTION

Took off from Moffett, overflowed Moffett Tacan, San Jose Vortac, and Crow's Landing Vortac. Landed at Crow's Landing. Taxied to Station "L". Navigated for 30 min. System turned off. Returned to Moffett.

5. DEVIATIONS FROM TEST PLAN

A. Unplanned failures

- 1. C and F gyro statistical failure during fine alignment.
- 2. Third gyro failure at 2,400 sec into navigation.
- 3. C PIPA 28 V dc PTE failure during fine alignment.
- 4. C PIPA temperature failure during fine alignment.
- 5. Driftmeter camera jammed at first waypoint.
- 6. Night watchman bad on computer B from fine aligning to end of flight.

B. Procedural changes

- 1. Operator errors - unrecorded DME time resets and frequency changes by technician during flight.
- 2. Operational necessities
 - a) Went into fine alignment with insufficient warmup due to change in flight schedule and loss of ground power source.
 - b) No driftmeter photos because of jammed camera.
 - c) No correlation between DME time resets and driftmeter marks because of circuitry problems.

- d) Went into navigation mode with C&F gyro statistical failures because of insufficient time available for recertification.

6. TIMES

A. Warmup 1 hr B. Fine align 20 min C. Navigation 1 hr 25 min
D. Flight 38 min

7. COMMENTS

C&F gyro failures and C PIPA temperature failure are probably due to insufficient warmup prior to going into fine alignment. Third failure not identified. F gyro recompensated and recertified at Station "L". Cause of C PIPA 28 V dc PTE failure undetermined. A measurement of the voltage proved normal. Wrong value of GMOA was entered for gyro A.

1. TEST OBJECTIVES:

Navigation performance test

2. SYSTEM CONFIGURATION

A. Computer

1. Configuration - A and B identical

2. FDI limits

a) Gyro statistical static	4 meru	0.06°/hr
b) Gyro statistical maximum dynamic increase	8 meru	.12°/hr
c) Gyro TSE MASE	18 pulses ²	.76°/hr
d) Gyro TSE maximum dynamic increase	20 pulses ²	.81°/hr
e) Accelerometer 1st failure MASE	72 pulses ²	.14 cm/sec ²
f) Accelerometer 2nd failure MASE	57.6 pulses ²	.13 cm/sec ²

B. Inertial components

1. Gyros - all operational

2. Accelerometers - all operational

3. FAILURES SCHEDULED

A. Inertial components - none

B. Computer - none

4. FLIGHT DESCRIPTION

Took off from Moffett, overflew Lick Observatory, Crow's Landing Tacan, landed at Crow's Landing. Taxied to Station "L". Engine off. Navigated for 5 min. Terminated program.

5. DEVIATIONS FROM TEST PLAN

Unplanned failures

1. Computer A failure prior to takeoff.

2. C,F gyro failure, A accelerometer failure while taxiing for takeoff.

3. A,B,C,D,E,F gyro failure at different times during flight. No accelerometer failures during flight.

4. All failures cleared except A&C gyro before landing.

5. B regulated power supply #2 failure during flight. Replaced fuse.

B. Procedural changes

1. Operator errors - none

2. Operational necessities - none

6. TIMES

A. Warmup 4 hr B. Fine alignment 30 min C. Navigation 40 min

D. Flight 22 min

7. COMMENTS

This flight was preceded by an aided calibration. The resultant compensation had all the gyro negative scale factor ramps unaccountably zeroed, the wrong sign was entered for the A accelerometer bias, and the wrong value of negative bias for the D gyro was entered. These compensation errors account for the many gyro failures and the A accelerometer failure and the resultant poor navigation performance. The power supply failure did not affect system performance because of power system redundancy.

1. TEST OBJECTIVES:

Navigation performance test

2. SYSTEM CONFIGURATION

A. Computer

1. Configuration -

2. FDI limits

a) Gyro statistical static	4	meru	0.06°/hr
b) Gyro statistical maximum dynamic increase	8	meru	.12°/hr
c) Gyro TSE MASE	18	pulses ²	.76°/hr
d) Gyro TSE maximum dynamic increase	20	pulses ²	.81°/hr
e) Accelerometer 1st failure MASE	72	pulses ²	.14 cm/sec ²
f) Accelerometer 2nd failure MASE	57.6	pulses ²	.13 cm/sec ²

B. Inertial components

1. Gyros - all operational

2. Accelerometers - all operational

3. FAILURES SCHEDULED

A. Inertial components - none

B. Computer - none

4. FLIGHT DESCRIPTION

Took off from Crow's Landing, overflew Los Banos, Fresno, Castle, Crow's Landing, landed at Crow's Landing. Taxied to Station "L". System turned off. Returned to Moffett.

5. DEVIATIONS FROM TEST PLAN

A. Unplanned Failures

1. Cabin temperature exceeded 90° F. Peaked at 100° F.

2. A,E,F gyro failures at various times during taxiing for takeoff.

3. A,C,E,F gyro failures at various times during flight.

4. High temperature coolant alarm.

B. Procedural changes

1. Operator errors - none

2. Operational necessities - none

6. TIMES

A. Warmup 6.3 hr B. Fine alignment 23 min

C. Navigation 100 min D. Flight 73 min

7. COMMENTS

This flight was preceded by an aided calibration at Moffett, Station A. The resultant compensation had the gyro negative scale factor ramp unaccountably zeroed, the wrong sign was entered for the A accelerometer bias, and the wrong value of D gyro negative bias was entered. These compensation errors and the high ambient temperatures account for the many failures and the resultant navigation performance.

SIRU FLIGHT TEST NO. 6/16A

1. TEST OBJECTIVES:

Verify operation of reference system interface.

2. SYSTEM CONFIGURATION

A. Computer

1. Configuration - A and B operational. Identical programs.

2. FDI limits

a) Gyro statistical static	4		0.06°/hr
b) Gyro statistical maximum dynamic increase	8	meru	.12°/hr
c) Gyro TSE MASE	18	pulses ²	.76°/hr
d) Gyro TSE maximum dynamic increase	20	pulses ²	.81°/hr
e) Accelerometer 1st failure MASE	72	pulses ²	.14 cm/sec ²
f) Accelerometer 2nd failure MASE	57.6	pulses ²	.13 cm/sec ²

B. Inertial components

1. Gyros - all operational
2. Accelerometers - all operational

3. FAILURES SCHEDULED

- A. Inertial components - none
- B. Computer - none

4. FLIGHT DESCRIPTION

Took off from Moffett, overflowed Moffett Tacan, San Jose Vortac, Lick Observatory, Crow's Landing Tacan, landed Crow's Landing. Taxied to Station "L". Navigated a few minutes. Terminated program.

5. DEVIATIONS FROM TEST PLAN

A. Unplanned failures

1. Night watchman bad computer B
2. A,B,C,F gyro failure, D accelerometer failure during taxiing.

B. Procedural changes

1. Operator errors - none
2. Operational necessities - none

6. TIMES

A. Warmup 4 hr B. Fine alignment 36 min C. Navigation 51 min
D. Flight 25 min

7. COMMENTS

Wrong value of -NBD entered in compensation for D gyro equivalent to 0.4°/hr. No gyro failures during flight.

1. TEST OBJECTIVES:

Verify operation of reference system interface.

2. SYSTEM CONFIGURATION

A. Computer

- 1. Configuration - A and B operational. Identical programs:
- 2. FDI limits
 - a) Gyro statistical static 4 meru 0.06°/hr
 - b) Gyro statistical maximum dynamic increase 8 meru .12°/hr
 - c) Gyro TSE MASE 18 pulses² .76°/hr
 - d) Gyro TSE maximum dynamic increase 20 pulses² .81°/hr
 - e) Accelerometer 1st failure MASE 72 pulses² .14 cm/sec²
 - f) Accelerometer 2nd failure MASE 57.6 pulses² .13 cm/sec²

B. Inertial components

- 1. Gyros - all operational
- 2. Accelerometers - all operational

3. FAILURES SCHEDULED

- A. Inertial components - none
- B. Computer - none

4. FLIGHT DESCRIPTION

Took off from Crow's Landing. Overflow Crow's Landing Tacan, Lick Observatory, San Jose Vortac, Moffett Tacan. Landed at Moffett. Taxied to Station A. Terminated program.

5. DEVIATIONS FROM TEST PLAN

A. Unplanned failures

- 1. Coolant high temperature alarm from beginning of navigation mode until landing at Moffett. Cabin temperature peaked 93° F.
- 2. A,B,C,F gyro failures during taxiing.
- 3. Night watchman bad computer B during flight.
- 4. A,C,E gyro failures in flight.
- 5. A,C,D gyro, E accelerometer failures after touchdown at Moffett.

B. Procedural changes

- 1. Operator errors - none
- 2. Operational necessities - none

6. TIMES

- A. Warmup 6.25 hr B. Fine alignment 23 min
- C. Navigation 36 min D. Flight 31 min

7. COMMENTS

Wrong value of -NBD entered in Compensation for D gyro. Equivalent to 0.4°/hr. One engine running during fine alignment. Inertial component failures believed caused by high cabin temperatures.

1. TEST OBJECTIVES:

Navigation performance test.

2. SYSTEM CONFIGURATION

A. Computer

1. Configuration - A (no Schuler compensation), B (Schuler compensation)

2. FDI Limits

a) Gyro statistical static	4	meru	0.06°/hr
b) Gyro statistical maximum dynamic increase	8	meru	.12°/hr
c) Gyro TSE MASE	18	pulses ²	.76°/hr
d) Gyro TSE maximum dynamic increase	20	pulses ²	.81°/hr
e) Accelerometer 1st failure MASE	72	pulses ²	.14 cm/sec ²
f) Accelerometer 2nd failure MASE	57.6	pulses ²	.13 cm/sec ²

B. Inertial components

1. Gyros - all operational
2. Accelerometers - all operational

3. FAILURES SCHEDULED

A. Inertial components - none

B. Computer - none

4. FLIGHT DESCRIPTION

Took off from Moffett. Overflew San Jose, Crow's Landing, Stockton, Sacramento, Stockton, Modesto, Crow's Landing, Fresno, Salinas, San Jose, Oakland, Buchanan, Sacramento. Landed at Moffett. Taxied to Station A. Navigated for 5 min. Terminated program.

5. DEVIATIONS FROM TEST PLAN

A. Unplanned failures

1. A,C,E gyro failures during taxiing for takeoff.
2. Intermittent B,C,E,D gyro and D accelerometer failures during flight.
3. B,C,F gyro failures in turns.
4. Camera driftmeter mark failed at 5051.00 sec (no SCORE reset).

B. Procedural changes

1. Operator errors - none
2. Operational necessities - none

6. TIMES

A. Warmup 11.6 hr B. Fine alignment 26 min
C. Navigation 4.3 hr D. Flight 3.9 hr

7. COMMENTS

E gyro recertified at 28.3 meru at 869.00 sec into navigation. All driftmeter marks after 5051.00 sec were manual (no SCORE resets). Wrong value of -NBD entered in compensation for D gyro. Equivalent to 0.4°/hr. Other compensation parameters derived from 5 position aided calibration were contaminated by this error.

1. TEST OBJECTIVES:

Evaluate system performance in a dynamic environment similar to STOL terminal environment.

2. SYSTEM CONFIGURATION

A. Computer

1. Configuration - A and B identical

2. FDI limits

a) Gyro statistical static	4	meru	0.06°/hr
b) Gyro statistical maximum dynamic increase	8	meru	.12°/hr
c) Gyro TSE MASE	18	pulses ²	.76°/hr
d) Gyro TSE maximum dynamic increase	20	pulses ²	.81°/hr
e) Accelerometer 1st fail MASE	72	pulses ²	.14 cm/sec ²
f) Accelerometer 2nd failure MASE	57.6	pulses ²	.13 cm/sec ²

B. Inertial components

1. Gyros - all operational

2. Accelerometers - all operational

3. FAILURES SCHEDULED

A. Inertial components - none

B. Computer - none

4. FLIGHT DESCRIPTION

Took off from Crow's Landing. Made several right and left turns at 10° and 20° bank angles. Landed at Crow's Landing. Taxied to Station "L". Navigated for 7 min. Terminated program.

5. DEVIATIONS FROM TEST PLAN

A. Unplanned failures

1. A,C,D,E gyro failures intermittent throughout flight. B,F accelerometer failures intermittent during flight.

B. Procedural changes

1. Operator errors - entered initial longitude as -121.0470 vs -121.1047

2. Operational necessities - none

6. TIMES

A. Warmup 3.1 hr B. Fine alignment 30 min

C. Navigation 57 min D. Flight 41 min

7. COMMENTS

A. C&D gyro failures seemed to correlate with turns. Wrong value of -NBD entered in compensation for D gyro. Equivalent to 0.4°/hr. Other compensation parameters, derived from 5-position aided calibration, were contaminated by this error.

1. TEST OBJECTIVES:

Navigation performance check.

2. SYSTEM CONFIGURATION

A. Computer

1. Configuration - A computer off.

2. FDI limits

a) Gyro statistical static	32	meru	0.48°/hr
b) Gyro statistical maximum dynamic increase	64	meru	.96°/hr
c) Gyro TSE MASE	40	pulses ²	1.13°/hr
d) Gyro TSE maximum dynamic increase	80	pulses ²	1.61°/hr
e) Accelerometer 1st failure MASE	72	pulses ²	.14 cm/sec
f) Accelerometer 2nd failure MASE	57.6	pulses ²	.13 cm/sec ²

B. Inertial components

1. Gyros - all operational
2. Accelerometers - all operational

3. FAILURES SCHEDULED

- A. Inertial components - none
- B. Computer - none

4. FLIGHT DESCRIPTION

Took off from Moffett, overflew Moffett Tacan, San Jose Vortac, Stockton Airport, Crow's Landing Tacan, San Jose Vortac, Moffett Tacan. Landed at Moffett, taxied to Station A, navigated for approximately 10 min. Terminated program.

5. DEVIATIONS FROM TEST PLAN

A. Unplanned failures

1. A,B,F gyros had transient failures during taxiing.
2. D gyro failure from 380 sec until 3640 sec, recertified with -0.01°/hr.
3. C gyro failure in turns during flight.
4. B gyro failure just prior to touchdown, intermittent while taxiing.
5. Cabin temperature exceeded 90° F prior to takeoff.
6. Coolant high temperature alarm prior to takeoff, cleared after takeoff.

B. Procedural changes

1. Operator errors - initial longitude entered as -121.0548 vs -122.0548 (1° error)
2. Operational necessities - none

6. TIMES

A. Warmup 1.5 hr B. Fine alignment 55 min
 C. Navigation 1.67 hr D. Flight 1.2 hr

7. COMMENTS

- A. Latitude vs longitude plot indicates flight originated at Crow's Landing vs Moffett. This is due to the 1° error in initial longitude entry by the operator. Moffett and Crow's are approximately same latitude and are approximately 1° apart in longitude.
- B. Gyro FDI limits increased to minimize "transient" gyro failures.
- C. A computer not used in order to get maximum data on tape.

1. TEST OBJECTIVES:

- A. Navigation performance to verify new accelerometer calibration.
- B. Evaluation of SIRU algorithms.

2. SYSTEM CONFIGURATION

A. Computer

- 1. Configuration - A and B identical
- 2. FDI limits
 - a) Gyro statistical static 32 meru 0.48°/hr
 - b) Gyro statistical maximum dynamic increase 64 meru .96°/hr
 - c) Gyro TSE MASE 40 pulses² 1.14°/hr
 - d) Gyro TSE maximum dynamic increase 80 pulses² 1.16°/hr
 - e) Accelerometer 1st failure MASE 72 pulses² .14 cm/sec²
 - f) Accelerometer 2nd failure MASE 57.6 pulses² .13 cm/sec²

B. Inertial components

- 1. Gyros - all operational
- 2. Accelerometers - all operational

3. FAILURES SCHEDULED

- A. Inertial components - none
- B. Computer - none

4. FLIGHT DESCRIPTION

Took off from Moffett. Overflow Lick Observatory, Crow's Landing, Stockton Airport, Modesto Airport, Castle Airport. Landed at Stockton. Taxied to reference point. Tape terminated.

5. DEVIATIONS FROM TEST PLAN

A. Unplanned failures

- 1. Computer B turned off because of disagreement with computer A (COP bad).
- 2. Numerous 3-phase 400-Hz power glitches.

B. Procedural changes

- 1. Operator errors - none
- 2. Operational necessities
 - a) Ran with one computer because of cross opinion bad.

6. TIMES

- A. Warmup 3.7 hr
- B. Fine alignment 45 min
- C. Navigation 1.6 hr
- D. Flight 1.2 hr

7. COMMENTS

- A. Choice of computer A vs B was based on best estimate of actual position. COP bad only indicates disagreement between computers. Does not indicate which is bad.

1. TEST OBJECTIVES:

- A. Provide flight data for SIRU response to programmed sequential sensor failures.

2. SYSTEM CONFIGURATION

A. Computer

1. Configuration - computer A only
2. FDI limits
 - a) Gyro statistical static 32 meru 0.48°/hr
 - b) Gyro statistical maximum dynamic increase 64 meru .96°/hr
 - c) Gyro TSE MASE 40 pulses² 1.13°/hr
 - d) Gyro TSE maximum dynamic increase 80 pulses² 1.61°/hr
 - e) Accelerometer 1st failure MASE 72 pulses² .14 cm/sec²
 - f) Accelerometer 2nd failure MASE 57.6 pulses² .13 cm/sec²

B. Inertial components

1. Gyros - all operational
2. Accelerometers - all operational

3. FAILURES SCHEDULED

- A. Inertial components - A gyro (10°/hr), C gyro (5°/hr)

- B. Computer - none

4. FLIGHT DESCRIPTION

Fine aligned at Stockton, reset latitude, longitude. Took off from Stockton. Overflew Modesto, failure C gyro. Overflew Castle, failure A gyro. Overflew Crow's Landing, Lick Observatory, San Jose. Landed at Moffett. Taxied to Station A. Removed gyro failure. Terminated program.

5. DEVIATIONS FROM TEST PLAN

A. Unplanned failures

1. Computer B turned off because of disagreement with computer A during flight 717A.
2. C PIP temperature failure.
3. C PIP 28V PTE failure.
4. PIP reg #1, C.

B. Procedural changes

1. Operator errors - none
2. Operational necessities - ran with computer A only.

6. TIMES

- A. Warmup 6.2 hr B. Fine alignment 20 min C. Navigation 1.2 hr
D. Flight 1.01 hr

7. COMMENTS

- A. Unable to verify C PIP 28V PTE failure of PIP reg #1, C failure.
- B. C PIP temperature indicated 5.38° F cold on diagnostic module. Cause undetermined at this time. Later determined that cold air was blowing on module from air conditioning.
- C. C gyro failure detected in 56 sec.
- D. A gyro failure detected in 44 sec.

1. TEST OBJECTIVES:

Navigation performance.

2. SYSTEM CONFIGURATION

A. Computer

1. Configuration A and B identical

2. FDI limits

a) Gyro statistical static	32	meru	0.48°/hr
b) Gyro statistical maximum dynamic increase	64	meru	.96°/hr
c) Gyro TSE MASE	40	pulses ²	1.14°/hr
d) Gyro TSE maximum dynamic increase	120	pulses ²	1.98°/hr
e) Accelerometer 1st failure MASE	288	pulses ²	.28 cm/sec ²
f) Accelerometer 2nd failure MASE	230.4	pulses ²	.25 cm/sec ²

B. Inertial components

1. Gyros - all operational

2. Accelerometers - all operational

3. FAILURES SCHEDULED

A. Inertial components - none

B. Computer - none

4. FLIGHT DESCRIPTION

Take off from Moffett, overflow San Jose, Lick Observatory, landed at Crow's Landing. Taxied to Station L. Navigated for 5 min. Terminated program.

5. DEVIATIONS FROM TEST PLAN

A. Unplanned failures

1. None

B. Procedural changes

1. Operator errors - none

2. Operational necessities

a) Gyro statistical FDI removed from navigation program by keyboard entry.

6. TIMES

A. Warmup 6.75 hr B. Fine alignment 20 min C. Navigation 40 min

D. Flight 21 min

7. COMMENTS

A. Gyro TSE maximum dynamic increase increased from 1.61°/hr to 1.96°/hr.

B. Accelerometer first failure MASE increased from 0.53 cm/sec² to .106 cm/sec².

C. Accelerometer second failure MASE increased from 0.047 cm/sec² to .095 cm/sec².

1. TEST OBJECTIVES:

Navigation performance with programmed sequential accelerometer failures.

2. SYSTEM CONFIGURATION

A. Computer

1. Configuration - A and B identical

2. FDI limits

a) Gyro statistical static	32	meru	0.48°/hr
b) Gyro statistical maximum dynamic increase	64	meru	.96°/hr
c) Gyro TSE MASE	40	pulses ²	1.14°/hr
d) Gyro TSE maximum dynamic increase	120	pulses ²	1.98°/hr
e) Accelerometer 1st failure MASE	288	pulses ²	.28 cm/sec ²
f) Accelerometer 2nd failure MASE	230.4	pulses ²	.25 cm/sec ²

B. Inertial components

1. Gyros - all operational

2. Accelerometers - all operational

3. FAILURES SCHEDULED

A. Inertial components - C PIPA (2 cm/sec²), E PIPA (3 cm/sec²) after first failure

B. Computer - none.

4. FLIGHT DESCRIPTION

Fine alignment at Station L. Took off from Crow's Landing. Overflow Stockton, Modesto failure C PIPA. Overflow Castle, failure E PIPA. Landed Crow's Landing. Taxied to Station L.

5. DEVIATIONS FROM TEST PLAN

A. Unplanned failures

1. Tape ran out immediately after touchdown at Crow's Landing.

B. Procedural changes

1. Operator errors - entered failures in both computers instead of computer B only. Altitude entered as 24830, not 2483 m.

2. Operational necessities

a) Gyro statistical FDI removed from navigation program by keyboard entry.

6. TIMES

A. Warmup 7.9 hr B. Fine alignment 25 min C. Navigation 58 min

D. Flight 39 min

7. COMMENTS

A. Both failures detected and taken off line.

1. TEST OBJECTIVES:

System performance with programmed sequential gyro and accelerometer failures. Evaluate performance by entering failure in one computer only.

2. SYSTEM CONFIGURATION

A. Computer

1. Configuration - A and B identical

2. FDI limits

a) Gyro statistical static	32	meru	0.48°/hr
b) Gyro statistical maximum dynamic increase	64	meru	.96°/hr
c) Gyro TSE MASE	40	pulses ²	1.14°/hr
d) Gyro TSE maximum dynamic increase	120	pulses ²	1.98°/hr
e) Accelerometer 1st failure MASE	288	pulses ²	.28 cm/sec ²
f) Accelerometer 2nd failure MASE	230.4	pulses ²	.25 cm/sec ²

B. Inertial components

1. Gyros - all operational
2. Accelerometers - all operational

3. FAILURES SCHEDULED

- A. Inertial components - C gyro (5°/hr), C PIP (2 cm/sec²) after first failure detected. A gyro (3°/hr) after second failure detected. B computer only.
- B. Computer - none.

4. FLIGHT DESCRIPTION

Fine alignment at Station L, Crow's Landing. Took off and overflow Stockton, failure C gyro. Overflow Modesto, failed C PIPA and A gyro. Overflow Castle, Crow's Landing. Terminated program. Returned to Moffett.

5. DEVIATIONS FROM TEST PLAN

A. Unplanned failures

1. Coolant high temperature alarm while taxiing for takeoff. Cabin temperature 90° F. (Alarm off 6 min after takeoff.)

B. Procedural Changes

1. Operator errors - none
2. Operational necessities
 - a) Gyro statistical FDI removed from navigation program by keyboard entry.

6. TIMES

- A. Warmup 9.25 hr
- B. Fine alignment 21 min
- C. Navigation 42 min
- D. Flight 36 min

7. COMMENTS

- A. Gyro and PIPA failures entered in B computer only.
- B. C PIPA recertified 850 sec after failure.
- C. All gyro and PIP failures detected and taken off line.

1. TEST OBJECTIVES:

Evaluate system performance with programmed sequential gyro failures.

2. SYSTEM CONFIGURATION

A. Computer

1. Configuration - A and B identical

2. FDI limits

a) Gyro statistical static	32	meru	0.48°/hr
b) Gyro statistical maximum dynamic increase	64	meru	.96°/hr
c) Gyro TSE MASE	40	pulses ²	1.14°/hr
d) Gyro TSE maximum dynamic increase	120	pulses ²	1.98°/hr
e) Accelerometer 1st failure MASE	288	pulses ²	.28 cm/sec ²
f) Accelerometer 2nd failure MASE	230.4	pulses ²	.25 cm/sec ²

B. Inertial components

1. Gyros - all operational

2. Accelerometers - all operational

3. FAILURES SCHEDULED

A. Inertial components - C gyro (3.5°/hr), D gyro (3.0°/hr) B computer only.

B. Computer - none

4. FLIGHT DESCRIPTION

Took off from Moffett. Overflow San Jose, Failure C and D gyros. Overflow Crow's Landing, Stockton, Modesto, Castle, Crow's Landing. Landed at Crow's Landing. Taxied to Station L. Terminated program.

5. DEVIATIONS FROM TEST PLAN

A. Unplanned failures

1. F gyro failure 2 min before going into navigation mode
2. B gyro failure during flight (B computer only)
3. C PIP temperature failure
4. Night watchman bad (B computer)
5. B gyro failure (A computer only) intermittent.
6. E gyro failure (A computer only) intermittent.
7. E gyro temperature failure.

B. Procedural changes

1. Operator errors - did not start data recording until 8 min after takeoff. (1110 sec into navigation)
2. Operational necessities
 - a) Statistical FDI removed from navigation program by keyboard entry.
 - b) Entered navigation mode with F gyro failure because of insufficient time for recertification.

6. TIMES:

- A. Warmup 2.1 hr
- B. Fine alignment 30 min
- C. Navigation 1.4 hr
- D. Flight 1.1 hr

7. COMMENTS

- A. Cause of B gyro failure undetermined
- B. C PIP temperature failure and E gyro temperature believed to be caused by cold air from air conditioning blowing on modules.
- C. C and D gyro failures detected and taken off line.
- D. Cause of F gyro failure undetermined.
- E. Once the deliberate C and D gyro failures are detected by computer B, it will not detect other gyro failures unless they are significantly larger in magnitude. Then the C and D failure indications will go off.

1. TEST OBJECTIVES:

Observe performance of system with programmed gyro failures of different magnitudes in each computer simultaneously.

2. SYSTEM CONFIGURATION

A. Computer

1. Configuration - A and B identical

2. FDI limits -

a) Gyro statistical static	32	meru	0.48°/hr
b) Gyro statistical maximum dynamic increase	64	meru	.96°/hr
c) Gyro TSE MASE	40	pulses ²	1.14°/hr
d) Gyro TSE maximum dynamic increase	120	pulses ²	1.98°/hr
e) Accelerometer 1st failure MASE	288	pulses ²	.28 cm/sec ²
f) Accelerometer 2nd failure MASE	230.4	pulses ²	.25 cm/sec ²

B. Inertial components

1. Gyros - all operational
2. Accelerometers - all operational

3. FAILURES SCHEDULED

- A. Inertial components - C gyro (2°/hr) B computer, (1.5°/hr) A computer.
- B. Computer - none

4. FLIGHT DESCRIPTION

Fine alignment at Station L. Took off from Crow's Landing. Entered C gyro failures. Overflew Crow's Landing, San Jose. Landed at Moffett. Taxied to Station A. Navigated 9 min. Terminated program.

5. DEVIATIONS FROM TEST PLAN

A. Unplanned failures

1. E gyro failure during fine alignment.
2. Night watchman bad (computer B).

B. Procedural changes

1. Operator errors - entered 0.5°/hr into A computer vs 1.5°/hr.
2. Operational Necessities
 - a) Statistical FDI removed from navigation program by keyboard entry.
 - b) Entered navigation mode with E gyro failure because of insufficient time for recertification.

6. TIMES

- | | | | | | |
|-----------|--------|-------------------|--------|---------------|--------|
| A. Warmup | 4.1 hr | B. Fine alignment | 25 min | C. Navigation | 45 min |
| D. Flight | 23 min | | | | |

7. COMMENTS

- A. E gyro failure attributed to cold air blowing on it from air conditioning.
- B. C gyro failure not detected on computer B because it was below TSE threshold.
- C. C gyro failure computer B intermittent because $2^\circ/\text{hr}$ is between the minimum and maximum TSE limits which makes detection dependent upon aircraft dynamics.

1. TEST OBJECTIVES:

Evaluate effect of induced computer failure in flight environment.

2. SYSTEM CONFIGURATION

A. Computer

1. Configuration - A and B identical

2. FDI limits

a) Gyro statistical static	6	meru	0.09°/hr
b) Gyro statistical maximum dynamic increase	-	meru	- °/hr
c) Gyro TSE MASE	40	pulses ²	1.14°/hr
d) Gyro TSE maximum dynamic increase	120	pulses ²	
	120	pulses ²	1.98°/hr
e) Accelerometer 1st failure MASE	288	pulses ²	.28 cm/sec ²
f) Accelerometer 2nd failure MASE	230.4	pulses ²	.25 cm/sec ²

B. Inertial components

1. Gyros - all operational

2. Accelerometers - all operational

3. FAILURES SCHEDULED

A. Inertial components - none

B. Computer (B only) Force program into infinite loop via keyboard change of contents of memory

4. FLIGHT DESCRIPTION

Took off from Moffett. Failure Computer B. Overflew Lick Observatory Landed at Crow's Landing. Taxied to Station L. Navigated for 5 min. Terminated program.

5. DEVIATIONS FROM TEST PLAN

A. Unplanned failures - none.

B. Procedural changes

1. Operator errors - none

2. Operational necessities - none

6. TIMES

A. Warmup 4.5 hr B. Fine alignment 1.1 hr C. Navigation 44 min

D. Flight 20 min

7. COMMENTS

A. Forced computer error detected as COP bad (Cross Opinion bad). Prime switched from Computer B to Computer A. Display stopped updating.

1. TEST OBJECTIVES:

Evaluate system performance with programmed simultaneous A and B Gyro failures of large equal magnitude.

2. SYSTEM CONFIGURATION

A. Computer

1. Configuration - A and B identical

2. FDI limits

a) Gyro statistical static	6	meru	0.09°/hr
b) Gyro statistical maximum dynamic increase	-	meru	- °/hr
c) Gyro TSE MASE	40	pulses ²	1.14°/hr
d) Gyro TSE maximum dynamic increase	120	pulses ²	1.98°/hr
e) Accelerometer 1st failure MASE	288	pulses ²	.28 cm/sec ²
f) Accelerometer 2nd failure MASE	230.4	pulses ²	.25 cm/sec ²

B. Inertial components

1. Gyros - all operational
2. Accelerometers - all operational

3. FAILURES SCHEDULED

A. Inertial components - A gyro 6167°/hr, B gyro 6167°/hr - Computer B only

B. Computer - none

4. FLIGHT DESCRIPTION

Fine alignment at Station L, Crow's Landing. Took off from Crow's Landing. Entered gyro failures. Landed at Crow's Landing. Taxied to Station L. Removed failures, reinitialized latitude and longitude. Took off, entered gyro failures. Landed Crow's Landing. Taxied to Station L. Terminated program.

5. DEVIATIONS FROM TEST PLAN

A. Unplanned failures

1. E gyro failure and E accelerometer failure during fine alignment and flight.

2. Night watchman bad (B computer) prior to taxiing for takeoff.

B. Procedural changes

1. Operator errors - none
2. Operational necessities

a) Entered navigation mode with E gyro failure because of insufficient time for recertification.

6. TIMES

A. Warmup 6.75 hr B. Fine alignment 37 min C. Navigation 35 min
D. Flight 22 min

7. COMMENTS

- A. Cause of E gyro failure and E accelerometer believed caused by high cabin temperature
- B. Gyro failures entered 20 sec apart. Detected immediately.

1. TEST OBJECTIVES:

Evaluate effect of induced computer failures in flight environment.

2. SYSTEM CONFIGURATION

A. Computer

1. Configuration - A and B identical

2. FDI limits

a) Gyro statistical static	6	meru	0.09°/hr
b) Gyro statistical maximum dynamic increase	-	meru	- °/hr
c) Gyro TSE MASE	40	pulses ²	1.14°/hr
d) Gyro TSE maximum dynamic increase	120	pulses ²	1.98°/hr
	120	pulses ²	1.98°/hr
e) Accelerometer 1st failure MASE	288.	pulses ²	.28 cm/sec ²
f) Accelerometer 2nd failure MASE	230.4	pulses ²	.25 cm/sec ²

B. Inertial components

1. Gyros - all operational

2. Accelerometers - all operational

3. FAILURES SCHEDULED

A. Inertial components - none

B. Computer - (1) Memory checksum error (Comp. A&B) (2) Arithmetic instruction failure (Comp. A) (3) Wordwatch failure (Comp. A) (4) Wraparound test failure (Comp. A) (5) Night watchman failure (Comp. A)

4. FLIGHT DESCRIPTION

Fine aligned at Station L. Took off from Crow's Landing. Induced computer failures. Overflew Fresno. Landed at Bakersfield. Taxied to reference point. Navigated a few minutes. Terminated program.

5. DEVIATIONS FROM TEST PLAN

A. Unplanned failures

1. E accelerometer intermittent failure during fine alignment and flight

2. E&F gyro failure during fine alignment. E gyro recertified at -6.5 meru (0.1°/hr)

3. Coolant high temperature alarm at liftoff. Cabin temperature 88° F.

4. Night watchman bad (computer B). Display did not respond to keyboard.

B. Procedural changes

1. Operator errors - none

2. Operational necessities

a) Raised gyro statistical static limit from 0.09°/hr to 0.18°/hr during fine alignment to reduce number of false failures.

b) Computer B turned off. No response to keyboard commands.

6. TIMES

A. Warmup 8.2 hr B. Fine alignment 56 min C. Navigation 1.13 hr
D. Flight 57 min

7. COMMENTS

- A. Computers responded correctly to induced failures except Computer B did not respond to memory checksum error.
- B. Cause of Computer B problems not determined at this time.
- C. Gyro and accelerometer failures may have been caused by high coolant temperature.

1. TEST OBJECTIVES:

Evaluate effect of induced computer failures in flight environment

2. SYSTEM CONFIGURATION

A. Computer

1. Configuration - A and B identical

2. FDI limits

a) Gyro statistical static	6	meru	0.09°/hr
b) Gyro statistical maximum dynamic increase	-	meru	- °/hr
c) Gyro TSE MASE	40	pulses ²	1.14°/hr
d) Gyro TSE maximum dynamic increase	120	pulses ²	1.98°/hr
e) Accelerometer 1st failure MASE	288	pulses ²	.28 cm/sec ²
f) Accelerometer 2nd failure MASE	230.4	pulses ²	.25 cm/sec ²

B. Inertial components

1. Gyros - all operational

2. Accelerometers - all operational

3. FAILURES SCHEDULED

A. Inertial components - none

B. Computer - (1) Memory checksum error (2) Wraparound test failure (3) Wordwatch failure (4) Arithmetic instruction failure (Computer B only).

4. FLIGHT DESCRIPTION

Fine aligned at reference point. Induced failures in Computer B. Took off from Bakersfield. Overflew Bakersfield, Fresno, Crow's Landing, Lick Observatory. Landed at Moffett. Taxied to Station A. Navigated for 3 min. Terminated program.

5. DEVIATIONS FROM TEST PLAN

A. Unplanned failures

1. E accelerometer and E gyro failure during fine alignment
2. Computer A failure just before taxiing for takeoff.
3. Computer B display not displaying data, only labels during flight right after takeoff.

B. Procedural changes

1. Operator errors - none
2. Operational necessities
 - a) Turned off Computer A due to apparent failure
 - b) No display photos due to display failure
 - c) No induced computer failures in flight because of Computer A failure. (Wanted one computer running normally)
 - d) Raised gyro statistical FDI limit from 0.09°/hr to 0.18°/hr during fine alignment to reduce number of false failures.
 - e) Did not land at Crow's Landing due to insufficient fuel.

6. TIMES

A. Warmup 10.5 hr B. Fine alignment 30 min C. Navigation 1.5 hr
D. Flight 1.2 hr

7. COMMENTS

A. Computer B responded correctly to induced failures.
B. System navigated and recorded data even though display was not working.
C. E accelerometer and E gyro failures believed caused by high cabin temperature.

1. TEST OBJECTIVES:

Evaluate system performance with programmed simultaneous gyro failures of different magnitudes.

2. SYSTEM CONFIGURATION

A. Computer

1. Configuration - A and B identical

2. FDI limits

a) Gyro statistical static	6	meru	0.09°/hr
b) Gyro statistical maximum dynamic increase	-	meru	-°/hr
c) Gyro TSE, MASE	40	pulses ²	1.14°/hr
d) Gyro TSE maximum dynamic increase	120	pulses ²	1.98°/hr
e) Accelerometer 1st failure MASE	288	pulses ²	.28 cm/sec ²
f) Accelerometer 2nd failure MASE	230.5	pulses ²	.25 cm/sec ²

B. Inertial components

1. Gyros - all operational

2. Accelerometers - all operational

3. FAILURES SCHEDULED

A. Inertial components - A gyro 6°/hr, B gyro 24°/hr (computer B only)

B. Computer - none

4. FLIGHT DESCRIPTION

Took off from Moffett. Overflew San Jose. Entered gyro failures over Lick Observatory. Landed at Crow's Landing. Taxied to Station L. Navigated a few minutes. Terminated program.

5. DEVIATIONS FROM TEST PLAN

A. Unplanned failures

1. E gyro failure during fine alignment. Recertified at 0.15°/hr

2. D gyro failure during fine alignment. Recertified at 0.15°/hr

B. Procedural changes

1. Operator errors - entered gyro failures into both computers instead of B computer only.

2. Operational necessities - none.

6. TIMES

A. Warmup 3.25 hr B. Fine alignment 1.6 hr C. Navigation 44 min

D. Flight 20 min

7. COMMENTS

A. Both gyro failures entered within 5 sec of each other. B gyro failure detected in 15 sec, A gyro failure detected in 20 sec.

B. Cause of D and E gyro failure undetermined. Recertified and back on line before going into navigation.

1. TEST OBJECTIVES:

Evaluate system performance with programmed simultaneous gyro failures of different magnitudes in a turn.

2. SYSTEM CONFIGURATION

A. Computer

1. Configuration - A and B identical

2. FDI limits

a) Gyro statistical static	6 meru	0.09°/hr
b) Gyro statistical maximum dynamic increase	- meru	- °/hr
c) Gyro TSE MASE	40 pulses ²	1.14°/hr
d) Gyro TSE maximum dynamic increase	120 pulses ²	1.98°/hr
e) Accelerometer 1st failure MASE	288 pulses ²	.28 cm/sec ²
f) Accelerometer 2nd failure MASE	230.4 pulses ²	.25 cm/sec ²

B. Inertial components

1. Gyros - all operational

2. Accelerometers - all operational

3. FAILURES SCHEDULED

A. Inertial components - A gyro 6°/hr, B gyro 24°/hr (Computer B only)

B. Computer - none

4. FLIGHT DESCRIPTION

Fine aligned at Station L. Took off from Crow's Landing. Failed gyros during climbing left turn to 1500 ft. Descending left turn. Landed at Crow's Landing. Taxied to Station L. Reinitialized latitude and longitude. Navigated for 5 min. Took off. Climbing left turn to 1000 ft. Descending left turn. Landed at Crow's. Taxied to Station L. Navigated for 2 min. Terminated program.

5. DEVIATIONS FROM TEST PLAN

A. Unplanned failures

1. Aircraft developed severe hydraulic leak during second flight.

B. Procedural changes

1. Operator errors - none

2. Operational necessities

a) Did not enter failures on second flight because of insufficient time. (Flight time 5 min)

6. TIMES

A. Warmup 4.2 hr B. Fine alignment 27 min C. Navigation 42 min

D. Flight 8.4 min

7. COMMENTS

A. Second flight aborted because of aircraft hydraulic leak. (Original flight plan was to overfly Stockton, Modesto, and Castle and land at Crow's Landing.)

1. TEST OBJECTIVES:

Evaluate system performance with programmed gyro failures of short duration in straight and level flight.

2. SYSTEM CONFIGURATION

A. Computer

1. Configuration - A and B identical

2. FDI limits

a) Gyro statistical static	6	meru	0.09°/hr
b) Gyro statistical maximum dynamic increase	-	meru	- °/hr
c) Gyro TSE MASE	40	pulses ²	1.14°/hr
d) Gyro TSE maximum dynamic increase	120	pulses ²	1.48°/hr
e) Accelerometer 1st failure MASE	288	pulses ²	.28 cm/sec ²
f) Accelerometer 2nd failure MASE	230.4	pulses ²	.25 cm/sec ²

B. Inertial components

1. Gyros - all operational

2. Accelerometers - all operational

3. FAILURES SCHEDULED

A. Inertial components - E gyro 6°/hr, F gyro 24°/hr, B computer only

B. Computer - none

4. FLIGHT DESCRIPTION

Took off from Moffett. Overflow San Jose. Entered failures. Removed failures. Overflow Lick Observatory. Landed at Crow's Landing. Taxied to Station L. Navigated for 2 min. Terminated program.

5. DEVIATIONS FROM TEST PLAN

A. Unplanned failures

1. A gyro failure during fine alignment only. Intermittent.

B. Procedural changes

1. Operator errors - none

2. Operational necessities - none

a) Reloaded program after F and D gyro failures during fine alignment.

6. TIMES

A. Warmup 3.3 hr B. Fine alignment 31 min C. Navigation 37 min

D. Flight 21 min

7. COMMENTS

A. F gyro failure detected in 10 sec.

B. E gyro failure detected in 60 sec.

C. E, F gyro failures removed 7 min after entry.

1. TEST OBJECTIVES:

Evaluate system performance with programmed gyro and accelerometers failures of short duration during straight and level flight.

2. SYSTEM CONFIGURATION

A. Computer

1. Configuration - A and B identical

2. FDI limits

a) Gyro statistical static	6	meru	0.09°/hr
b) Gyro statistical maximum dynamic increase	-	meru	- °/hr
c) Gyro TSE MASE	40	pulses ²	1.14°/hr
d) Gyro TSE maximum dynamic increase	120	pulses ²	1.48°/hr
e) Accelerometer 1st failure MASE	288	pulses ²	.28 cm/sec ²
f) Accelerometer 2nd failure MASE	230.4	pulses ²	.25 cm/sec ²

B. Inertial components

1. Gyros - all operational

2. Accelerometers - all operational

3. FAILURES SCHEDULED

A. Inertial components - A gyro 6°/hr, B gyro 24°/hr, A accelerometer 1 cm/sec², B accelerometer 4 cm/sec² - B computer only

B. Computer - none

4. FLIGHT DESCRIPTION

Fine alignment at Station L. Entered accelerometer failures during taxiing. Took off from Crow's Landing. Removed failures. Ended at Crow's Landing.

5. DEVIATIONS FROM TEST PLAN

A. Unplanned failures

1. F gyro failure during fine alignment

2. Coolant high temperature alarm during taxiing. Cabin temperature 90° F.

B. Procedural Changes

1. Operator errors

a) F gyro loop opened in flight (closed at Station L)

b) Insufficient negative error entered to remove B accelerometer failure.

2. Operational necessities

a) Entered navigation mode with F gyro failure because of insufficient time for recertification.

b) Did not fail gyros because of unscheduled F gyro failures.

6. TIMES

A. Warmup 5.1 hr B. Fine alignment 37 min C. Navigation 53 min

D. Flight 33 min

7. COMMENTS

- A. A PIP failure detected in 110 sec.
- B. B PIP failure detected in 100 sec.
- C. B PIP failure removal intermittent
- D. A PIP failure not removed until after landing.
- E. F gyro failure believed caused by high temperature.

1. TEST OBJECTIVES:

Evaluate system performance with programmed gyro failure of short duration.

2. SYSTEM CONFIGURATION

A. Computer

1. Configuration

2. FDI limits

a) Gyro statistical static	6	meru	0.09°/hr
b) Gyro statistical maximum dynamic increase	-	meru	- °/hr
c) Gyro TSE MASE	40	pulses ²	1.14°/hr
d) Gyro TSE maximum dynamic increase	120	pulses ²	1.48°/hr
e) Accelerometer 1st failure MASE	288	pulses ²	.28 cm/sec ²
f) Accelerometer 2nd failure MASE	230.4	pulses ²	.25 cm/sec ²

B. Inertial components

1. Gyros - all operational
2. Accelerometers - all operational

3. FAILURES SCHEDULED

- A. Inertial components - E gyro 6°/hr - computer B only
- B. Computer - none

4. FLIGHT DESCRIPTION

Fine alignment Station L. Took off from Crow's Landing. Failed E gyro just before 180° turn. Removed failure. Landed at Crow's Landing, taxied to Station L. Navigated for 3 min. Terminated program.

5. DEVIATIONS FROM TEST PLAN

A. Unplanned failures

1. Coolant high temperature alarm during fine alignment. Cabin temperature 89° F.
2. F gyro failure during fine alignment.
3. A computer address error and echo check bad immediately after touchdown.

B. Procedural changes

1. Operator errors -
2. Operational necessities
 - a) Entered navigation mode with F gyro failure because of insufficient time for recertification.

6. TIMES

A. Warmup 6.6 hr B. Fine alignment 29 min C. Navigation 39 min
D. Flight 25 min

7. COMMENTS

- A. E gyro failure detected in 50 sec
- B. E gyro failure removed after 710 sec
- C. F gyro failure believed cause by high cabin temperature.

1. TEST OBJECTIVES:

Evaluate system performance with programmed accelerometer failures during straight and level flight.

2. SYSTEM CONFIGURATION

A. Computer

1. Configuration - A and B identical

2. FDI limits

a) Gyro statistical static	6	meru	0.09°/hr
b) Gyro statistical maximum dynamic increase	-	meru	- °/hr
c) Gyro TSE MASE	40	pulses ²	1.14°/hr
d) Gyro TSE maximum dynamic increase	120	pulses ²	1.48°/hr
e) Accelerometer 1st failure MASE	288	pulses ²	.28 cm/sec ²
f) Accelerometer 2nd failure MASE	230.4	pulses ²	.25 cm/sec ²

B. Inertial components

1. Gyros - all operational

2. Accelerometers - all operational

3. FAILURES SCHEDULED

A. Inertial components - C accelerometer 1 cm/sec, D accelerometer 4 cm/sec - B computer only

B. Computer - none

4. FLIGHT DESCRIPTION

Fine alignment at Station L. Took off from Crow's Landing. Entered accelerometer failures. Overflew Lick Observatory, San Jose. Landed at Moffett. Taxied to Station A. Terminated program.

5. DEVIATIONS FROM TEST PLAN

A. Unplanned failures

1. Computer A display failure. Loose connector.

2. Coolant high temperature alarm. Cabin temperature 92° F.

3. E and F gyro failure during fine alignment.

B. Procedural changes

1. Operator errors - none

2. Operational necessities

a) Entered navigation mode with E and F gyro failures because of insufficient time for recertification.

b) Night watchman bad (computer B).

c) C gyro temperature failure.

6. TIMES

A. Warmup 8.3 hr B. Fine alignment 27 min C. Navigation 32 min

D. Flight 23 min

7. COMMENTS

- A. E and F gyro failures probably caused by high cabin temperature.
- B. C accelerometer failure detected in 80 sec.
- C. D accelerometer failure detected in 70 sec.
- D. Accelerometer failures not removed.

1. TEST OBJECTIVES:

- A. Evaluate system performance with controlled turns, bank angles, and climb rates to simulate STOL maneuvers.
- B. Collect raw inertial instrument data for later analysis.

2. SYSTEM CONFIGURATION

A. Computer

- 1. Configuration - A and B identical
- 2. FDI limits
 - a) Gyro statistical static 12 meru 0.18°/hr
 - b) Gyro statistical maximum dynamic increase - meru - °/hr
 - c) Gyro TSE MASE 40 pulses 1.14°/hr
 - d) Gyro TSE maximum dynamic increase 120 pulses² 1.98°/hr
 - e) Accelerometer 1st failure MASE 288 pulses² .28 cm/sec²
 - f) Accelerometer 2nd failure MASE 230.4 pulses² .25 cm/sec²

B. Inertial components

- 1. Gyros - all operational
- 2. Accelerometers - all operational

3. FAILURES SCHEDULED

- A. Inertial components - none
- B. Computer - none

4. FLIGHT DESCRIPTION

Took off from Moffett. Touch and go at Crow's Landing (Runway 30). Climbed at maximum rate. Turned left (30° bank), climbed to 3000 ft (915 m); crosswind level (3 knots). 360° turn to right (60° bank). Level downwind. Descending left turn. Touch and go at Crow's Landing. Repeated above. Landed at Crow's Landing. Taxied to Station L.

5. DEVIATIONS FROM TEST PLAN

A. Unplanned failures

- 1. F gyro failure in fine alignment. Recertified at +0.12°/hr

B. Procedural changes

- 1. Operator errors - none
- 2. Operational necessities. Runway 30 used vs Runway 35.

6. TIMES

- A. Warmup 1.25 hr
- B. Fine alignment 1.1 hr
- C. Navigation 62 min
- D. Flight 41 min

7. COMMENTS

- A. Cabin temperature 74° F to 82° F

1. TEST OBJECTIVES:

- A. Evaluate system performance with controlled turns, bank angles, and climb rates to simulate STOL maneuvers.
- B. Collect raw instrument data for later analysis.

2. SYSTEM CONFIGURATION

A. Computer

- 1. Configuration
- 2. FDI limits
 - a) Gyro statistical static 12 meru 0.18°/hr
 - b) Gyro statistical maximum dynamic increase - meru -°/hr
 - c) Gyro TSE MASE 40 pulses² 1.14°/hr
 - d) Gyro TSE maximum dynamic increase 120 pulses² 1.98°/hr
 - e) Accelerometer 1st failure MASE 288 pulses² .28 cm/sec²
 - f) Accelerometer 2nd failure MASE 230.4 pulses² .25 cm/sec²

B. Inertial components

- 1. Gyros - all operational
- 2. Accelerometers - all operational

3. FAILURES SCHEDULED

- A. Inertial components - none
- B. Computer - none

4. FLIGHT DESCRIPTION

Took off from Runway 12, Crow's Landing. Climbed to 3000 ft (915 m) turned left (45° bank) crosswind 3 min. 360° left turn (60° bank). Downwind. Descending right turn (30° bank). Touch and go at Crow's Landing. Repeated above. Landed at Crow's Landing. Taxied to Station L. Terminated tape.

5. DEVIATIONS FROM TEST PLAN

- A. Unplanned failures - none
- B. Procedural changes
 - 1. Operator errors - none
 - 2. Operational necessities - none

6. TIMES

- A. Warmup 1.25 hr
- B. Fine alignment 1.1 hr
- C. Navigation 1.9 hr
- D. Flight 30 min

7. COMMENTS

- A. Lost radar tracking in 360° turn.
- B. Navigation time includes 1 hr from flight test 910A
- C. No fine alignment or initialization of latitude and longitude was done at Station L. Therefore, flight started with errors accumulated during flight test 910A.

1. TEST OBJECTIVES:

- A. Evaluate system performance with controlled turns, bank angles, and rate of climb to simulate STOL maneuvers.
- B. Collect raw inertial instrument data for later analysis.

2. SYSTEM CONFIGURATION

A. Computer

- 1. Configuration - A and B identical
- 2. FDI limits
 - a) Gyro statistical static 12 meru 0.18°/hr
 - b) Gyro statistical maximum dynamic increase - meru -°/hr
 - c) Gyro TSE MASE 40 pulses² 1.14°/hr
 - d) Gyro TSE maximum dynamic increase 120 pulses² 1.98°/hr
 - e) Accelerometer 1st failure MASE 288 pulses² .28 cm/sec²
 - f) Accelerometer 2nd failure MASE 230.4 pulses² .25 cm/sec²

B. Inertial components

- 1. Gyros - all operational
- 2. Accelerometers - all operational

3. FAILURES SCHEDULED

- A. Inertial components - none
- B. Computer - none

4. FLIGHT DESCRIPTION

Took off from Runway 12, Crow's Landing. Performed various turn maneuvers at bank angles from 10° to 45° (see latitude-longitude plot) and touch-and-go operations. Landed at Crow's Landing. Taxied to Station L. Terminated tape.

5. DEVIATIONS FROM TEST PLAN

- A. Unplanned failures - none
- B. Procedural changes
 - 1. Operator errors - none
 - 2. Operational necessities
 - a) Unable to perform all touch-and-go maneuvers because of runway restrictions. Made low passes instead. Marked intersection of Runways 30 and 35 instead of touchdown on these passes.

6. TIMES

- A. Warmup 1.25 hr
- B. Fine alignment 1.1 hr
- C. Navigation 2.7 hr
- D. Flight 33 min

7. COMMENTS

- A. Navigation time includes 1.9 hr accumulated in flight tests 910A and 910B.
- B. No fine alignment or initialization of latitude and longitude was done at Station L. Therefore, flight started with errors accumulated during flight tests 910A and 910B.

1. TEST OBJECTIVES:

Navigation performance.

2. SYSTEM CONFIGURATION

A. Computer

1. Configuration - A and B identical

2. FDI limits

a) Gyro statistical static	12	meru	0.18°/hr
b) Gyro statistical maximum dynamic increase	-	meru	- °/hr
c) Gyro TSE MASE	40	pulses ²	1.14°/hr
d) Gyro TSE maximum dynamic increase	120	pulses ²	1.98°/hr
e) Accelerometer 1st failure MASE	288	pulses ²	.28 cm/sec ²
f) Accelerometer 2nd failure MASE	230.4	pulses ²	.25 cm/sec ²

B. Inertial components

1. Gyros - all operational

2. Accelerometers - all operational

3. FAILURES SCHEDULED

A. Inertial components - none

B. Computer - none

4. FLIGHT DESCRIPTION

Took off from Crow's Landing. Landed at Moffett. Taxied to Station A. Navigated 2 min. Terminated program.

5. DEVIATIONS FROM TEST PLAN

A. Unplanned failures

1. None

B. Procedural changes

1. Operator errors - none

2. Operational necessities

a) Did not overfly Lick Observatory and San Jose because of insufficient time

6. TIMES

A. Warmup 1.25 hr 2. Fine alignment 1 hr C. Navigation 3.4 hr

D. Flight 19 min

7. COMMENTS

A. Navigation time includes 2.7 hr accumulated during flight tests 910A, 910B, and 910C.

B. No fine alignment or initialization of latitude or longitude was done at Station L. Therefore, flight started with errors accumulated during flight tests 910A, 910B, and 910C.

1. TEST OBJECTIVES:

- A. Evaluate system performance in a dynamic environment similar to a STOL terminal environment.
- B. Collect raw inertial instrument data for later analysis.

2. SYSTEM CONFIGURATION

A. Computer

- 1. Configuration - A and B identical
- 2. FDI limits
 - a) Gyro statistical static 12 meru 0.18°/hr
 - b) Gyro statistical maximum dynamic increase - meru - °/hr
 - c) Gyro TSE MASE 40 pulses² 1.14°/hr
 - d) Gyro TSE maximum dynamic increase 120 pulses² 1.98°/hr
 - e) Accelerometer 1st failure MASE 288 pulses² .28 cm/sec²
 - f) Accelerometer 2nd failure MASE 230.4 pulses² .25 cm/sec²

B. Inertial components

- 1. Gyros - all operational
- 2. Accelerometers - all operational

3. FAILURES SCHEDULED

- A. Inertial components - none
- B. Computer - none

4. FLIGHT DESCRIPTION

Took off from Moffett. Direct to Crow's Landing. Overflow intersection Runways 30 and 35 at 1000 ft. Climbed to 3000 ft (915 m). Turned left 90°. Two min crosswind. Turned left 90°. Two min downwind. Made 2 right and 2 left 360° turns at bank angle of 45°. Overflow intersection, made right and left 360° turns at bank angles of 25°. Landed at Crow's Landing. Taxied to Station L. Terminated tape.

5. DEVIATIONS FROM TEST PLAN

A. Unplanned failures.

- 1. F gyro failure in fine alignment. Recertified at 0.09°/hr

B. Procedural changes

- 1. Operator errors - missed intersection mark at end of first pattern.
- 2. Operational necessities
 - a) Flew at 2000 ft (712 m) vs 3000 ft (914 m).
 - b) Second pattern aborted because of incorrect pilot procedure and insufficient time remaining on tape.

6. TIMES

- A. Warmup 1.5 hr
- B. Fine alignment 1.7 hr
- C. Navigation 1.1 hr
- D. Flight 48 min

7. COMMENTS

1. TEST OBJECTIVES:
 - A. Evaluate system performance in a dynamic environment similiar to a STOL terminal environment.
 - B. Collect raw inertial instrument data for later analysis.

2. SYSTEM CONFIGURATION
 - A. Computer
 1. Configuration - A and B identical
 2. FDI limits

a) Gyro statistical static	12	meru	0.18°/hr
b) Gyro statistical maximum dynamic increase	-	meru	- °/hr
c) Gyro TSE MASE	40	pulses ²	1.14°/hr
d) Gyro TSE maximum dynamic increase	120	pulses ²	1.98°/hr
e) Accelerometer 1st failure MASE	288	pulses ²	.28 cm/sec ²
f) Accelerometer 2nd failure MASE	230.4	pulses ²	.25 cm/sec ²
 - B. Inertial components
 1. Gyros - all operational
 2. Accelerometers - all operational

3. FAILURES SCHEDULED
 - A. Inertial components - none
 - B. Computer - none

4. FLIGHT DESCRIPTION

Took off from Crow's Landing. Made several right and left 360° turns at 45° bank angle. Made low approach over intersection of Runways 30 and 35. Made several right and left 360° turns at 25° bank angle. Landed at Crow's Landing. Taxied to Station L. Terminated tape.

5. DEVIATIONS FROM TEST PLAN
 - A. Unplanned failures
 1. None
 - B. Procedural changes
 1. Operator errors - none
 2. Operational necessities
 - a) Patterns flown at 2000 ft (712 m) vs 3000 ft (914 m)
 - b) Low approaches made at 500 ft (152 m) vs 100 ft (30 m)

6. TIMES
 - A. Warmup 1.5 hr
 - B. Fine alignment 1.7 hr
 - C. Navigation 2.0 hr
 - D. Flight 40 min

7. COMMENT
 - A. Navigation time includes 1.1 hr accumulated in flight test 918A
 - B. No fine alignment or initialization of latitude and longitude before takeoff. Therefore, flight begins with errors accumulated in flight test 918A.

1. TEST OBJECTIVES:

- A. Evaluate system performance in a dynamic environment similar to a STOL terminal environment.
- B. Collect raw inertial sensor data for later analysis.

2. SYSTEM CONFIGURATION

A. Computer

- 1. Configuration - A and B identical
- 2. FDI limits
 - a) Gyro statistical static 12 meru 0.18°/hr
 - b) Gyro statistical maximum dynamic increase - meru - °/hr
 - c) Gyro TSE MASE 40 pulses² 1.14°/hr
 - d) Gyro TSE maximum dynamic increase 120 pulses² 1.98°/hr
 - e) Accelerometer 1st failure MASE 288 pulses² .28 cm/sec²
 - f) Accelerometer 2nd failure MASE 230.4 pulses² .25 cm/sec²

B. Inertial components

- 1. Gyros - all operational
- 2. Accelerometers - all operational

3. FAILURES SCHEDULED

- A. Inertial components - none
- B. Computer - none

4. FLIGHT DESCRIPTION - Took off from Crow's Landing. Made right and left 360° turns at 25° bank angles. Overflew intersection of Runways 30 and 35. Made 2 right and 2 left 360° turns at 15° bank angle. Landed at Crow's Landing. Taxied to Station L. Terminated tape.

5. DEVIATIONS FROM TEST PLAN

A. Unplanned failures

- 1. None

B. Operational necessities

- 1. Reduced number of 360° turns because of insufficient time on tape.

6. TIMES

- A. Warmup 1.5 hr B. Fine alignment 1.7 hr C. Navigation 3.0 hr
- D. Flight 41 min

7. COMMENTS

- A. Navigation time includes 2.0 hr accumulated in flight tests 918A and 918B
- B. No fine alignment or initialization of latitude and longitude before takeoff. Therefore, flight begins with errors accumulated in flight tests 918A and 918B.

1. TEST OBJECTIVES:

Evaluate navigation performance

2. SYSTEM CONFIGURATION

A. Computer

1. Configuration - A and B identical

2. FDI limits

a) Gyro statistical static	12	meru	0.18°/hr
b) Gyro statistical maximum dynamic increase	-	meru	- °/hr
c) Gyro TSE MASE	40	pulses ²	1.14°/hr
d) Gyro TSE maximum dynamic increase	120	pulses ²	1.98°/hr
e) Accelerometer 1st failure MASE	288	pulses ²	.28 cm/sec ²
f) Accelerometer 2nd failure MASE	230.4	pulses ²	.25 cm/sec ²

B. Inertial components

1. Gyros - all operational

2. Accelerometers - all operational

3. FAILURES SCHEDULED

A. Inertial components - none

B. Computer - none

4. FLIGHT DESCRIPTION

Fine alignment at Station L. Took off from Crow's Landing. Overflew Lick Observatory, San Jose. Landed at Moffett. Taxied to near Station A. Terminated program.

5. DEVIATIONS FROM TEST PLAN

A. Unplanned failures

1. E&F gyro failure during fine alignment

2. Coolant high temperature alarm. Cabin temperature 90° F

3. E accelerometer failure during flight, then off

B. Procedural changes

1. Operator errors - none

2. Operational necessities. Entered navigation mode with E and F gyro failures because of insufficient time for recertification.

6. TIMES

A. Warmup 6.5 hr B. Fine alignment 37 min C. Navigation 26 min

D. Flight 18 min

7. COMMENTS

A. E & F gyro failure believed caused by high cabin temperature.

B. E accelerometer failure believed caused by high cabin temperature.

1. TEST OBJECTIVES:

Evaluate long term navigation performance

2. SYSTEM CONFIGURATION

A. Computer

1. Configuration - A and B identical

2. FDI limits

a) Gyro statistical static	12	meru	0.18°/hr
b) Gyro statistical maximum dynamic increase	-	meru	- °/hr
c) Gyro TSE MASE	40	pulses ²	1.14°/hr
d) Gyro TSE maximum dynamic increase	120	pulses ²	1.98°/hr
e) Accelerometer 1st failure MASE	288	pulses ²	.28 cm/sec ²
f) Accelerometer 2nd failure MASE	230.4	pulses ²	.25 cm/sec ²

B. Inertial components

1. Gyros - all operational

2. Accelerometers - all operational

3. FAILURES SCHEDULED

A. Inertial components - none

B. Computer - none

4. FLIGHT DESCRIPTION

Took off from Moffett. Overflow Lick Observatory, Crow's Landing, Stockton, Sacramento, Stockton, Crow's Landing, Modesto, Castle, Fresno, Visalia, Bakersfield, Visalia, Fresno, Castle, Modesto, Crow's Landing, Lick Observatory. Landed at Moffett. Taxied to Station A. Navigated 3 min. Terminated program.

5. DEVIATIONS FROM TEST PLAN

A. Unplanned failures

1. Scaler #1 intermittent failure

2. Intermittent local keyboard failure. Used remote keyboard.

B. Procedural changes

1. Operator errors - none

2. Operational necessities - none

6. TIMES

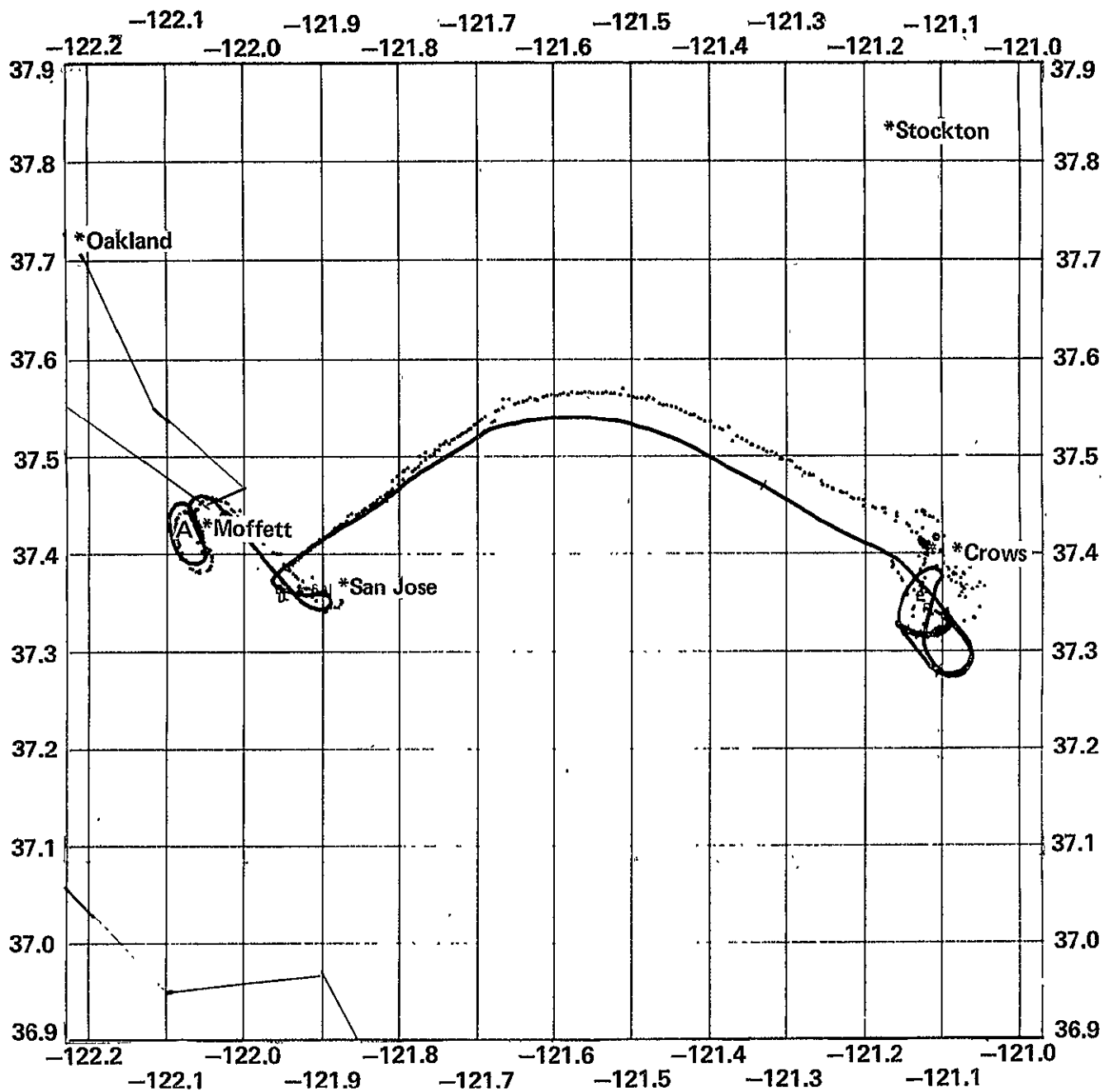
A. Warmup 3.1 hr B. Fine alignment 47 min C. Navigation 4.4 hr

D. Flight 4.0 hr

7. COMMENTS

A. Ran aided calibration prior to flight in hangar. Wrote new flight tape.

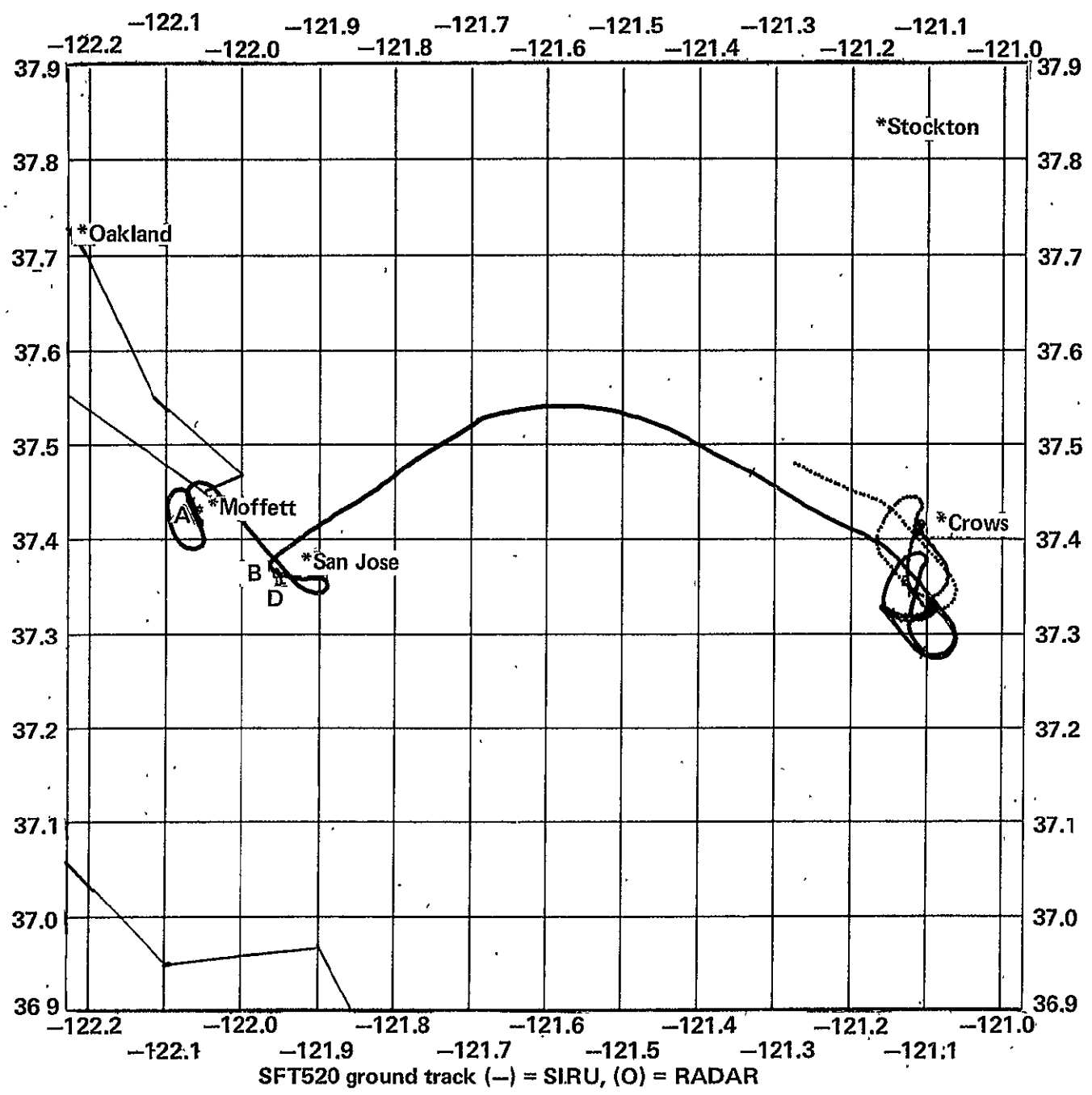
B. Lost power while moving from hangar to Station A. Ran on battery.



54

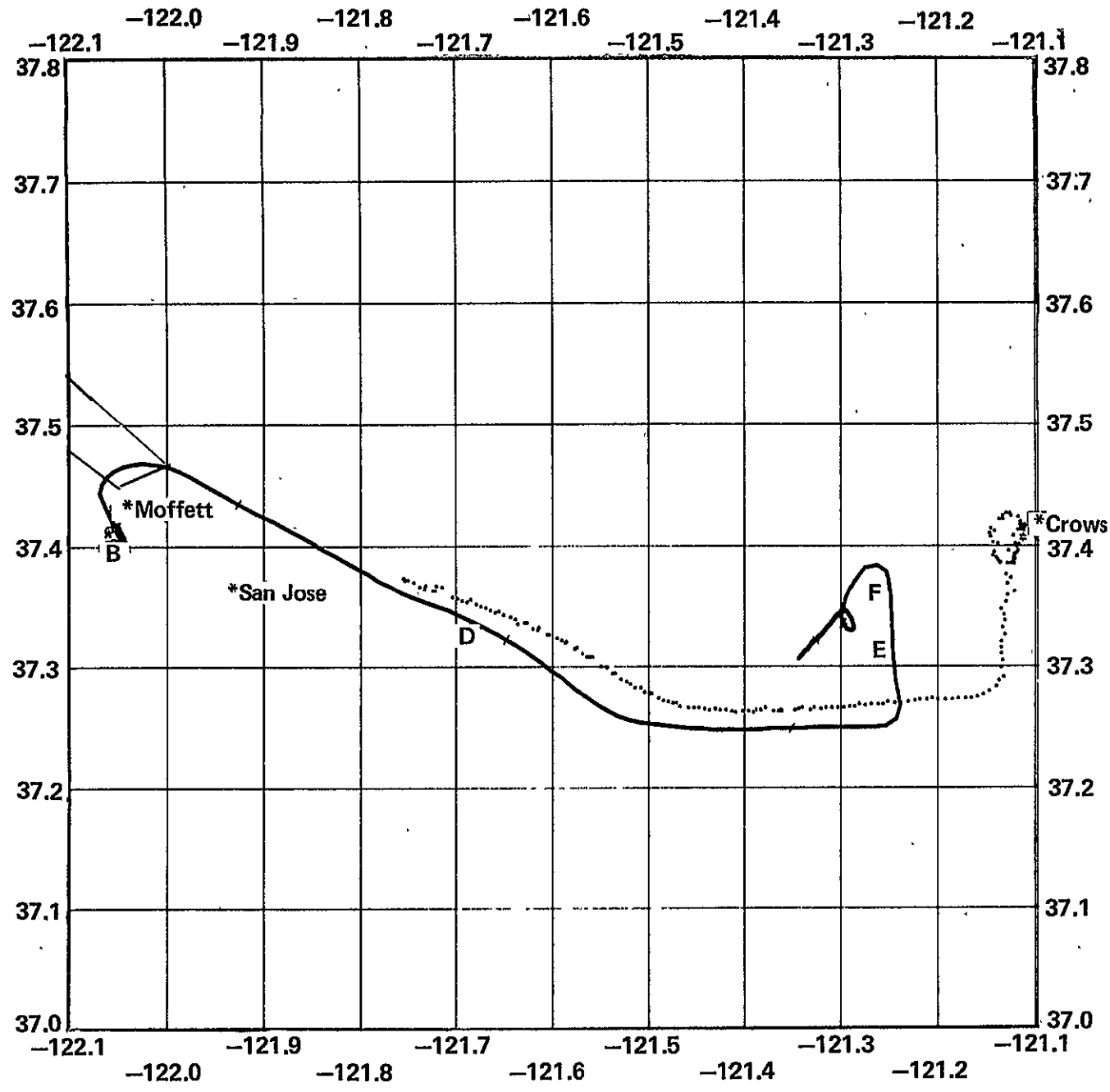
SFT520 ground track (-) = SIRU, (O) = DME
Figure A.1 SFT520 SIRU/DME ground track

55

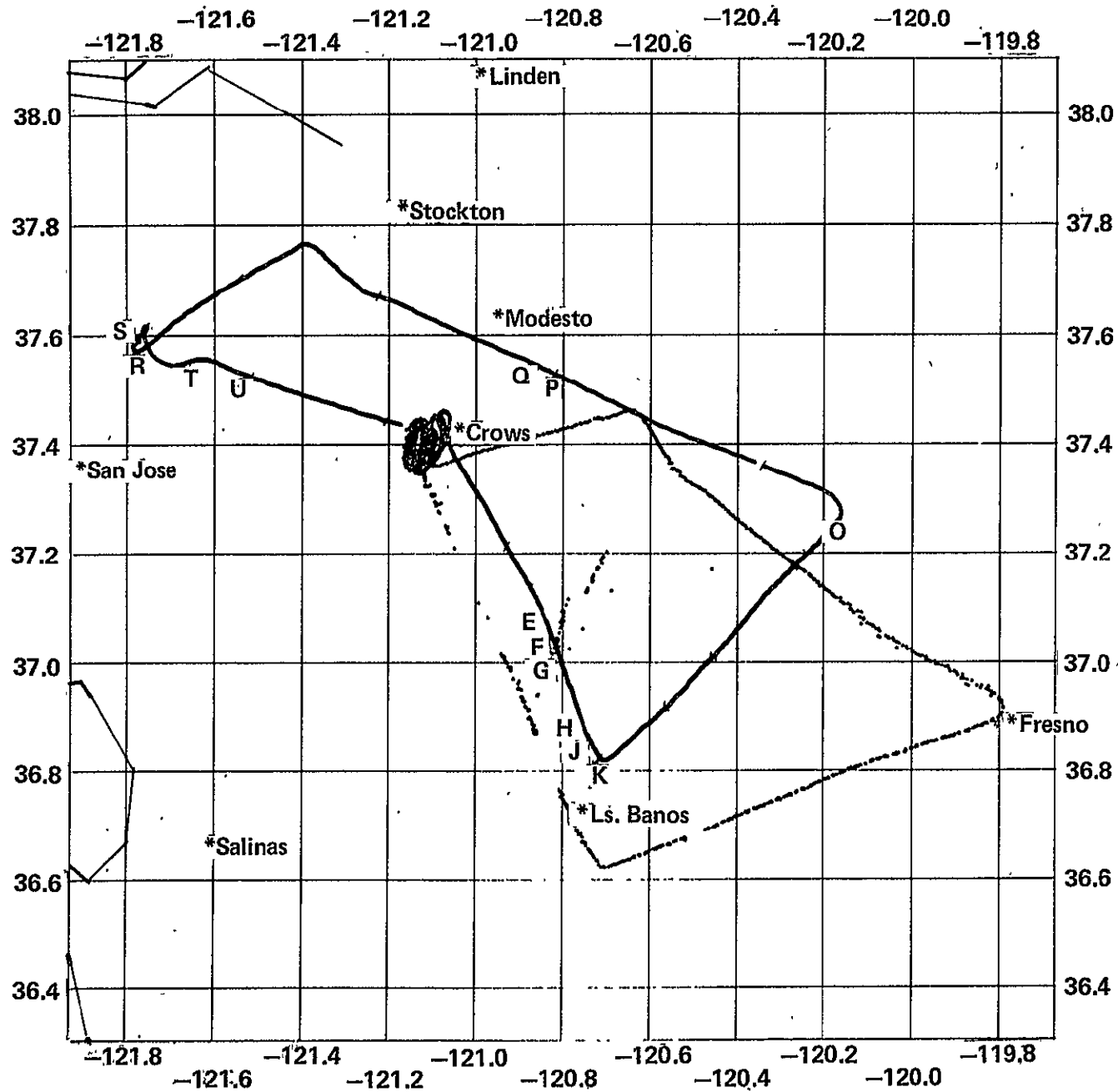


SFT520 ground track (-) = SIRU, (O) = RADAR

Figure A.2 SFT520 SIRU/radar ground track



SFT530A ground track (-) = SIRU, (O) = DME
Figure A.3 SFT530A SIRU/DME ground track

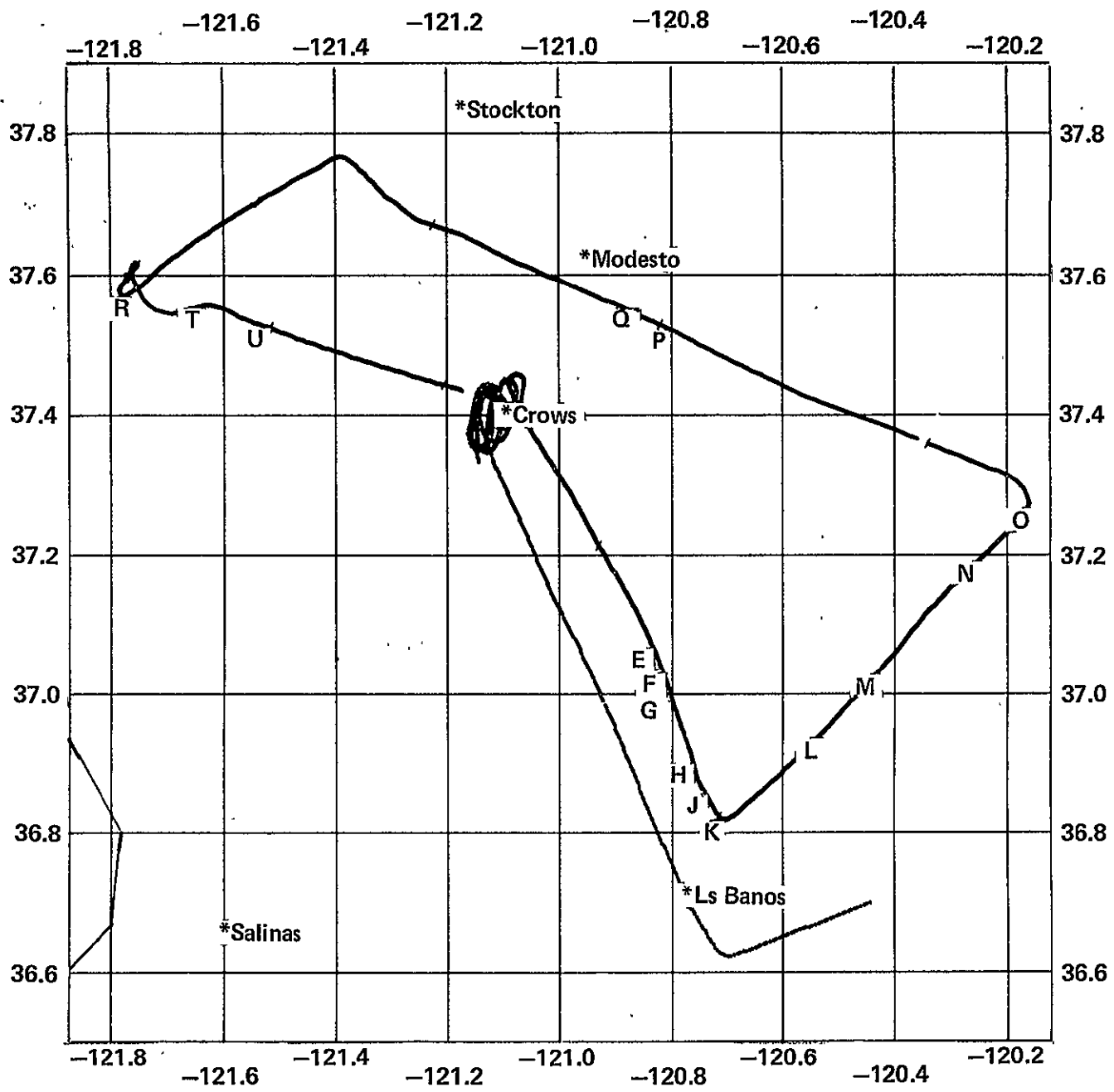


57

SFT530B ground track (-) = SIRU, (O) = DME

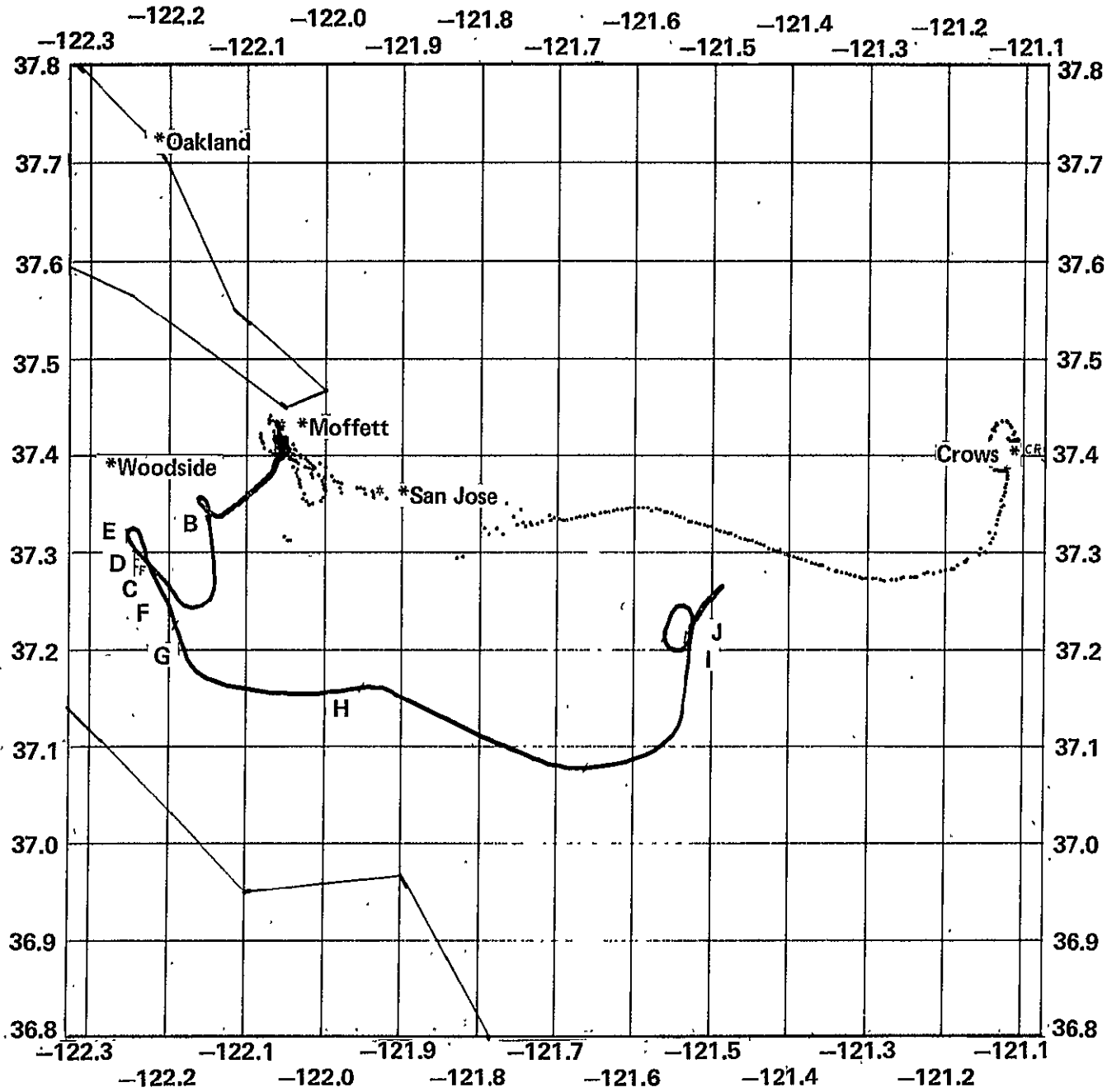
Figure A.4 SFT530B SIRU/DME ground track

58



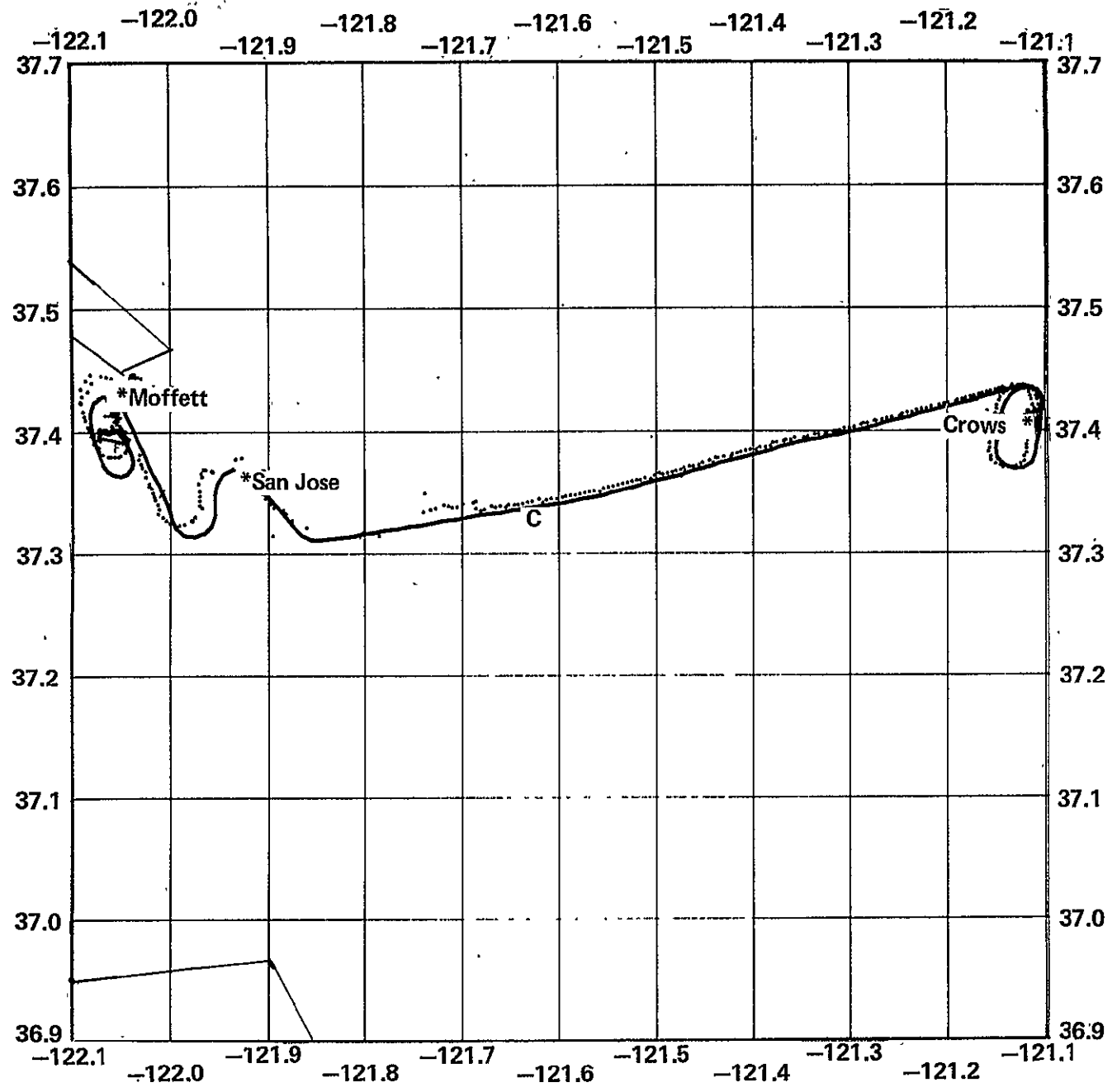
SFT530B ground track (—) = SIRU, (---) = RADAR

Figure A.5 SFT530B SIRU/radar ground track



SFT616A ground track (-) = SIRU, (O) = DME

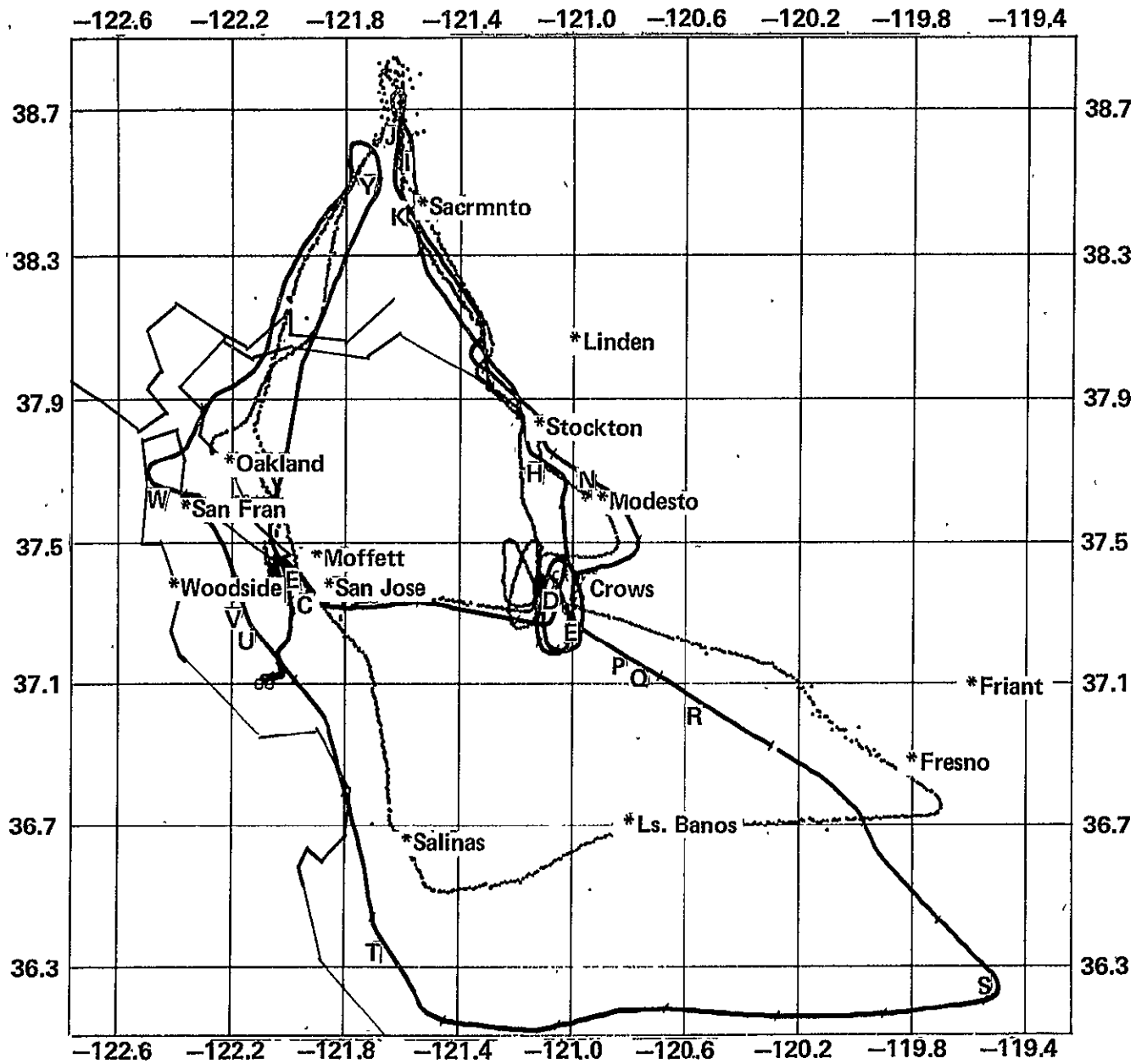
Figure A.6 SFT616A SIRU/DME around track



60

SFT616B ground track (-) = SIRU, (O) = DME
Figure A.7 SFT616B SIRU/DME ground track

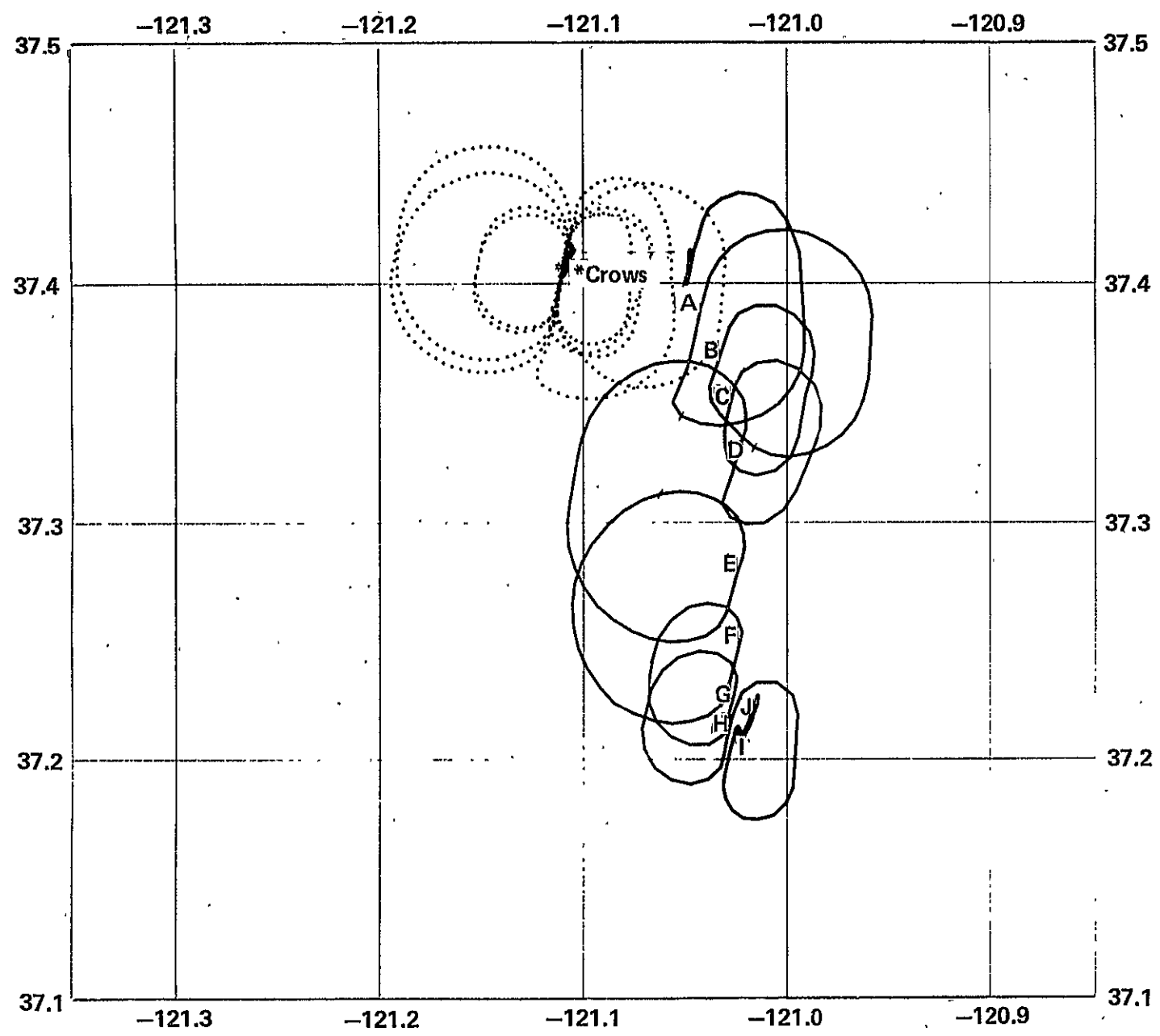
T9



SFT618 ground track (-) = SIRU, (O) = DME

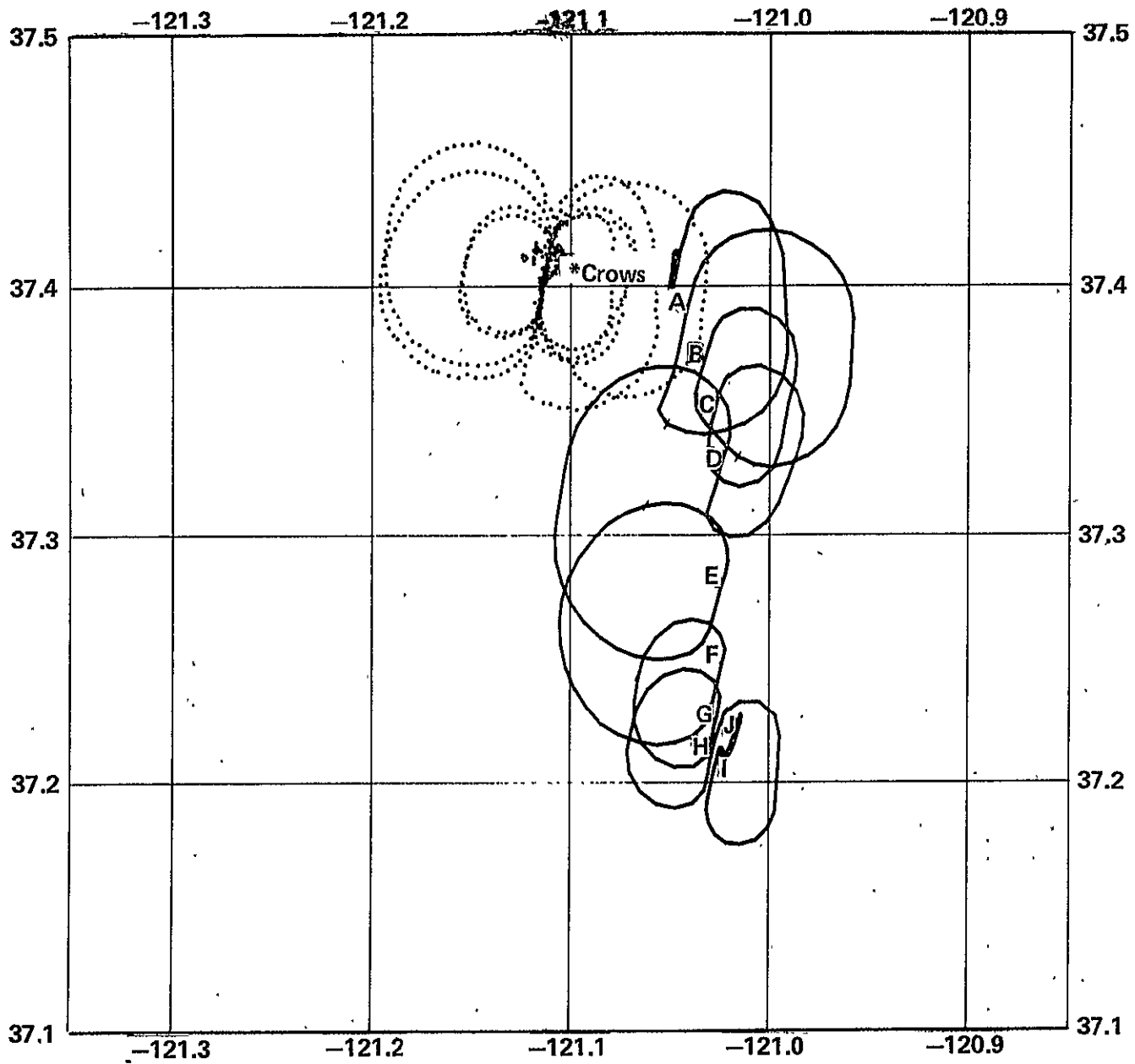
Figure A.8 SFT618 SIRU/DME ground track

62



SFT625 ground track (-) = SIRU, (O) = DME

Figure A.9 SFT625 SIRU/DME ground track

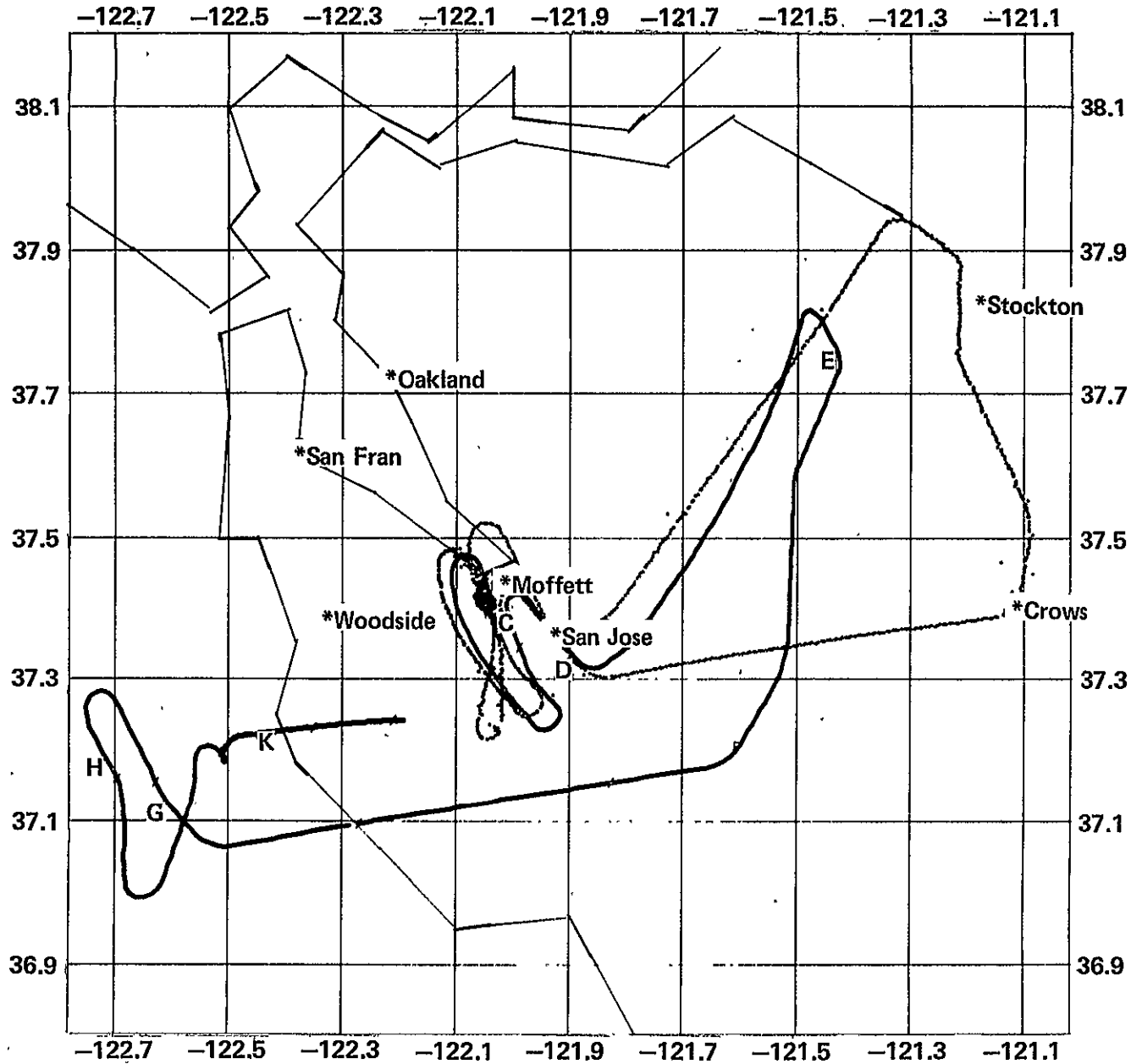


63

SFT625 ground track (-) = SIRU, (O) = RADAR

Figure A.10 SFT625 SIRU/radar ground track

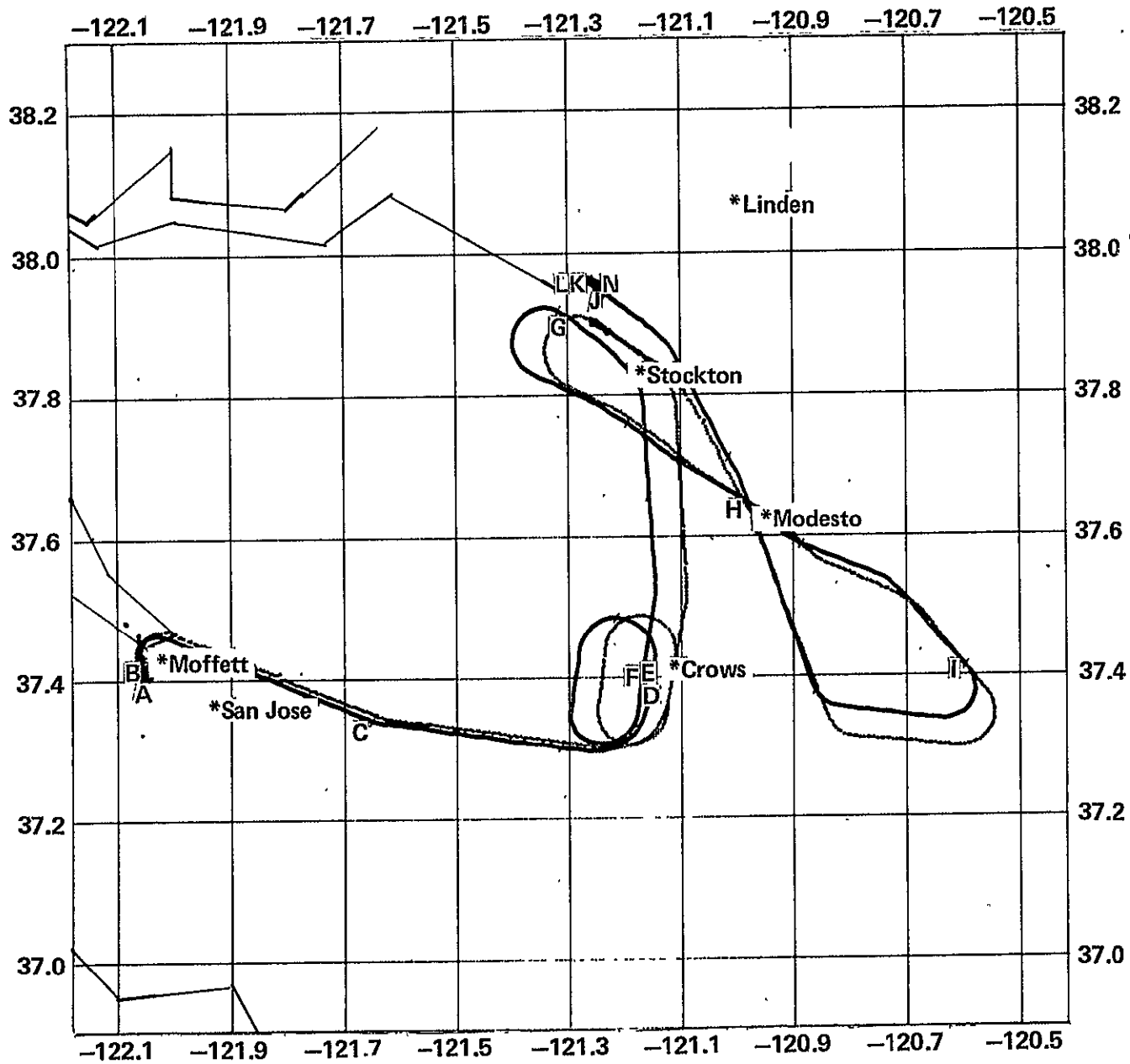
64



SFT714 ground track (-) = SIRU, (O) = DME

Figure A.11 SFT714 SIRU/DME ground track

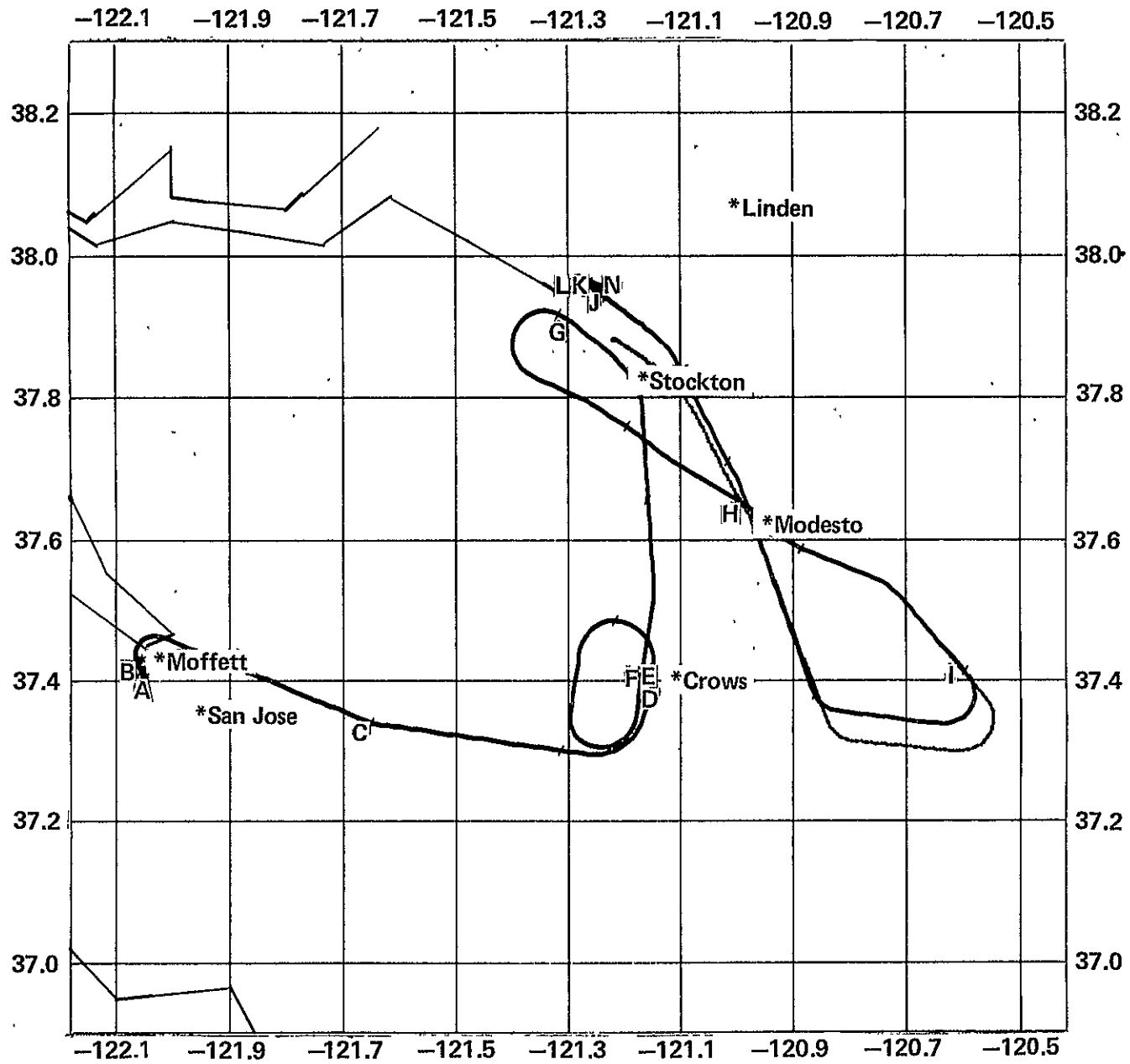
65



SFT717A ground track (-) = SIRU, (O) = DME

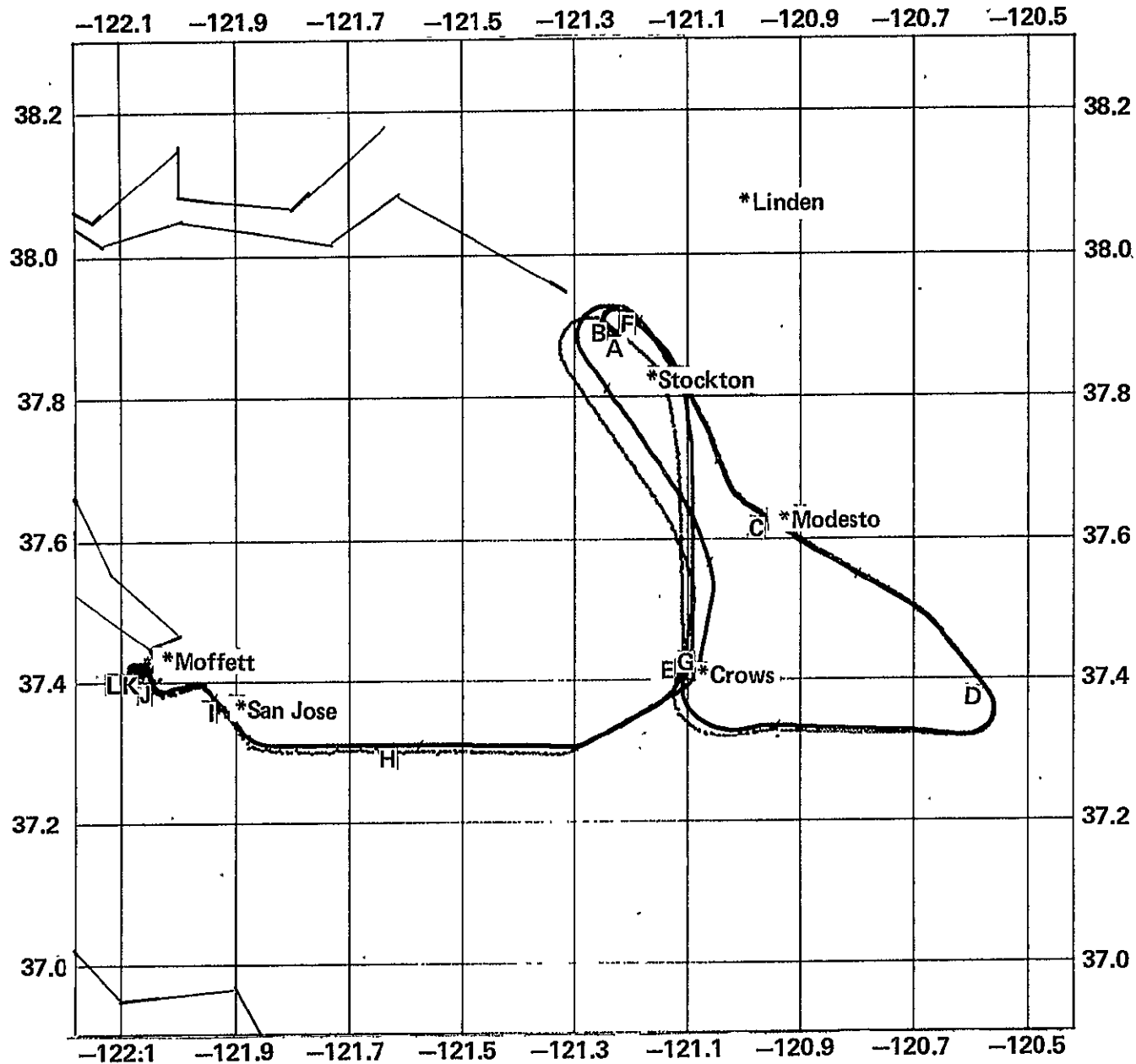
Figure A.12 SFT717A SIRU/DME ground track

99



SFT717A ground track (-) = SIRU, (O) = RADAR

Figure A.13 SIRU/radar ground track

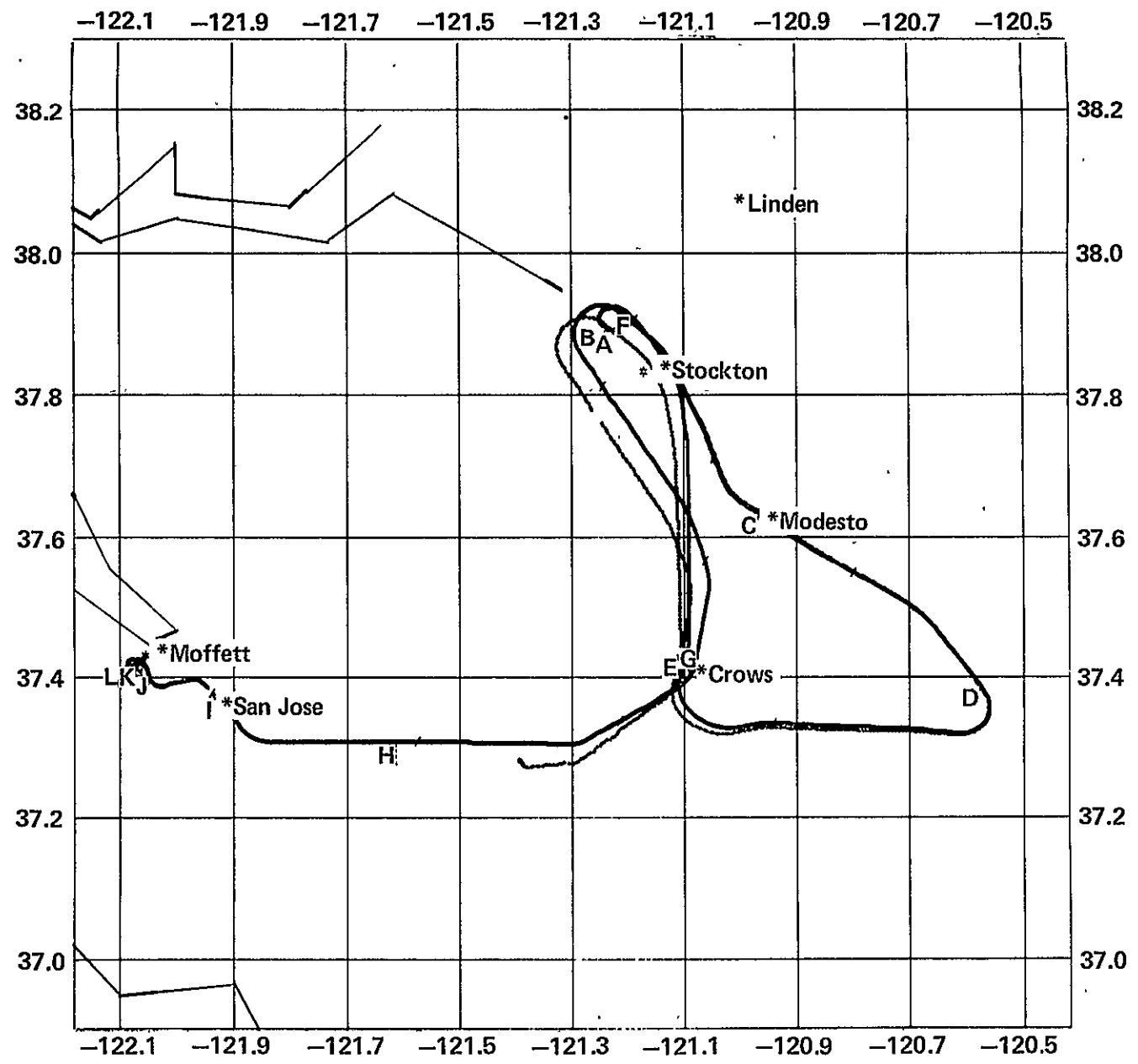


67

SFT717B ground track (—) = SIRU, (O) = DME

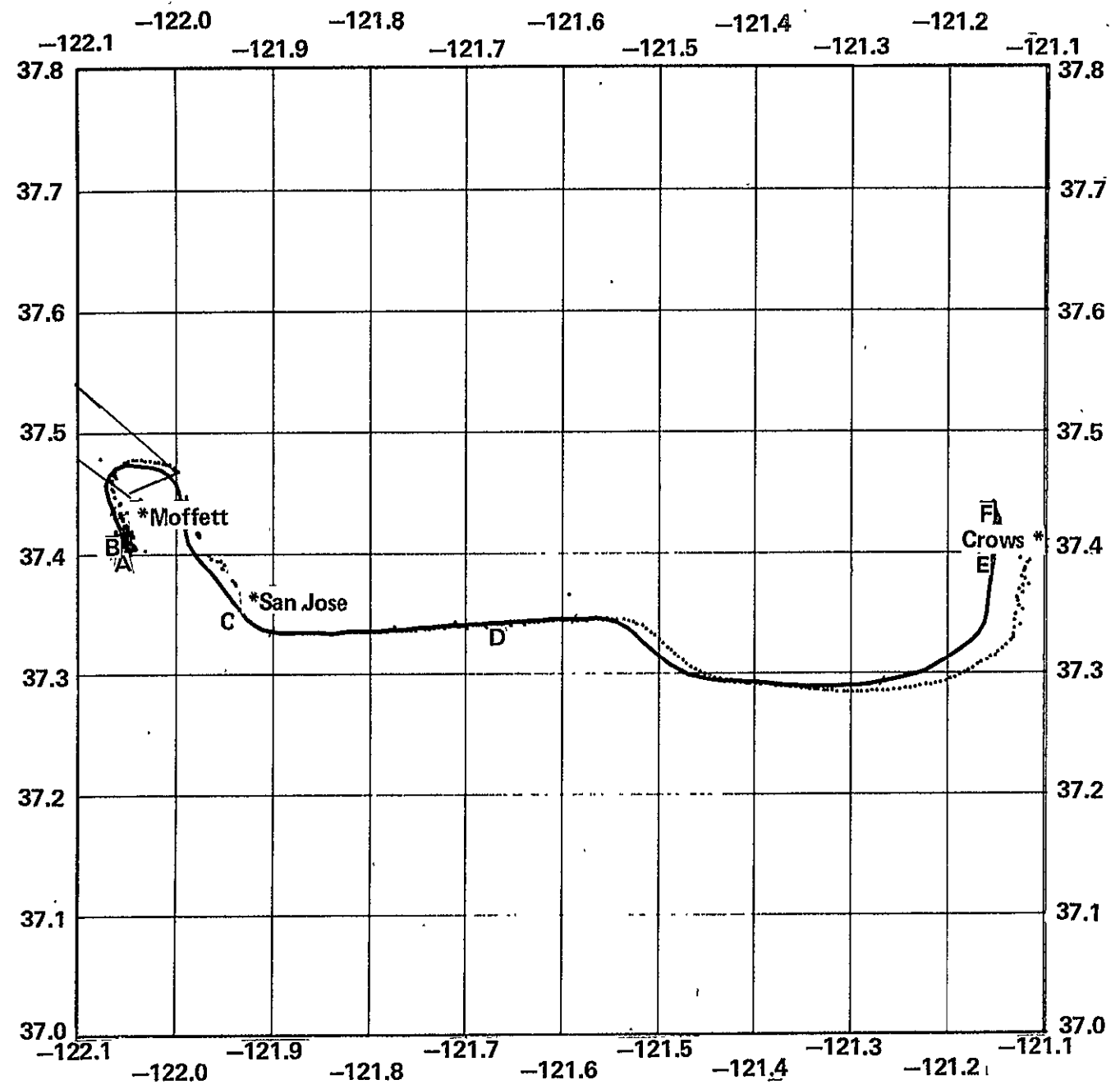
Figure A.14 SFT717B SIRU/DME ground track

89



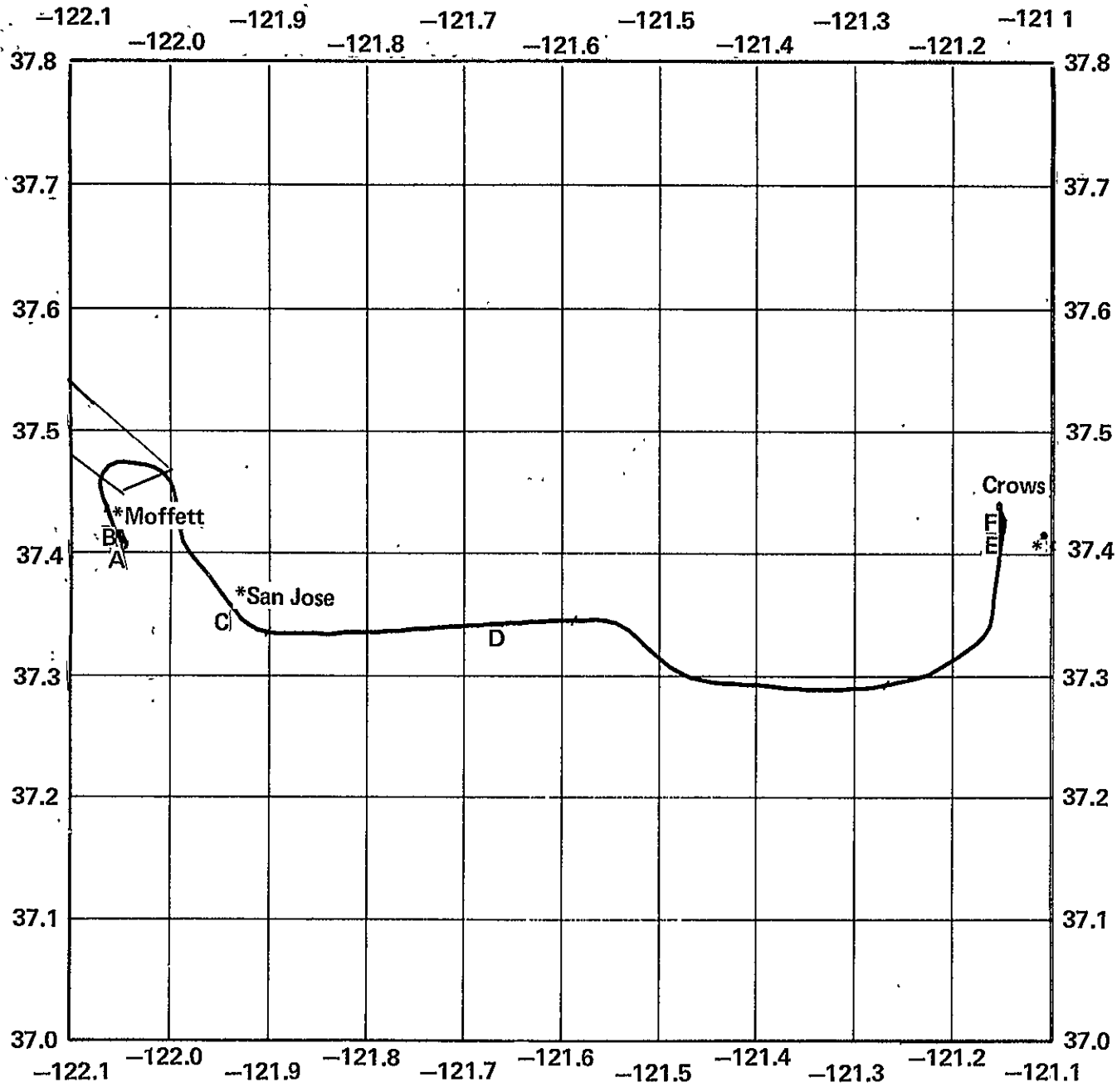
SFT717B ground track (-) = SIRU, (O) = RADAR

Figure A.15 SFT717B SIRU/radar ground track



SFT724A ground track (-) = SIRU, (O) = DME
Figure A.16 SFT724A SIRU/DME ground track

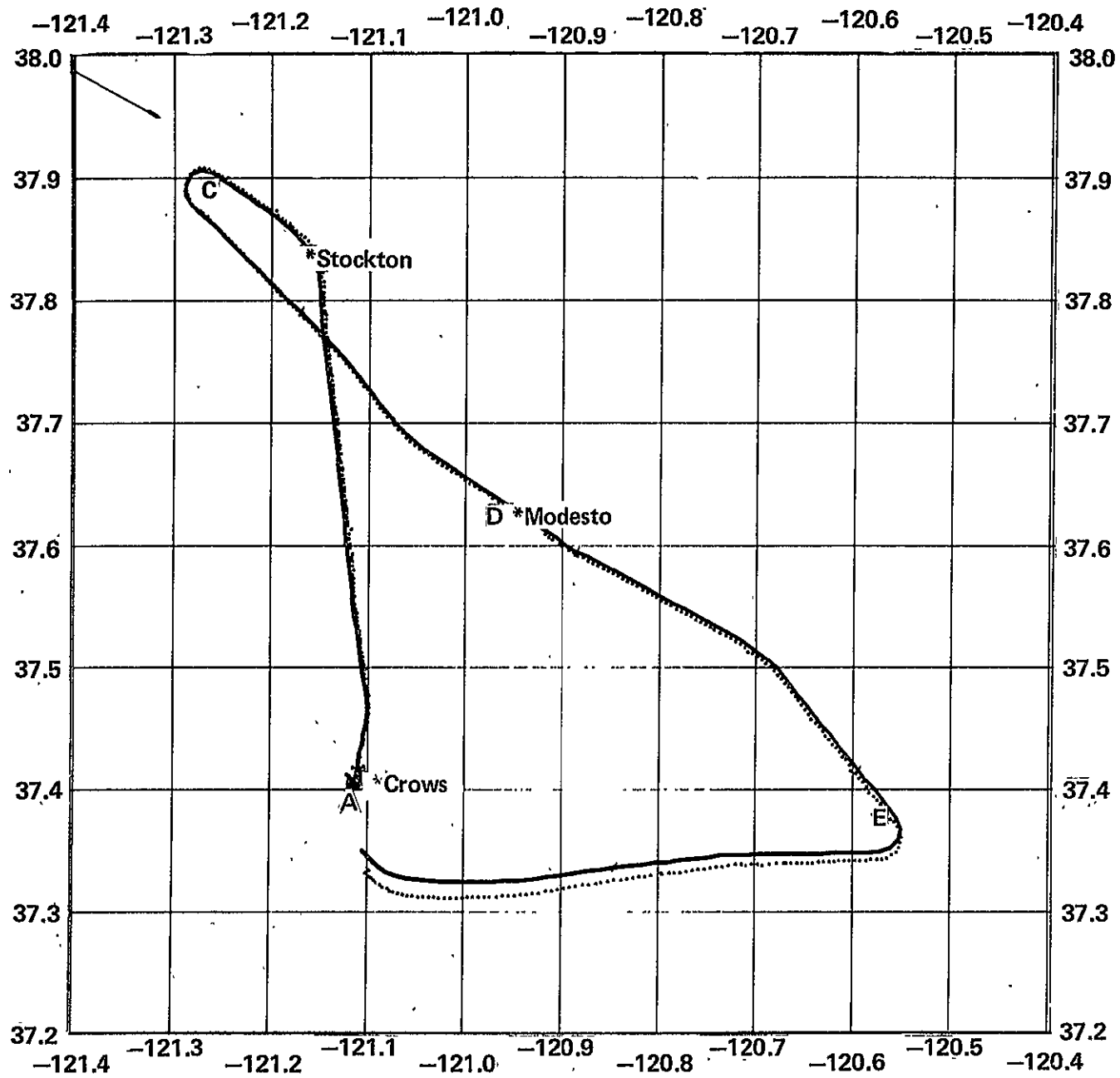
70



SFT724A ground track (-) = SIRU, (O) = RADAR

Figure A.17 SFT724A SIRU/radar ground track

71



SFT724B ground track (-) = SIRU, (O) = DME

Figure A.18 SFT724B SIRU/DME ground track

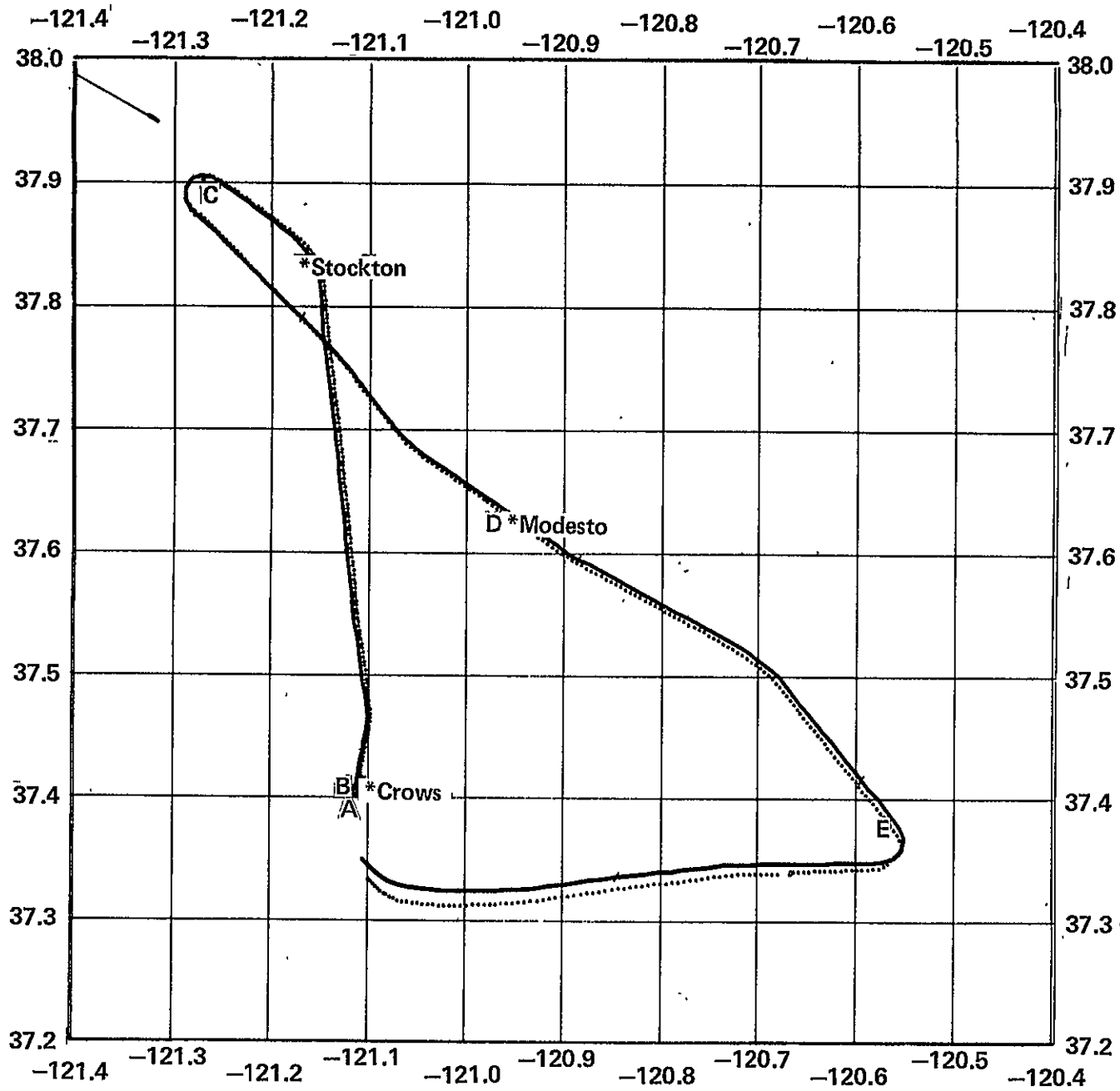
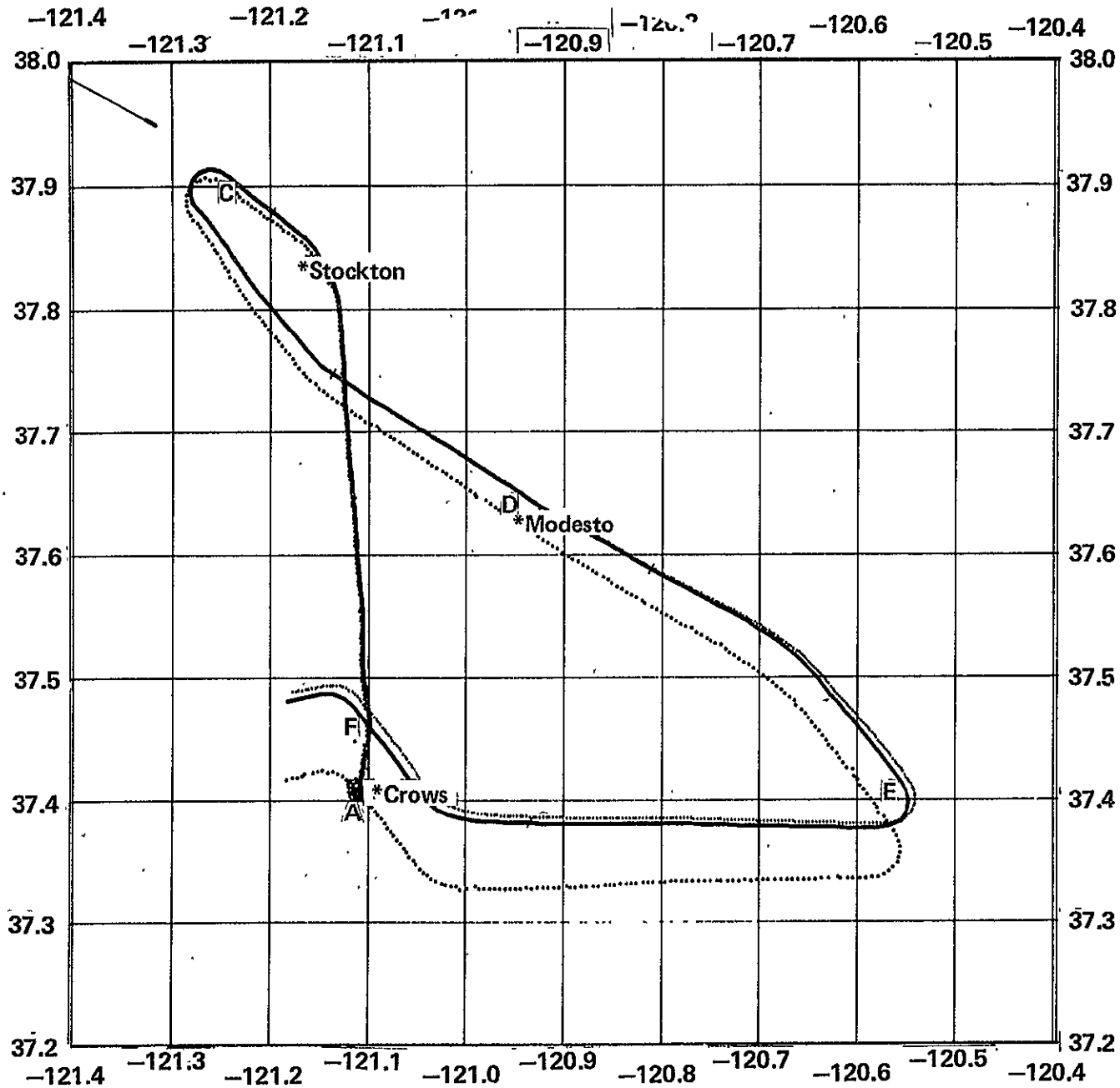


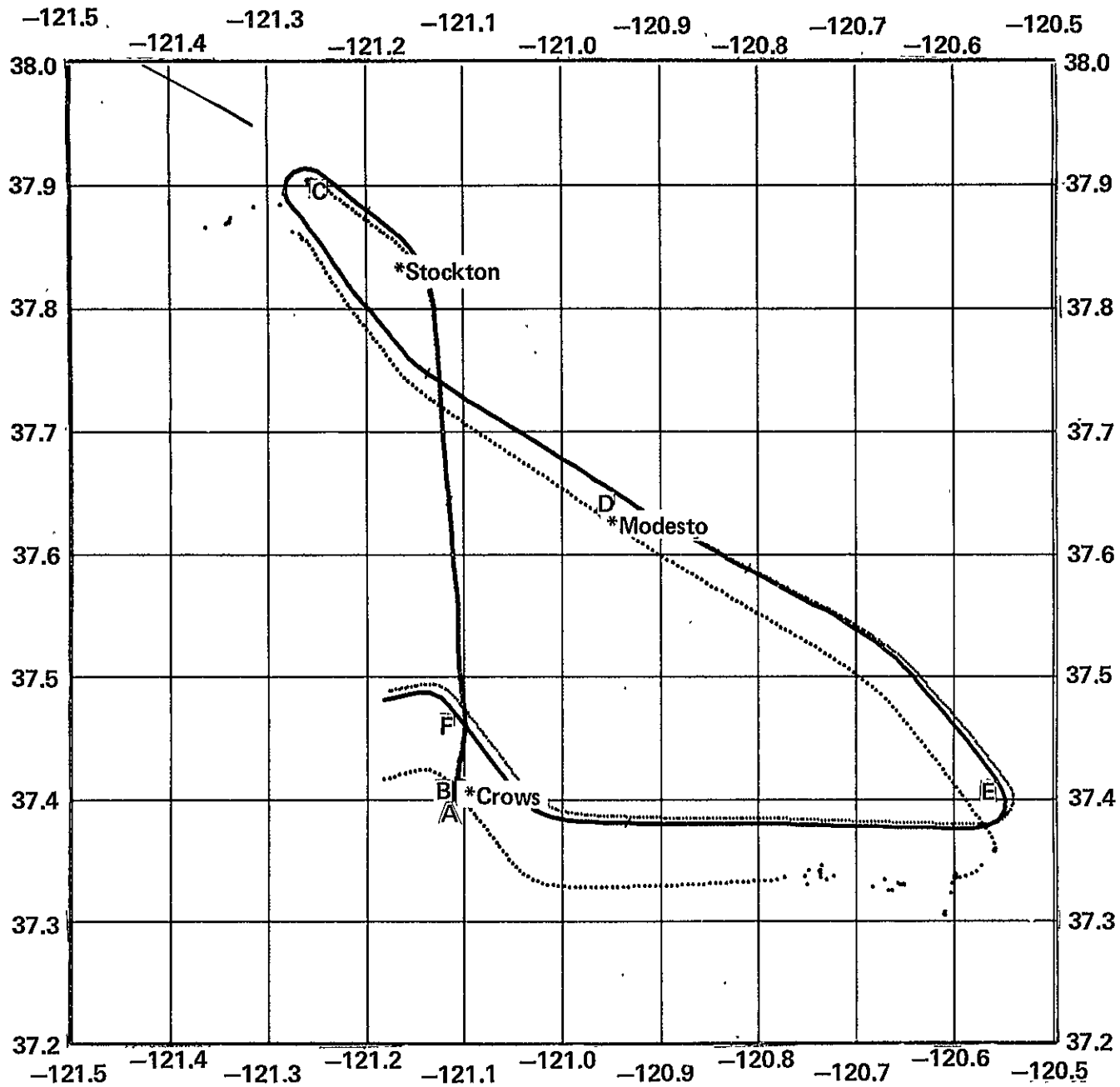
Figure A.19 SFT724B SIRU/radar ground track

72



73

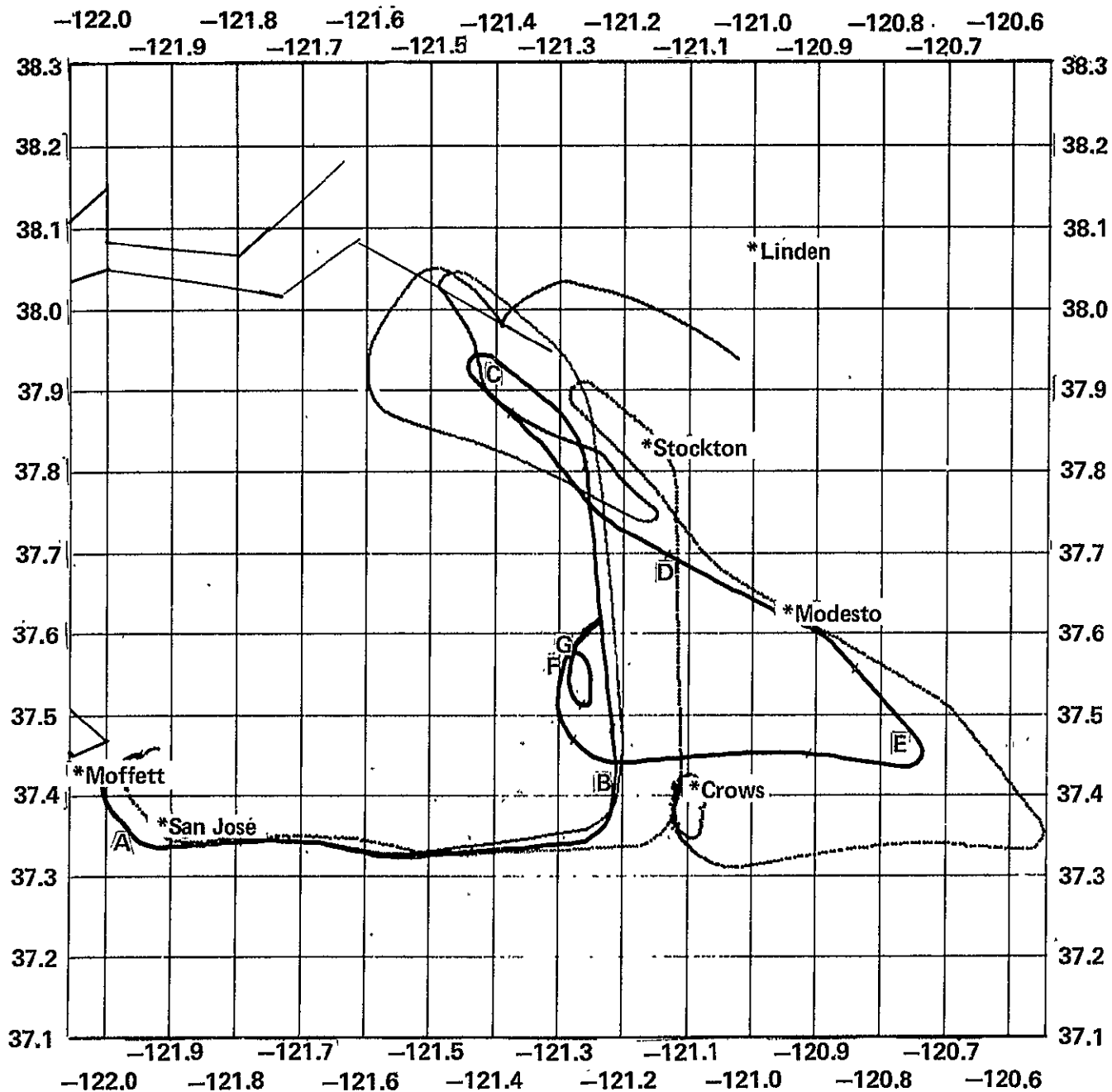
SFT724C track (-) = SIRUA, (.) = SIRUB, (O) = DME
Figure A.20 SFT724C SIRU A/SIRU B/DME ground tracks



74

SFT724C track (—, -) = SIRU A, B (O) = RADAR

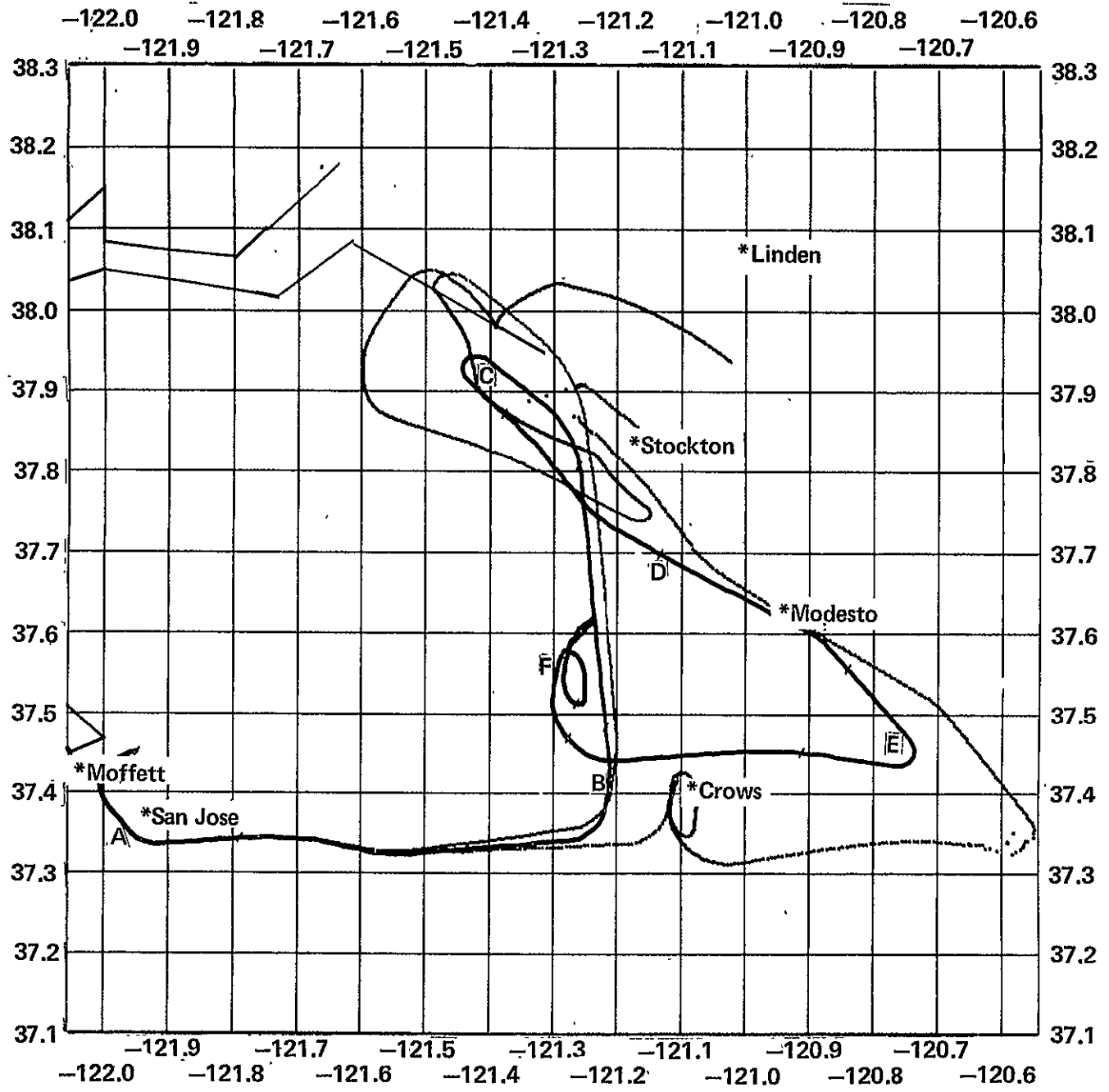
Figure A.21 SFT724C SIRU A/SIRU B/radar ground tracks



75

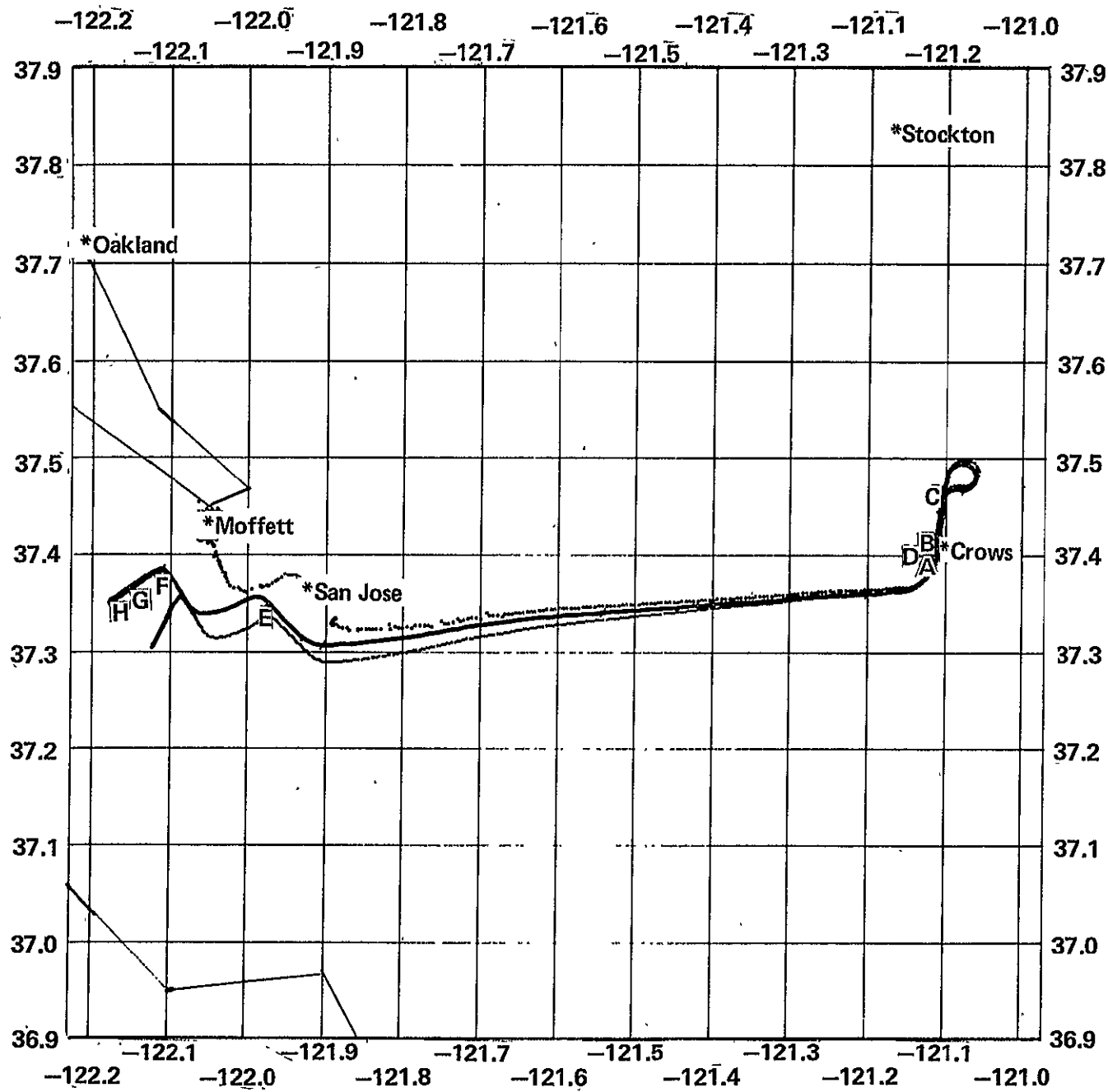
SFT729A track (-) = SIRUA, (.) = SIRUB, (O) = DME
 Figure A.22 SFT729A SIRU A/SIRU B/DME ground tracks

76



SFT729A track (-,.) = SIRUA, B (O) = RADAR
 Figure A.23 SFT729A SIRU A/SIRU B/radar ground tracks

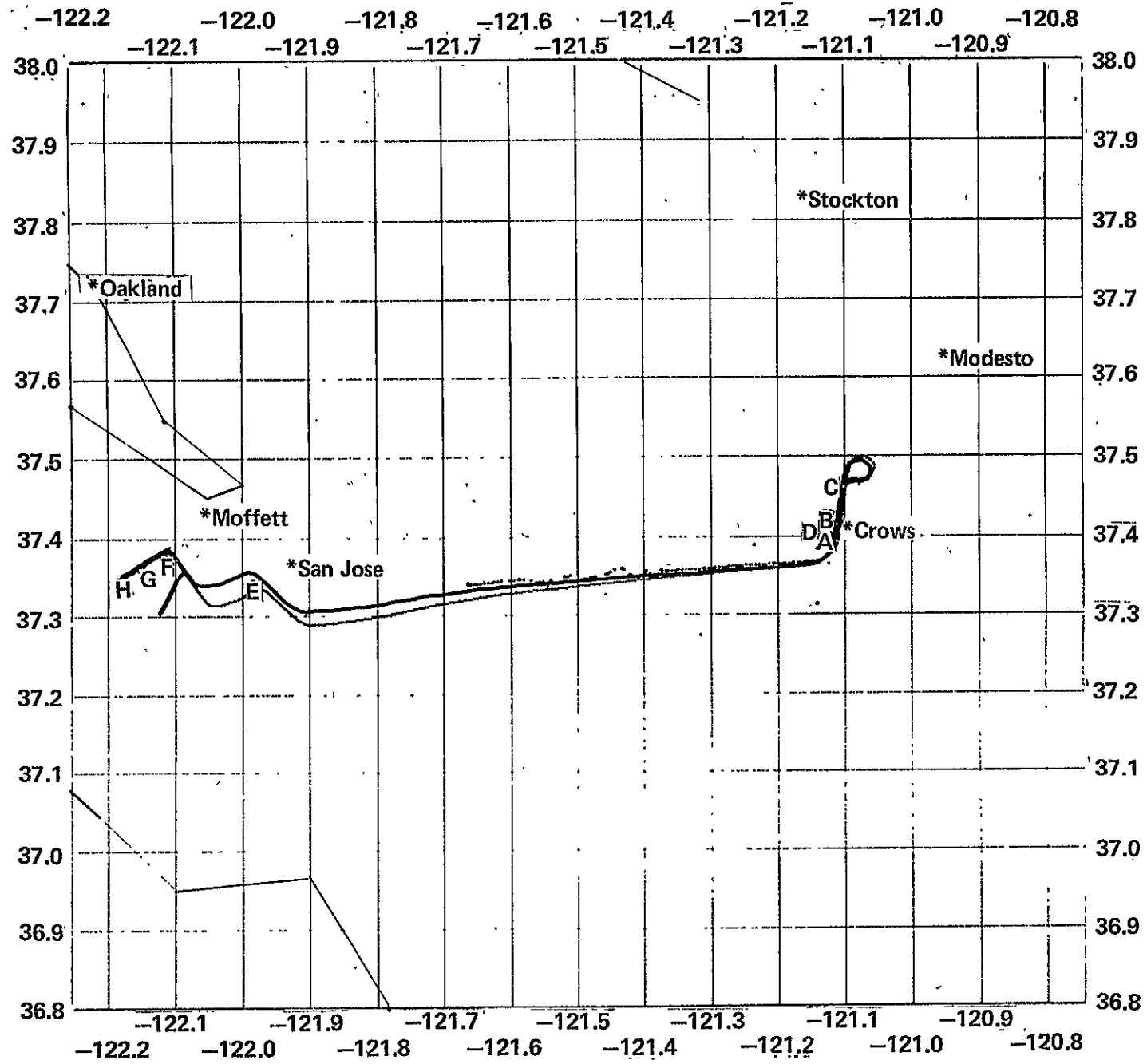
77



SFT729B track (—) = SIRUA, (.) = SIRUB, (O) = DME

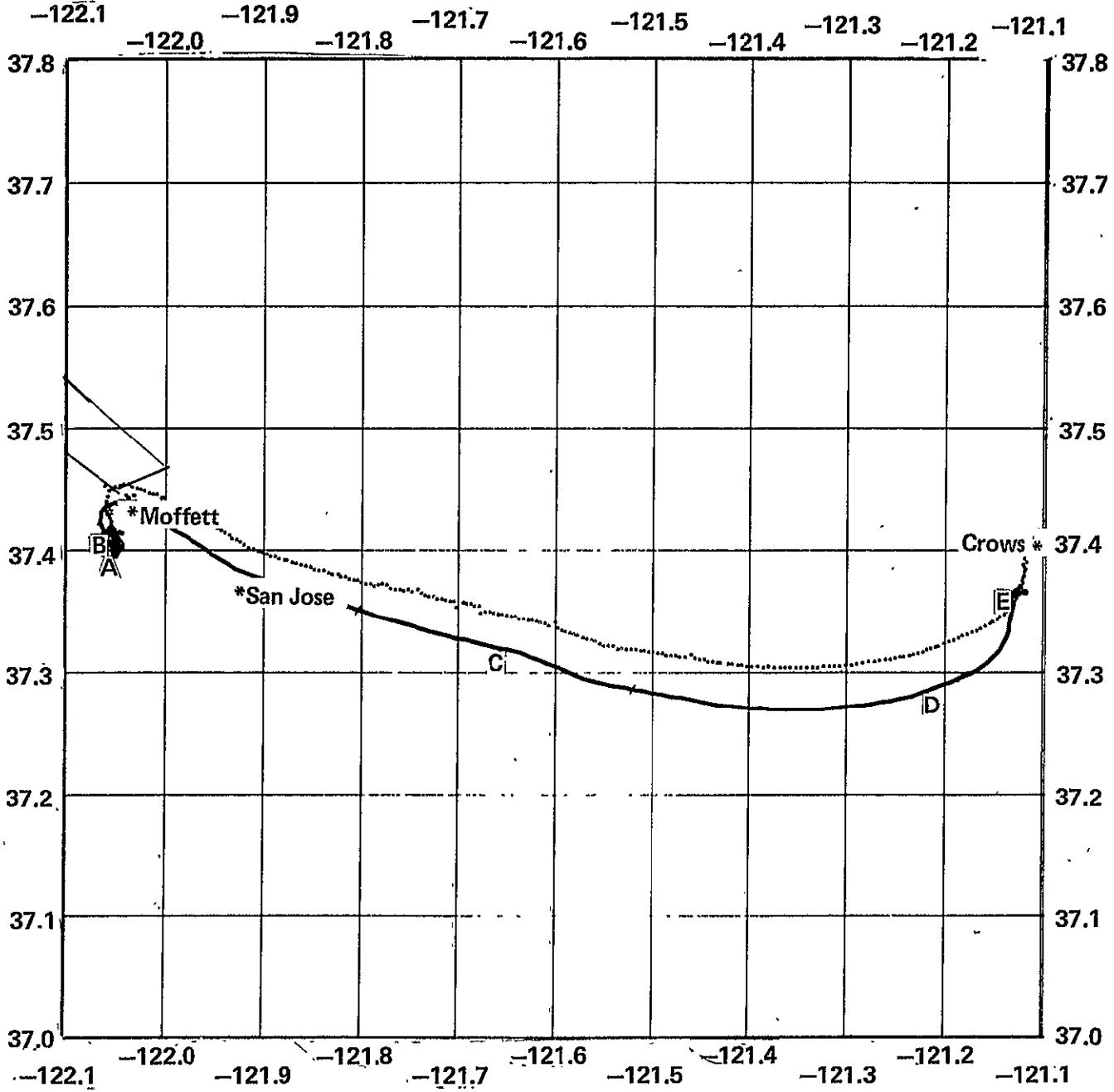
Figure A.24 SFT729B SIRU A/SIRU B/DME ground tracks

78



SFT729B track (-) = SIRUA, B (0) = RADAR
 Figure A.25 SFT729B SIRU A/SIRU B/radar ground tracks

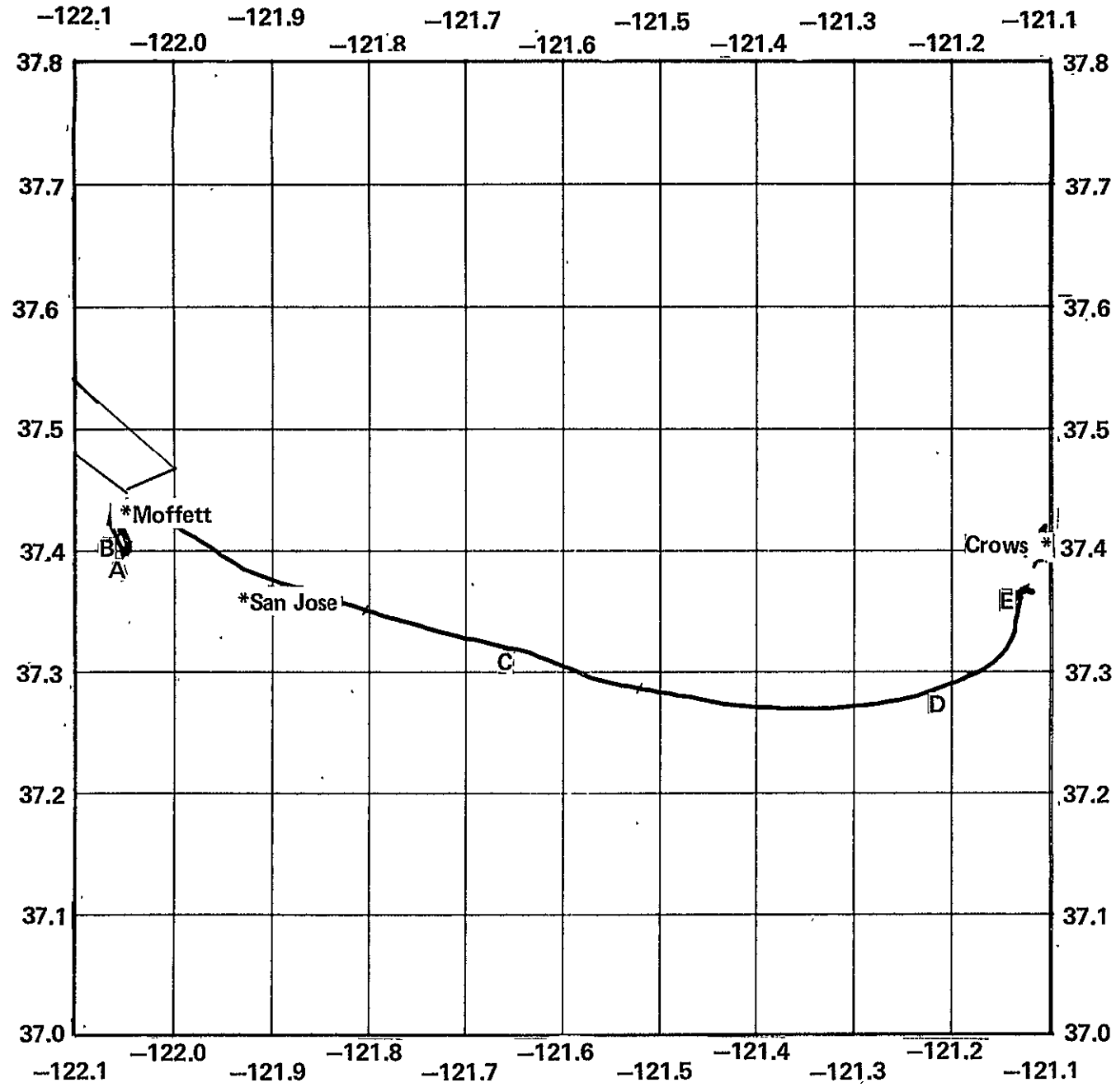
79



SFT822A ground track (-) = SIRU, (O) = DME

Figure A.26 SFT822A SIRU/DME ground tracks

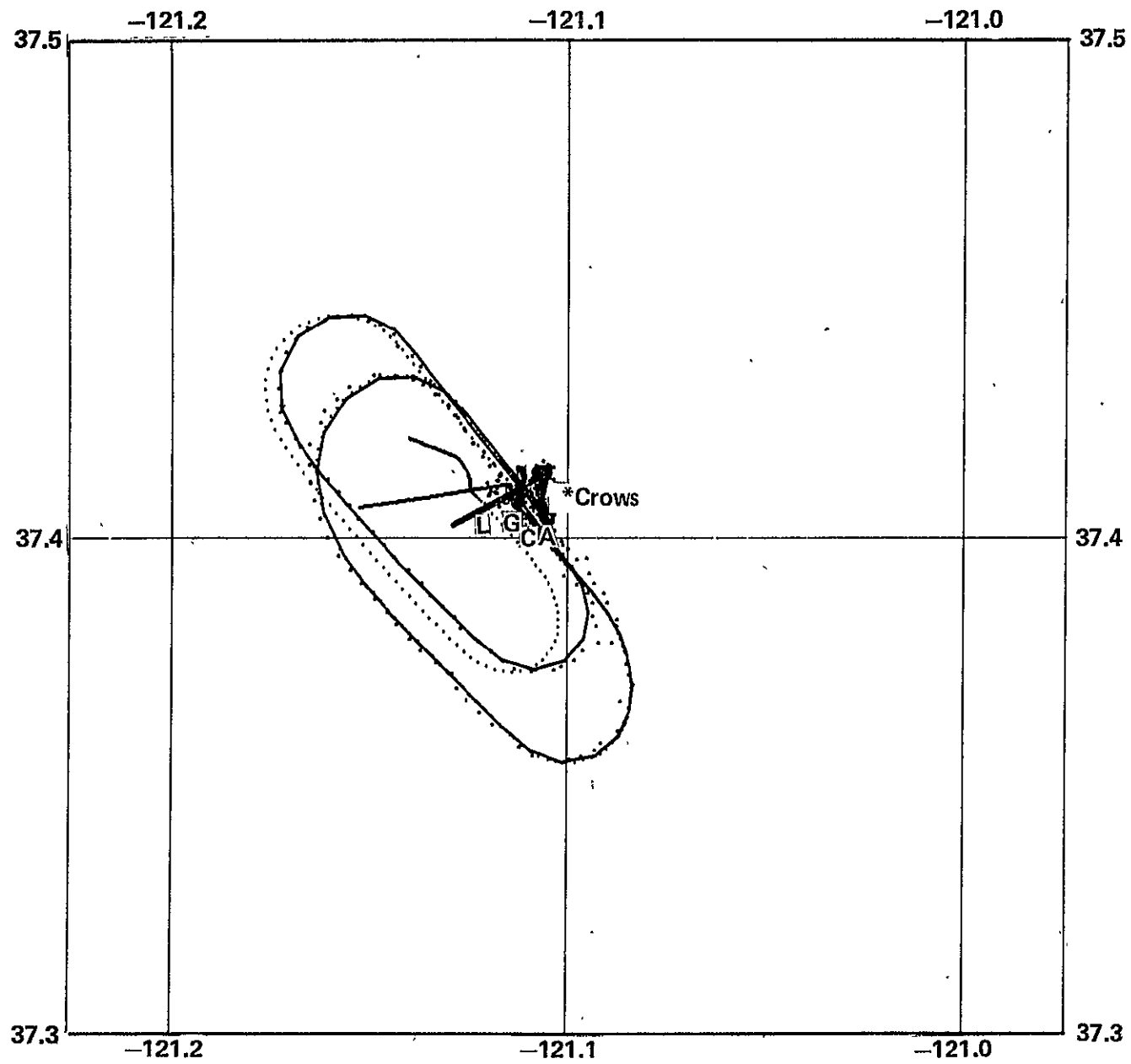
08



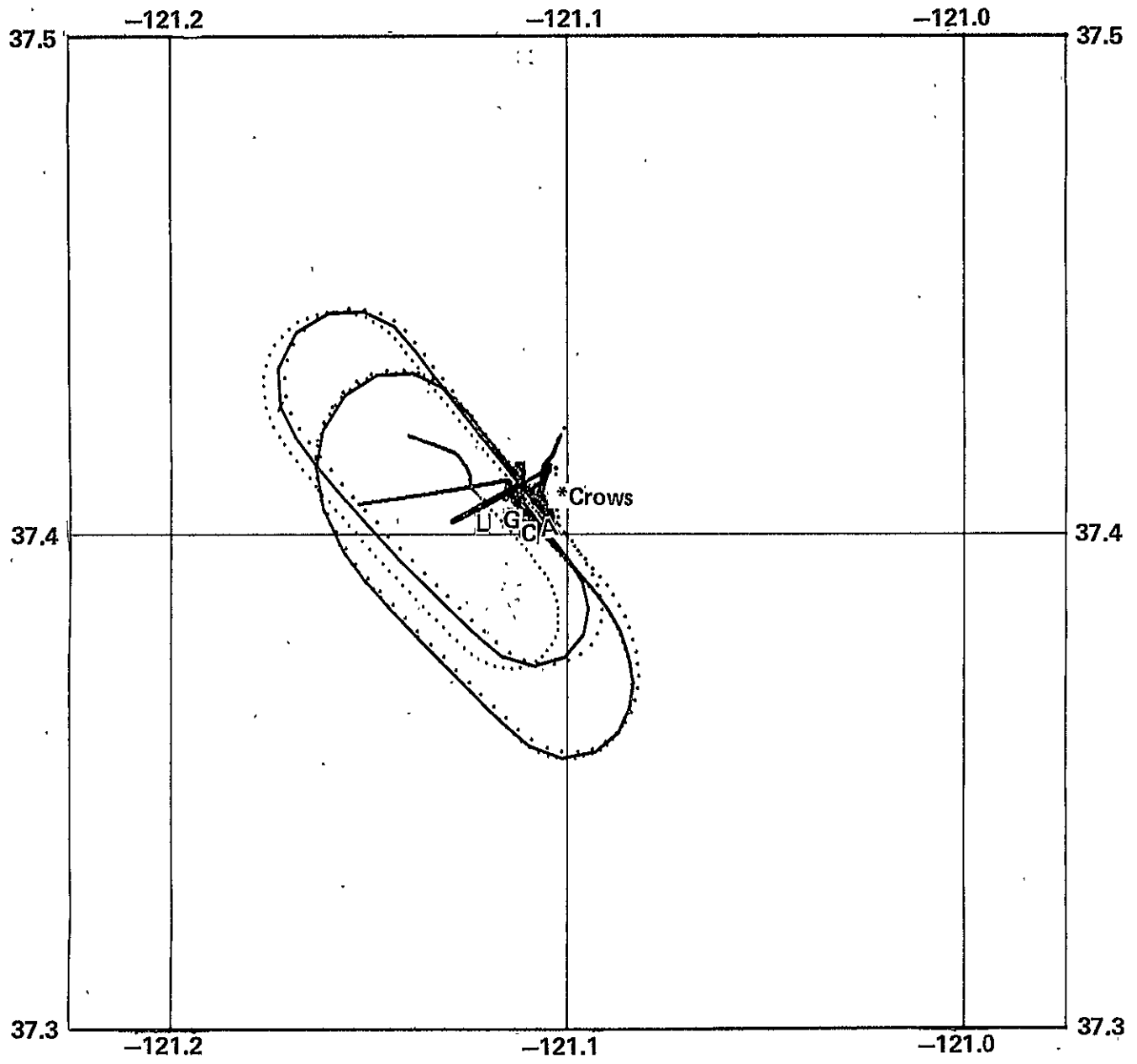
SFT822A ground track (-) = SIRU, (O) = DME

Figure A.27 SFT822A SIRU/radar ground tracks

81



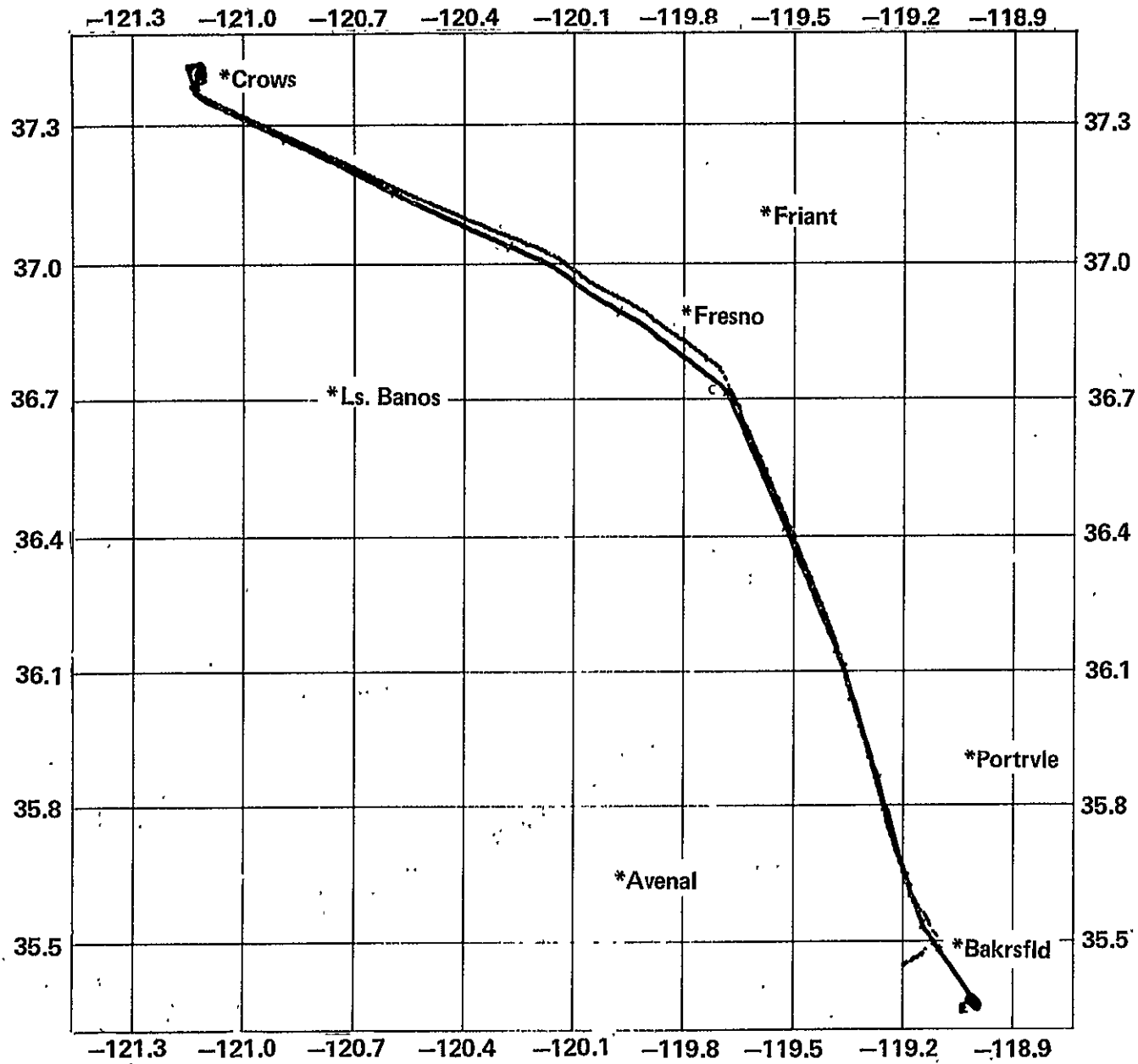
SFT822B track (-) = SIRUA, (.) = SIRUB, (O) = DME
Figure A.28 SFT822B SIRU A/SIRU B/DME ground tracks



82

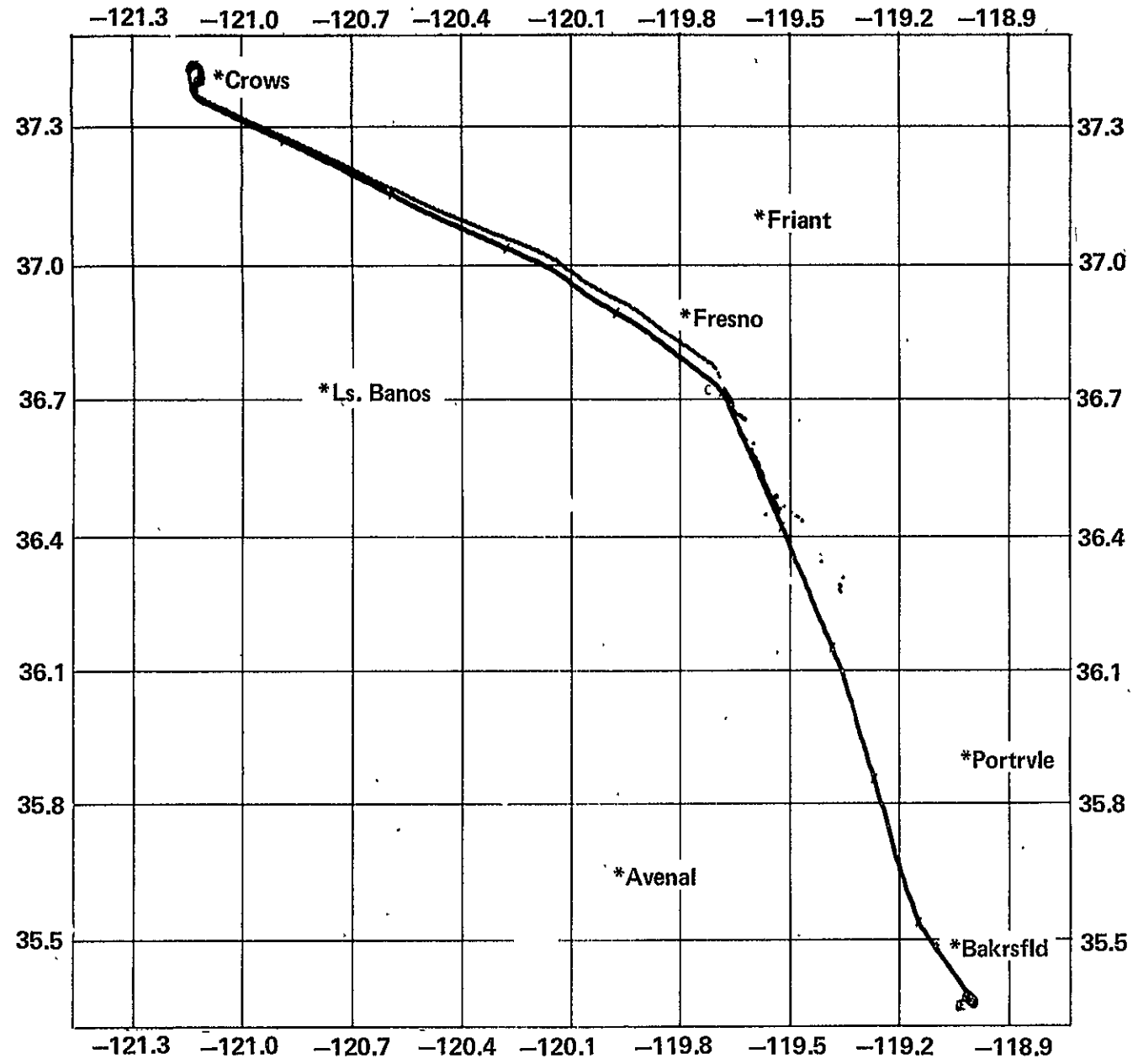
SFT822B track (-.-) = SIRUA, B (O) = RADAR

Figure A.29 SFT822B SIRU A/SIRU B/radar ground tracks



83

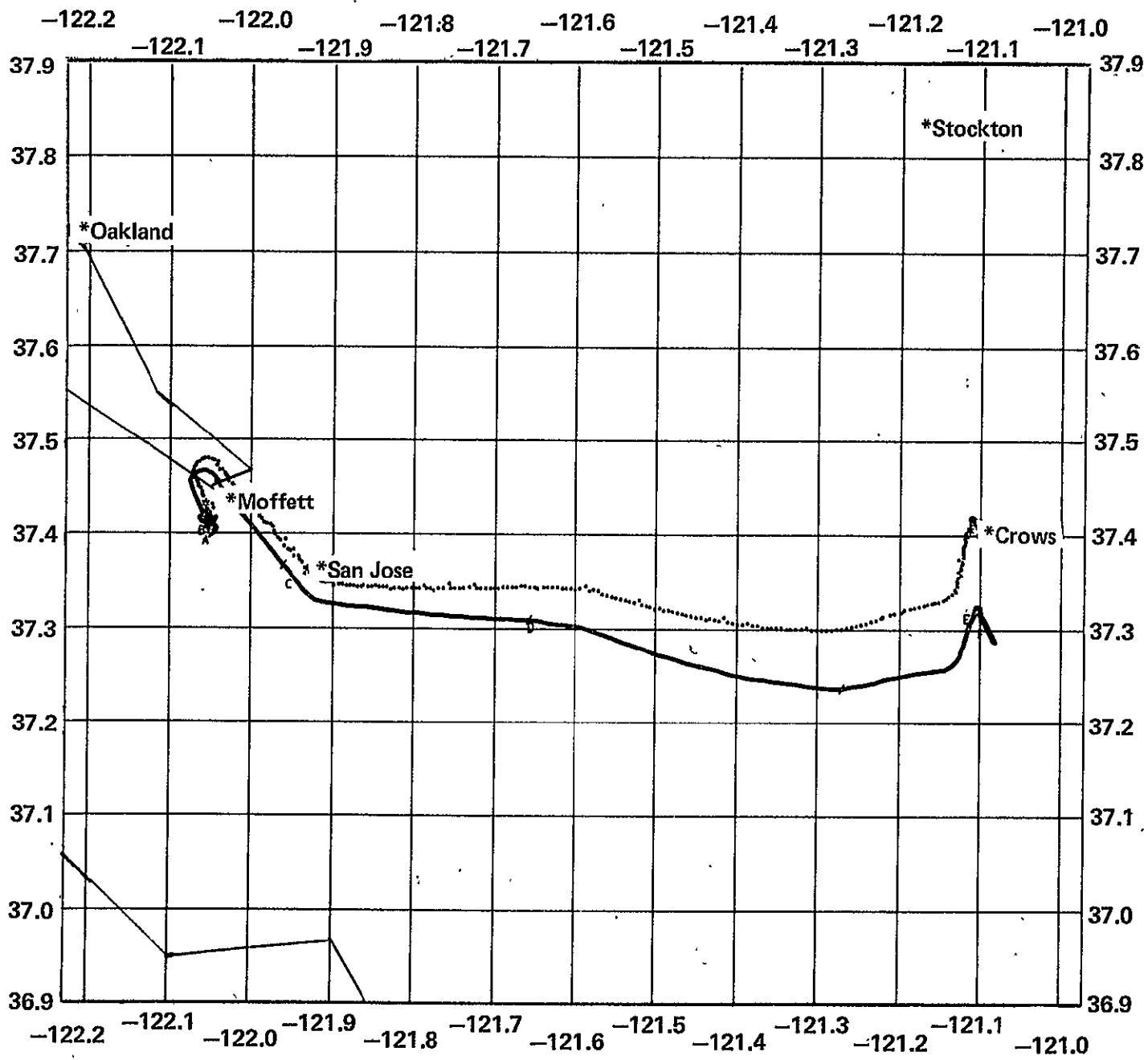
SFT822C ground track (—) = SIRU, (---) = DME
Figure A.30 SFT822C SIRU/DME ground tracks



SFT822C ground track (—) = SIRU, (---) = RADAR

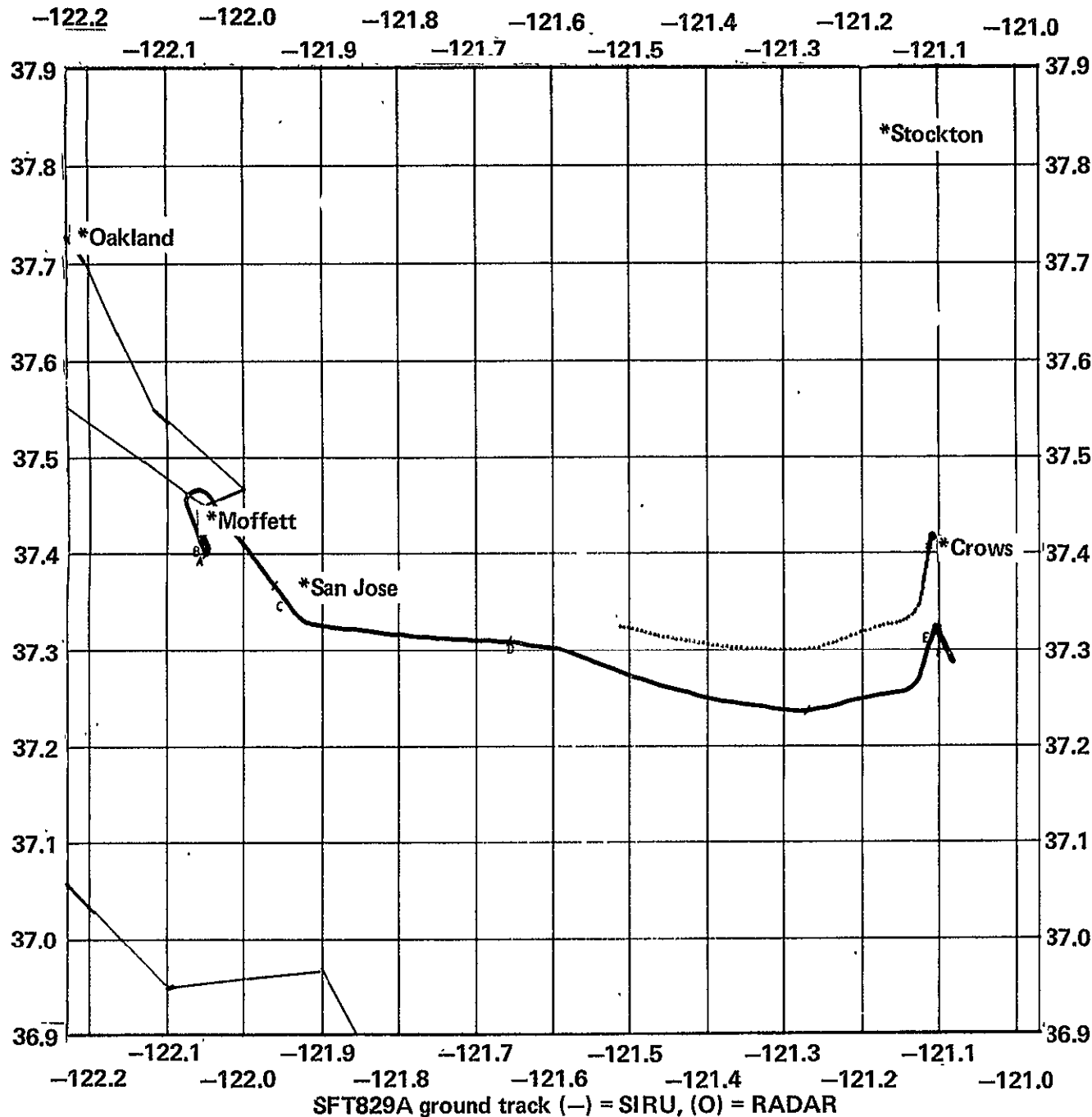
Figure A.31 SFT822C SIRU/radar ground tracks

85



SFT829A ground track (-) = SIRU, (O) = DME

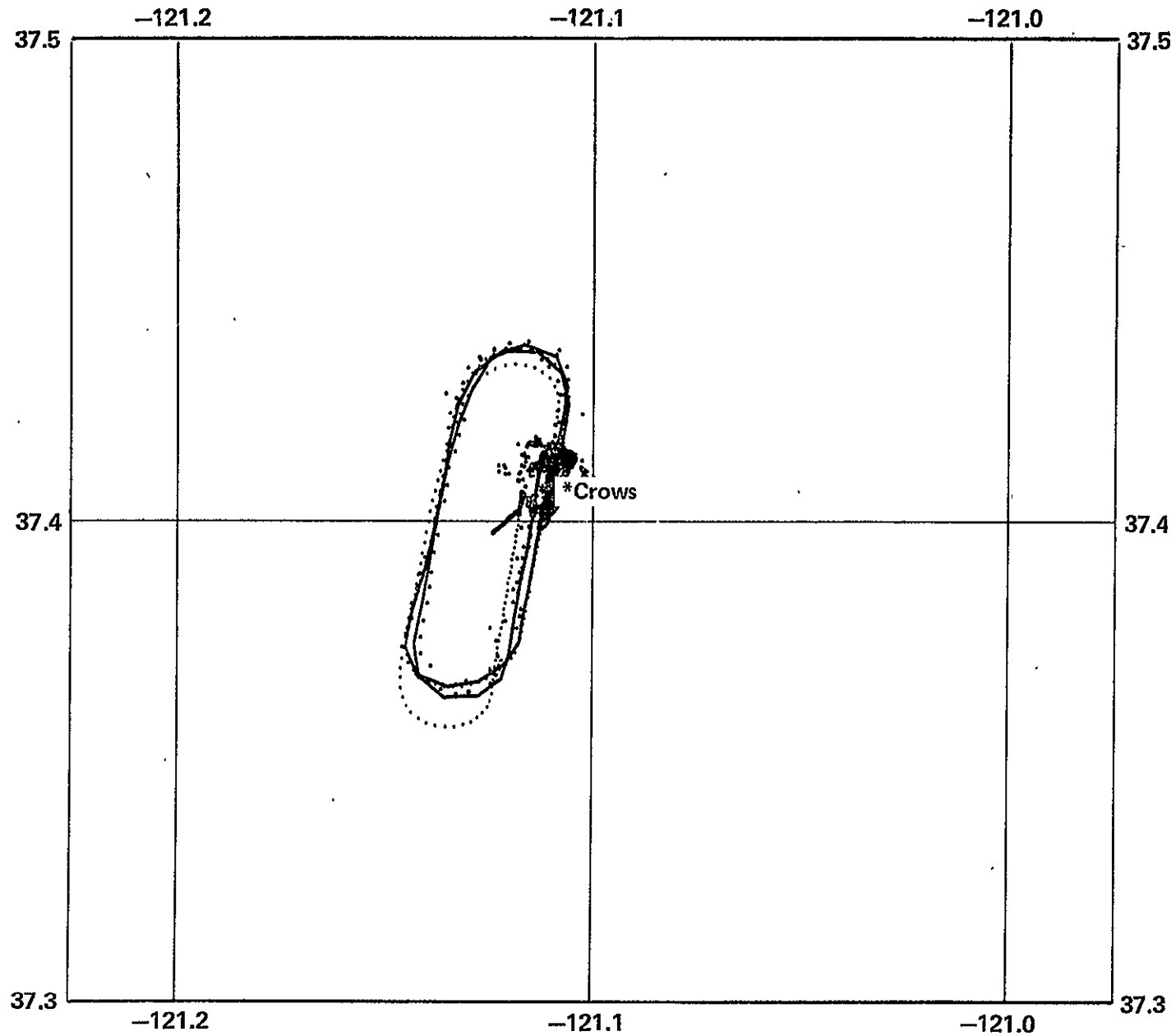
Figure A.32 SFT829A SIRU/DME ground tracks



SFT829A ground track (-) = SIRU, (O) = RADAR

Figure A.33 SFT829A SIRU/radar ground tracks

86

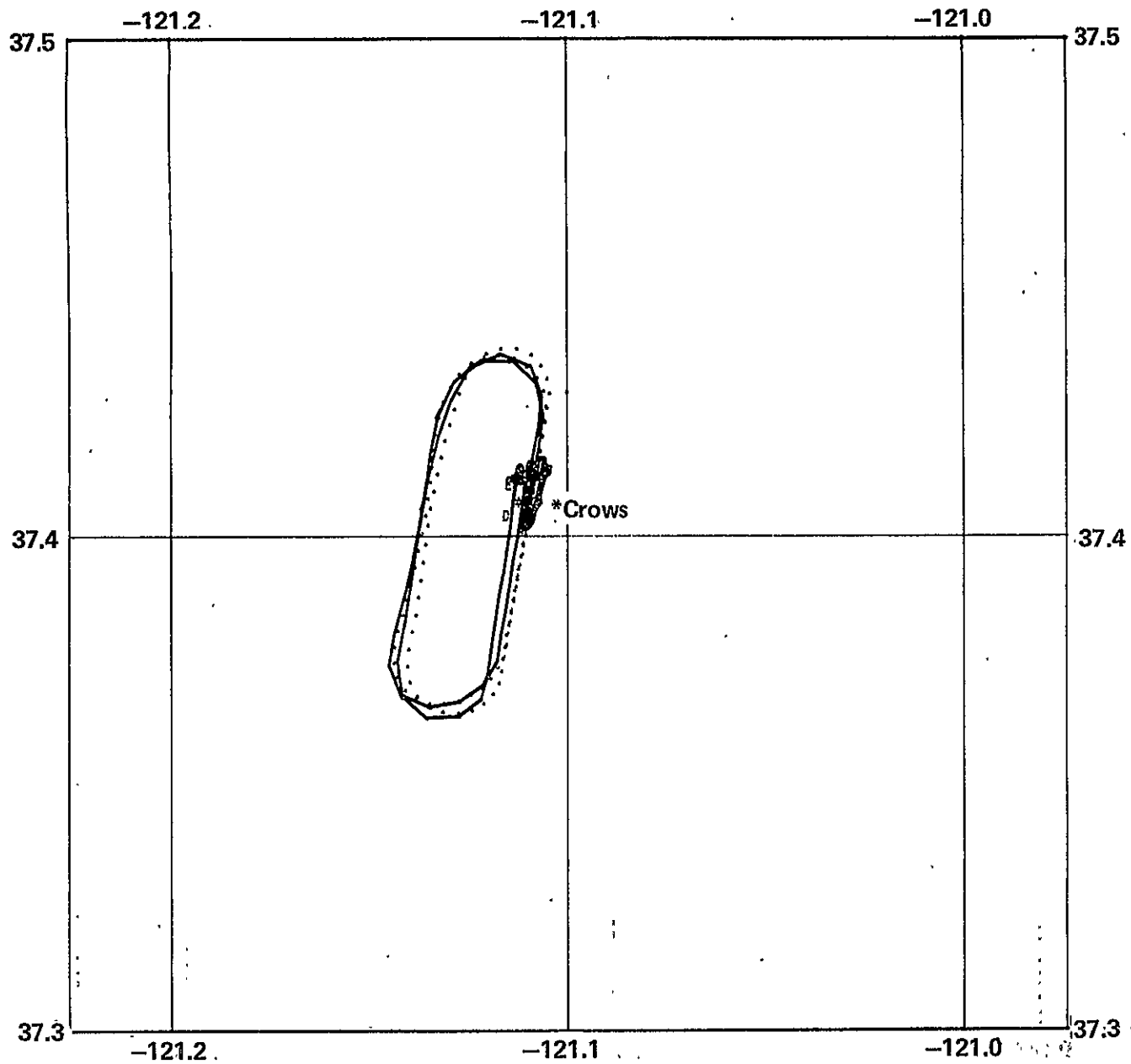


87

SFT829B track (-) SIRUA, (.) = SIRUB, (O) = DME

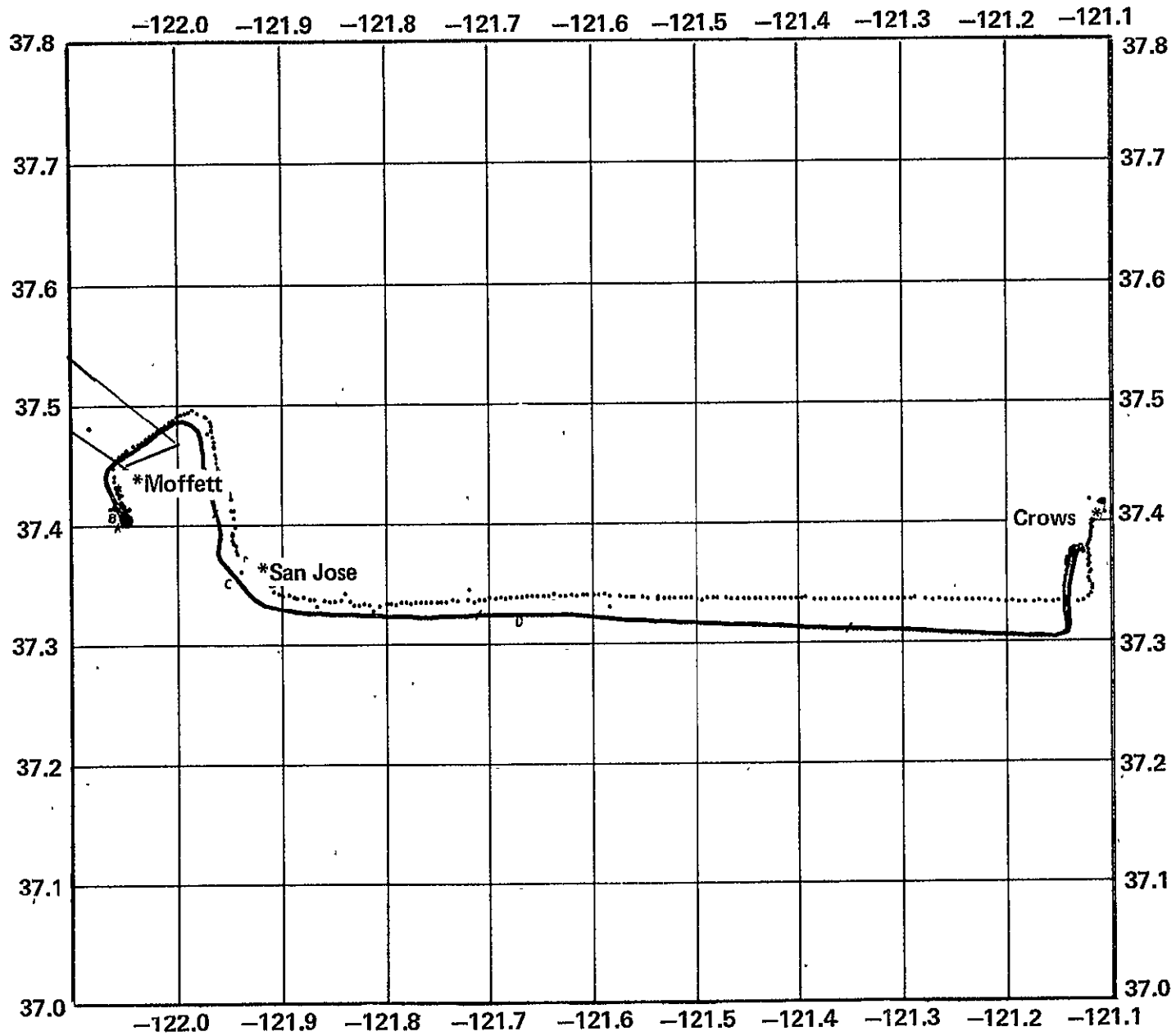
Figure A.34 SFT829B SIRU A/SIRU B/DME ground tracks

88



SFT829B ground track (-) = SIRU, (O) = RADAR

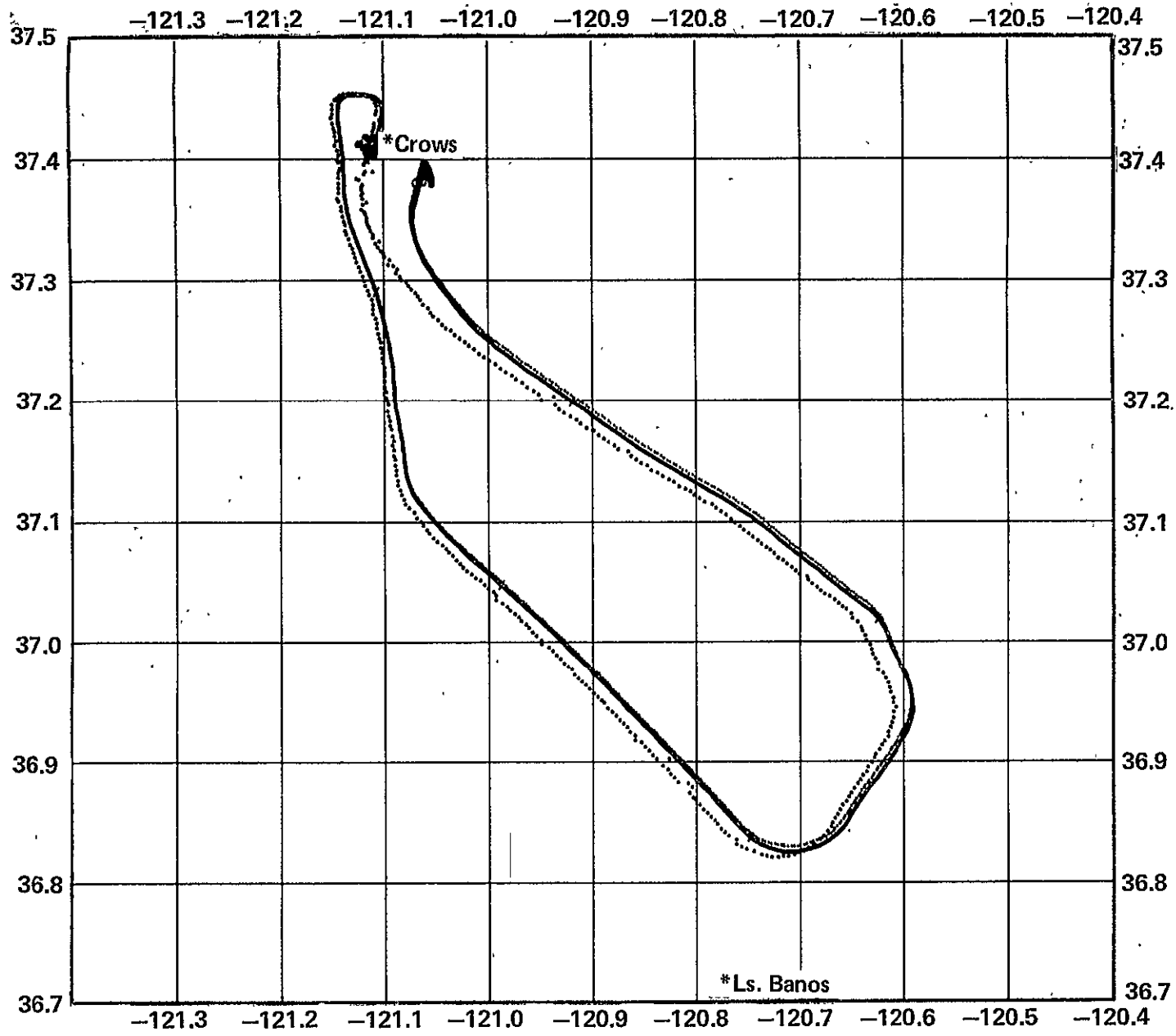
Figure A.35 SFT829B SIRU/radar ground tracks



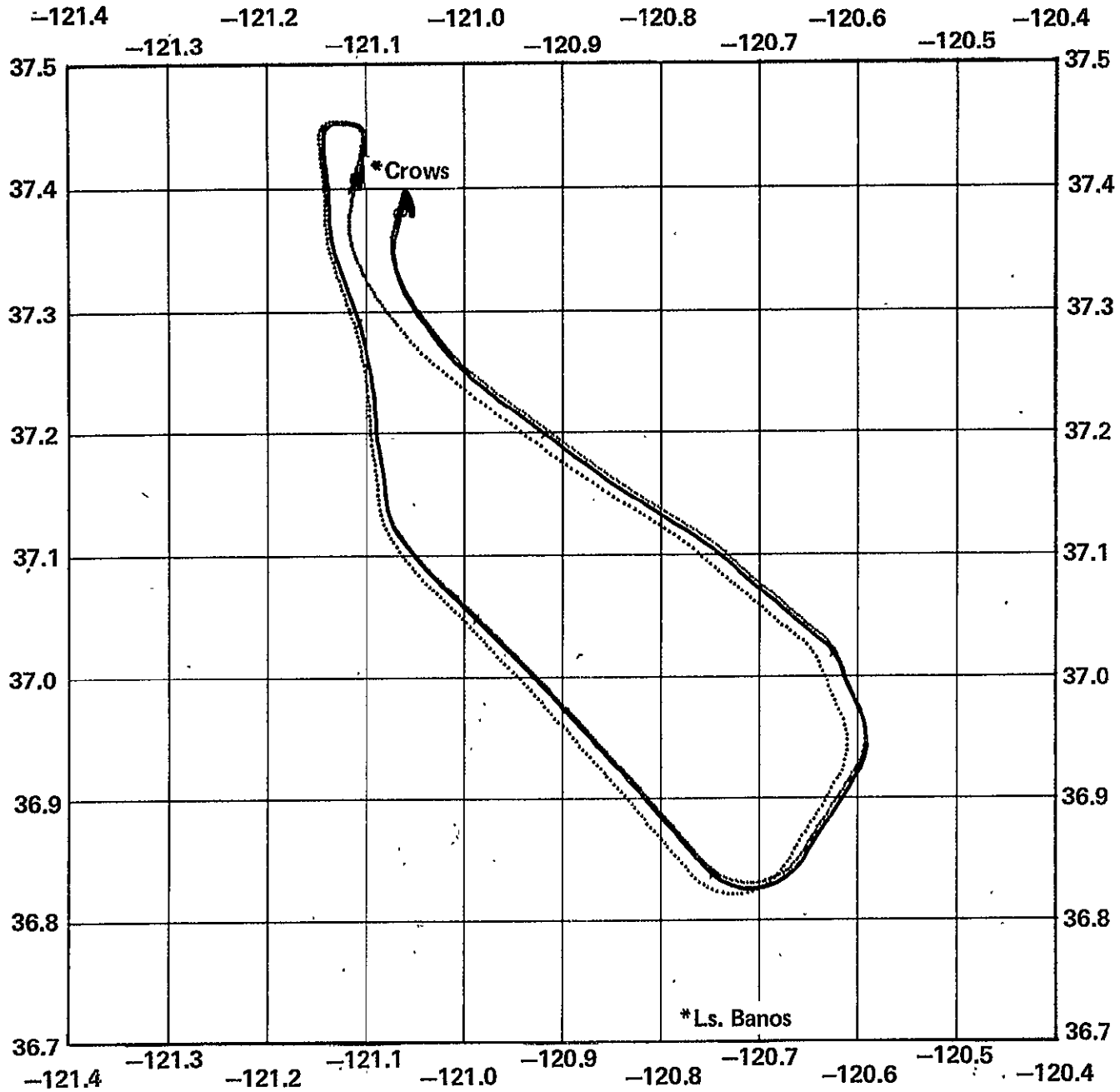
SFT905A track (-) = SIRUA, (.) = SIRUB, (O) = DME

Figure A.36 SFT905A SIRU A/SIRU B/DME ground tracks

06



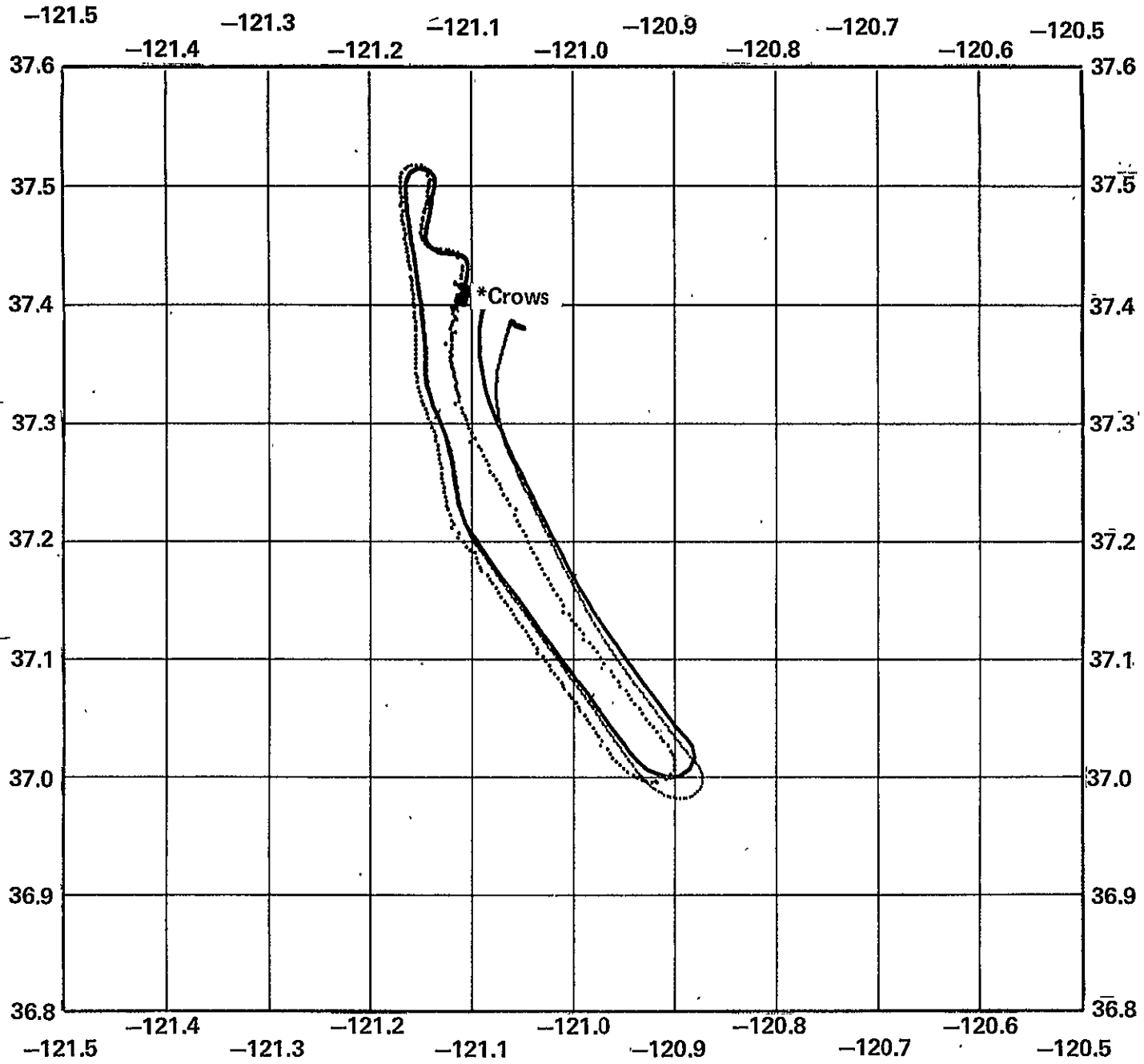
SFT905B track (-) = SIRUA, (.) = SIRUB, (O) = DME
Figure A.37 SFT905B SIRU A/SIRU B/DME ground tracks



I6

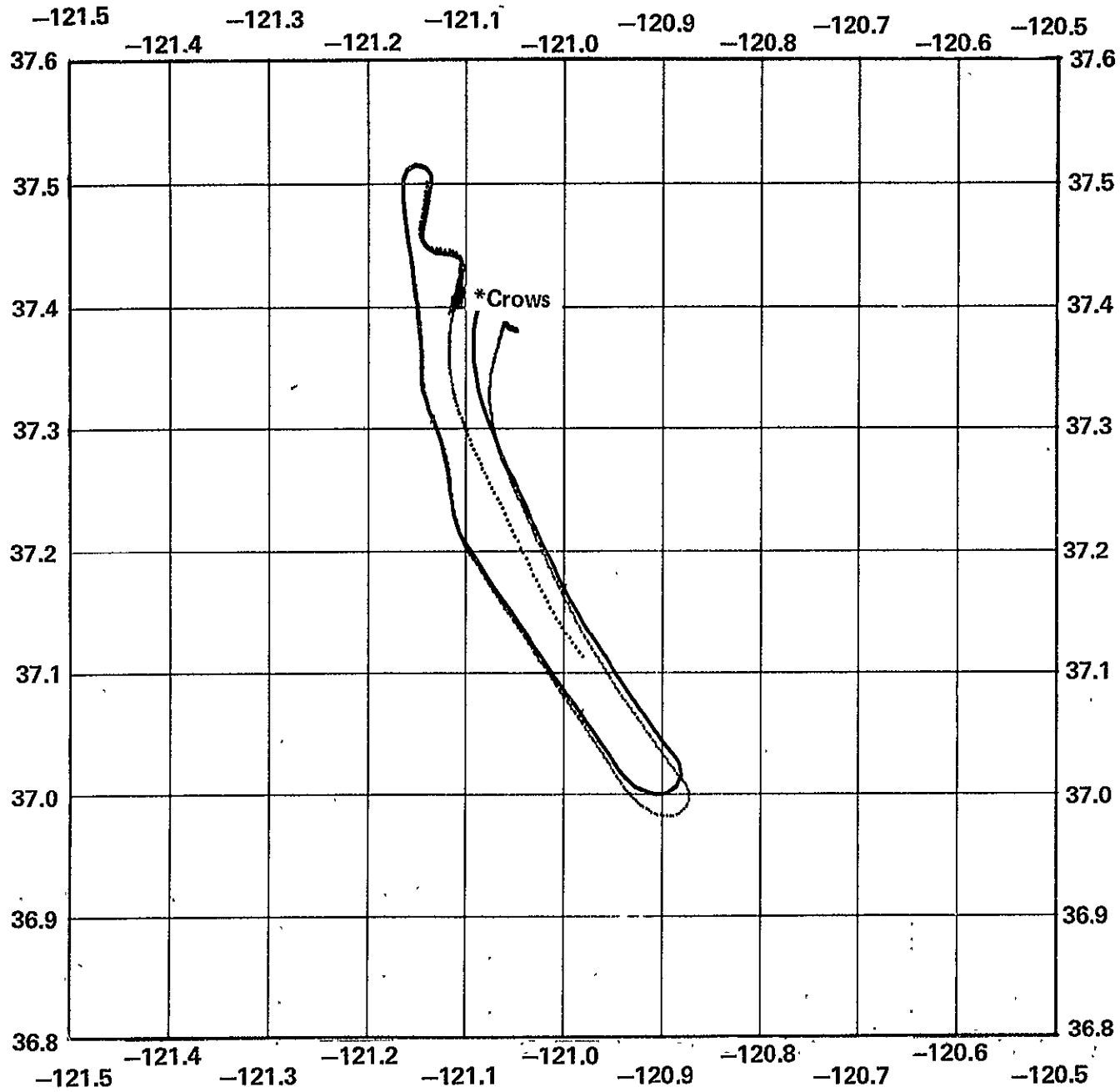
SFT905B track (-,.) = SIRUA,B (O) = RADAR

Figure A.38 SFT905B SIRU A/SIRU B/radar ground tracks



92

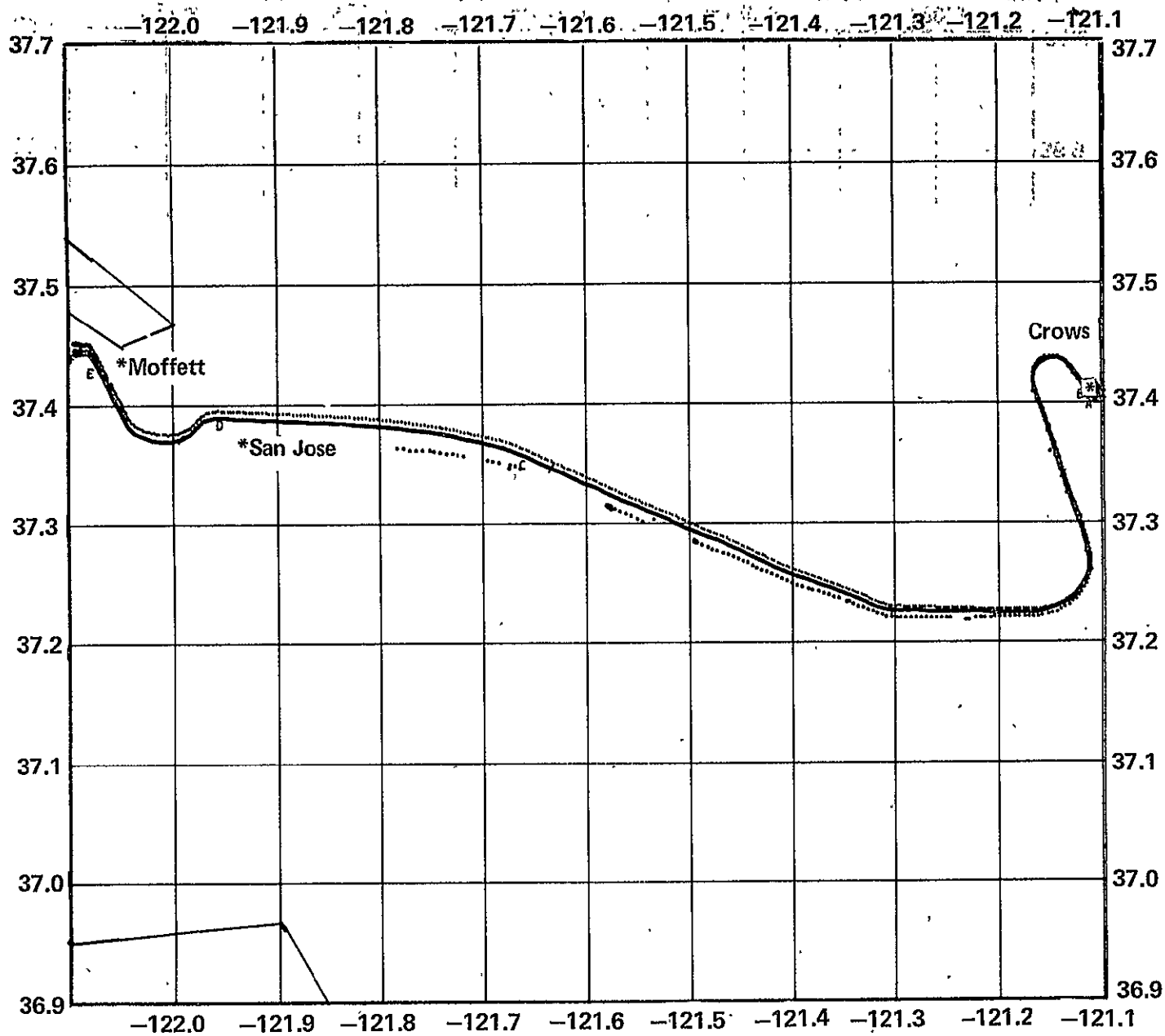
SFT905C track (-) = SIRUA, (.) = SIRUB, (o) = DME
Figure A.39 SFT905C SIRU A/SIRU B/DME ground tracks



93

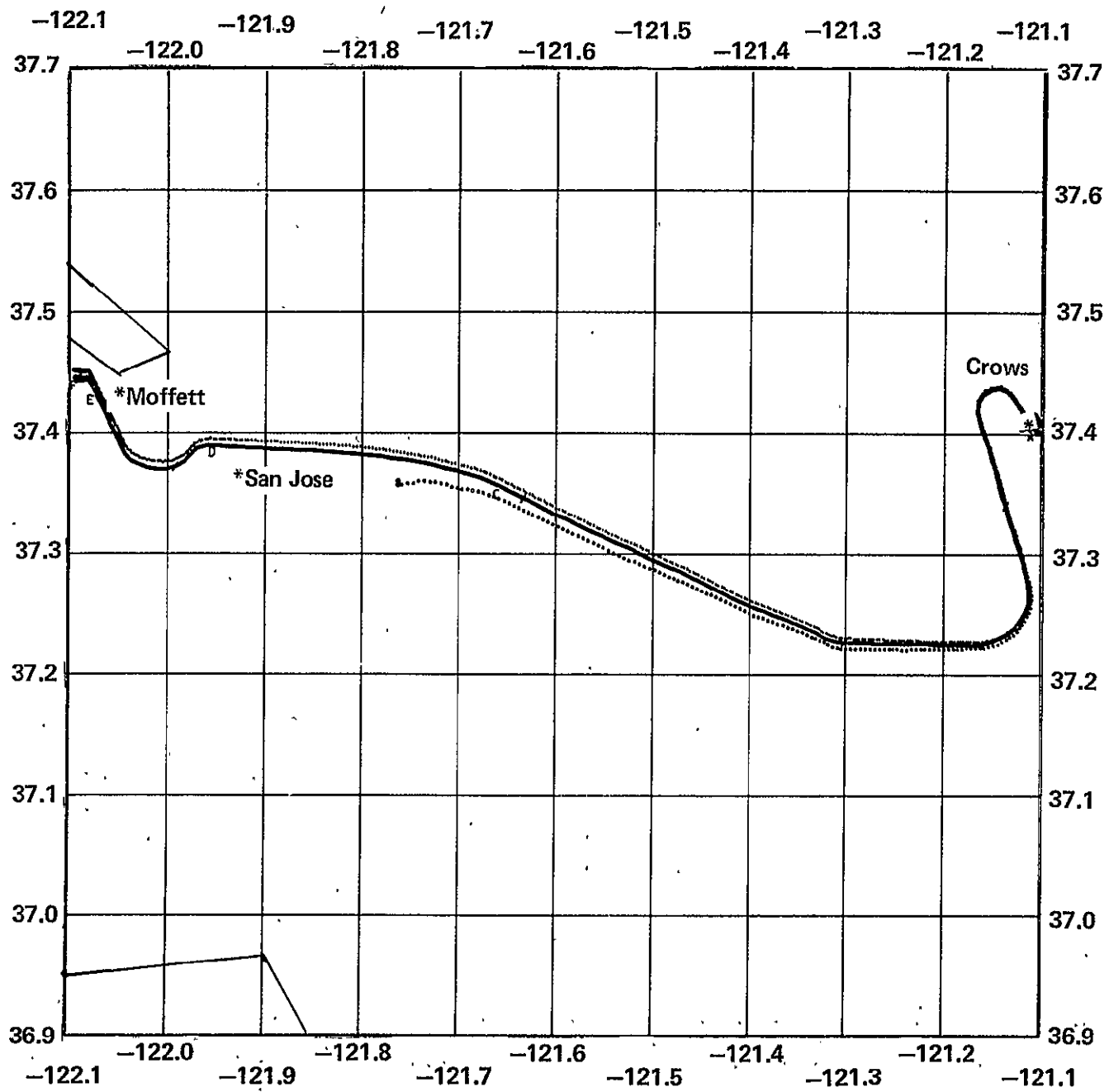
SFT905C track (-,.) = SIRUA, B (O) = RADAR

Figure A.40 SFT905C SIRU A/SIRU B/radar ground tracks



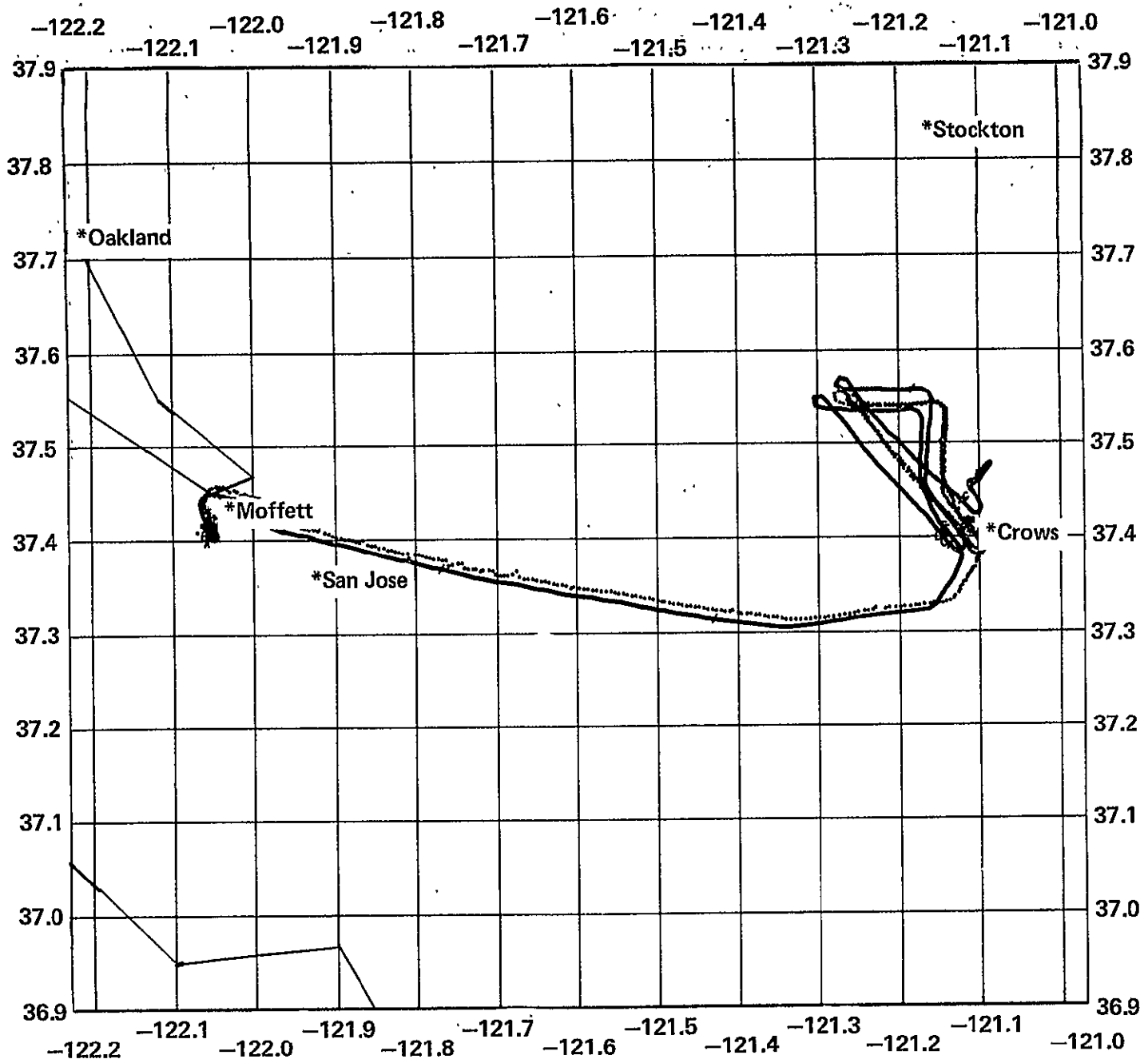
94

SFT905D track (-) = SIRUA, (.) = SIRUB, (O) = DME
 Figure A.41 SFT905D SIRU A/SIRU B/DME ground tracks



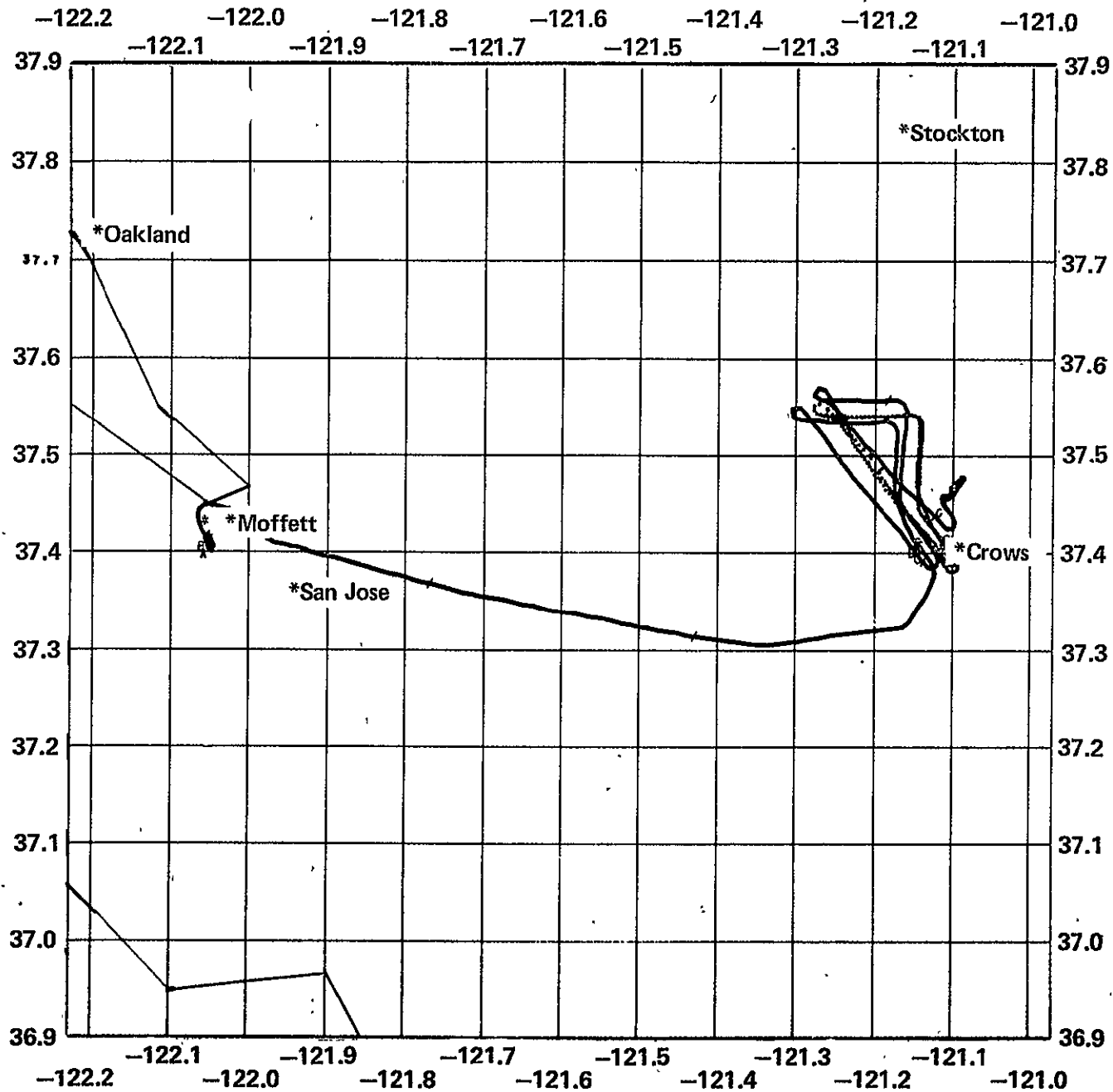
96

SFT905D track (-,.) = SIRUA, B (O) = RADAR
Figure A.42 SFT905D SIRU A/SIRU B/radar ground tracks



SFT910A ground track (-) = SIRU, (O) = DME

Figure A.43 SFT910A SIRU/DME ground tracks



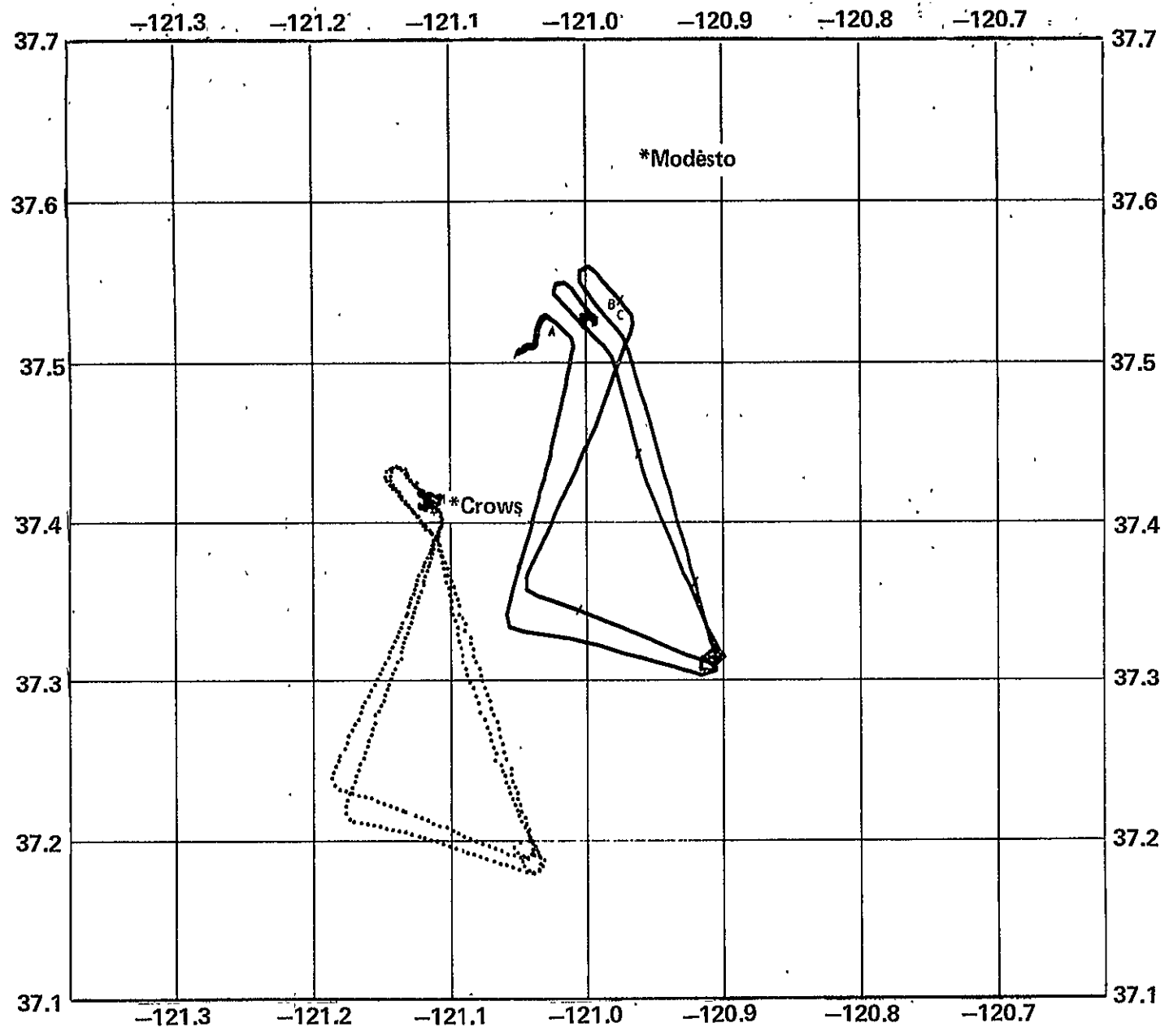
A
B
C
D
E
F
G
H

97

SFT910A ground track (-) = SIRU, (O) = RADAR

Figure A.44 SFT910A SIRU/radar ground tracks

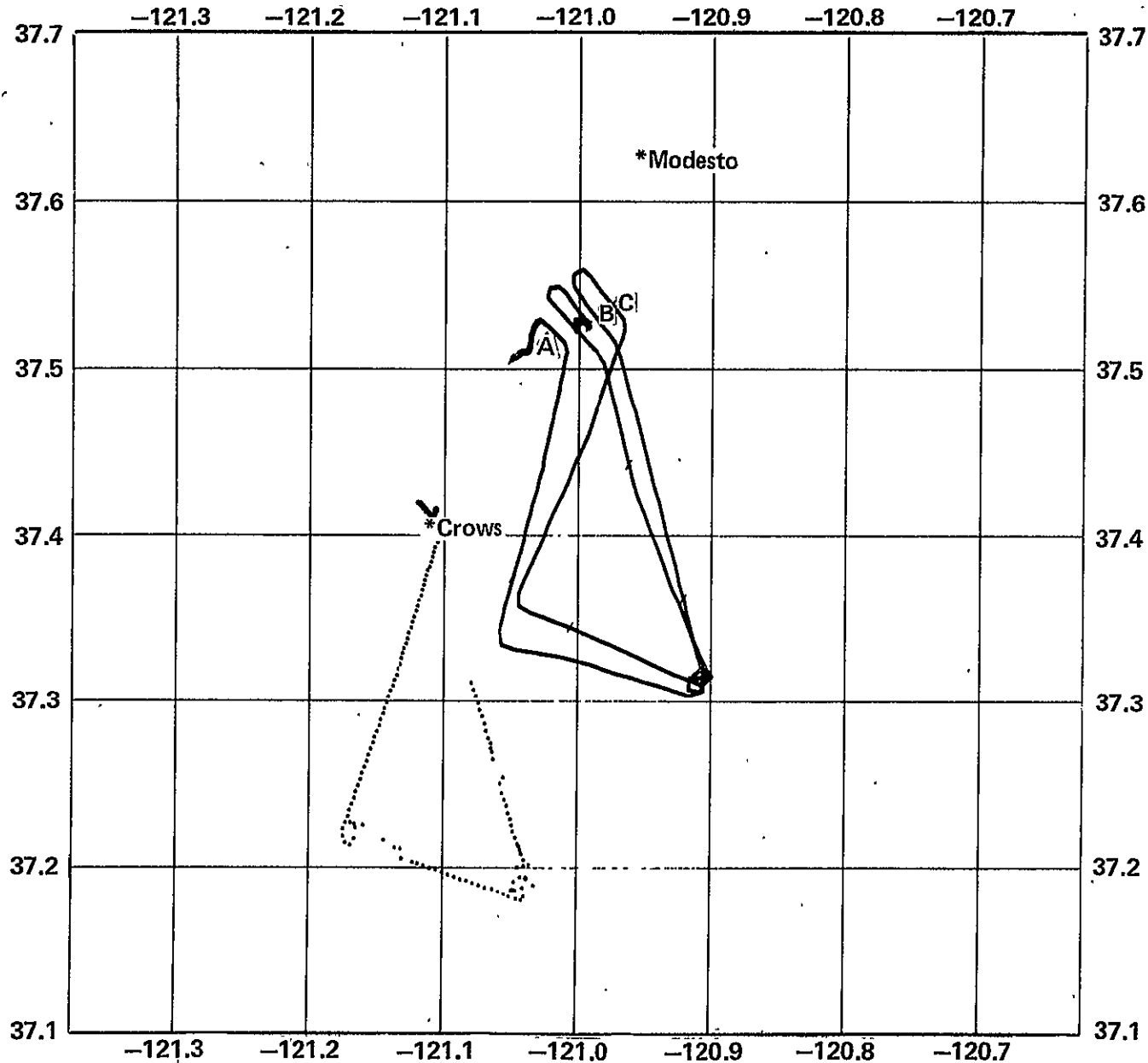
3-2



86

SFT910B ground track (-) = SIRU, (O) = DME
 Figure A.45 SFT910B SIRU/DME ground tracks

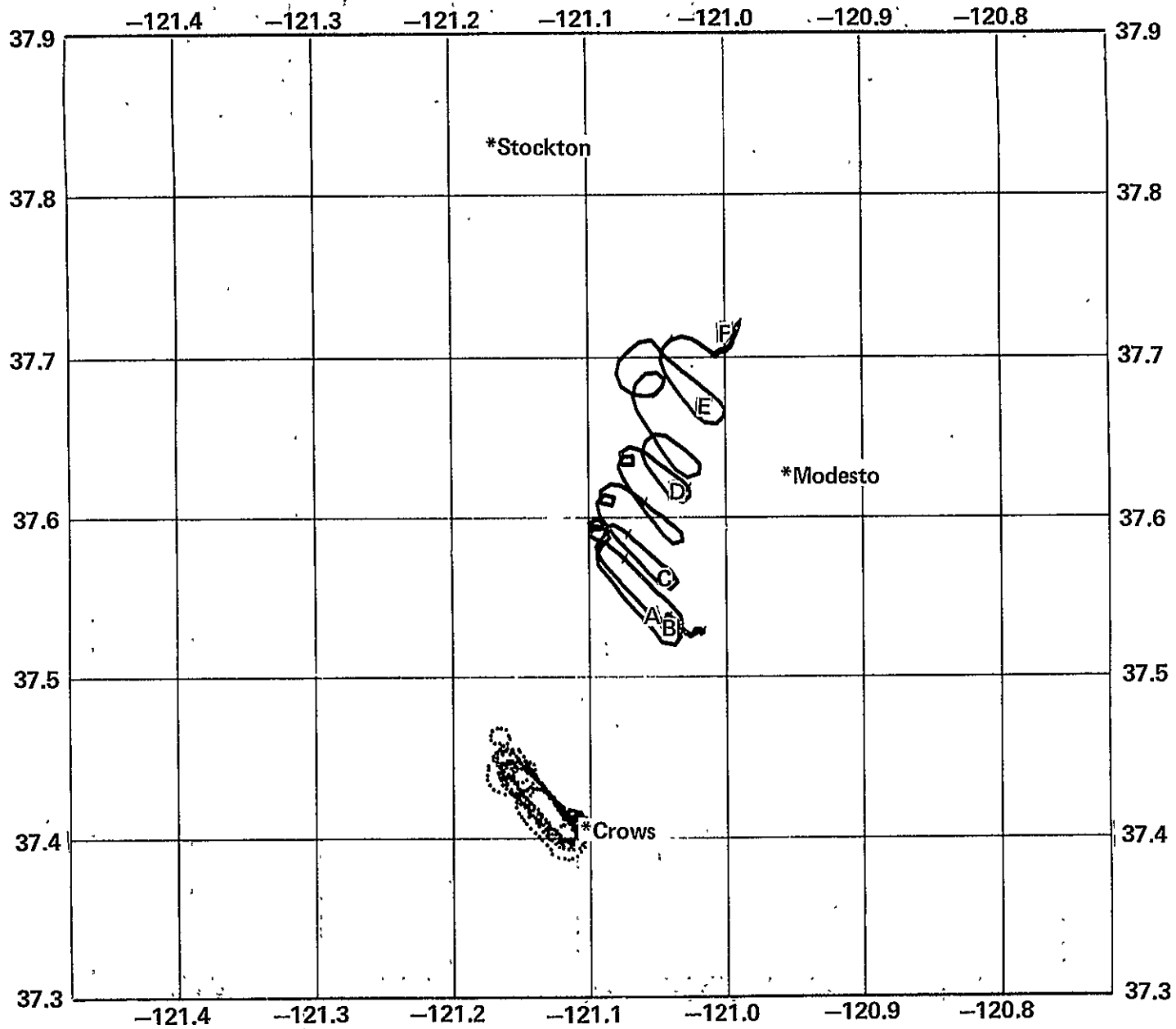
66



SFT910B ground track (-) = SIRU, (O) = RADAR

Figure A.46 SFT910B SIRU/radar ground tracks

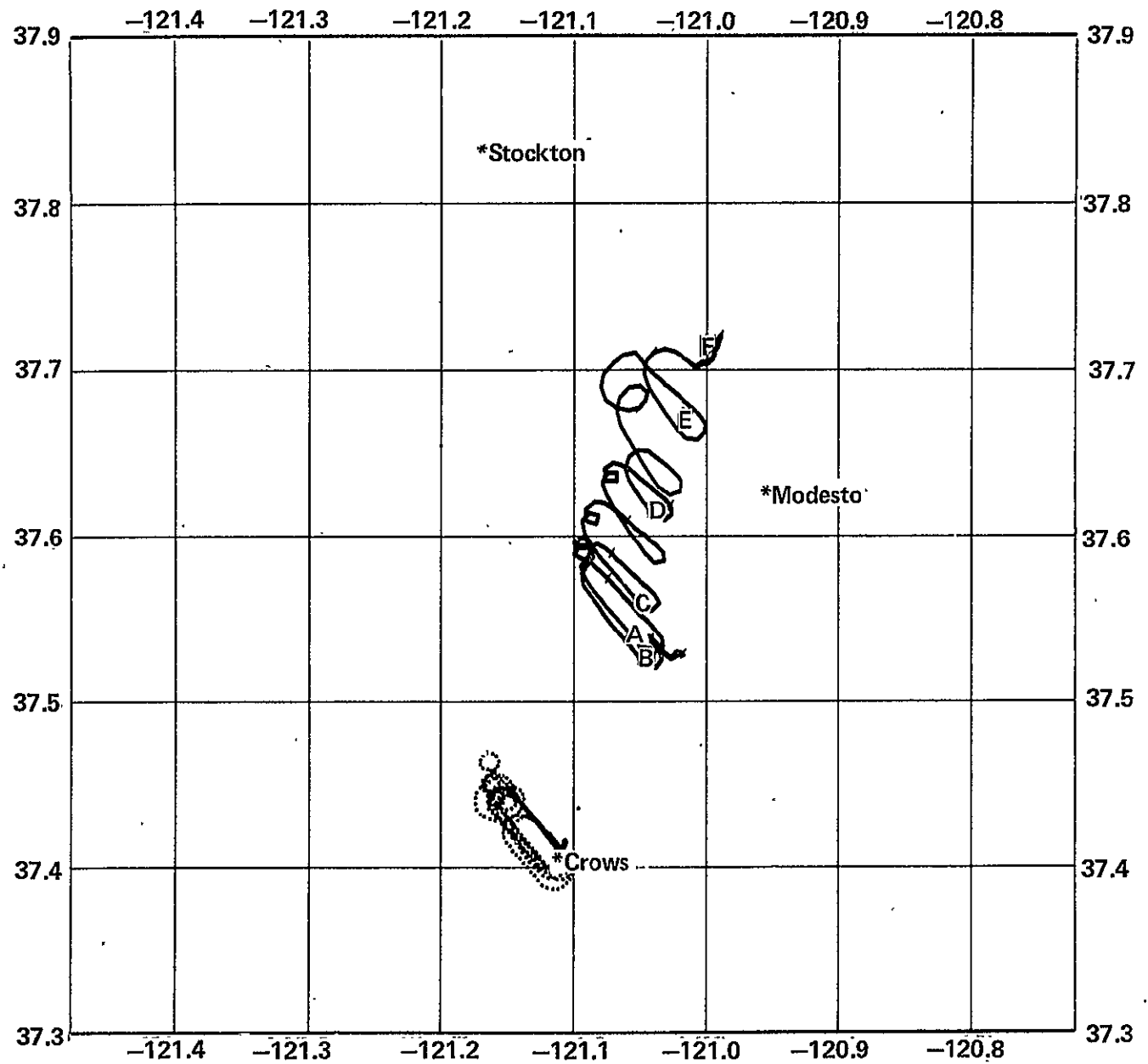
100



SFT910C ground track (—) = SIRU, (O) = DME

Figure A.47 SFT910C SIRU/DME ground tracks

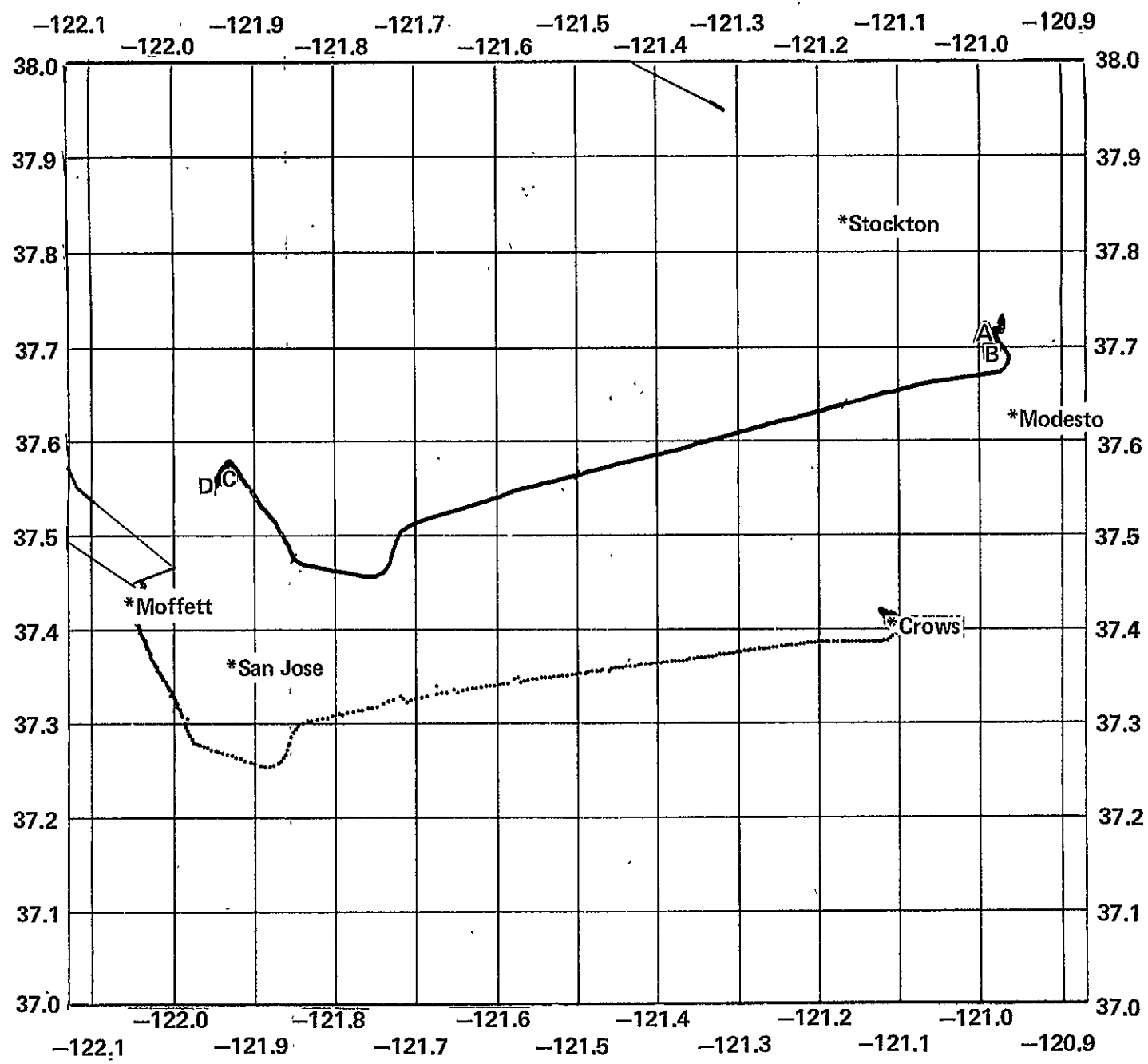
101



SFT910C ground track (—) = SIRU, (O) = RADAR

Figure A.48 SFT910C SIRU/radar ground tracks

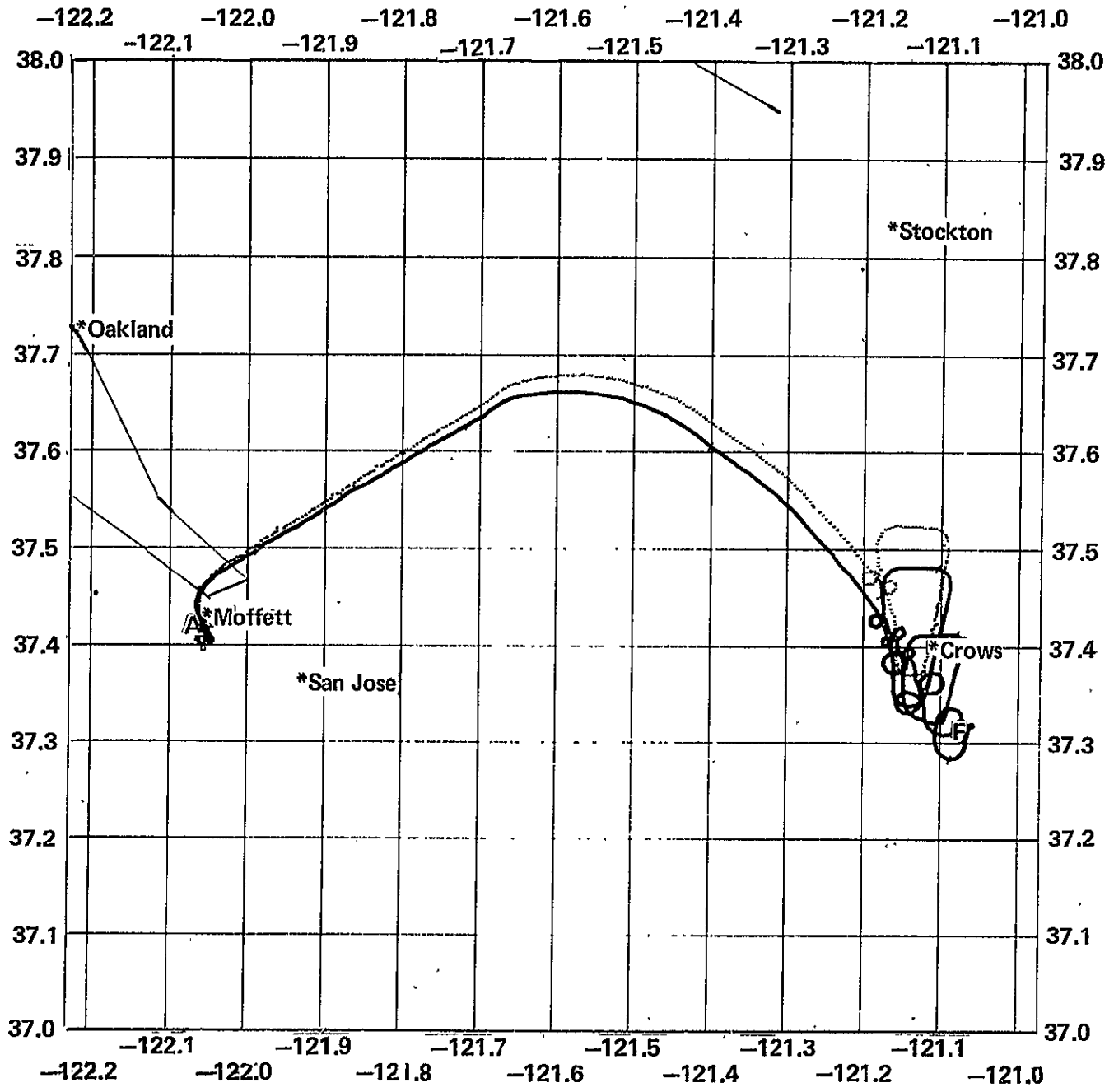
102



SFT910D ground track (-) = SIRU, (O) = DME

Figure A.49 SIRU/DME ground tracks

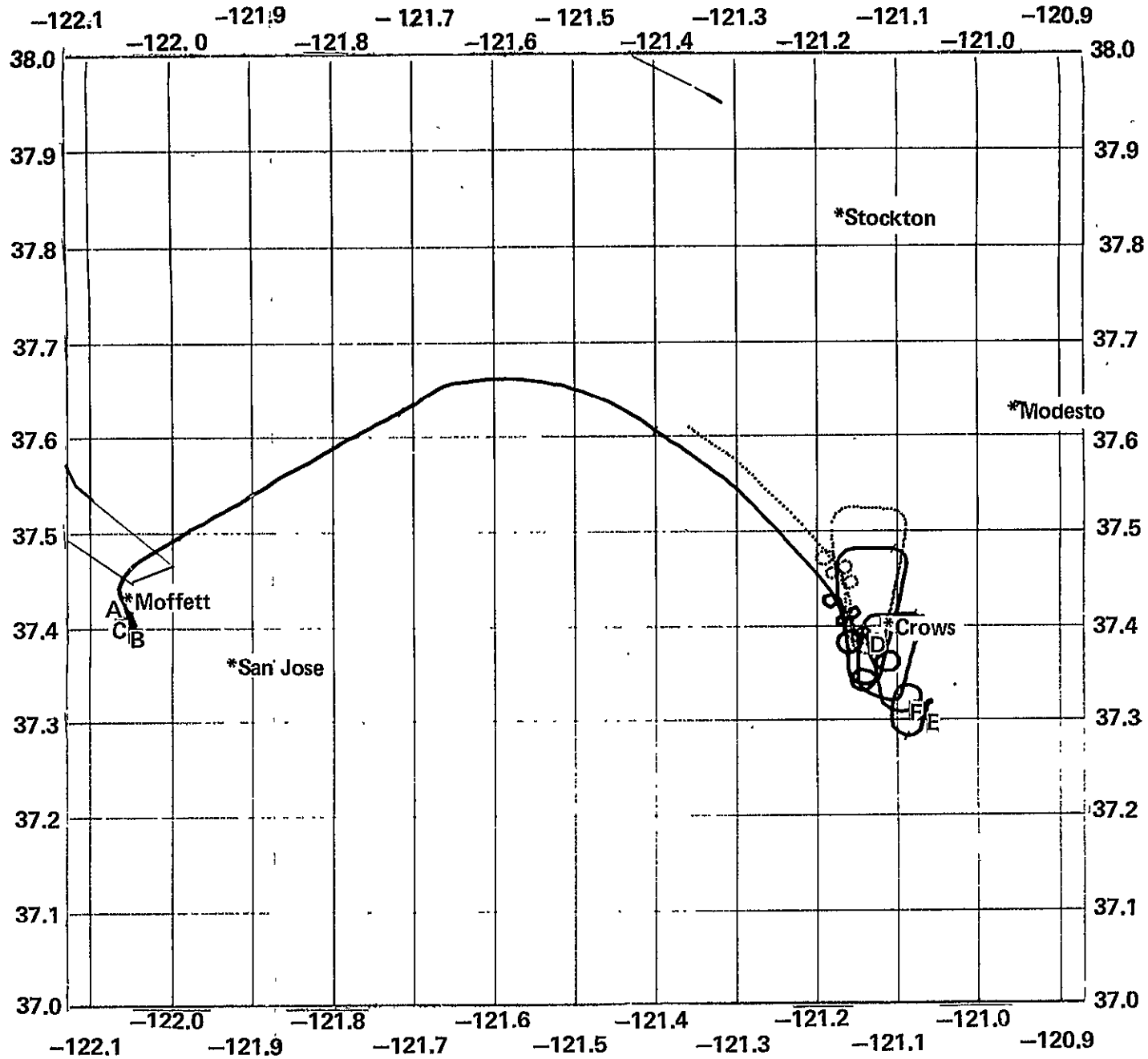
103



SFT918A ground track (-) = SIRU, (O) = DME

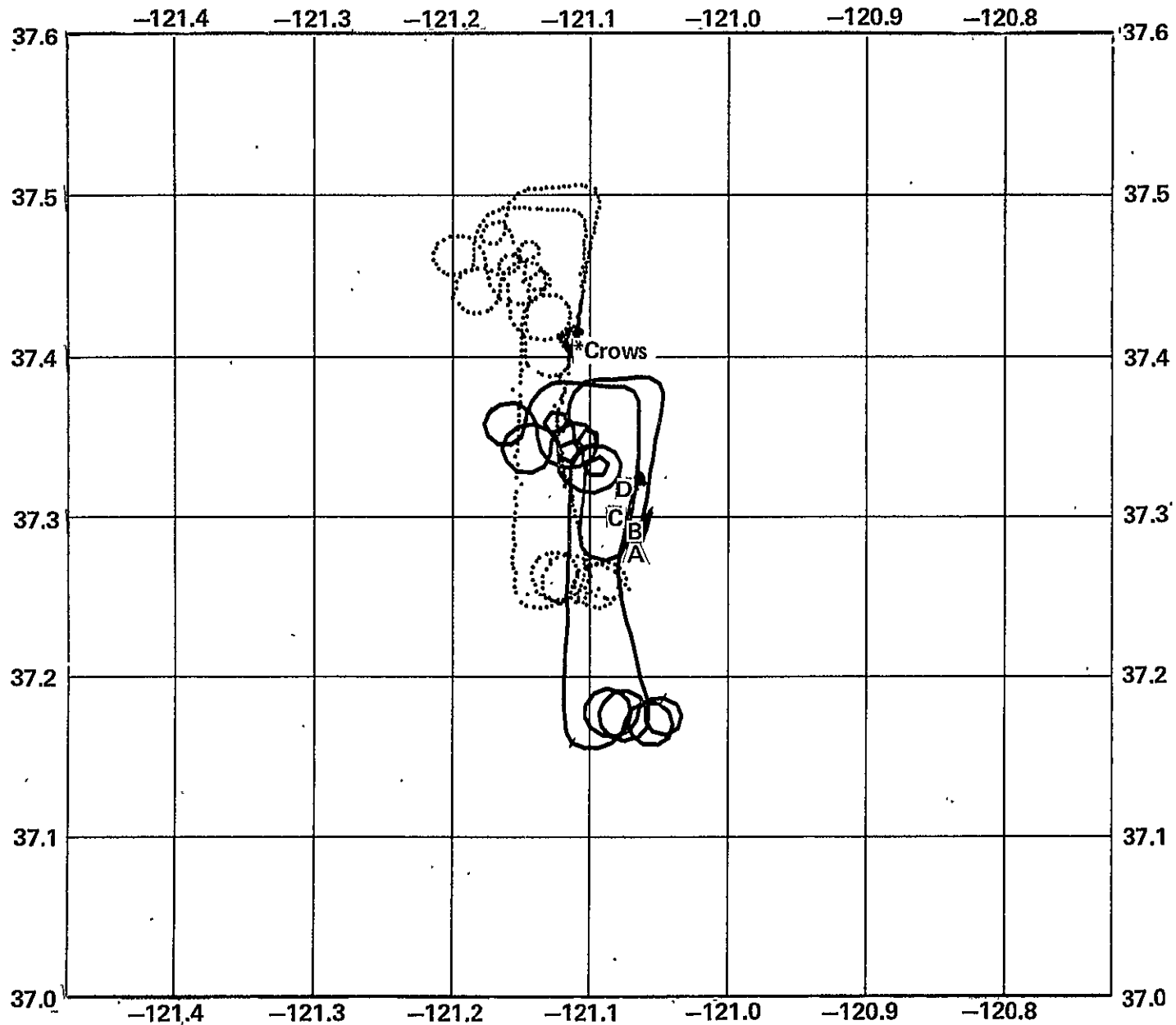
Figure A.50 SFT918A SIRU/DME ground tracks

104



SFT918A ground track (—) = SIRU, (O) = RADAR

105

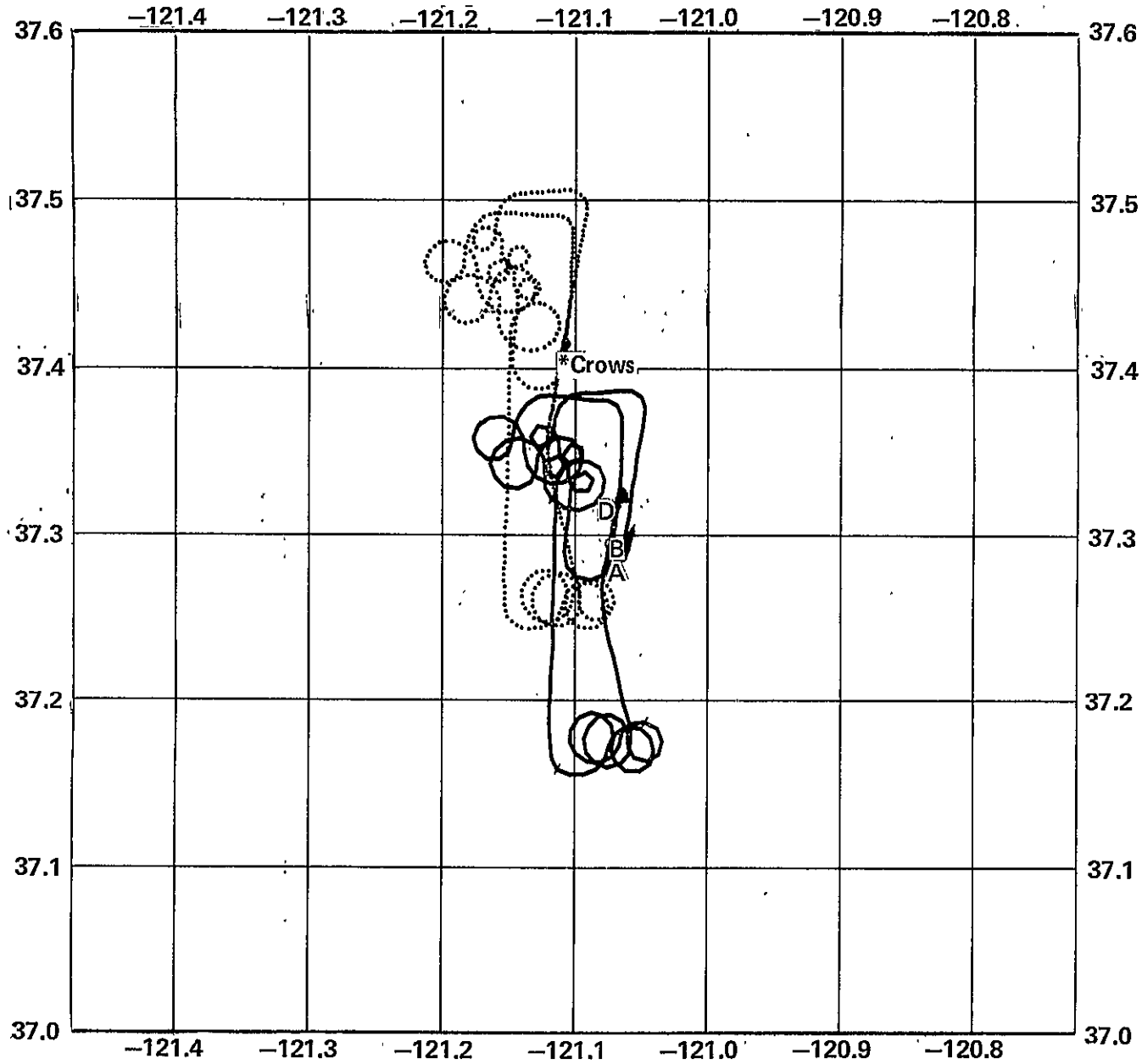


A
B
C
D
E
F

SFT918B ground track (-) = SIRU, (O) = DME

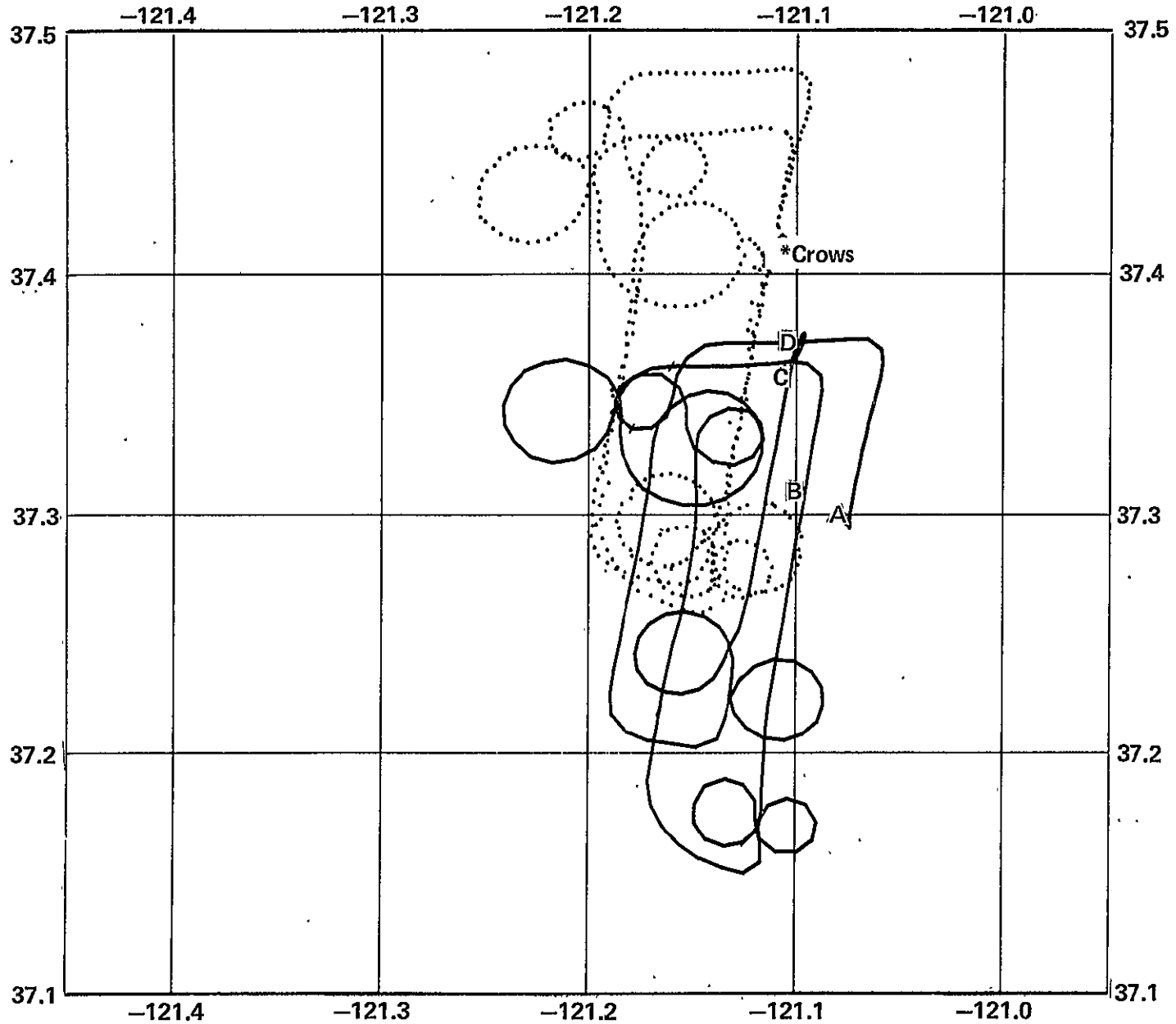
Figure A.52 SFT918B SIRU/DME ground tracks

106



SFT918B ground track (—) = SIRU, (O) = RADAR

Figure A.53 SFT918B SIRU/radar ground tracks

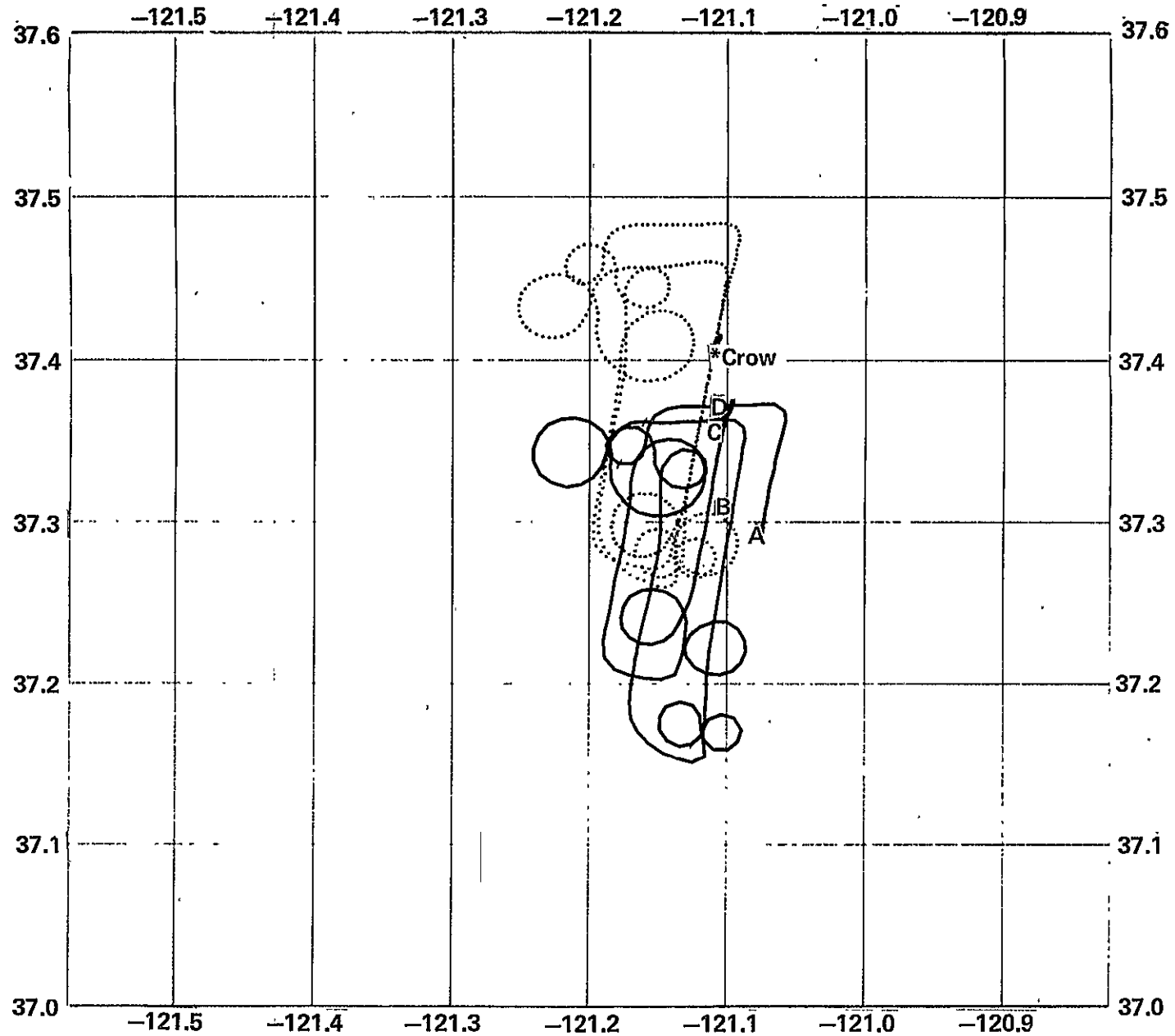


107

SFT918C ground track (-) = SIRU, (O) = DME

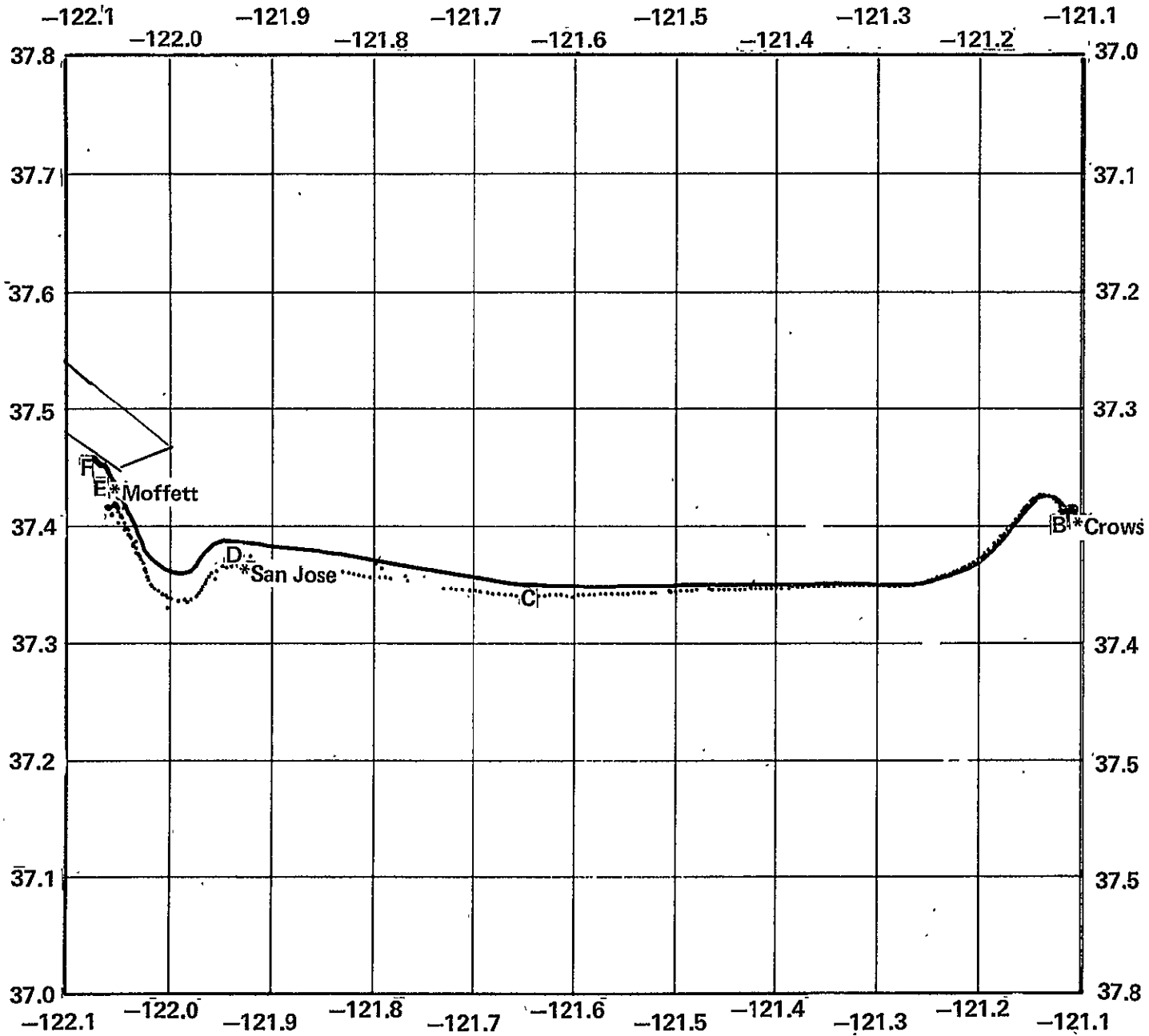
Figure A.54 SFT918C SIRU/DME ground tracks

108



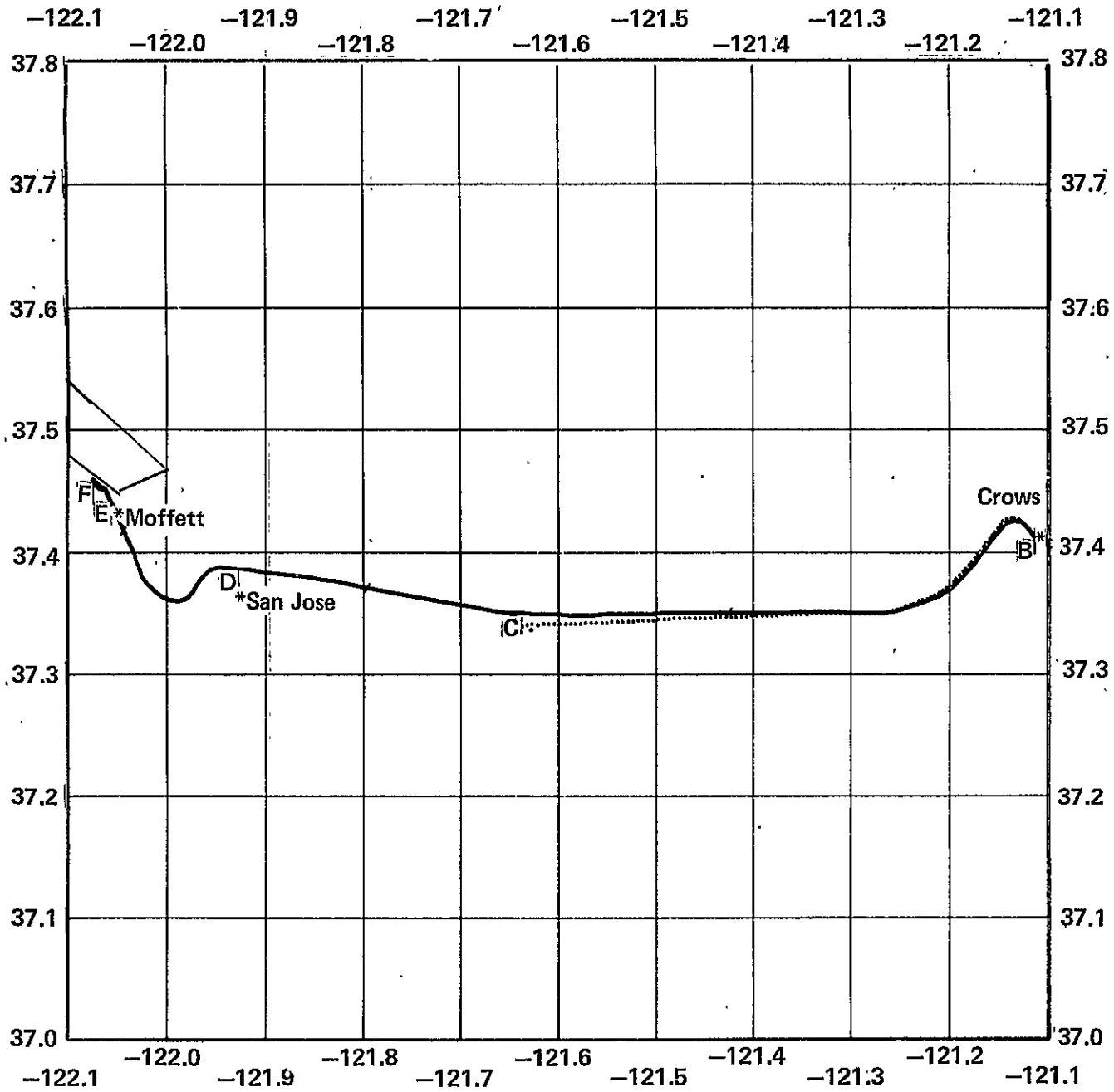
SFT918C ground track (-) = SIRU, (O) = RADAR
Figure A.55 SFT918C SIRU/radar ground tracks

109



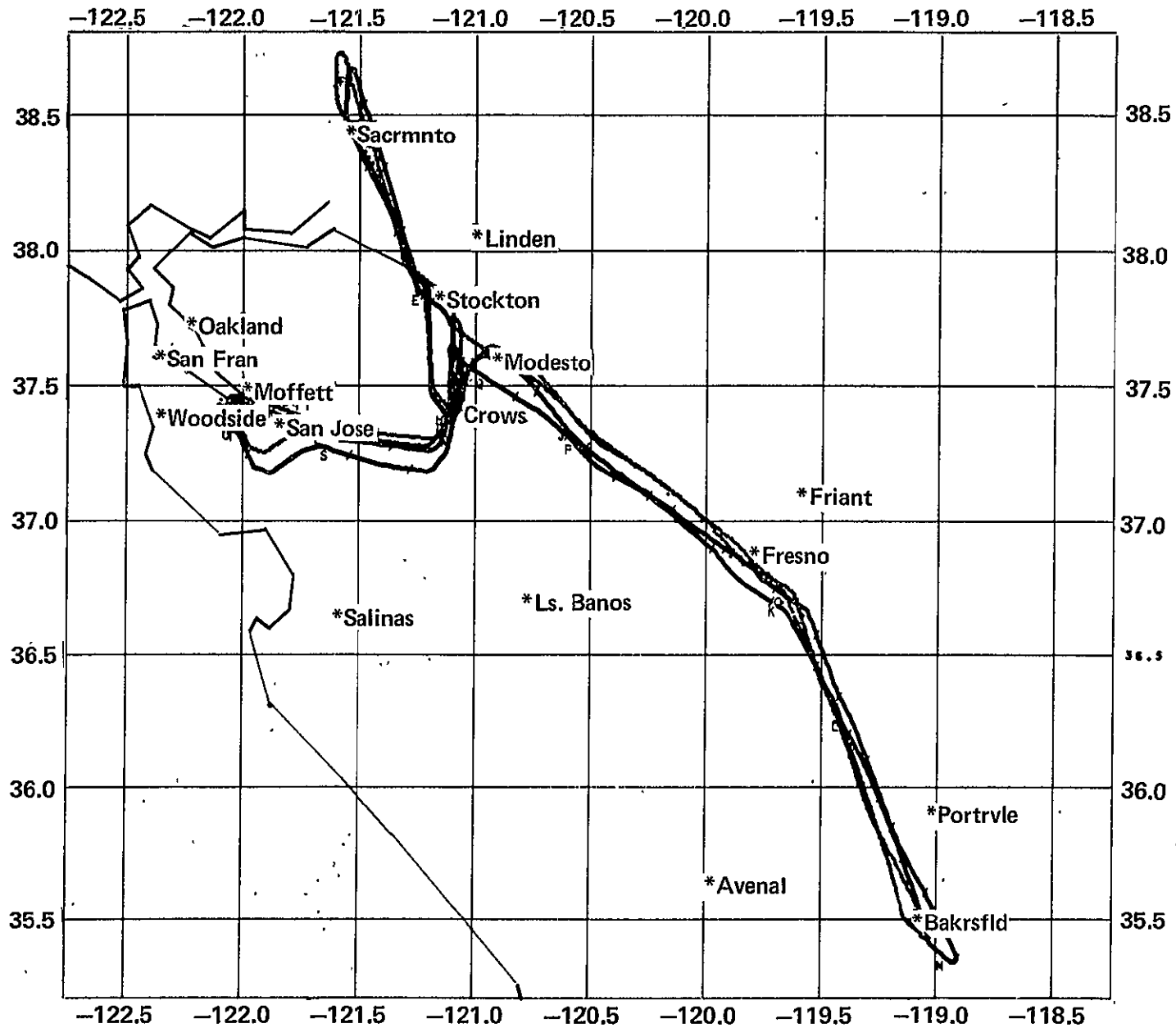
SFT918D ground track (-) = SIRU, (O) = DME

Figure A.56 SFT918D SIRU/DME ground tracks



SFT918D ground track (-) = SIRU, (O) = RADAR

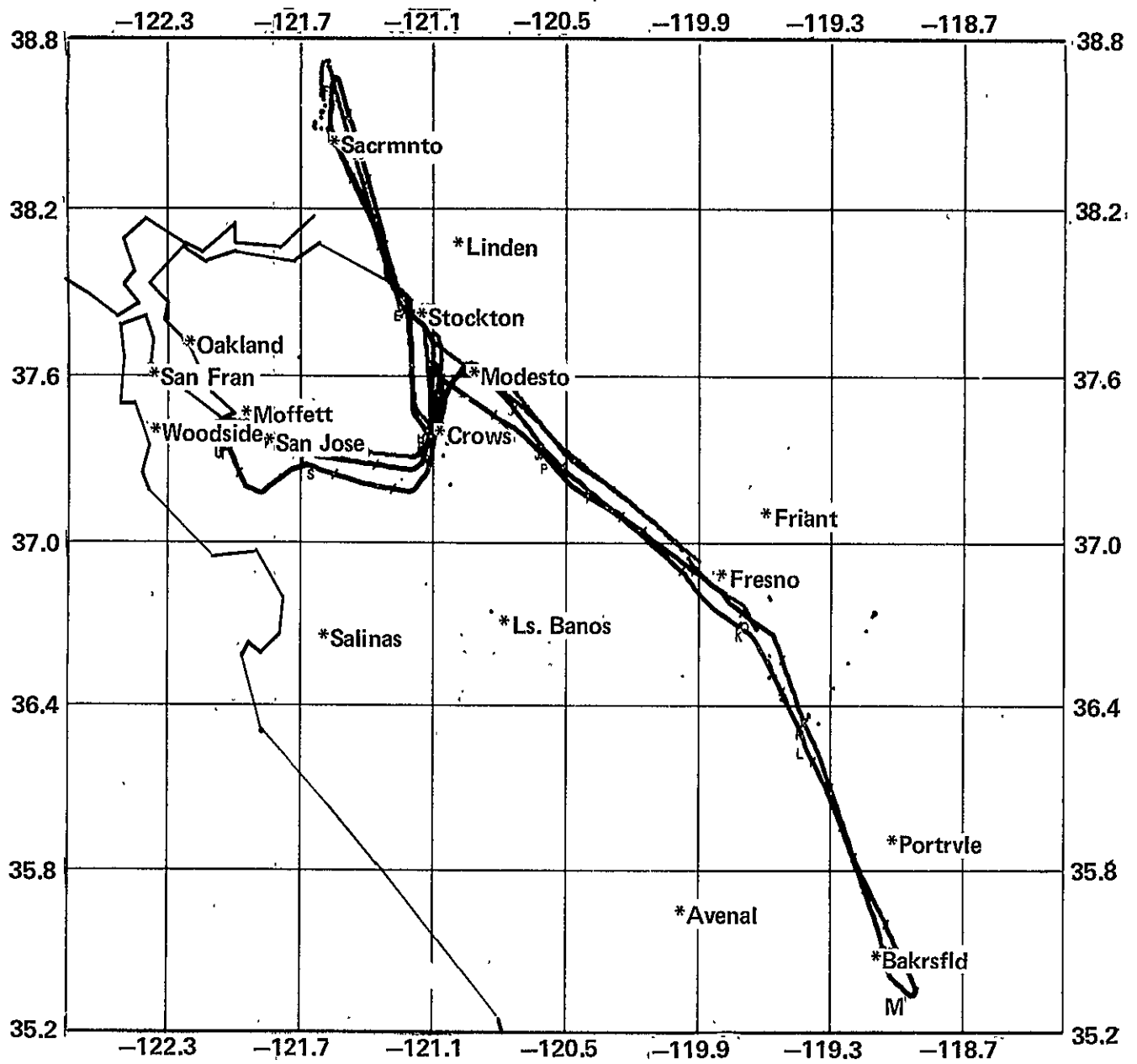
Figure A.57 SFT918D SIRU/radar ground tracks



111

SFT924 ground track (—) = SIRU, (O) = DME

Figure A.58 SFT924 SIRU/DME ground tracks



SFT924 ground track (-) = SIRU, (O) = RADAR

Figure A.59 SFT924 SIRU/radar ground tracks

APPENDIX B

NAVIGATION RESIDUAL PLOTS

This appendix presents position residuals between SIRU's best estimate of the trajectory and the trajectory derived from DME or radar data. Three residual histories are contained in each plot:

1. northward position residual
2. eastward position residual
3. root-sum-square or radial position residual.

All three residual histories are plotted in units of nautical miles. Scales vary, however, so individual scale labels should be noted. The flight segment and external reference (i.e., DME or radar) are identified in the figure's title.

The sense of the residuals is DME-SIRU or radar-SIRU, so that the indicated external reference position is SIRU plus residual. That is, the DME or radar aircraft position is (northward residual) nautical miles north of SIRU's indicated position and (eastward residual) nautical miles east of SIRU's indicated position.

The specific flight to which the residuals apply is indicated by the legend SFT+ (month)(day); for example, figure B.1 applies to SFT520 which is SIRU Flight Test of May 20. SIRU always presents a smooth, continuous position estimate, so noise or discontinuous behavior should be attributed to the external source. The radar position residuals are generally seen to be smoother than the DME position residuals.

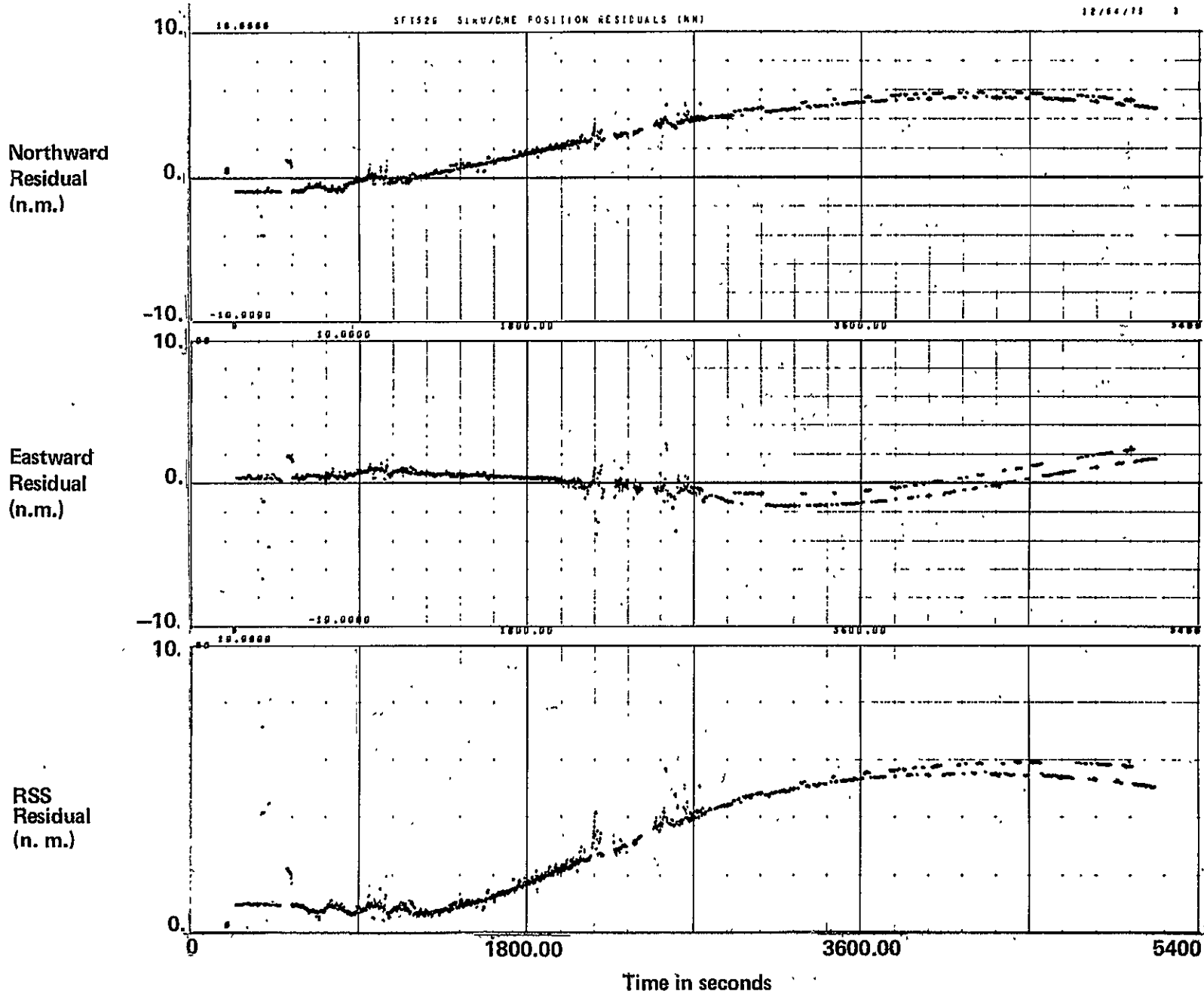
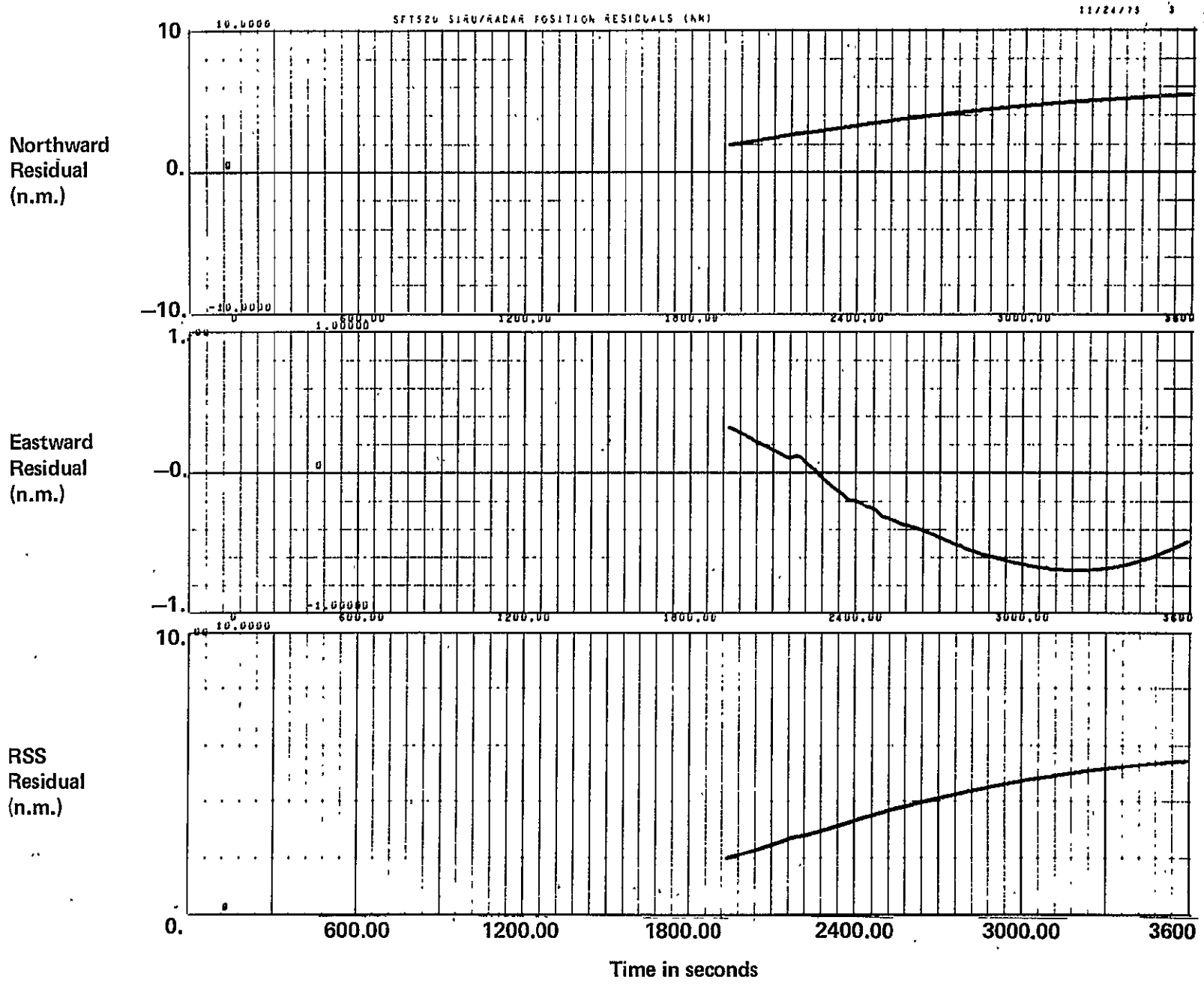


Figure B.1 SFT520 SIRU/DME position residuals

114

ORIGINAL PAGE IS
OF POOR QUALITY



115

ORIGINAL PAGE IS OF POOR QUALITY

Figure B.2 SFT520 SIRU/radar position residuals

116

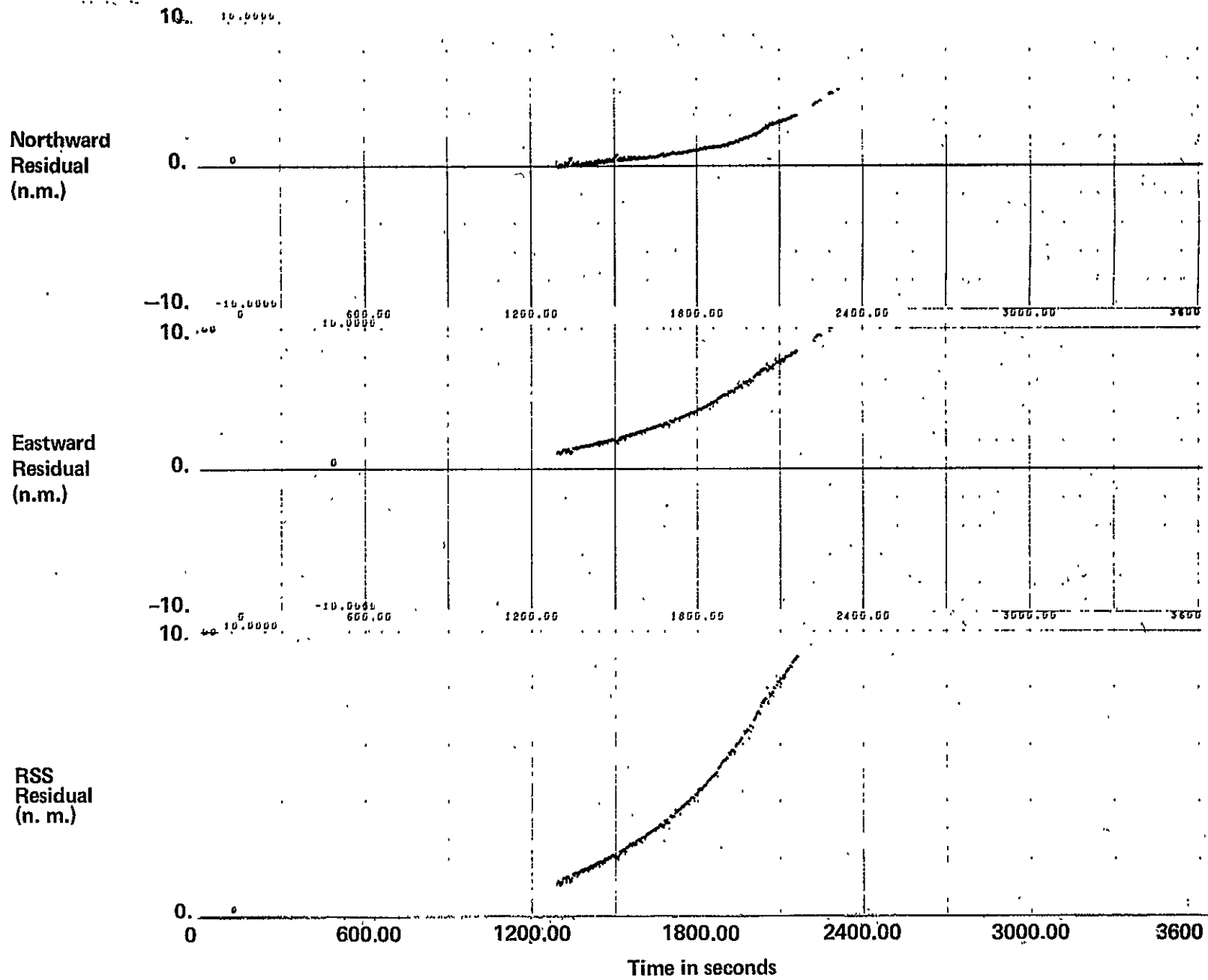


Figure B.3 SFT530A SIRU/DME position residuals

ORIGINAL PAGE IS
OF POOR QUALITY

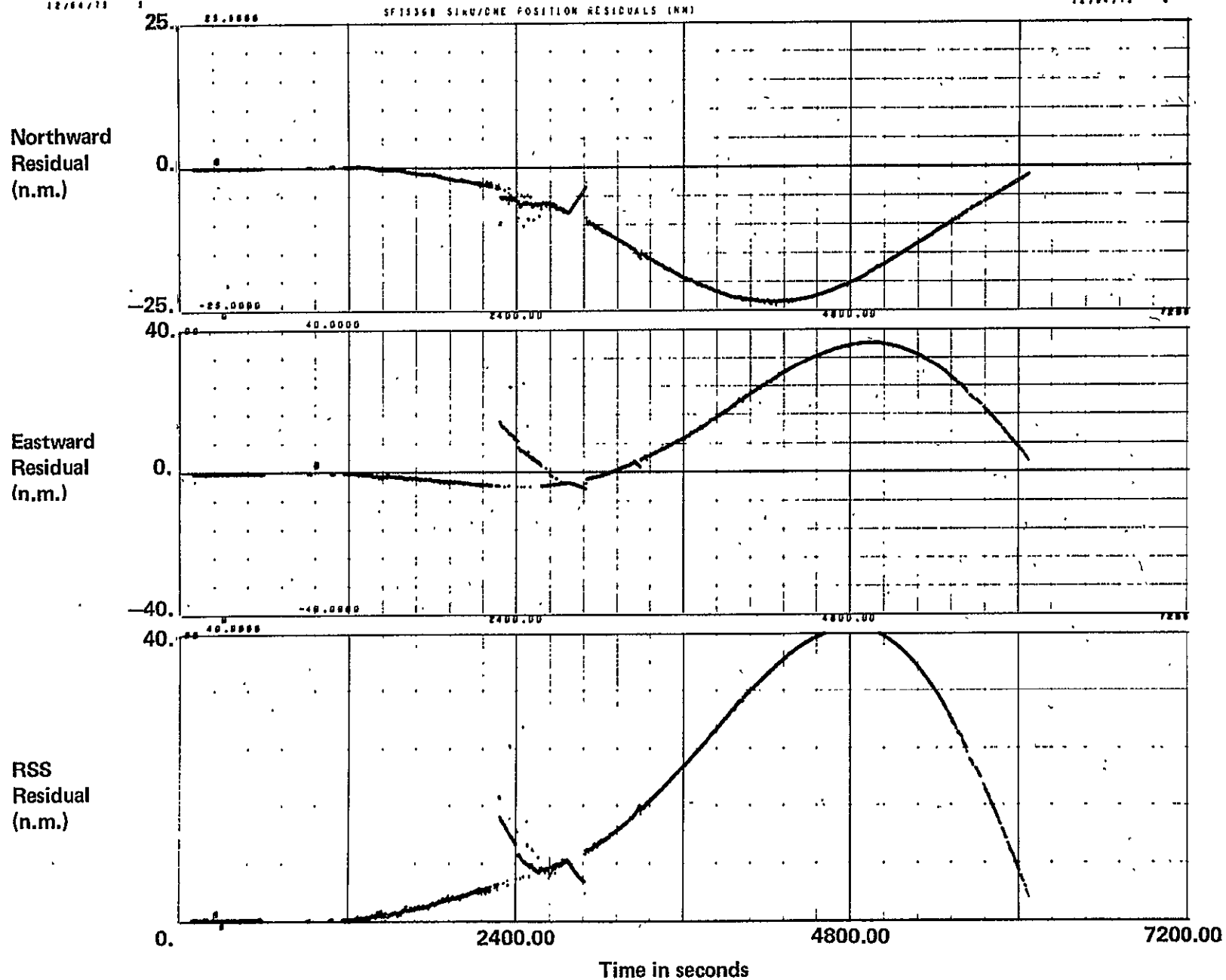


Figure B.4 SFT530B SIRU/DME position residuals

ORIGINAL PAGE IS
OF POOR QUALITY

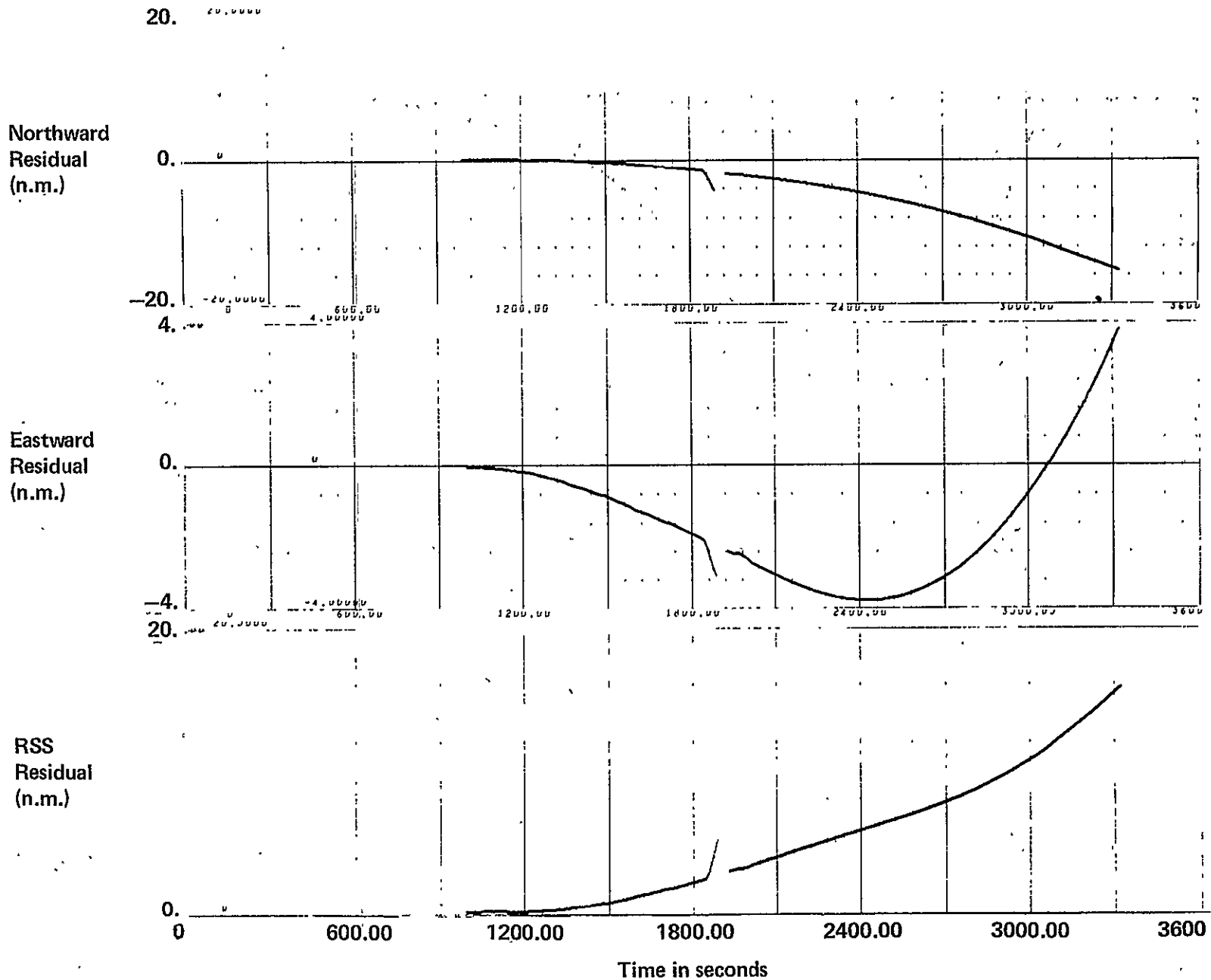


Figure B.5 SFT530B SIRU/radar position residuals

611

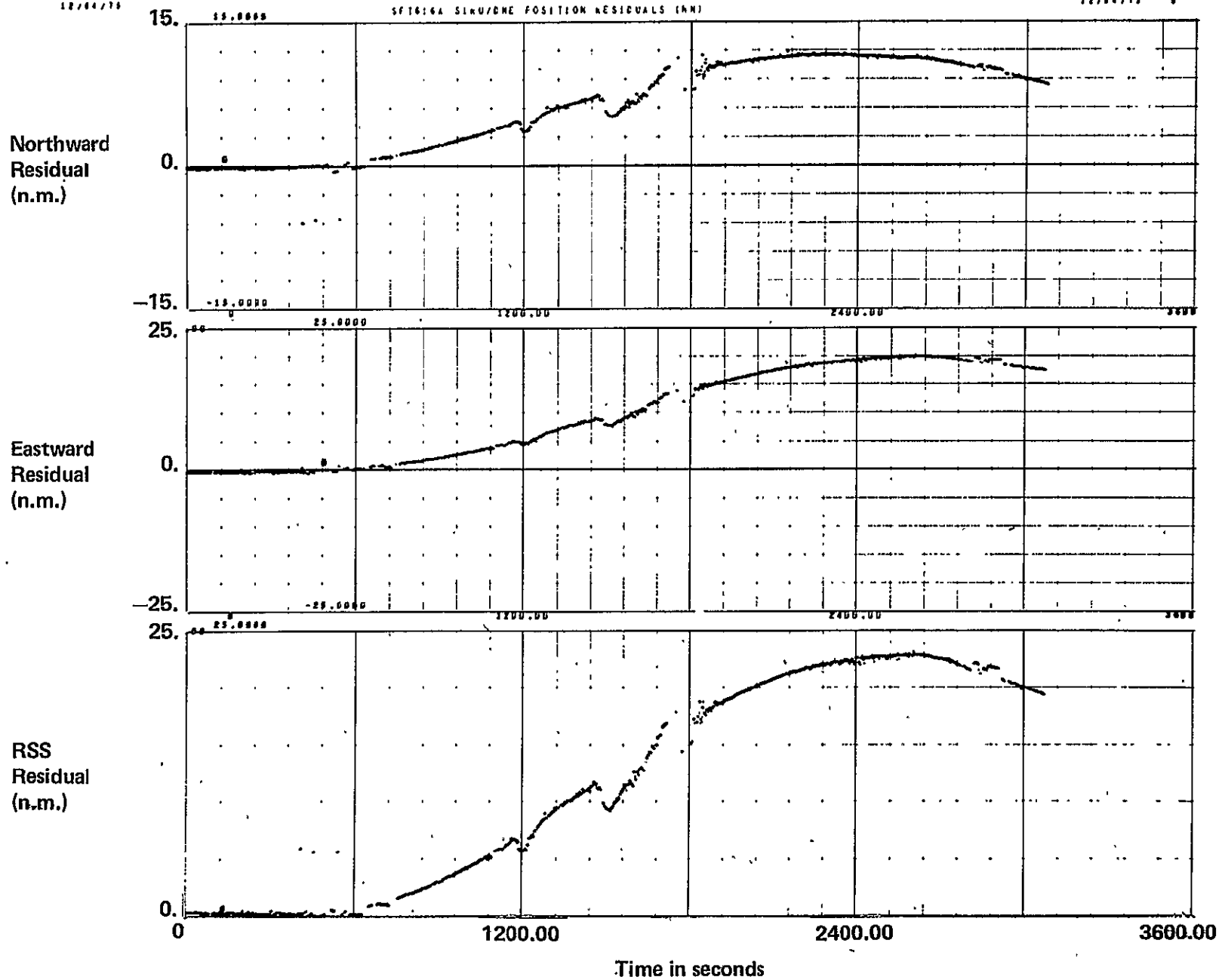


Figure B.6 SFT616A SIRU/DME position residuals

5. 5.00000

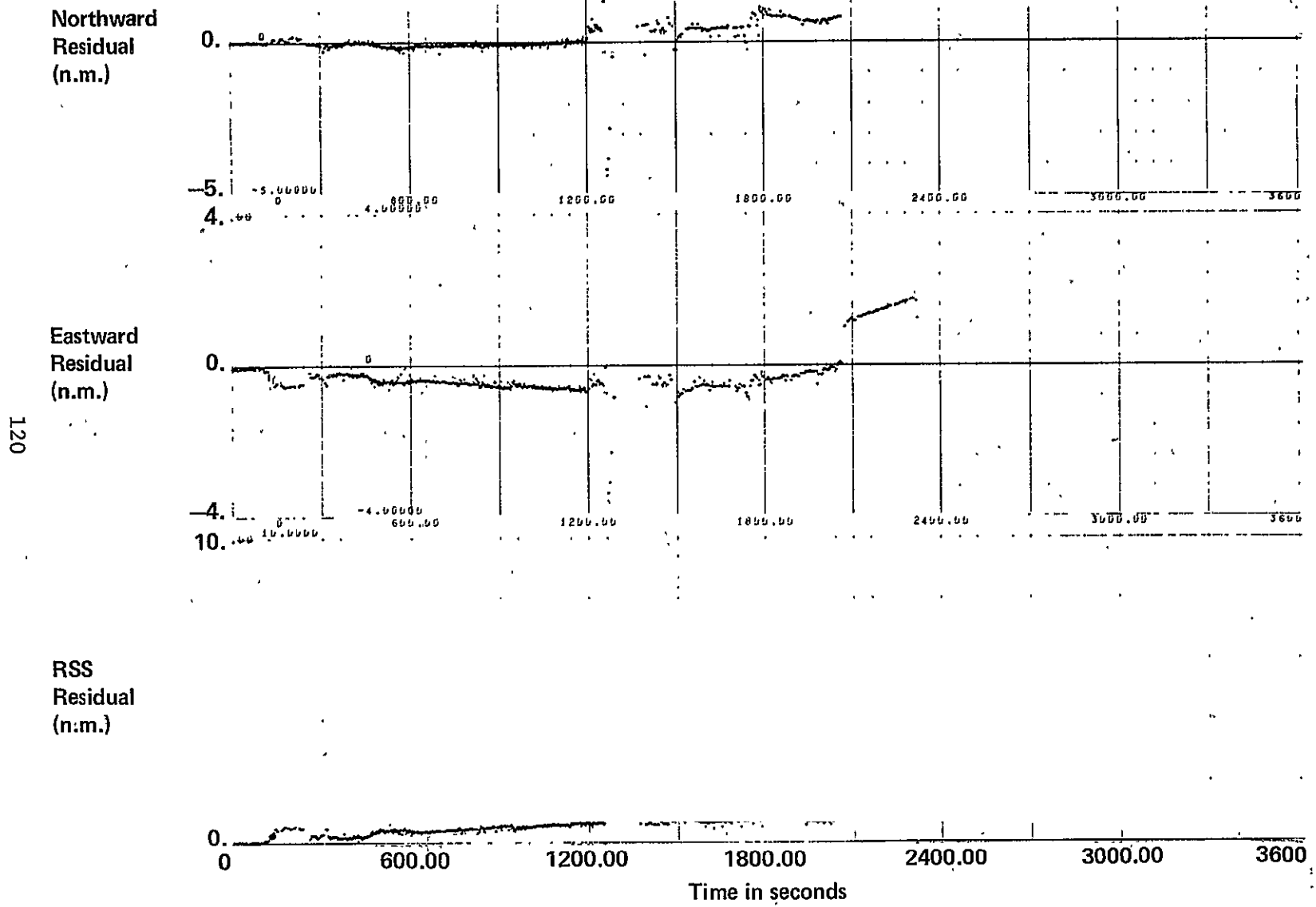
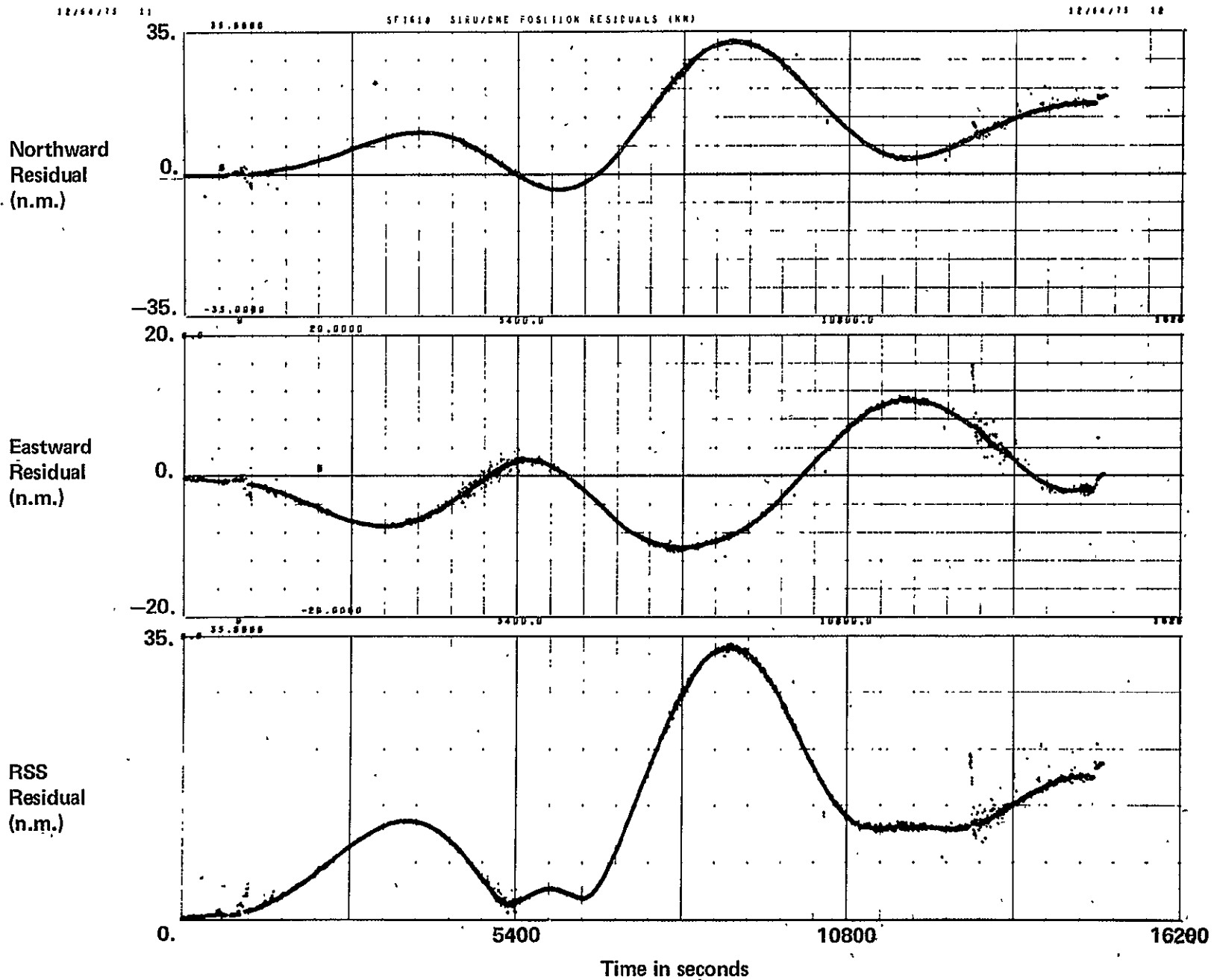


Figure B.7 SFT616B SIRU/DME position residuals

ORIGINAL PAGE IS
OF POOR QUALITY



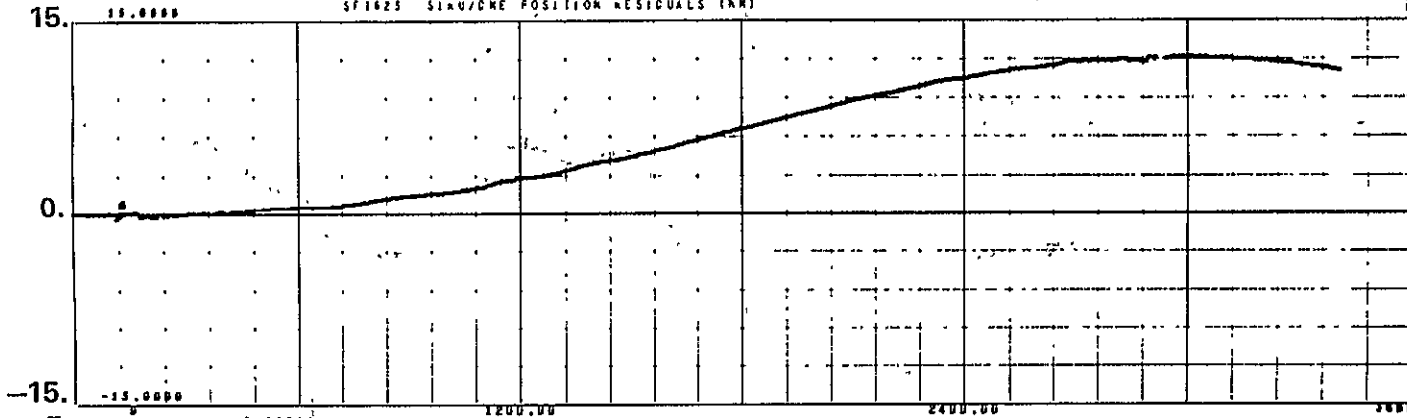
121

Figure B.8 SFT618 SIRU/DME position residuals

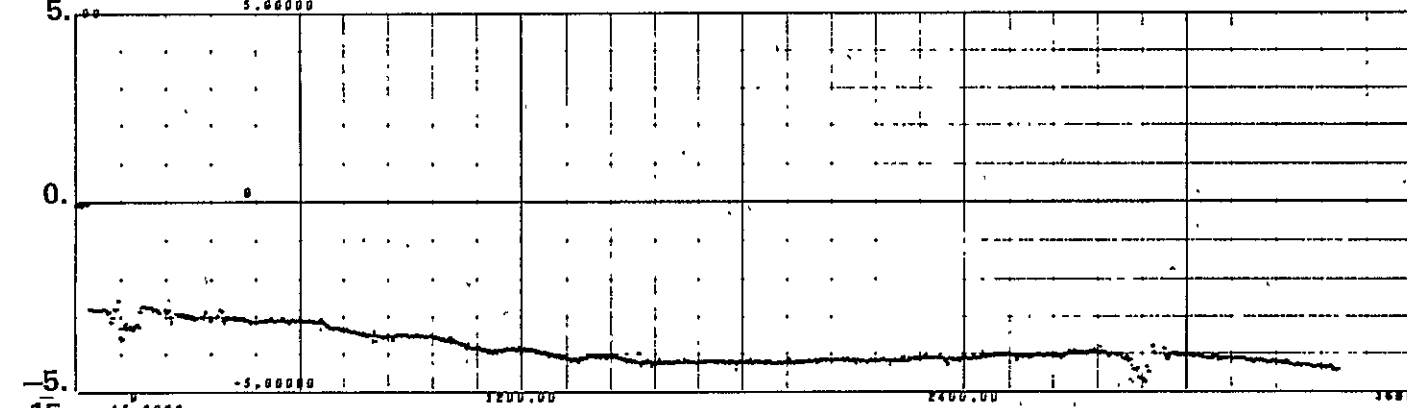
ORIGINAL PAGE IS
OF POOR QUALITY

SFT625 SIRU/DME POSITION RESIDUALS (NM)

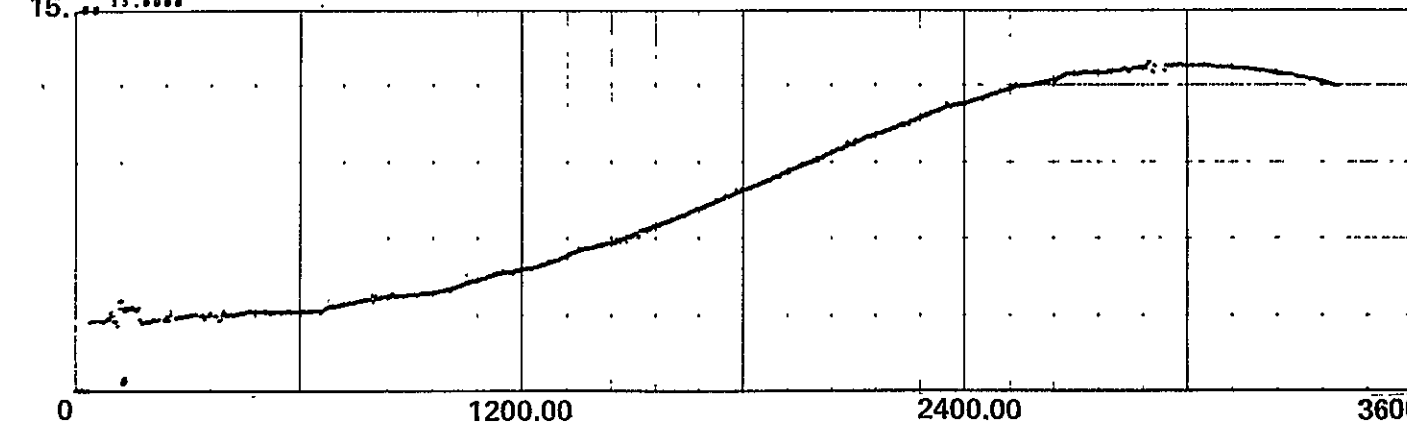
Northward Residual (n.m.)



Eastward Residual (n.m.)



RSS Residual (n.m.)

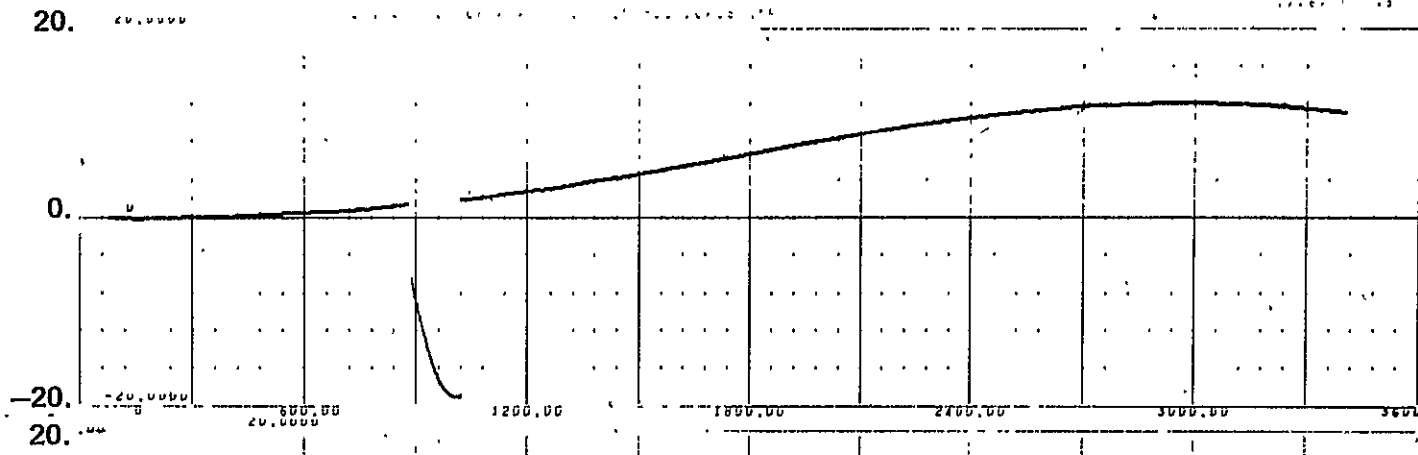


Time in seconds

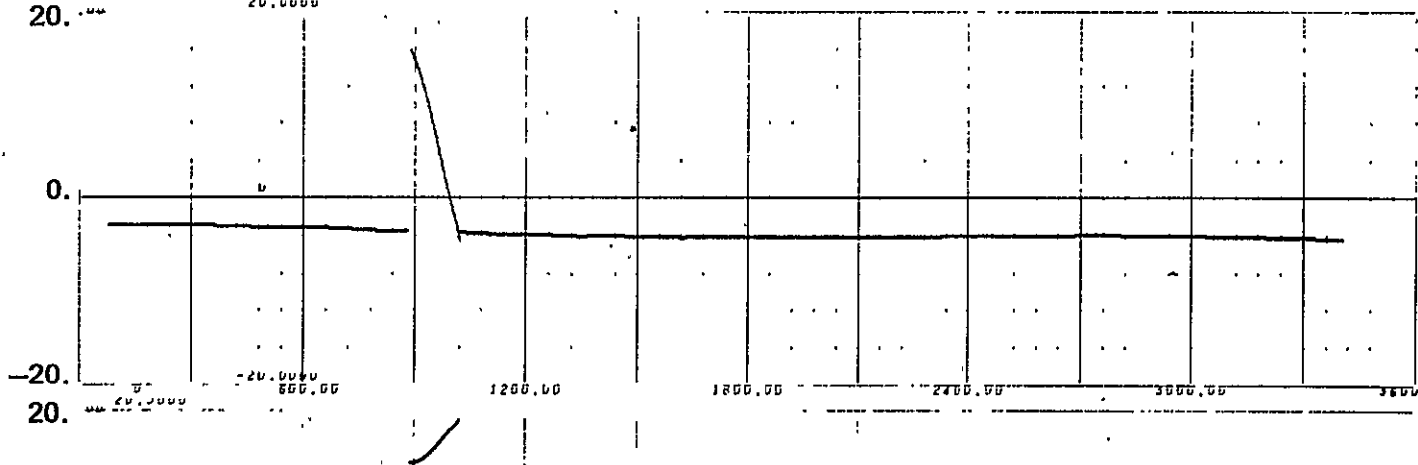
Figure B.9 SFT625 SIRU/DME position residuals

122

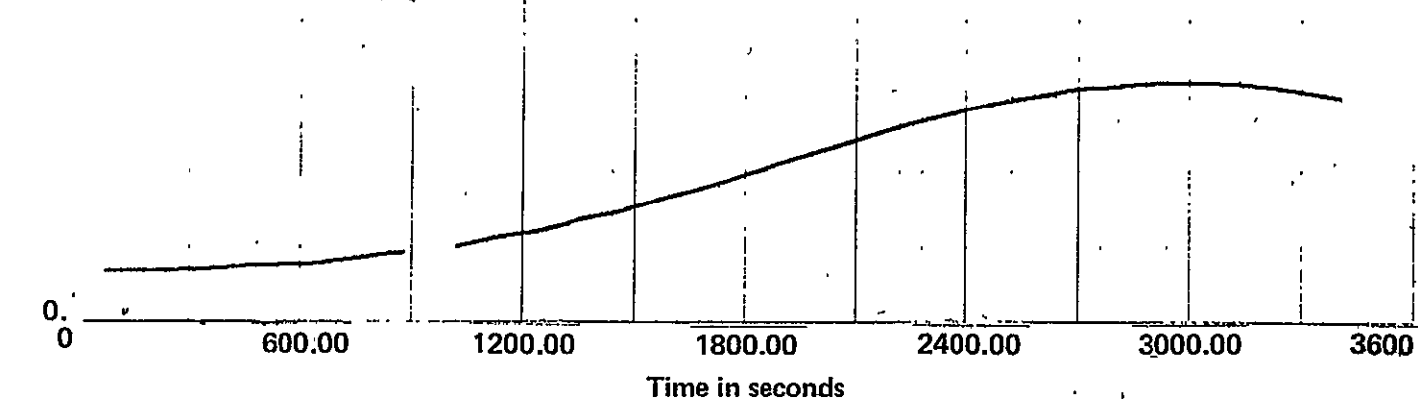
Northward
Residual
(n.m.)



Eastward
Residual
(n.m.)



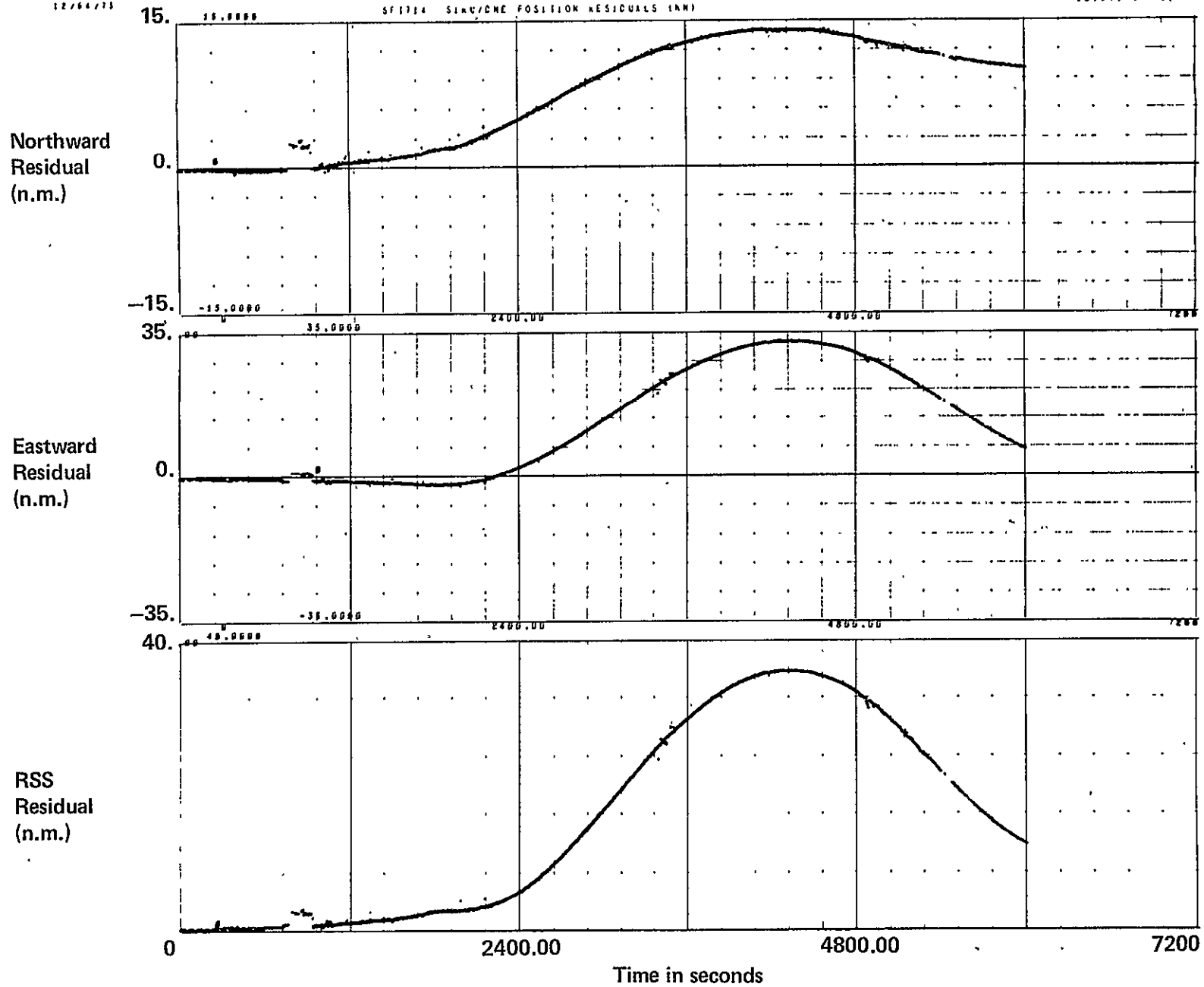
RSS
Residual
(n.m.)



123

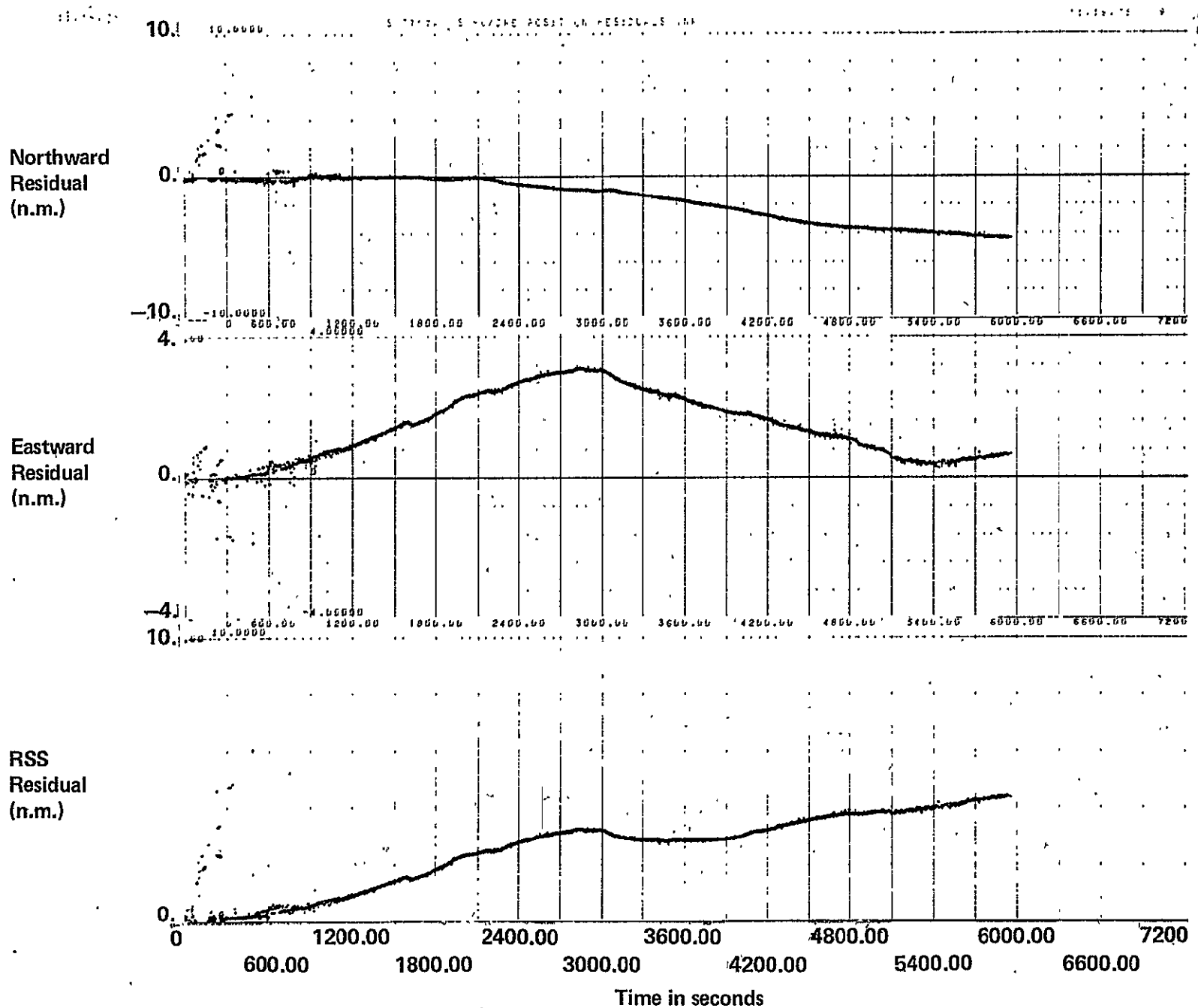
Figure B.10 SFT625 SIRU/radar position residuals

ORIGINAL PAGE IS
OF POOR QUALITY



124

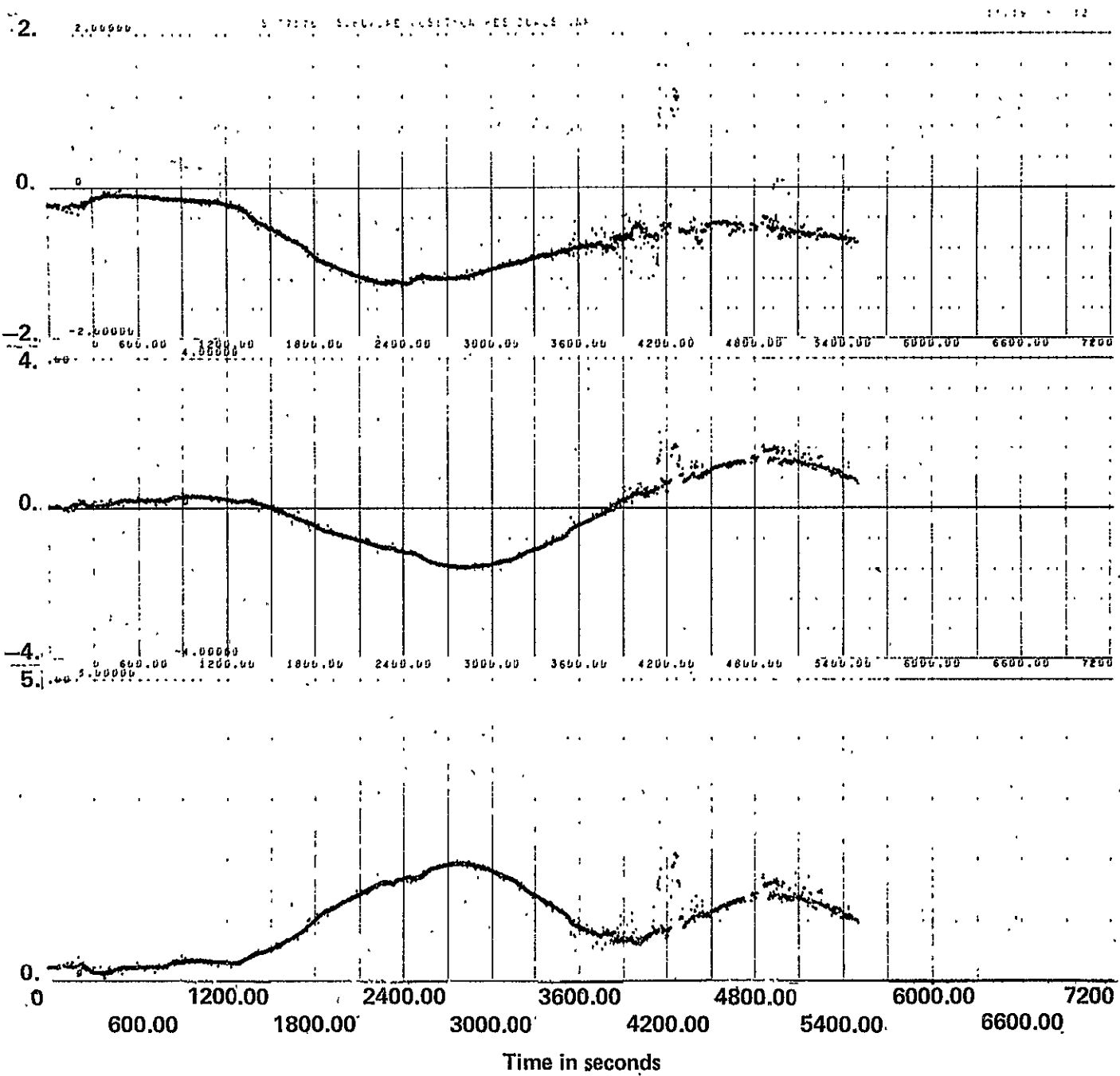
Figure B.11 SFT714 SIRU/DME position residuals



125

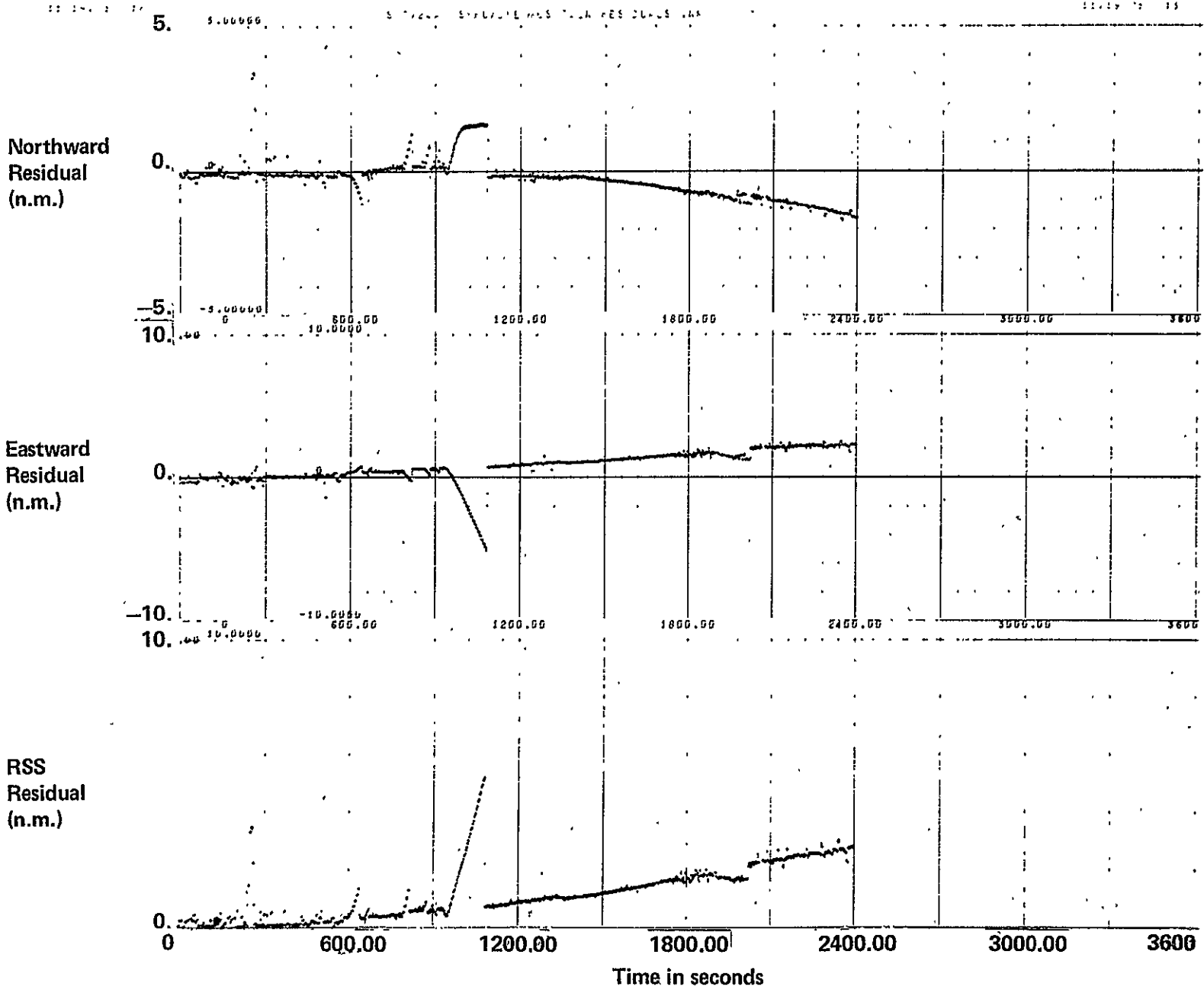
ORIGINAL PAGE IS
OF POOR QUALITY

Figure B.12 SFT717A SIRU/DME position residuals



126

Figure B.13 SFT717B SIRU/DME position residuals



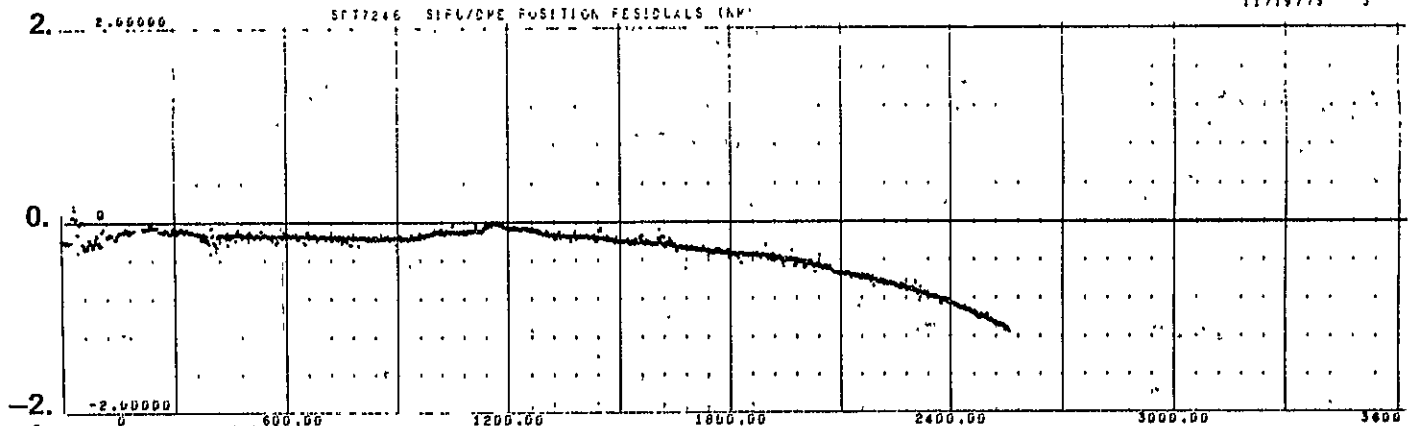
127

Figure B.14 SFT724A SIRU/DME position residuals

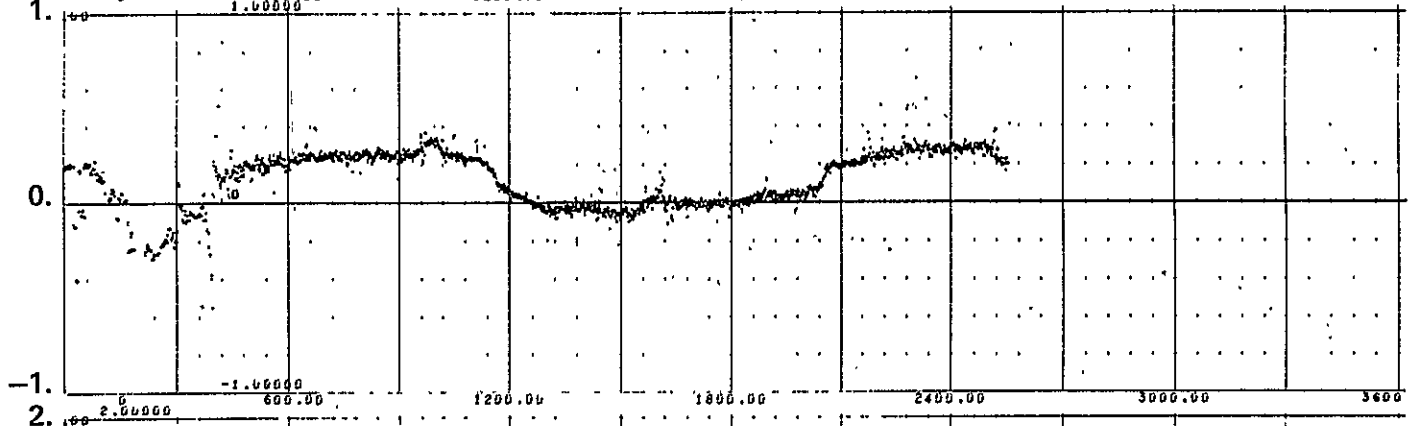
ORIGINAL PAGE IS
OF POOR QUALITY

SFT724B SIRU/DME POSITION RESIDUALS (NM)

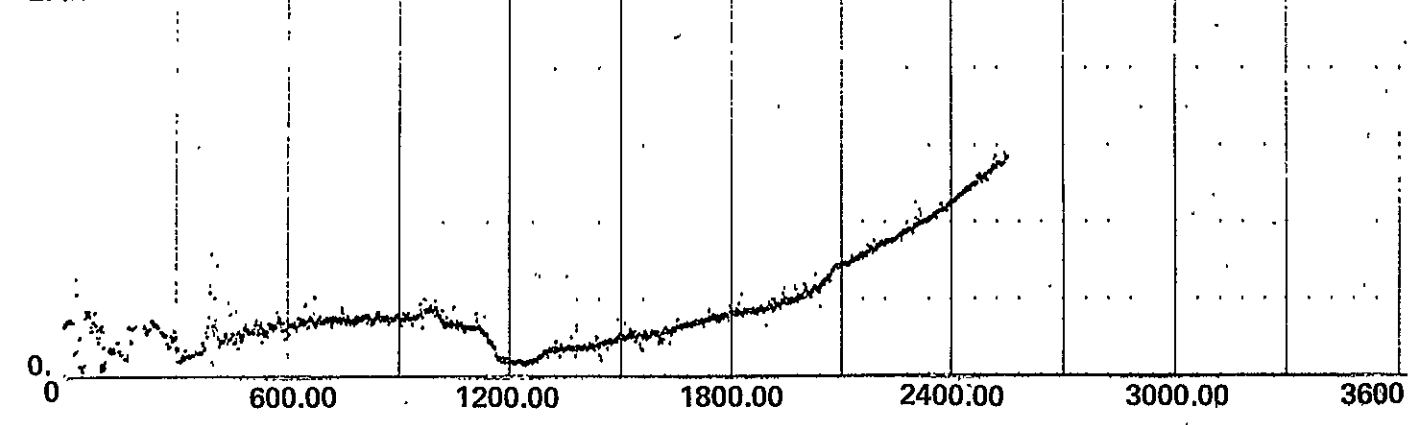
Northward Residual (n.m.)



Eastward Residual (n.m.)



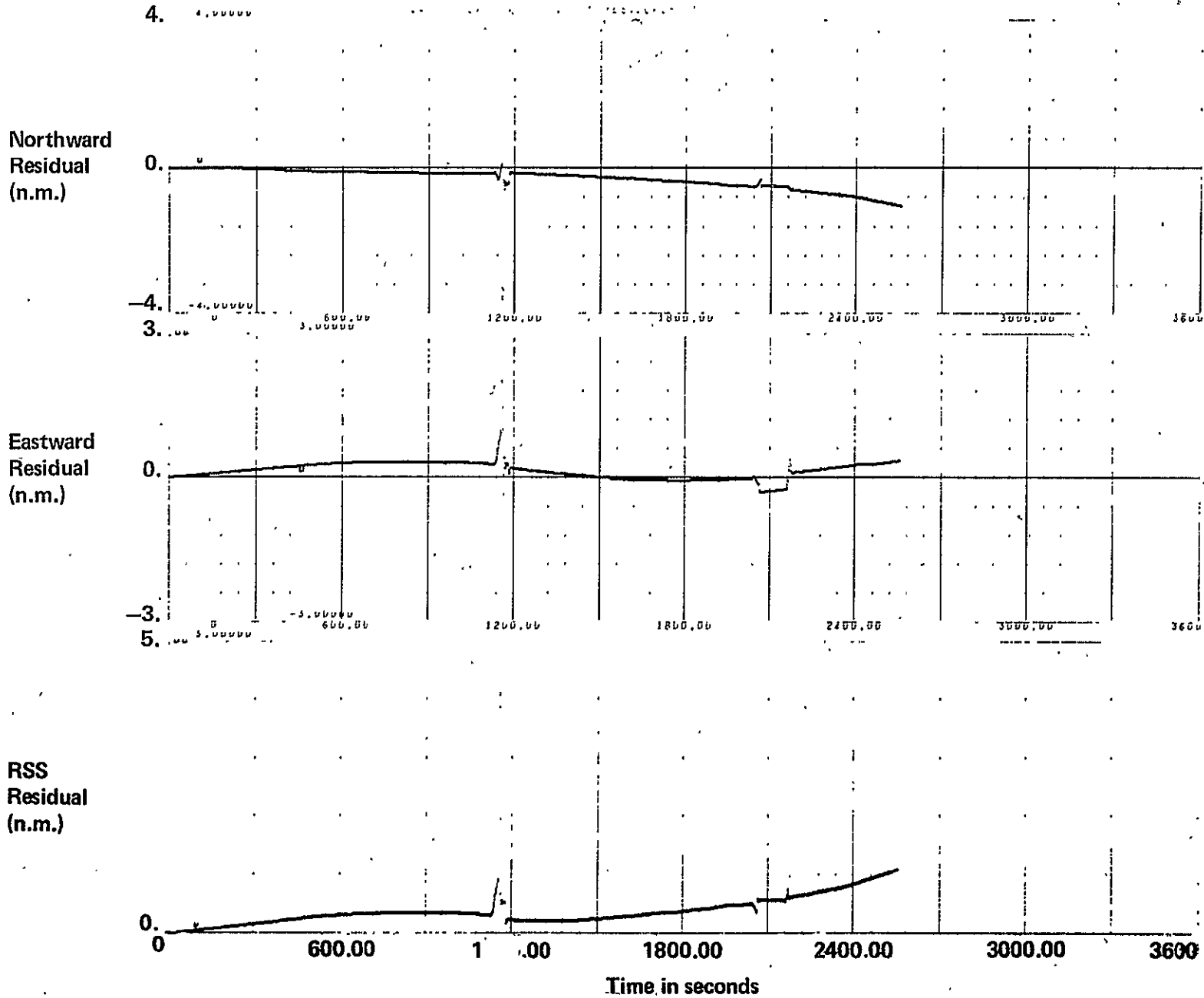
RSS Residual (n.m.)



Time in seconds

Figure B.15 SFT724B SIRU/DME position residuals

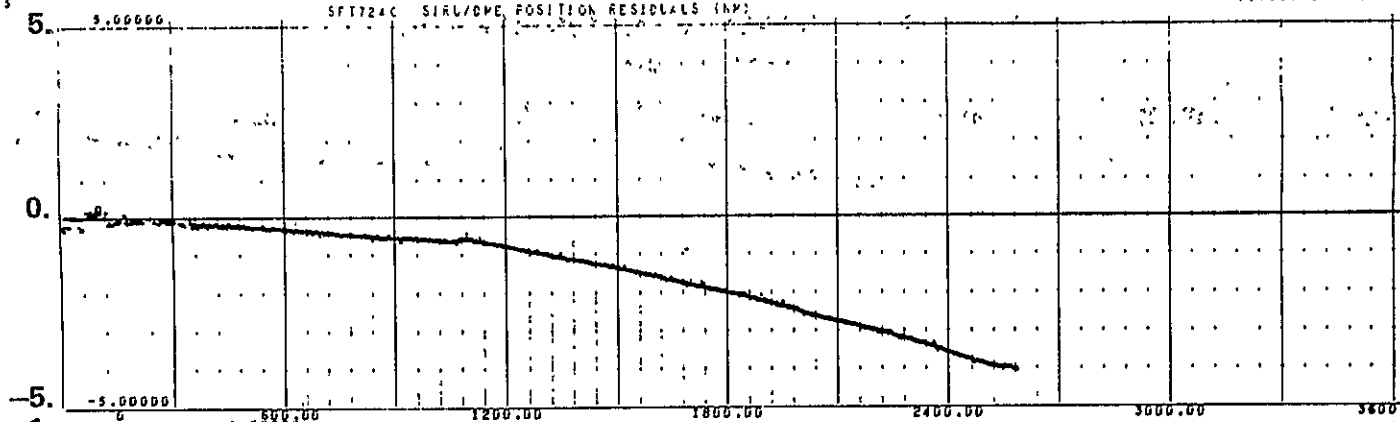
ORIGINAL PAGE IS
OF POOR QUALITY



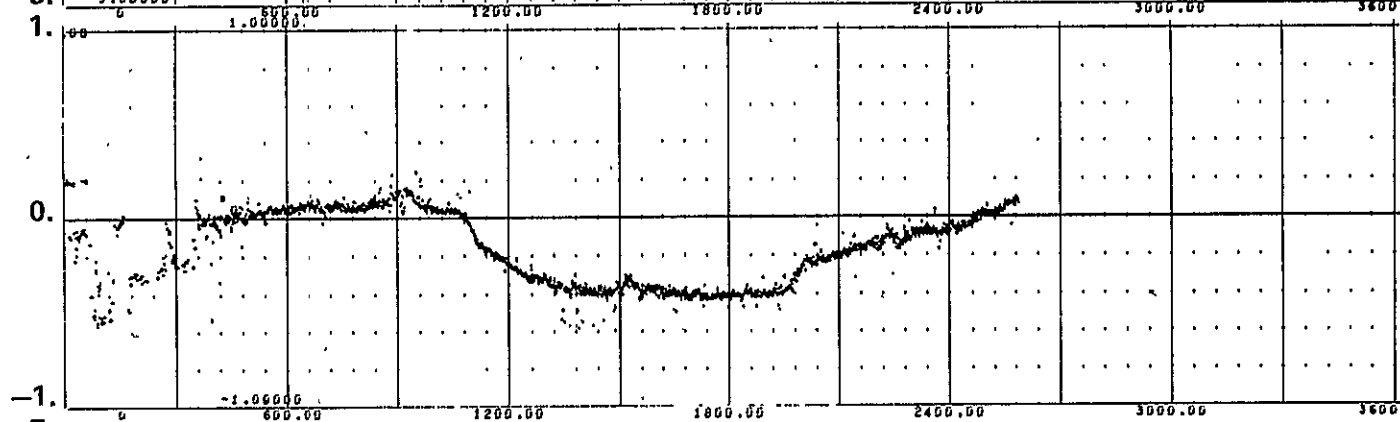
129

Figure B.16 SFT724B SIRU/radar position residuals

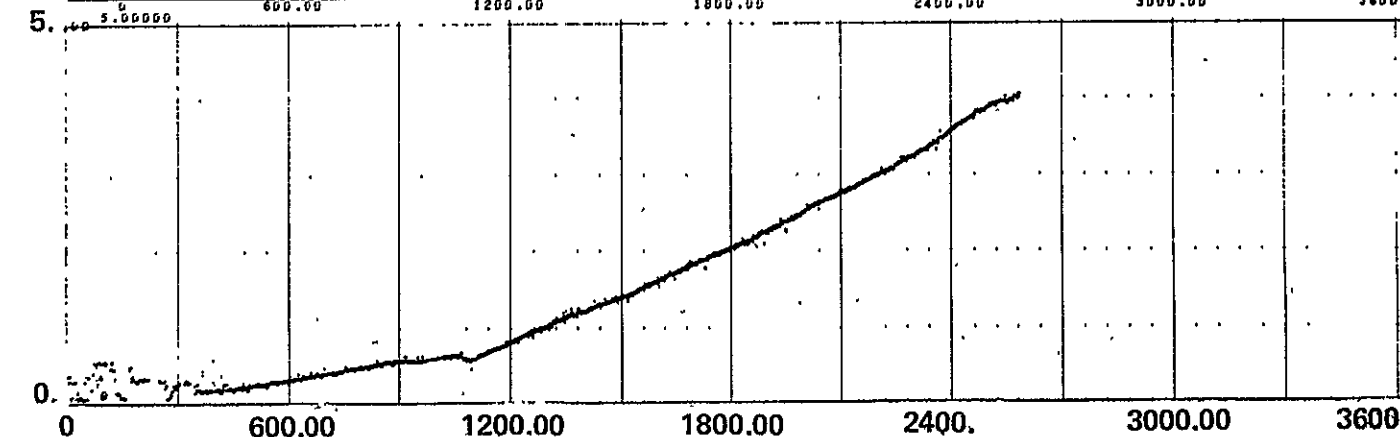
Northward
Residual
(n.m.)



Eastward
Residual
(n.m.)



RSS
Residual
(n.m.)



Time in seconds

Figure B.17 SFT724C SIRU/DME position residuals

130

131

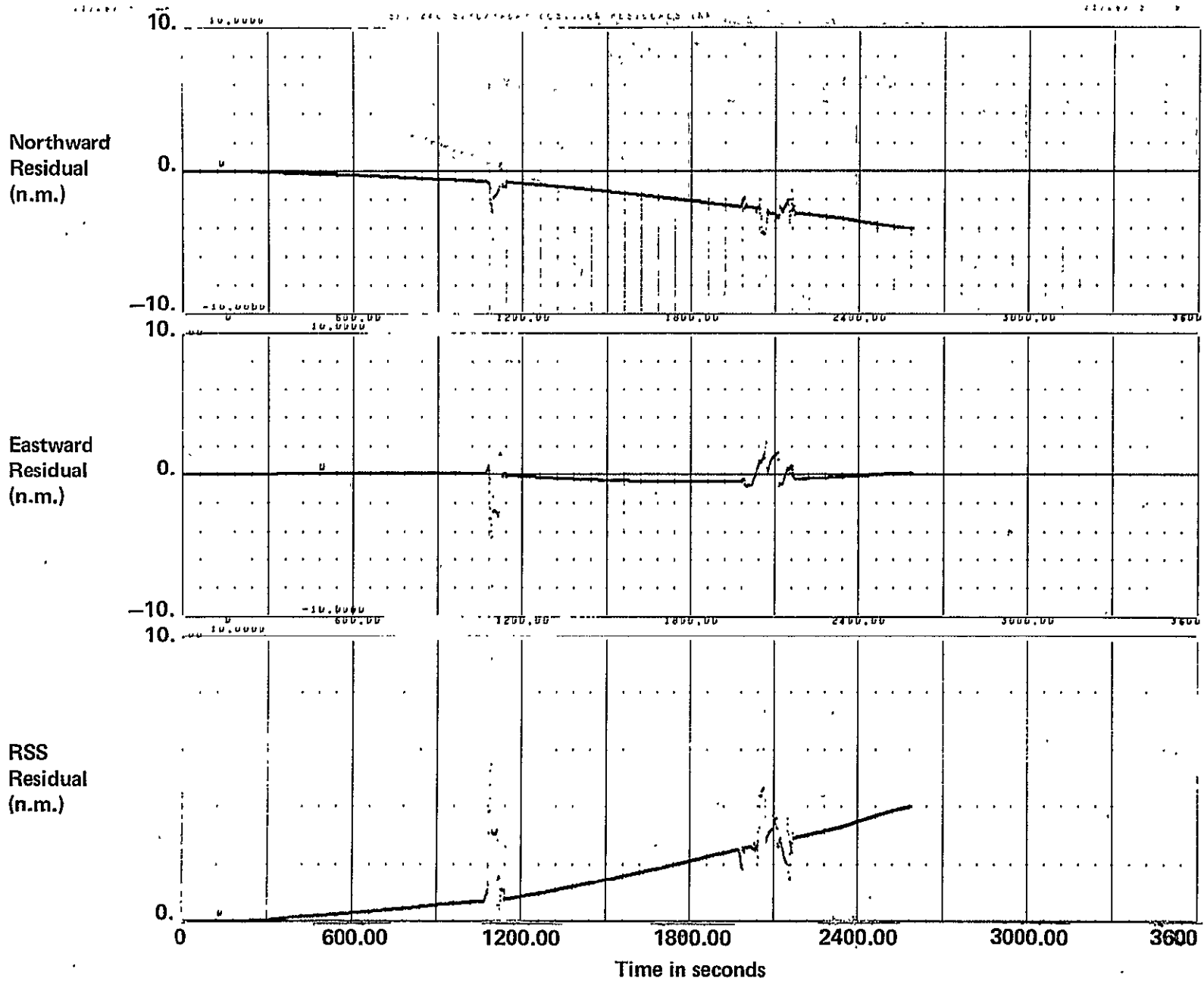


Figure B.18 SFT724C SIRU/radar position residuals

ORIGINAL PAGE IS
OF POOR QUALITY

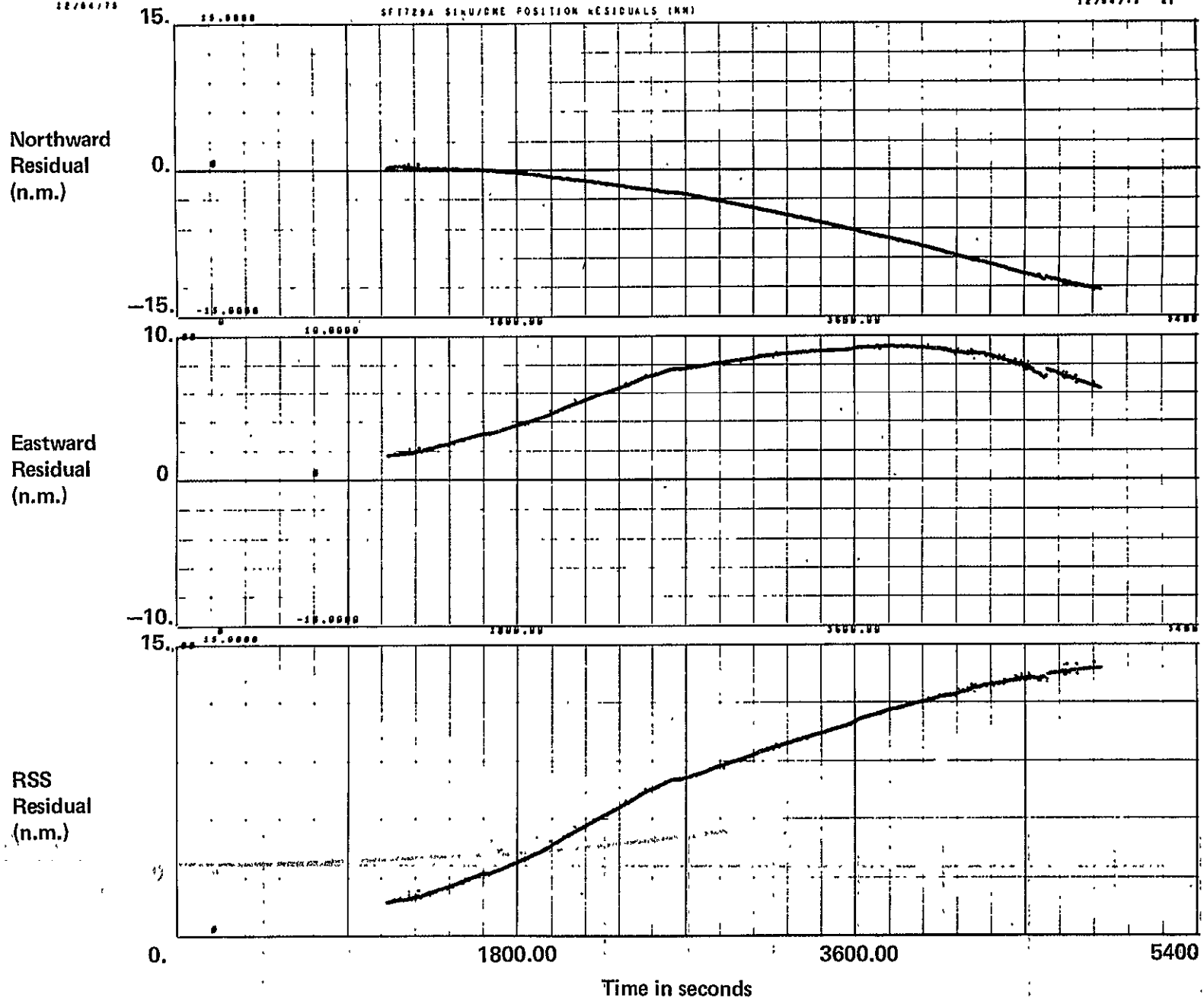


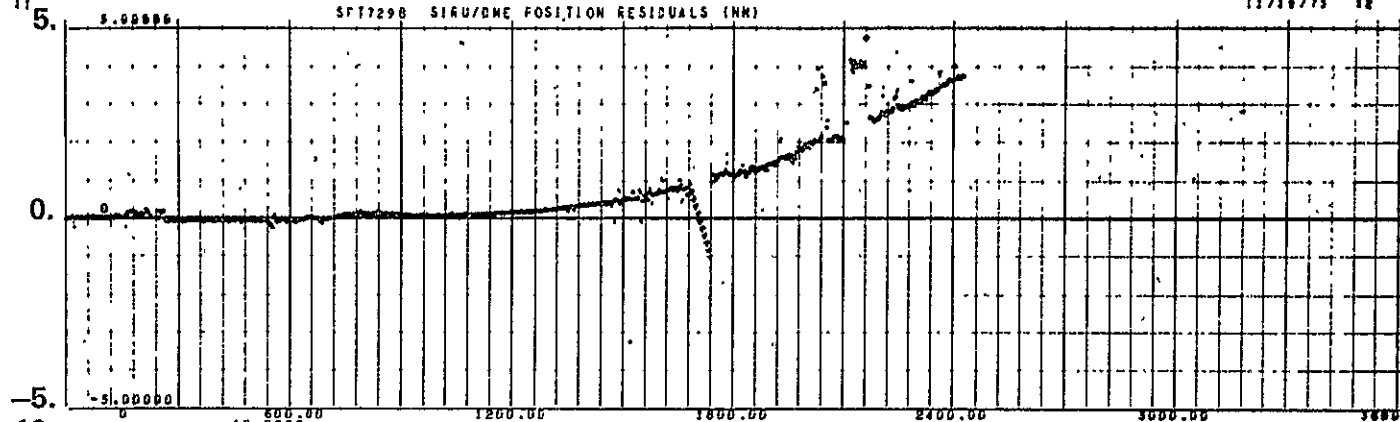
Figure B.19 SFT729A SIRU/DME position residuals

11/19/75

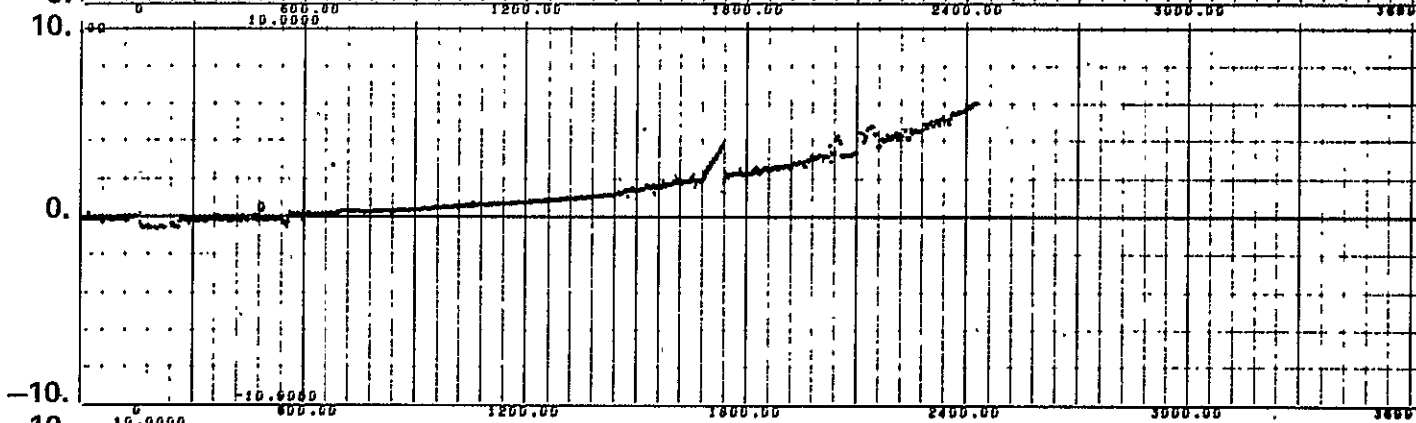
11/19/75 12

SFT729B SIRU/DME POSITION RESIDUALS (NM)

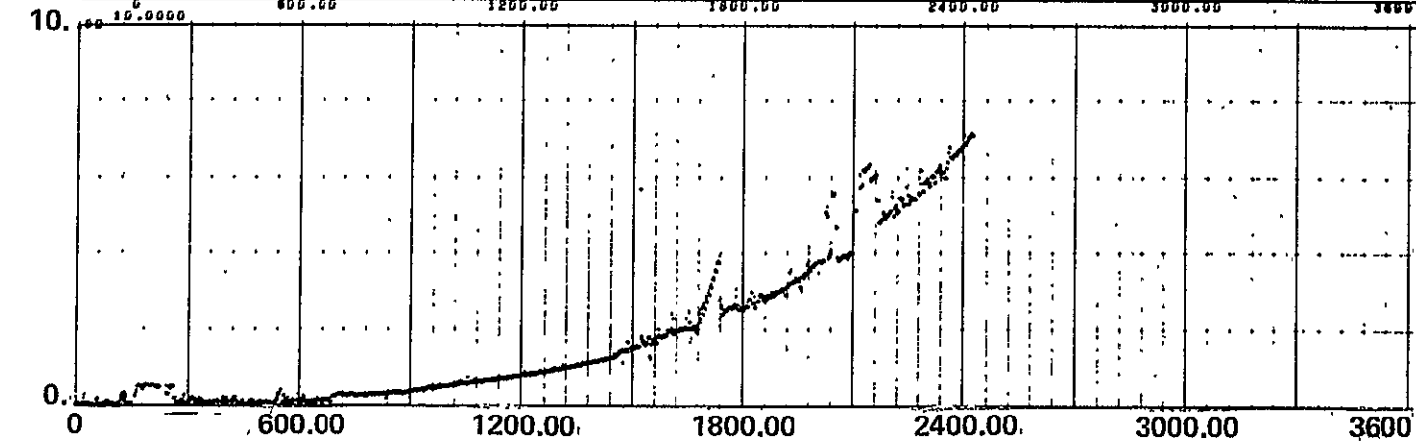
Northward Residual (n.m.)



Eastward Residual (n.m.)



RSS Residual (n.m.)

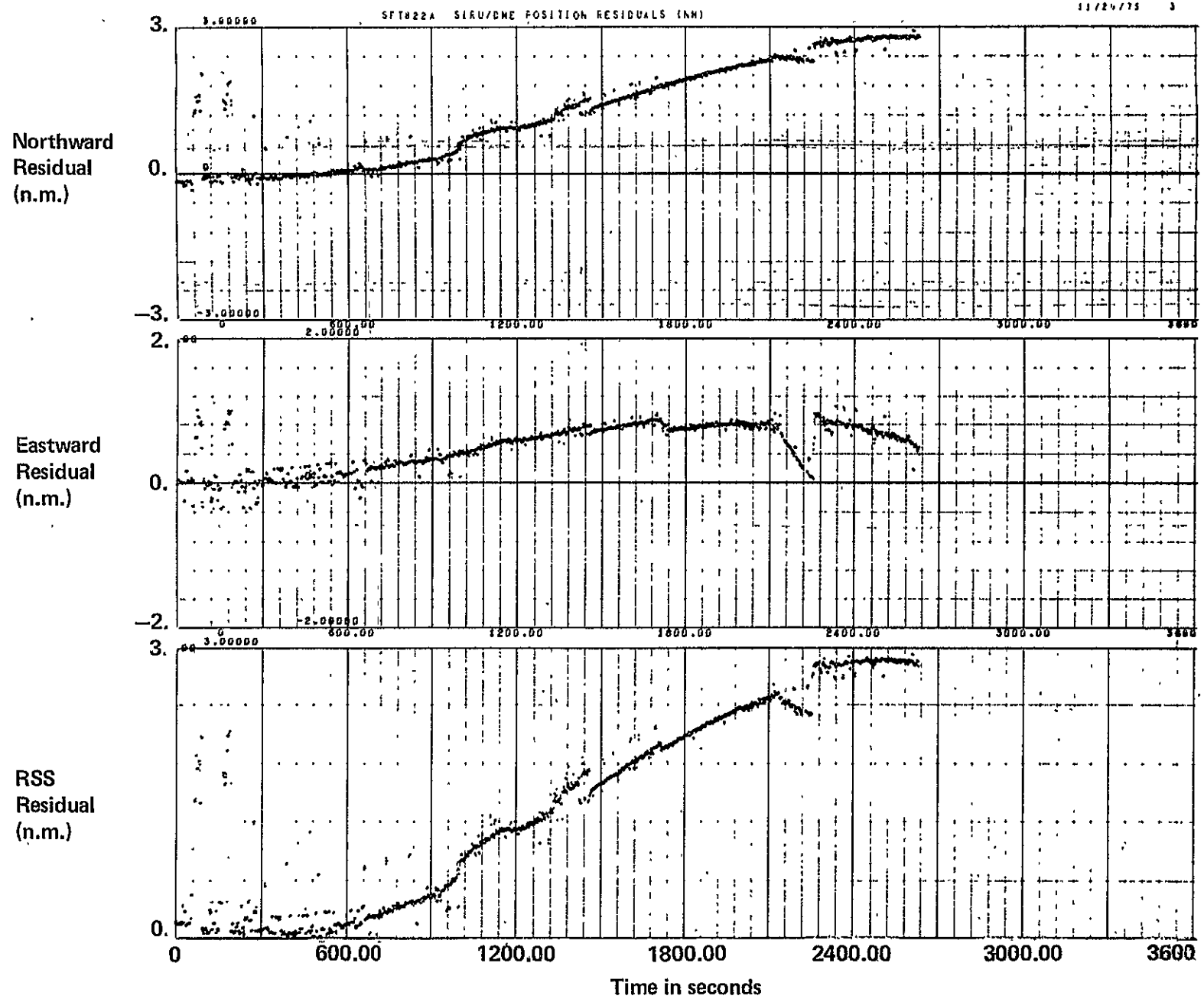


Time in seconds

Figure B.20 SFT729B SIRU/DME position residuals

ORIGINAL PAGE IS
OF POOR QUALITY

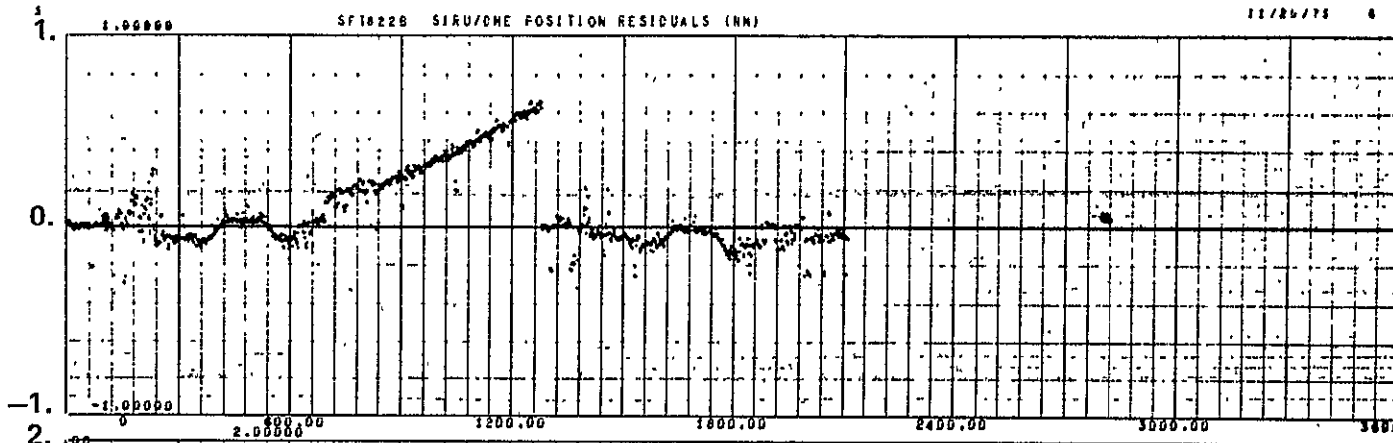
133



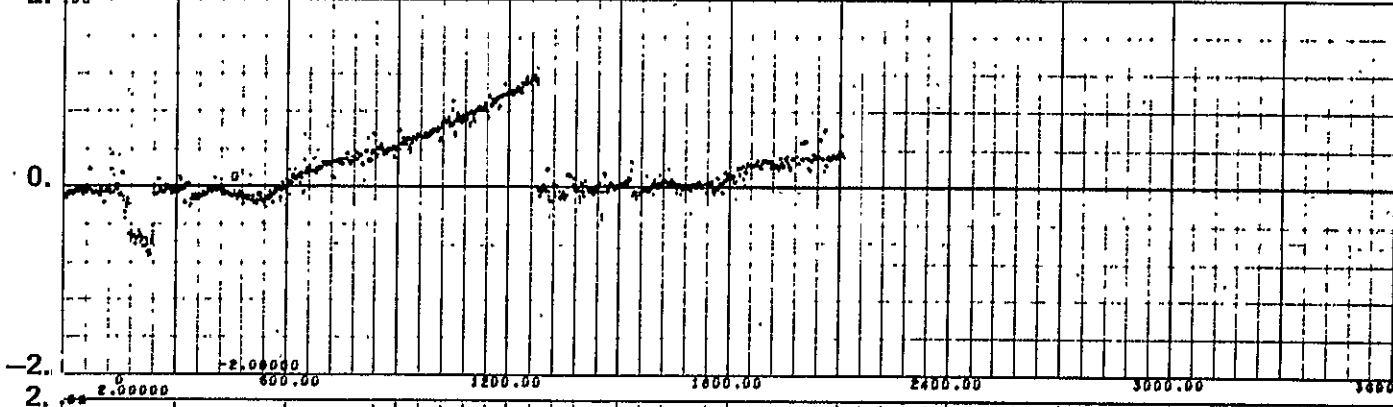
134

Figure B.21 SFT822A SIRU/DME position residuals

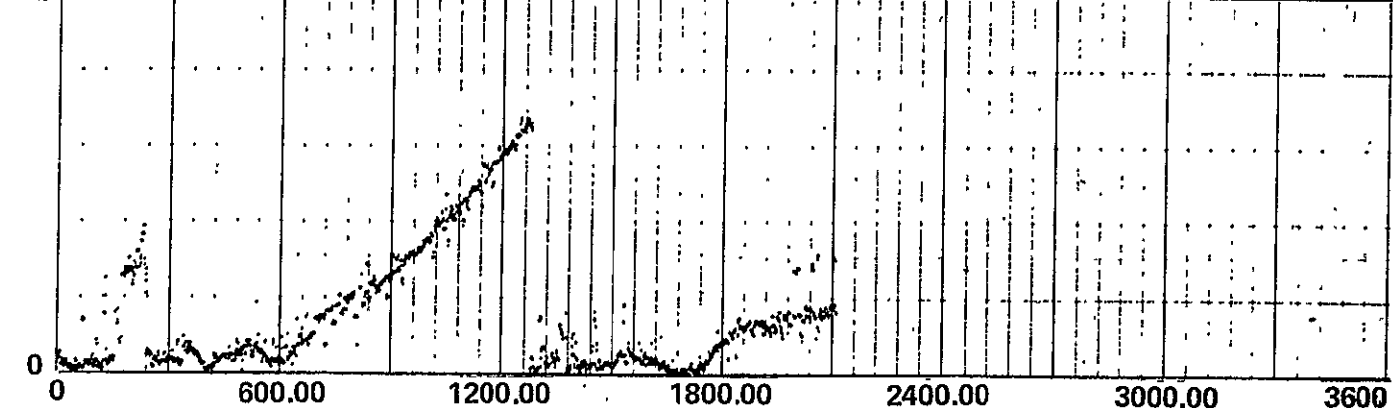
Northward
Residual
(n.m.)



Eastward
Residual
(n.m.)



RSS
Residual
(n.m.)

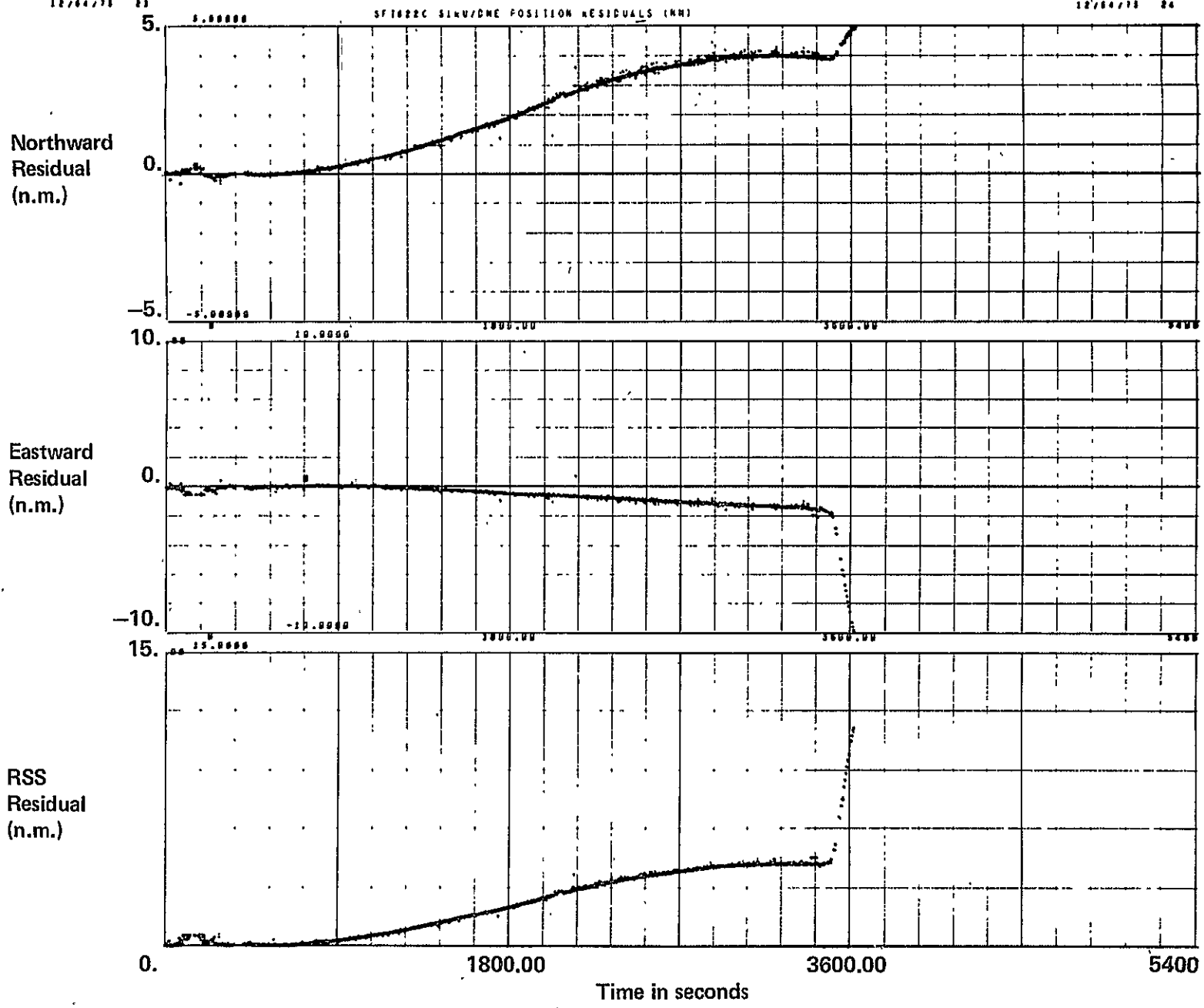


Time in seconds

Figure B.22 SFT822B SIRU/DME position residuals

135

ORIGINAL PAGE IS
OF POOR QUALITY



136

Figure B.23 SFT822C SIRU/DME position residuals

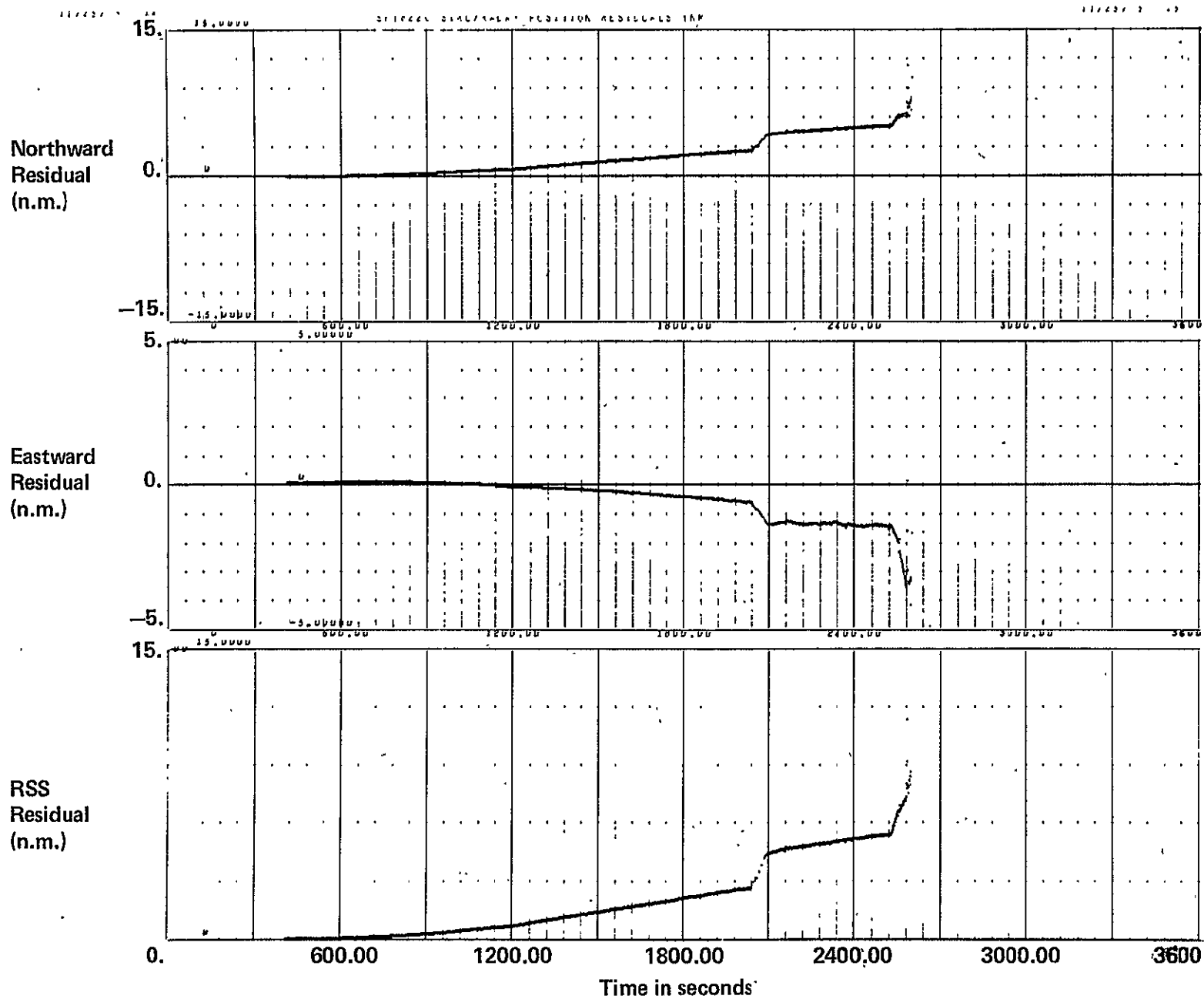
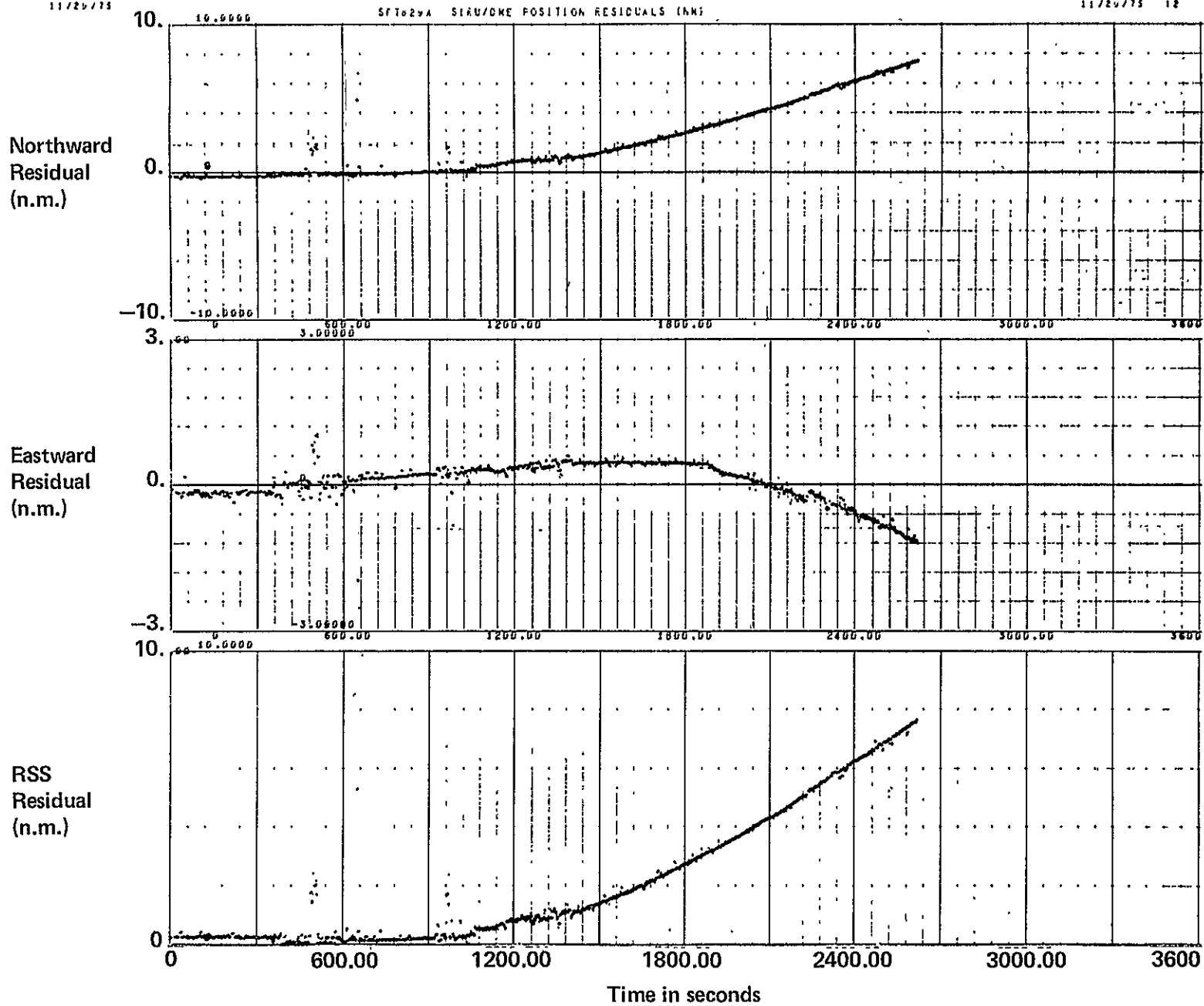


Figure B.24 SFT822C SIRU/radar position residuals

137

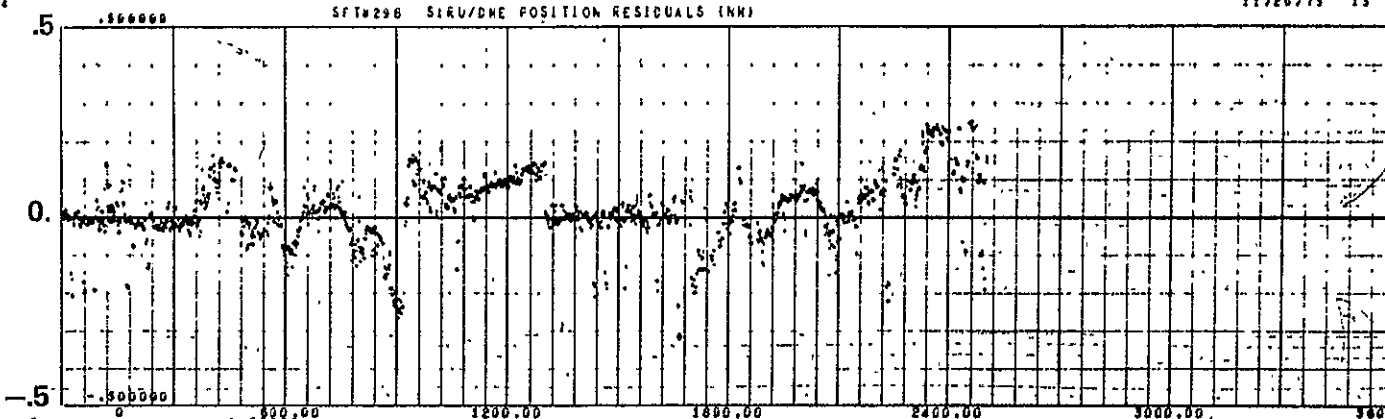
ORIGINAL PAGE IS
OF POOR QUALITY



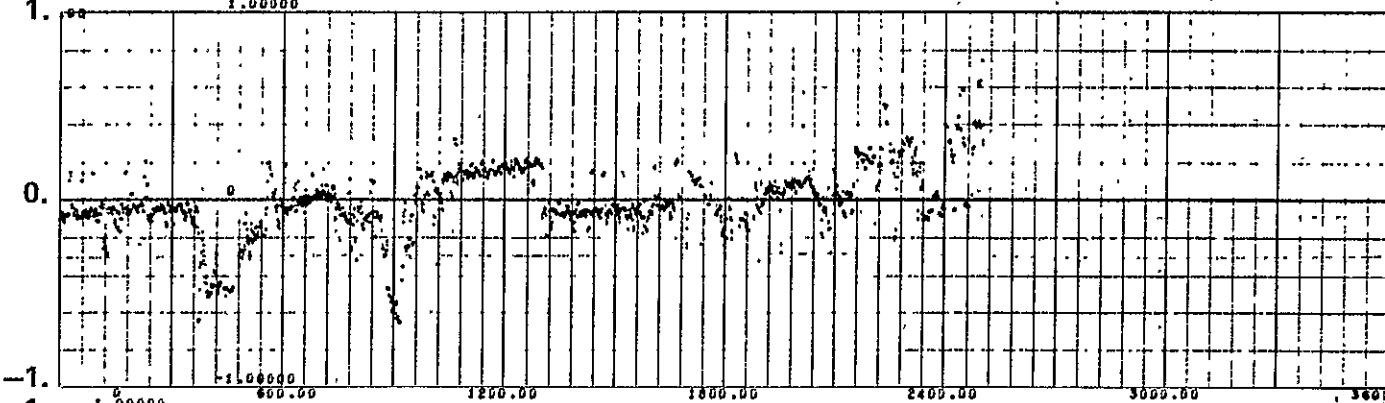
138

Figure B.25 SFT829A SIRU/DME position residuals

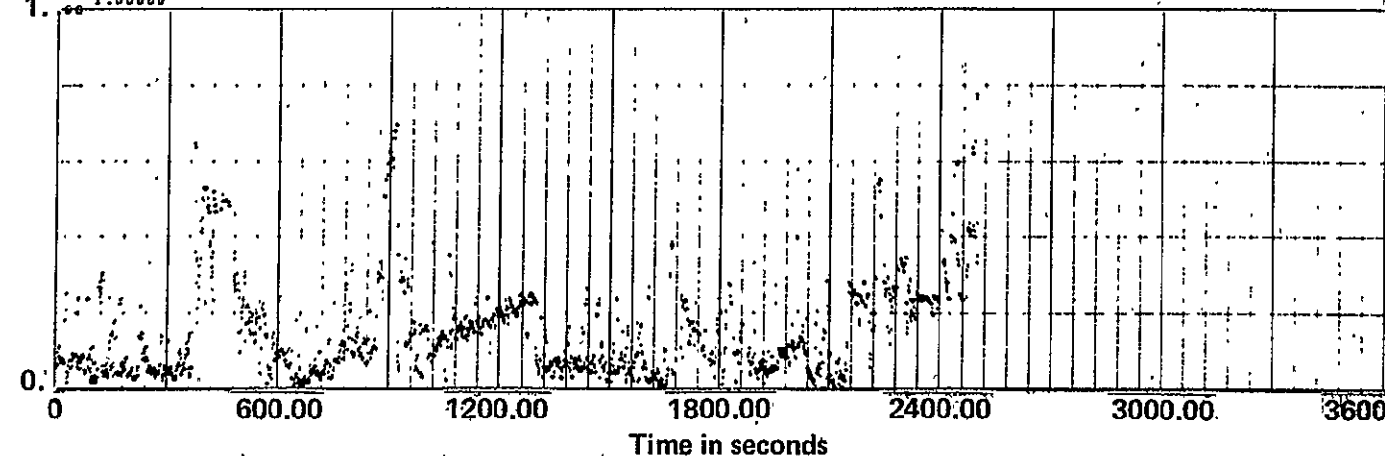
Northward Residual (n.m.)



Eastward Residual (n.m.)



RSS Residual (n.m.)

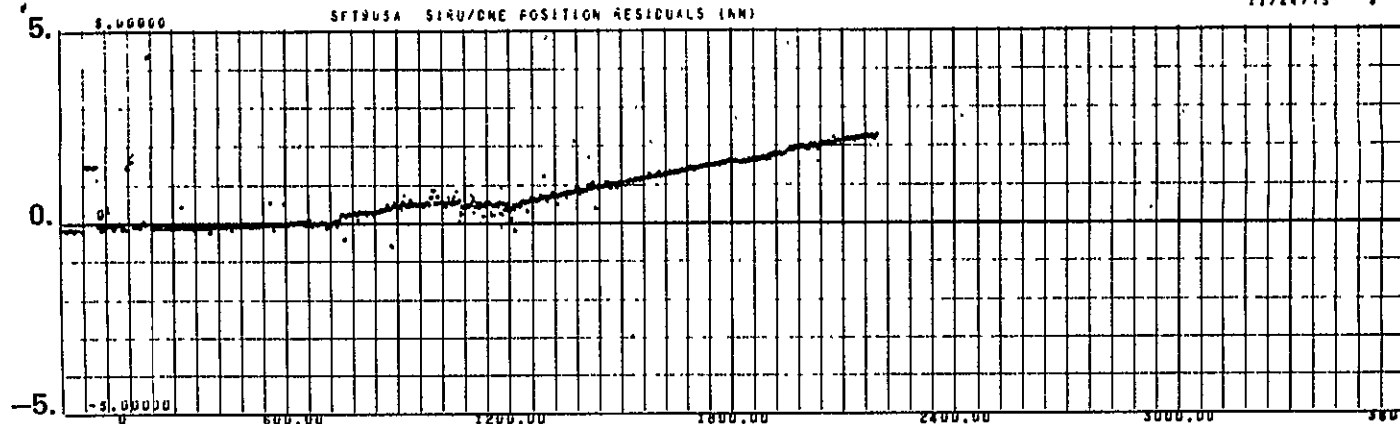


139

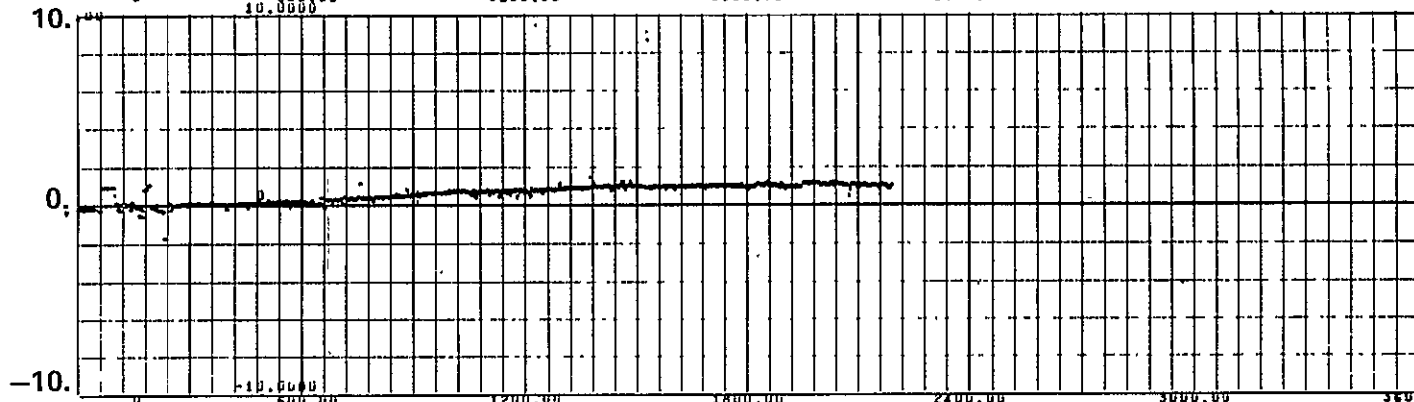
ORIGINAL PAGE IS OF POOR QUALITY

Figure B.26 SFT829B SIRU/DME position residuals

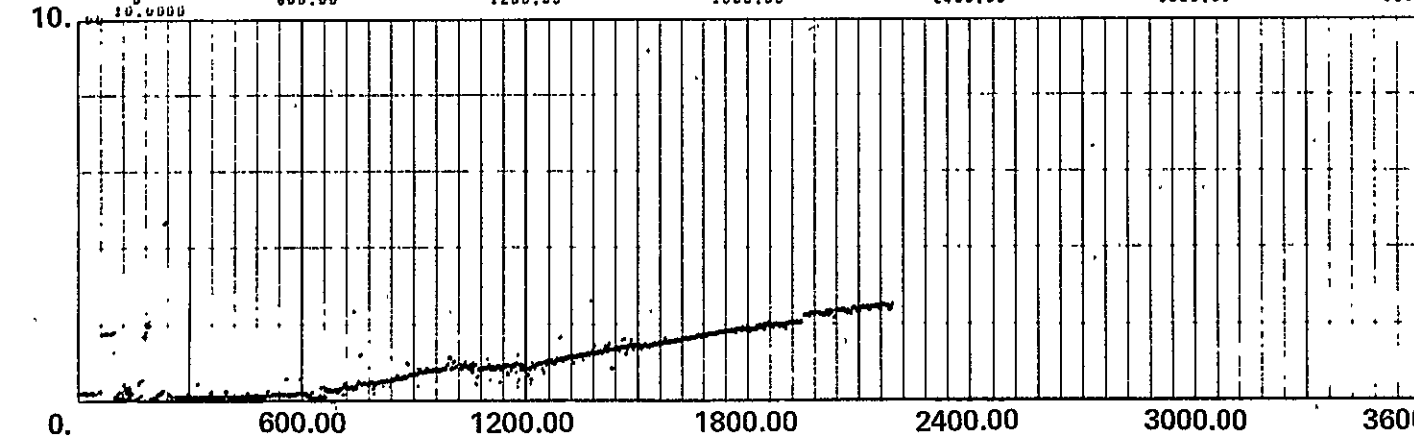
Northward
Residual
(n.m.)



Eastward
Residual
(n.m.)



RSS
Residual
(n.m.)

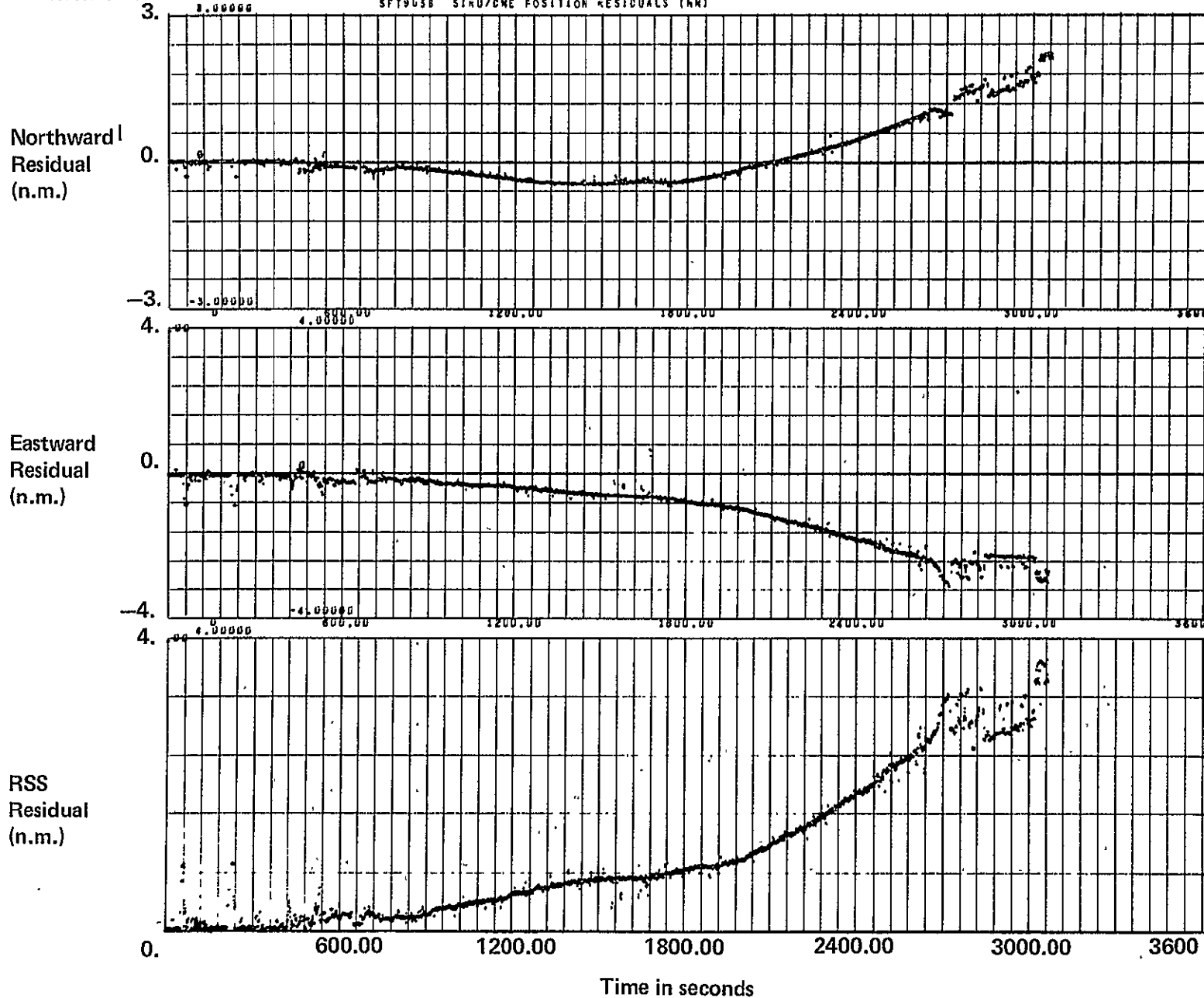


Time in seconds

Figure B.27 SFT905A SIRU/DME position residuals

140

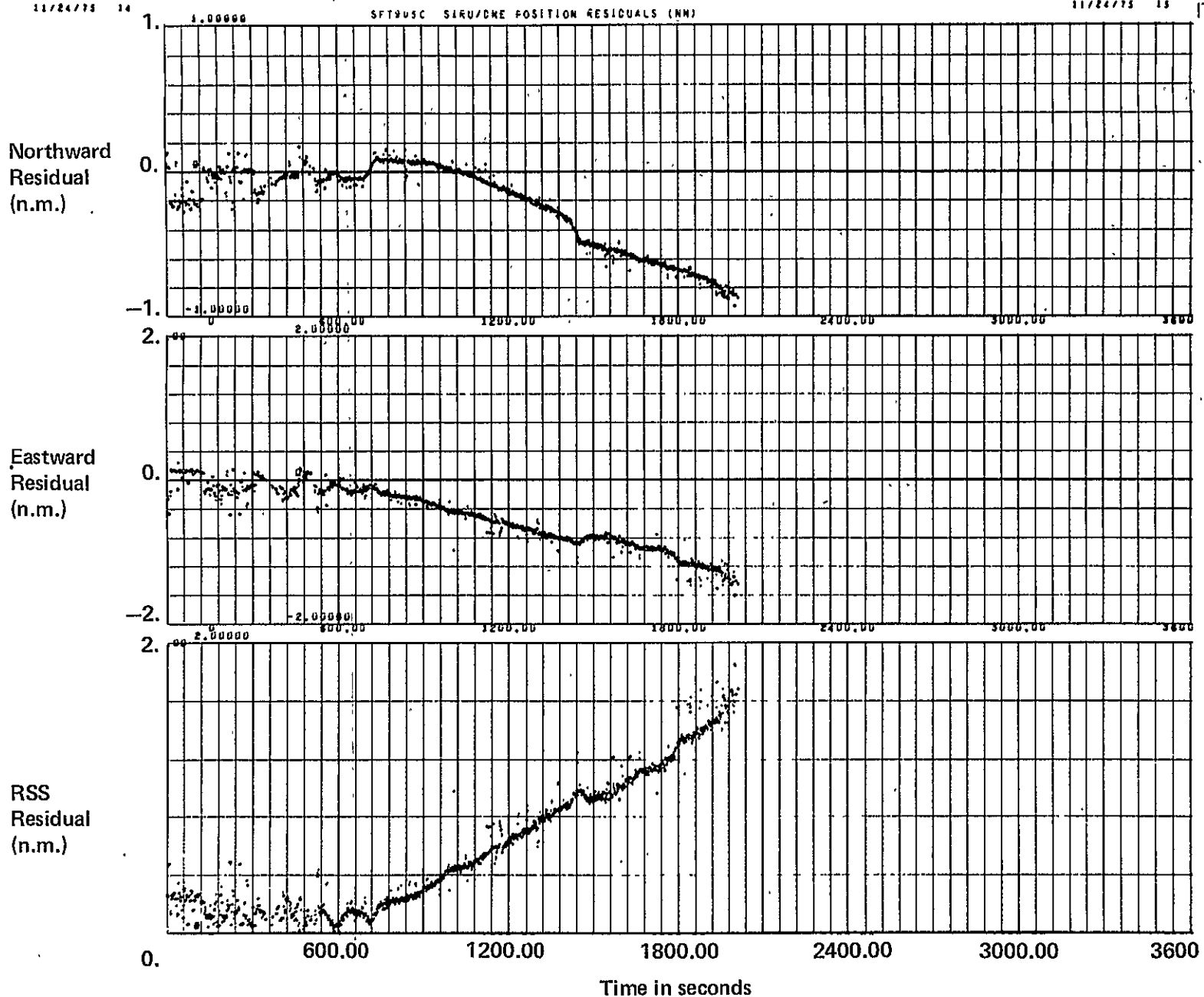
SFT905B SIRU/DME POSITION RESIDUALS (NM)



141

ORIGINAL PAGE IS
OF POOR QUALITY

Figure B.28 SFT905B SIRU/DME position residuals



142

Figure B.29 SFT905C SIRU/DME position residuals

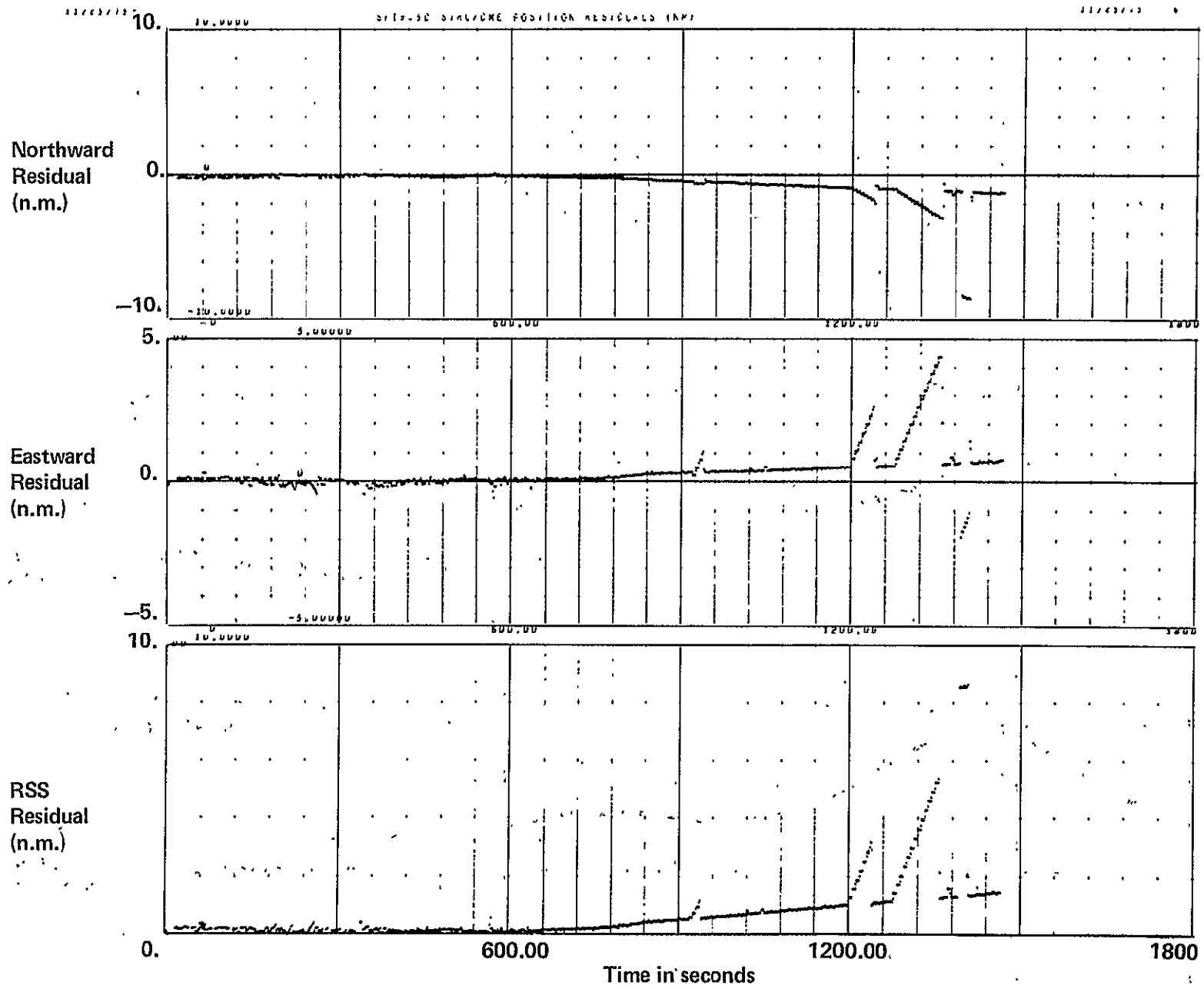


Figure B.30 SFT905D SIRU/DME position residuals

ORIGINAL PAGE IS
OF POOR QUALITY

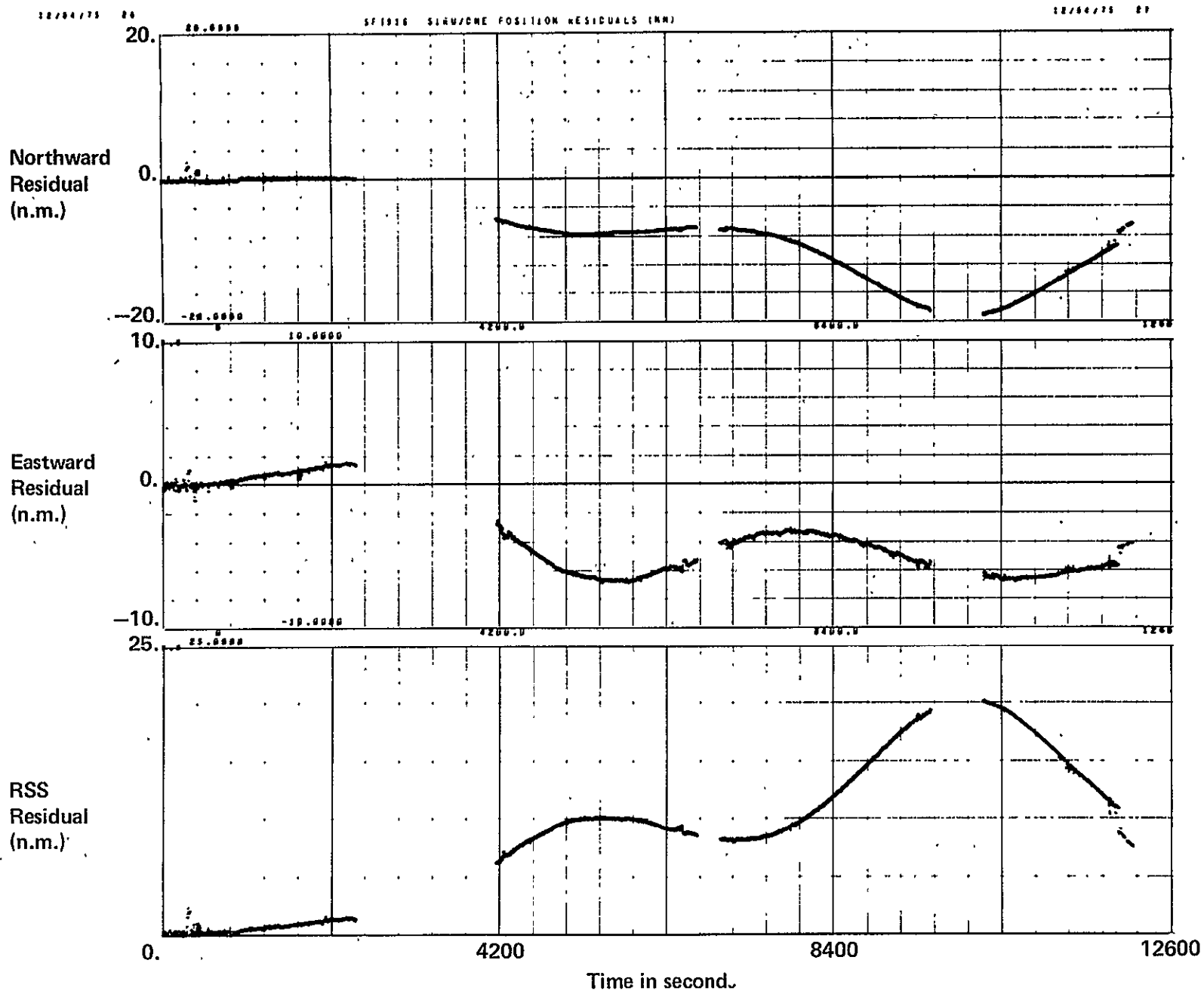
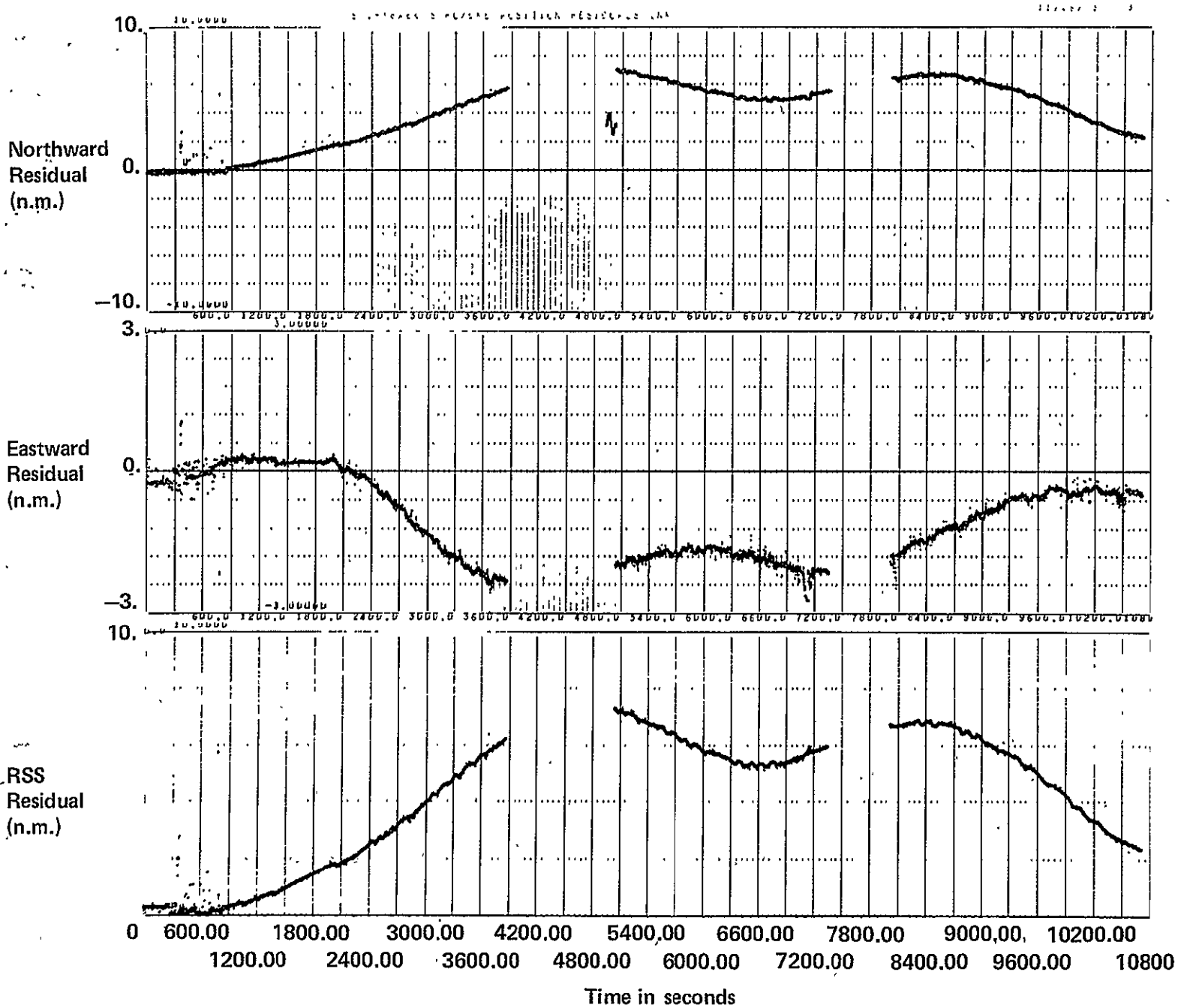


Figure B.31 SFT910 SIRU/DME position residuals



ORIGINAL PAGE IS
OF POOR QUALITY

Figure B.32 SFT918ABC SIRU/DME position residuals

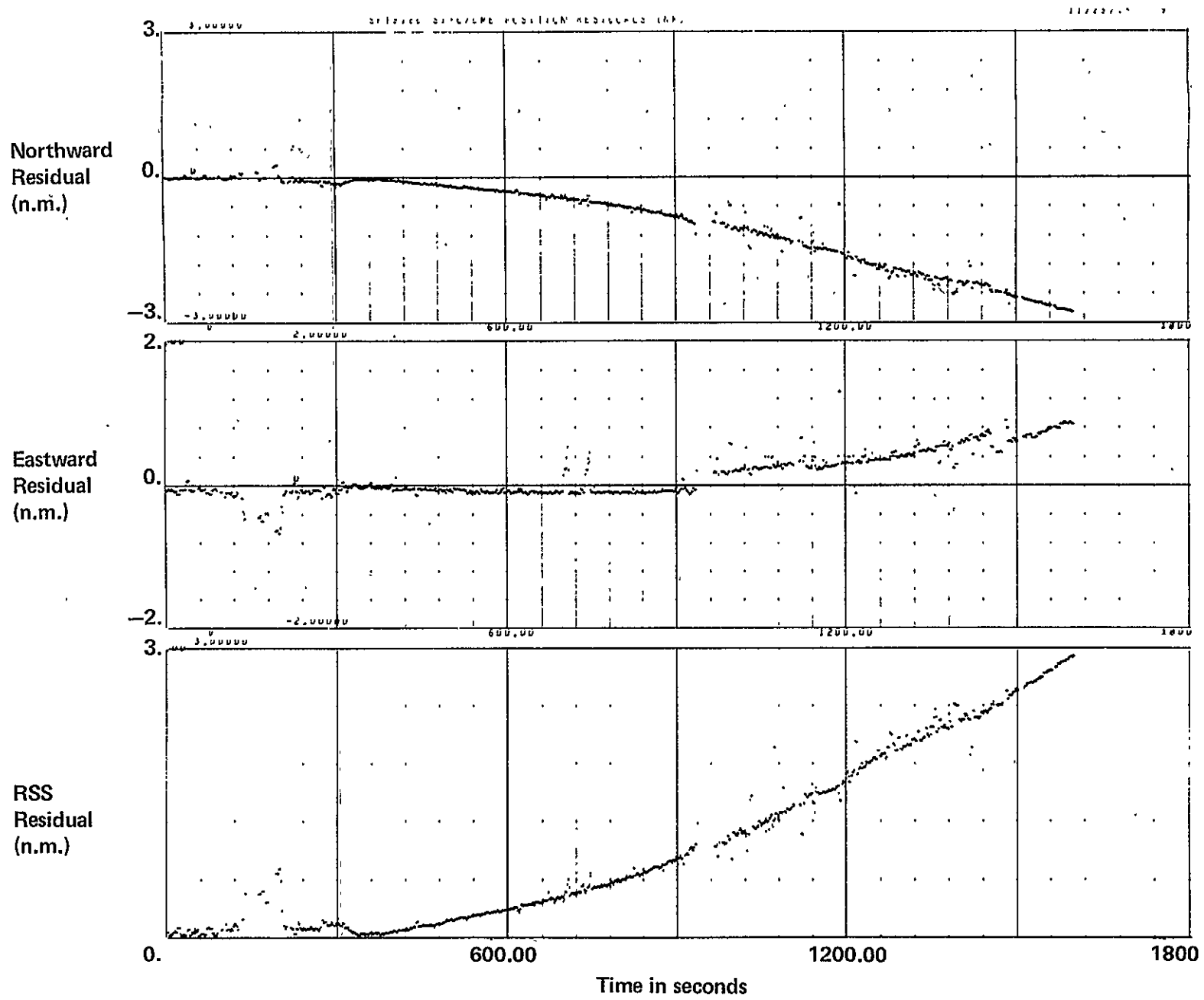


Figure B.33 SFT918D SIRU/DME position residuals

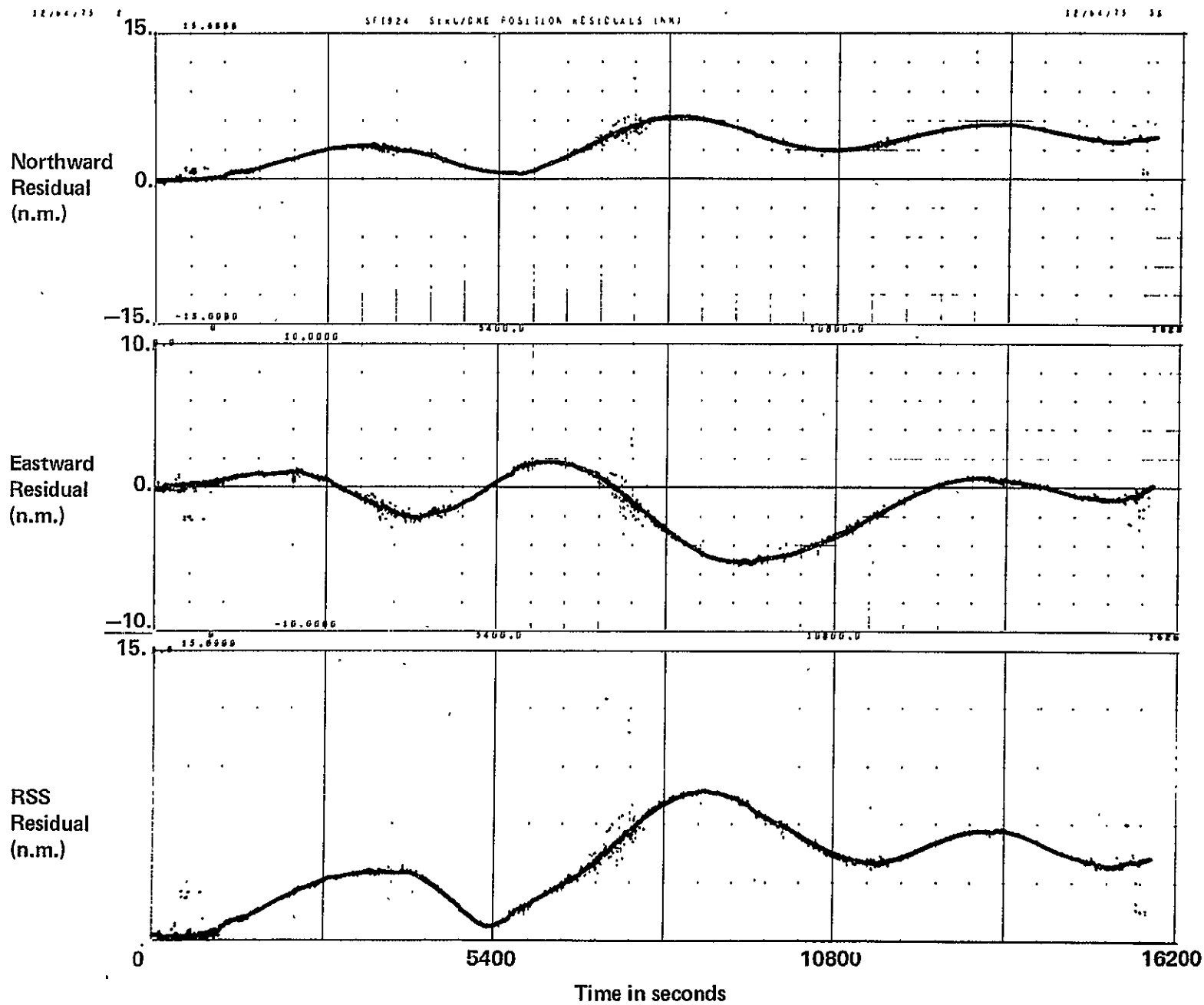


Figure B.34 SFT924 SIRU/DME position residuals

147

PAGE INTENTIONALLY BLANK

APPENDIX C

EFFECTS OF APPROXIMATIONS IN NAVIGATION ALGORITHMS

Velocity Algorithm Errors - Interval Integration

A small amount of bounded position error is present in all navigation test data due to using the computed body velocity at the end of each 1-sec navigation update to approximate the average velocity over that update. By itself, this algorithmic defect causes acceleration-induced position errors only; vehicle velocity is correctly updated over each interval. Therefore, position error propagation in the absence of significant vehicle acceleration is negligible.

In a simplified form, the navigation algorithm which was used is:

$$\begin{aligned}\bar{V}^N(nT) &= \bar{V}^N[(n-1)T] + \Delta\bar{V}^N(nT) \\ \bar{S}^N(nT) &= \bar{S}^N[(n-1)T] + \bar{V}^N(nT) \cdot T\end{aligned}$$

where \bar{V}^N and \bar{S}^N are velocity and position vectors in the pseudo-inertial N-frame (local-level coordinates corrected for earth-rotation). The navigation algorithm update period, T, is one second in this case. It will also be noted at this point that most of this algorithmic error can be eliminated by making a first-order correction to the position update:

$$\bar{S}^N(nT) = \bar{S}^N[(n-1)T] + \bar{V}^N[(n-1)T] + \frac{\Delta\bar{V}^N(nT)}{2} \cdot T$$

For the case of straight-line vehicle acceleration up to a cruise velocity, V, with uniform acceleration over each T-second interval, the position error is:

$$\bar{\epsilon}(nT) \equiv \hat{\bar{S}}(nT) - \bar{S}(nT) = 1/2 \bar{V}(nT) \cdot T$$

Straight-line acceleration in the CV340 up to $\bar{V} = 200$ knots produces an indicated position 55 m (170 ft) ahead of actual position. Deceleration (straight-line) to $\bar{V} = 0$ causes this position error to return uniformly to zero.

Vehicle acceleration of constant magnitude perpendicular to its velocity vector produces circular motion. When perpendicular acceleration is removed, straight-line motion resumes with an acceleration-caused position offset. This position error is conveniently expressed in local-level vehicle coordinates with \bar{i}_z down and with \bar{i}_x and \bar{i}_y defined, respectively, by the projections of the vehicle's nose and right wing into the level plane. It is assumed that navigation updates occur fast enough (every T sec), compared

to the maximum sustained angular velocity, ω , that $\sin(\omega T)$ can be approximated as (ωT) . For the simple case of a constant rate turn starting at $t = 0$, the resulting position error is approximately:

$$\begin{aligned} \epsilon(t) \equiv \epsilon(\omega t) = & \bar{i}_x \left\{ c_x \sin(\omega t) + c_y [1 - \cos(\omega t)] \right\} \\ & + \bar{i}_y \left\{ c_y \sin(\omega t) + c_x [\cos(\omega t) - 1] \right\} \end{aligned}$$

where

$$c_x = V\omega T^2/2$$

$$c_y = VT/2$$

For a typical 3°/sec CV340 turn ($\omega = 0.05$, $V = 118.5$ knots), we have

$$c_x = 2.3 \text{ m (7.5 ft)}$$

$$c_y = 45.7 \text{ m (150 ft)}$$

The position error vector for various amounts of turn is then:

$$\bar{\epsilon}(45^\circ) = \bar{i}_x \cdot 15 \text{ m} + \bar{i}_y \cdot 33 \text{ m}$$

$$\bar{\epsilon}(90^\circ) = \bar{i}_x \cdot 48 \text{ m} + \bar{i}_y \cdot 43 \text{ m}$$

$$\bar{\epsilon}(180^\circ) = \bar{i}_x \cdot 91 \text{ m} - \bar{i}_y \cdot 4.6 \text{ m}$$

$$\bar{\epsilon}(360^\circ) = \bar{i}_x \cdot 0 + \bar{i}_y \cdot 0$$

It is seen that this error approaches its maximum value for turns in the vicinity of 180° and returns to zero magnitude for complete circles.

Effects of Failure Detection and Isolation Algorithm Operation on Navigation Accuracy

Two aspects of navigation are dependent upon FDI actions. One aspect is the deterioration of accuracy caused by a slightly bad gyro or accelerometer whose error magnitude is just under the detection level of the relevant FDI algorithm. The second aspect concerns the magnitude of navigation errors which occur when an instrument has a "hard fail" and (typically) is detected and put off-line within a few seconds after failure.

A keyboard modification midway through the SIRU flight tests made it possible to add software bias errors to instruments in the B computer while

continuing normal (baseline) operations in the A computer. This allows comparison of navigation performance with and without the hard fail occurrence.

An accelerometer "hard fail" causes a velocity increment to be added to the system's navigation velocity. (For simplicity, the system is assumed initially to have all instruments on-line with low total squared errors (TSEs) up to the point of the single instrument degradation.) This accelerometer failure has a minor, second-order effect on the attitude of the failed system since the accelerometer outputs couple into the gyro data by way of g-sensitive compensation.

The magnitude of the velocity error increment which corrupts the navigation performance depends on both the MASE value and the orientation of the accelerometer which is failing. Only the horizontal velocity error affects navigation. The later months of flight testing had a first-fail search accelerometer maximum allowable squared error (MASE) of 288 pulses² (4 cm/sec was the design pulse value). Assume all accelerometers are error-free except for one horizontal instrument with bias error, b_e cm/sec². If this bias error is begun at $t = 0$, then the accumulated instrument velocity error is

$$V_e(t) = b_e t$$

and the TSE is

$$\text{TSE}(t) = (b_e t)^2 + 5(0.2(b_e t)^2) = 2(b_e t)^2$$

The bad accelerometer is taken off-line at the point when $\text{TSE}(t) \geq \text{MASE}$. Define V_e^* as the value of $V_e(t)$ just prior to that point. The worse case V_e^* is then found:

$$2(V_e^*)^2 = \text{MASE} = 288 \text{ pulse}^2$$

$$V_e^* = 12 \text{ pulses} = 48 \text{ cm/sec}$$

This total instrument velocity error is reduced by a factor of two in the transformation to body coordinates, so the worst-case maximum velocity error increment is

$$\frac{\sqrt{\text{MASE}/2}}{2} = 24 \frac{\text{cm}}{\text{sec}} = 0.79 \frac{\text{ft}}{\text{sec}} = 0.47 \text{ knots}$$

This maximum value of velocity error occurs only if the aircraft maintains a constant heading during the instrument degradation period. If the aircraft is turning, the velocity error magnitude and direction will be modulated accordingly. In either case, a consistent velocity error in the navigation frame results. Unfortunately, none of the four flight tests which had scheduled accelerometer failures yielded a clear example of comparative (A vs B) navigation performance for a single accelerometer failure. (This was due to operating both computers identically on some flights and to scheduling multiple instrument failures on others.)

A more serious aspect of FDI operation concerns a low level instrument degradation which escapes detection, thereby degrading navigation for the duration of a flight. The maximum TSE accumulation period is 4 min, so the maximum undetected accelerometer bias error (b_{ϵ}^*) is found from:

$$(b_{\epsilon}^* \cdot 4 \text{ min}) = V_{\epsilon}^* = \sqrt{(\text{MASE}/2)}$$

For MASE = 288 pulse², this reduces to:

$$b_{\epsilon}^* = \frac{48 \text{ cm/sec}}{240 \text{ sec}} = 0.2 \frac{\text{cm}}{\text{sec}^2}$$

Again, this instrument bias error is attenuated by a factor of 2 in conversion to body coordinates. This constant bias error of ($b_{\epsilon}^*/2$) can produce a maximum position error (for degraded horizontal accelerometer in straight - line flight):

$$\epsilon^*(t) = 1/2(b_{\epsilon}^*/2)t^2 = 0.05 \frac{\text{cm}}{\text{sec}^2} t^2$$

This theoretical maximum results in a 3.5-n. mi. position error 1 hr after the bias error begins. This bias error, b_{ϵ}^* , is a *change* in instrument bias after navigation has begun. The alignment procedure cancels the effects of initial biases.

APPENDIX D

VIBRATION SPECTRUM OF THE CV-340 AIRCRAFT

Inertial instrument data have been analyzed for vibration content as an *aïd* to investigating potential SIRU navigation error sources. Gyro data have been spectral-analyzed for angular vibration content while accelerometer data have been analyzed for linear vibration content. Only compensated body-axis angular rate and acceleration data are discussed here. The X, Y, and Z strapdown system axes are in close alignment with the aircraft's roll, pitch, and yaw axes, respectively.

Two typical data regimes were analyzed from data recorded during flight 14. The first was a preflight period in which the aircraft was on the ground (stationary), but with both engines operating. The second regime analyzed was a level flight segment in which aircraft heading was nearby constant. Data were recorded at full rate (20 frames/sec) so that the maximum frequency which may be reconstructed is 10 Hz.

Angular vibration data for the static section are shown in figures D.1 through D.3, which present the power spectral density (PSD) magnitude for each axis. Structural vibration resonances are evident for each axis. Motion about the aircraft's roll axis has a sharp resonance at 7.5 Hz, while motion about the pitch axis has a dominant resonance of similar magnitude just above 1 Hz. Aircraft oscillations about the vertical are also dominant at just over 1 Hz.

Linear vibration data for the static section are shown in figures D.4 through D.6. If the x-y body plane is approximately level (as in the SIRU flight tests), then small angular vibrations about the X-axis will cause linear acceleration vibrations along the Y-axis. A sinusoidal oscillation of amplitude b yields:

$$\theta_x(t) = \theta_{x0} + b \sin(\omega t)$$

$$\dot{\theta}_x(t) \equiv \omega_x(t) = b\omega \cos(\omega t)$$

The deviation in acceleration along the Y-axis is:

$$\begin{aligned} \delta a_y(t) &= -g \cdot \sin[b \sin(\omega t)] \cdot \cos(\theta_{x0}) \\ &\approx -g \cdot b \sin(\omega t) \end{aligned}$$

and the velocity deviation:

$$\begin{aligned}\delta V_y(t) &= \int_0^t \delta a_y(\tau) d\tau \\ &= \frac{gz}{\omega} \cos(\omega t)\end{aligned}$$

The body acceleration data (actually delta-velocity data) from SIRU tests are integrated to obtain velocity before doing spectral analysis. The ratio of the velocity deviation to the applied angular velocity (in the example above) is:

$$\frac{\delta V_y(t)}{\omega_x(t)} = \frac{g}{\omega^2}$$

With this background, the ΔV_X and ΔV_Y data are seen to have many of the same natural frequencies as the corresponding angular data.

A static aircraft's vibratory characteristics are of primary importance with respect to calibration and alignment algorithm performance, and primary interest is with the angular (gyro) data.

In-flight vibrational data (from level cruise) differ from ground data primarily in having much larger amplitudes at much lower frequencies (<1 Hz). Angular data are presented in figures D.7 through D.9. All three axes have angular excursions with typical periods of from 2 to 10 sec. High-frequency engine vibrations did not lie within the detection bandwidth of the sampling rate. Linear vibrational data (figs. D.10 through D.12) have very low-frequency velocity excursions, as would be expected in flight.

The data presented here is a spectral analysis of the inertial system's *output*. There are two limitations to using pulse-rebalanced instruments for this purpose - low bandwidth (due to low sampling rate) and low-amplitude distortion (due to pulse quantization). A comprehensive analysis of vibratory effects on a strapdown system would require better knowledge of the real spectral content (*input* to the strapdown system). Analog instruments and a continuous tape recorder should be used to obtain vibrational data for this purpose.

Ground WX

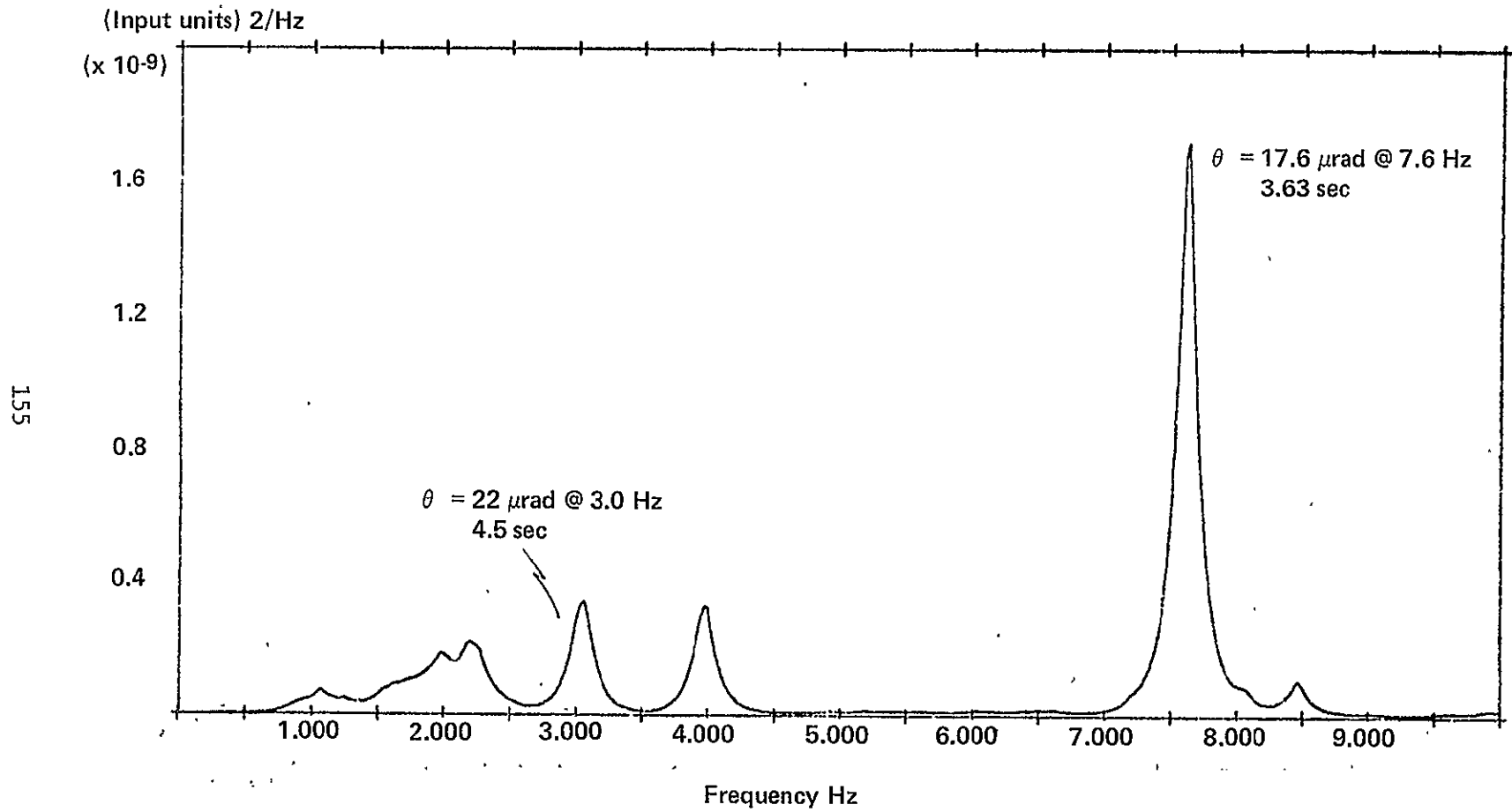


Figure D.1

Ground WY

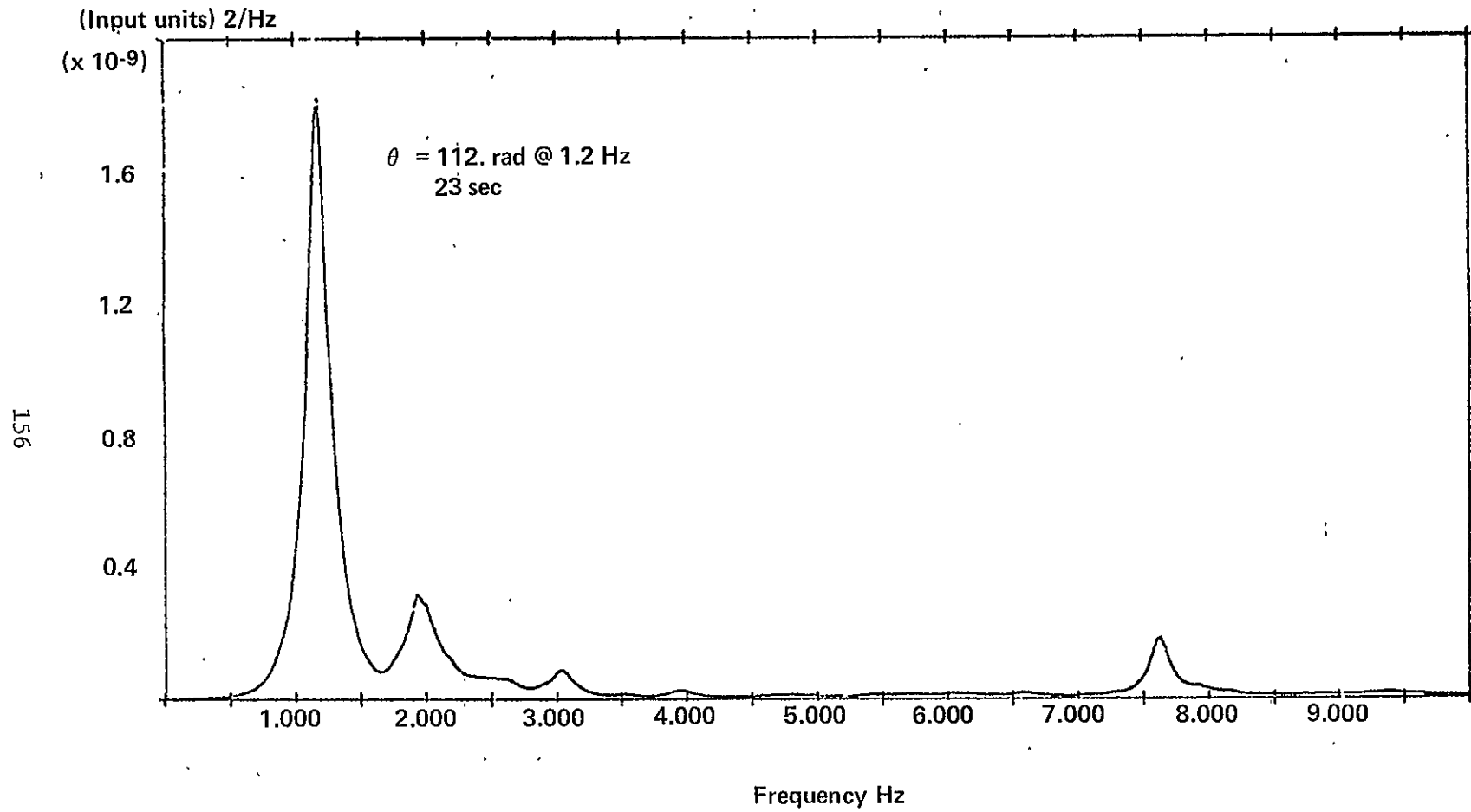


Figure D.2

Ground WZ

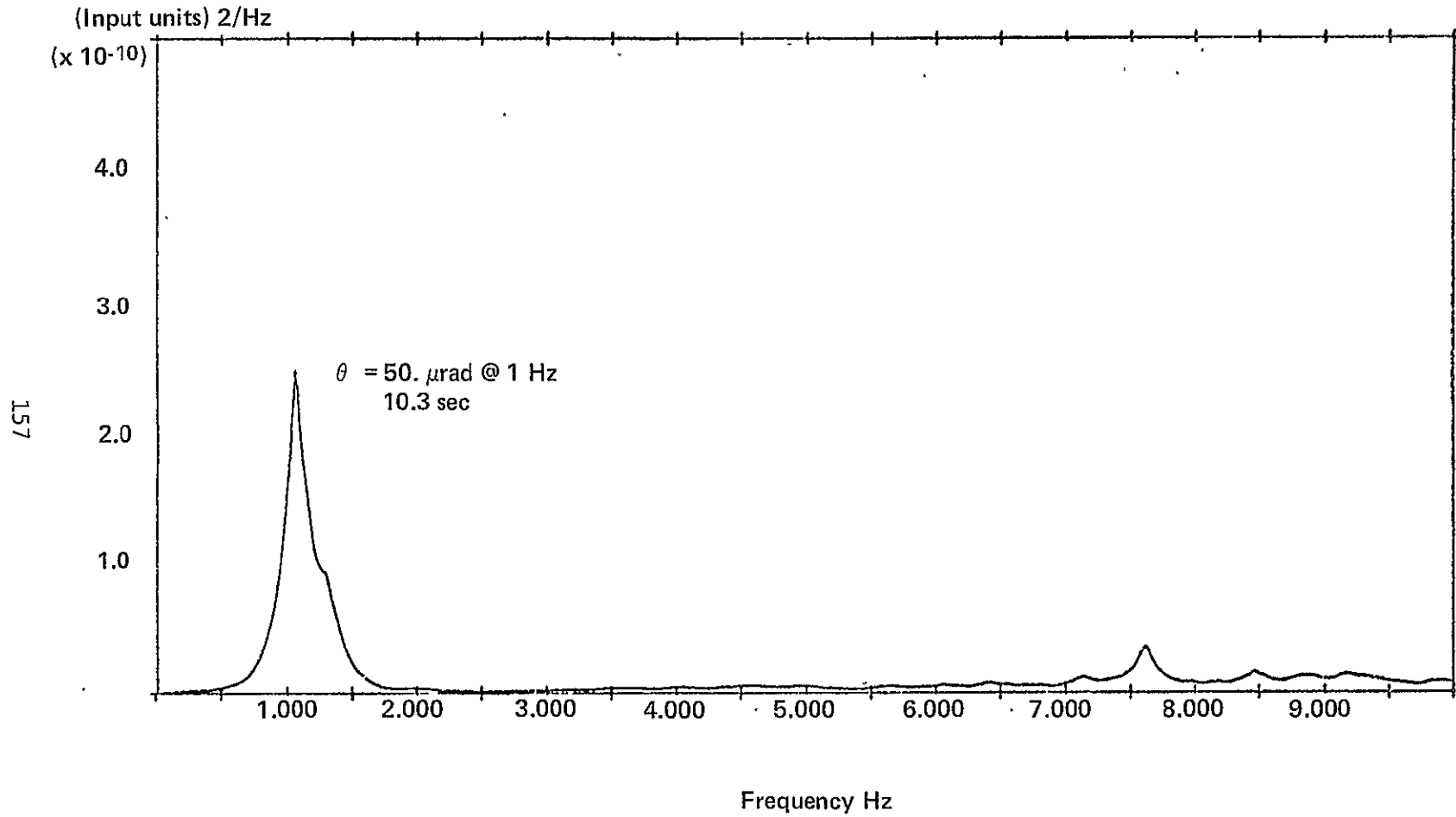


Figure D.3

Ground ΔV_X

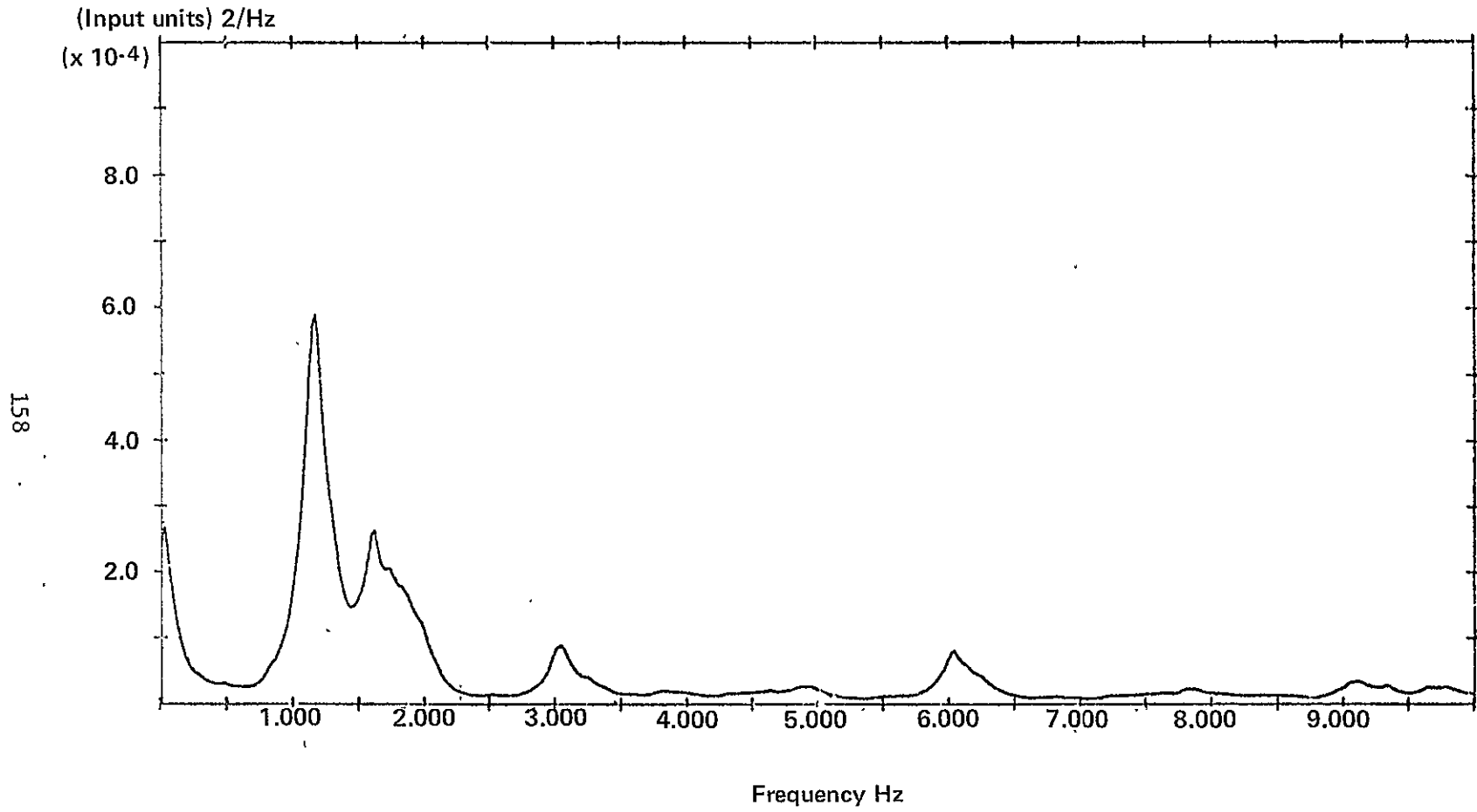


Figure D.4

Ground ΔV_Y

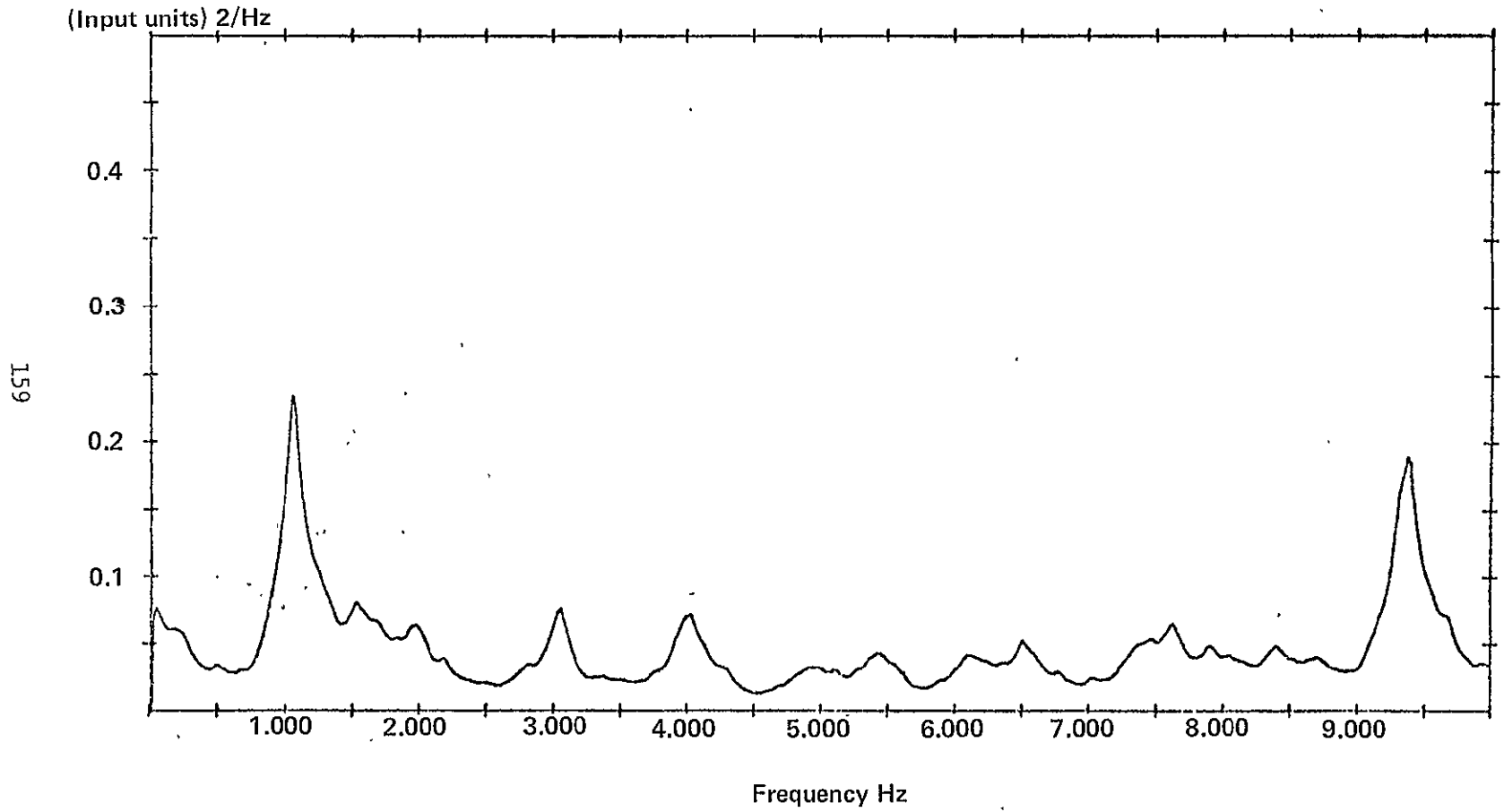


Figure D.5

Ground ΔV_Z

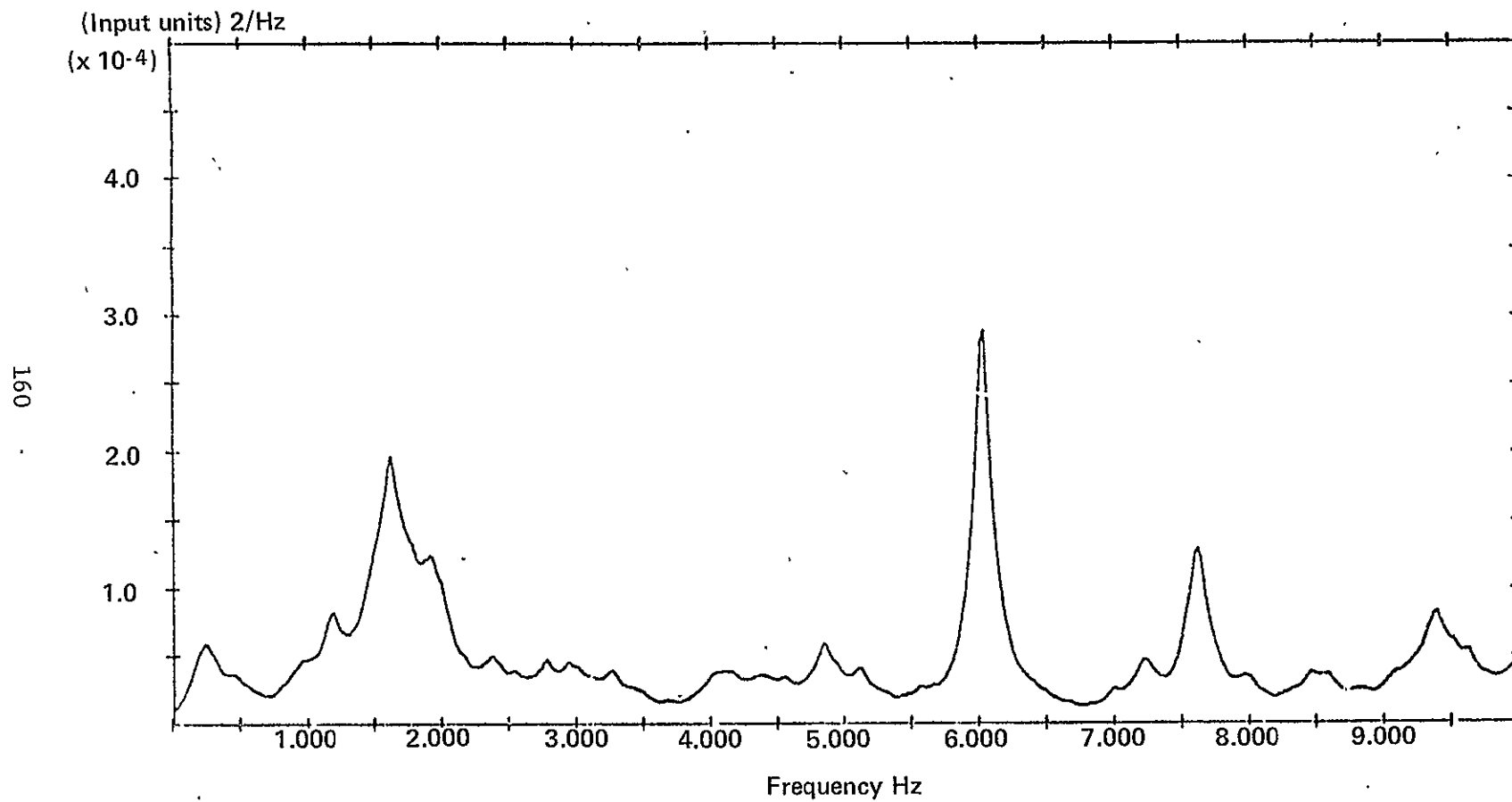


Figure D.6

Cruise WX

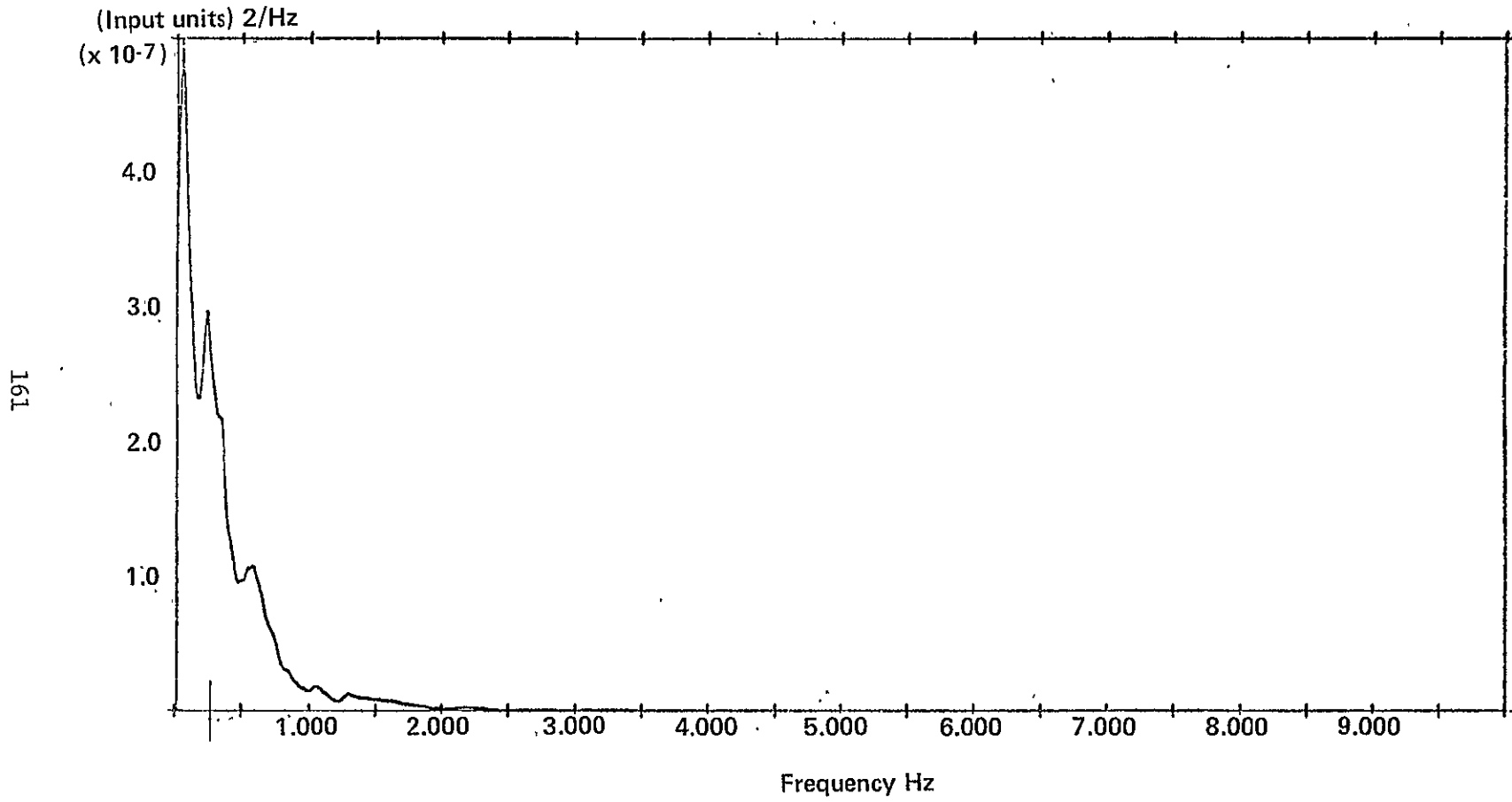
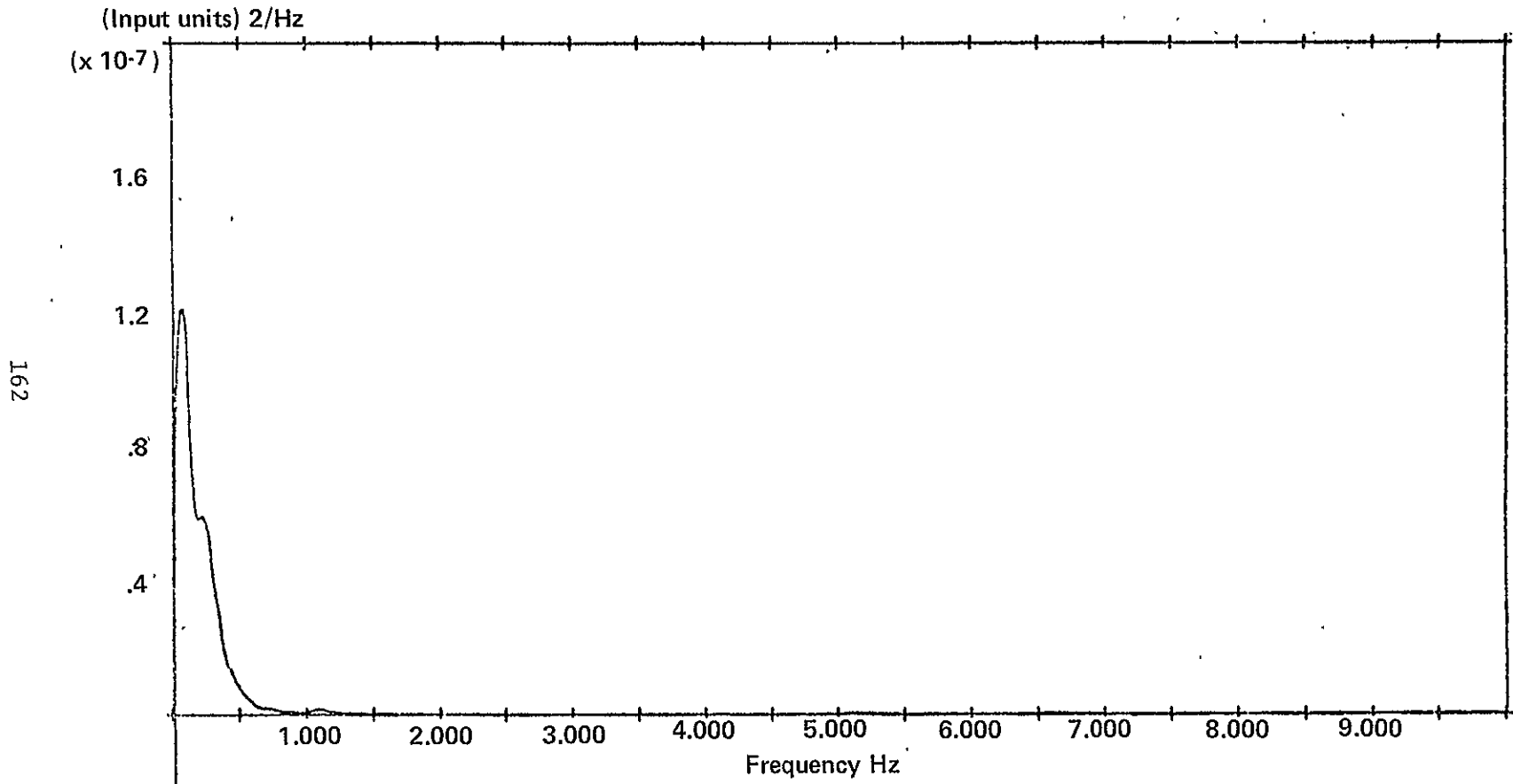


Figure D.7

Cruise WY



162

Figure D.8

Cruise WZ

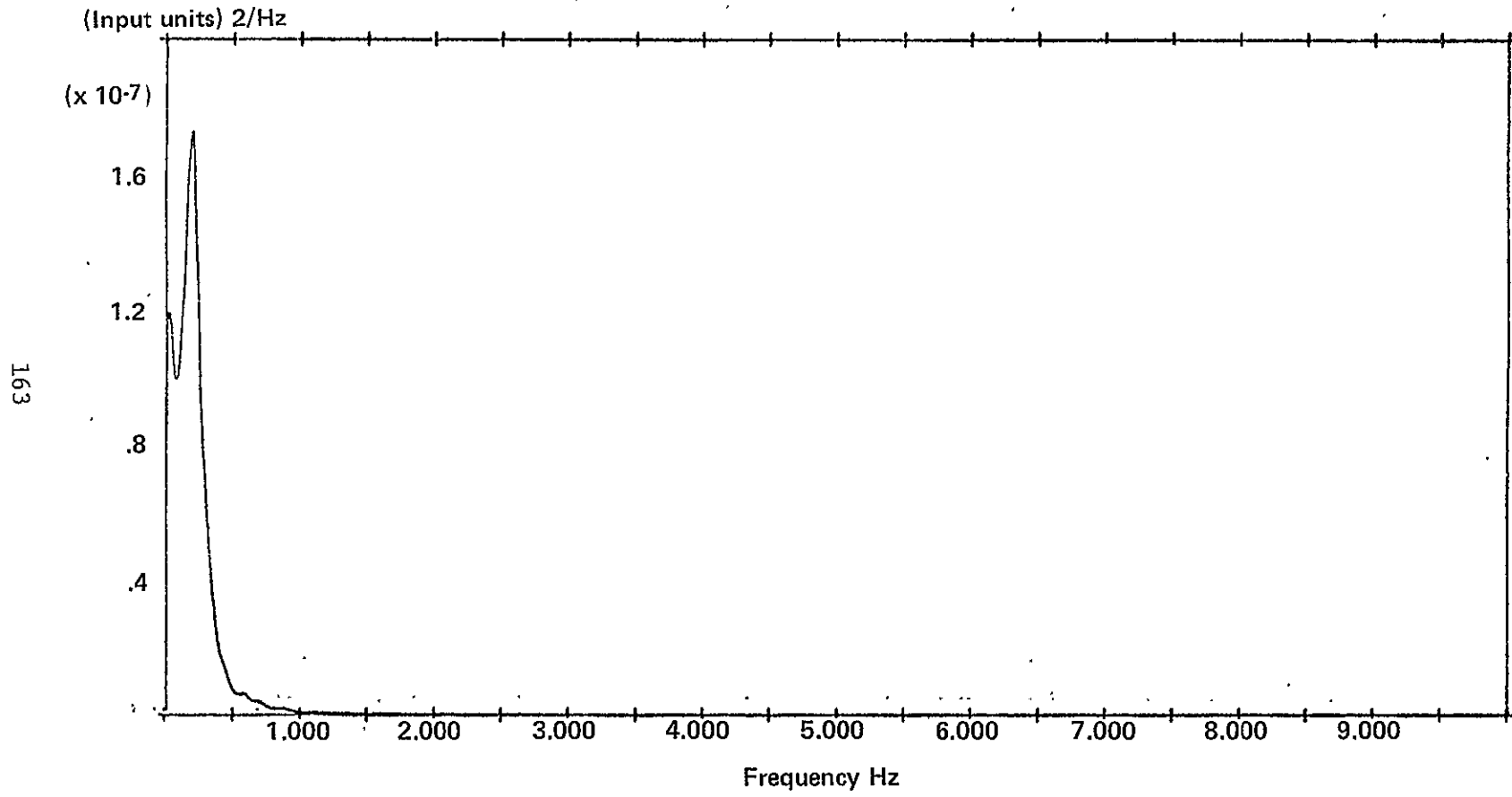


Figure D.9

Cruise ΔV_X

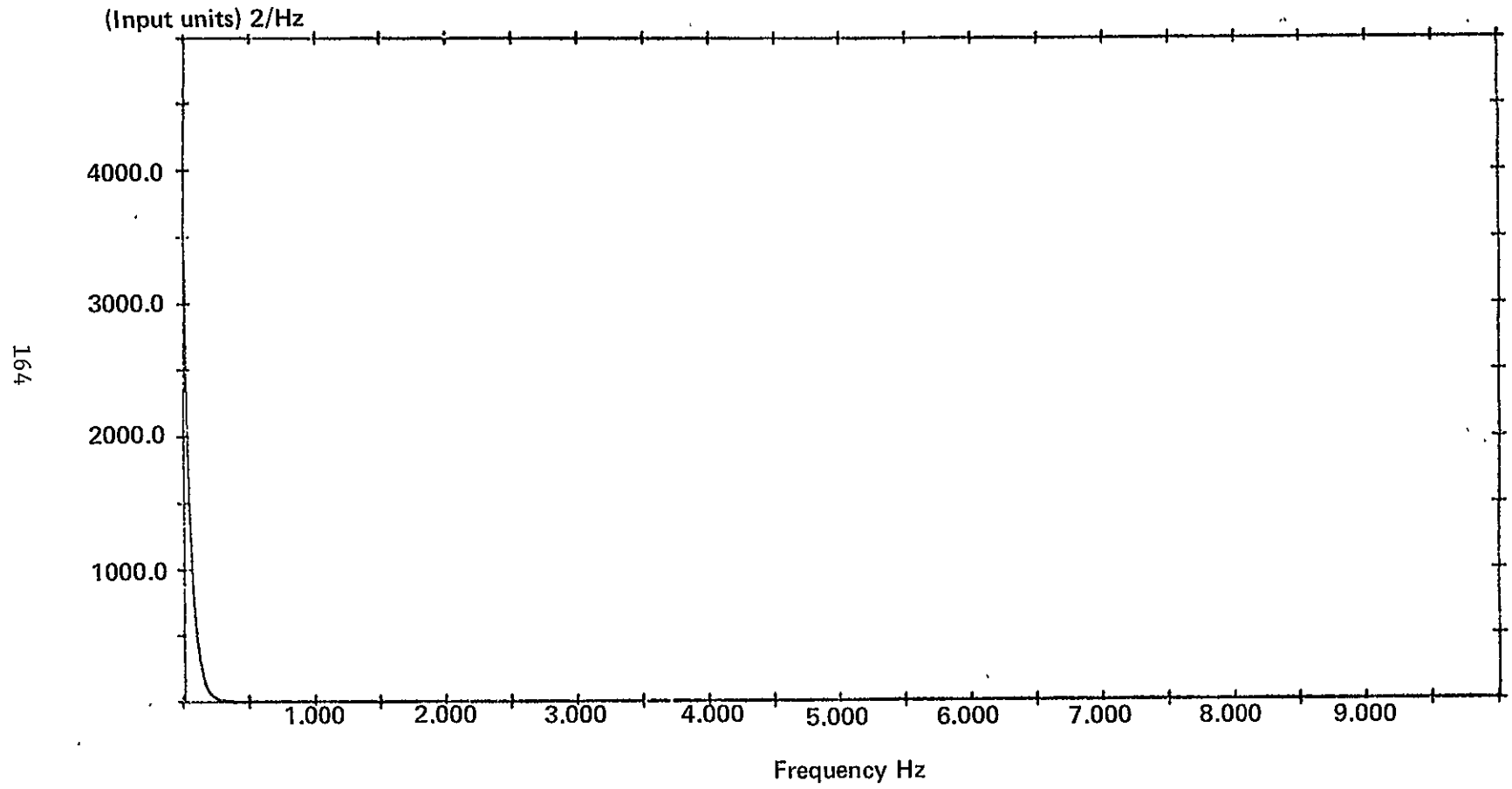


Figure D.10

Cruise ΔVY

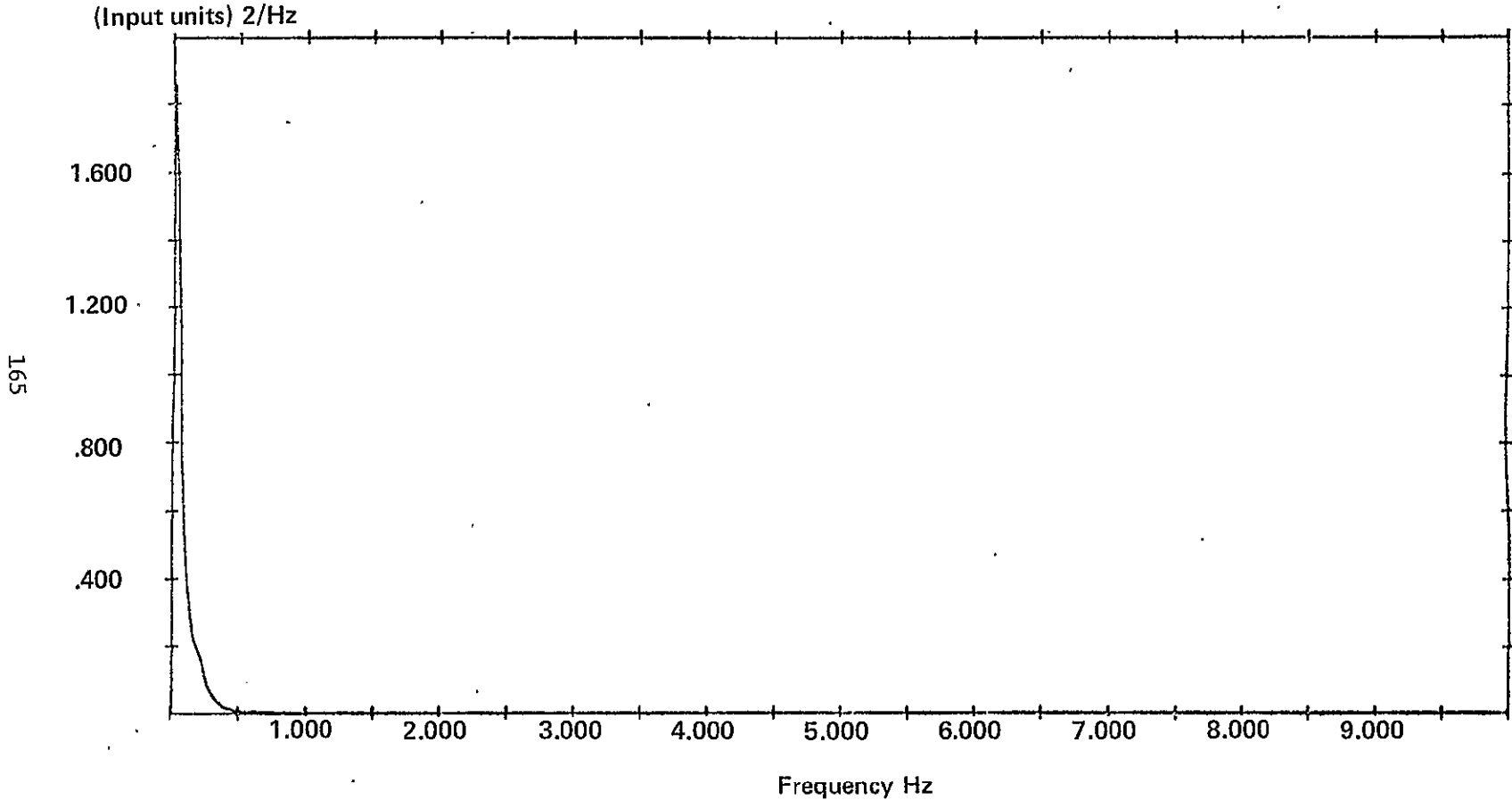


Figure D.11

Cruise ΔVZ

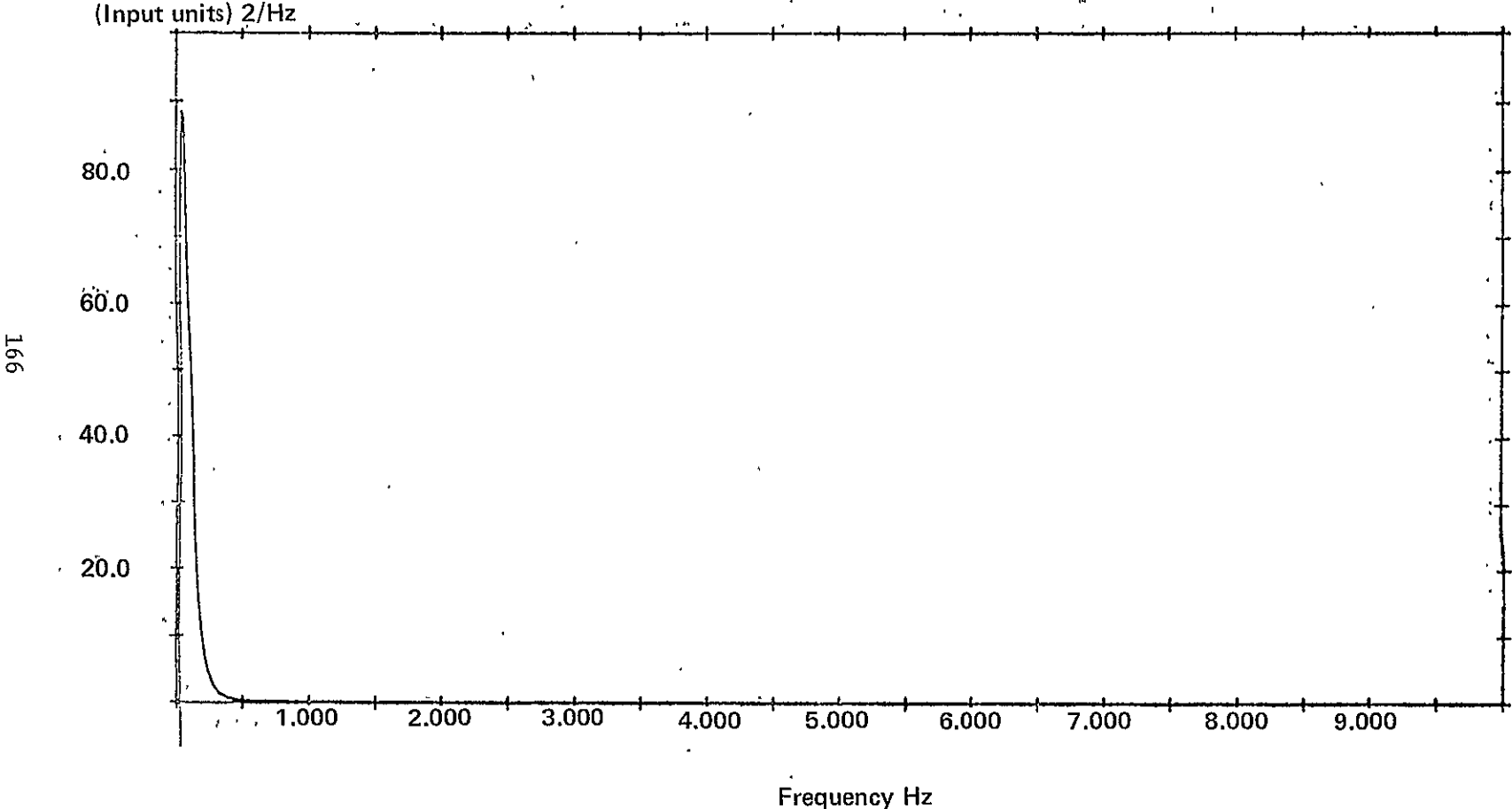


Figure D.12

APPENDIX E

MODIFICATION OF THE STATISTICAL FDICR ALGORITHM PARAMETERS FOR THE FLIGHT ENVIRONMENT

INTRODUCTION

During the SIRU flight tests, it was observed that the gyro total squared error (TSE) residuals were significantly larger in the flight environment than those observed in data taken during dynamic testing in the laboratory. Analysis of flight results were required before an adjusted set of Failure Detection and Isolation (FDI) system parameters could be derived to match the observed gyro residuals in the flight environment. This appendix presents the computations of the FDI parameters required to implement the statistical failure detection capability (also called failure detection isolation classification and recertification or FDICR algorithm) in a future flight with the environment of the CV-340 aircraft.

The essence of the FDI algorithms is to make decisions on the basis of the sequential cumulative information provided by recent sensor measurement history. The detection logic must decide whether a failure has occurred and, in making this decision, must trade off the risk of an erroneous decision against the inevitable attitude or velocity errors which result from detection time delays. A long wait to make a conservative decision results in excessive system performance error. On the other hand, if a decision is made too soon, false alarms may occur. The design of FDI algorithms for detection of failures in aircraft represents a balance of these two opposing factors.

The decision logic of SIRU's statistical FDICR algorithm process is based on sequential probability ratio tests. These tests are based on statistical assumptions which require definition of certain empirical and judgmental parameters. For each sensor measurement, y_n , a decision function, λ_n , is generated recursively as

$$\lambda_n = \lambda_{n-1} + \frac{b}{\sigma^2} \left(y_n - \frac{b}{2} \right) \quad (1)$$

where b is the specified *failure threshold* to be detected and σ is the standard deviation of noise errors in y_n . A *decision threshold*, B , is defined, based on a specified mean time, T , between two false alarms.

$$B = \ln \left[\frac{1}{2} \left(\frac{b}{\sigma} \right)^2 \frac{T}{\Delta} \right] \quad (2)$$

where Δ is the sampling interval. Failure detection is accomplished by comparing λ_n with the decision threshold, B . Then the following action is taken:

$$\begin{aligned} \lambda_n \geq B & : \text{Declare failure} \\ 0 \leq \lambda_n < B & : \text{Take more data} \\ \lambda_n < 0 & : \text{Reset } \lambda_n \text{ and continue taking data.} \end{aligned} \quad (3)$$

For the specified T , the mean detection time, $\tau(T)$, is given approximately by

$$\tau(T) \cong \left[2 \left(\frac{\sigma}{b} \right)^2 (B - 1.5) \right] \Delta \quad (4)$$

The failure threshold, b , and the decision threshold, B , are the two basic parameters to be specified for proper functioning of the FDI process.

SUGGESTED STATISTICAL FDICR ALGORITHM IMPLEMENTATION CHANGES

The proper parameters of both failure threshold, b , and decision threshold, B , are now derived for the aircraft flight environment, and theoretical estimates of detection performance are made. On the basis of laboratory and flight test experience, three parameter sets are required, corresponding to (a) ground operations, (b) level flight, and (c) turning flight. Each of these is discussed.

The failure detection system functioned properly during ground operations using the parameters derived from laboratory test data. No modifications of failure or decision thresholds are required.

For level flight, the following parameters are used to specify the failure threshold, b , and the decision threshold, B . The parity residual standard deviation, σ , was computed to be the RMS of the six parity residual errors from flight 905C (SIRU flight of September 5, C-leg). Results and assumptions were:

$$\begin{aligned} \text{Residual: } \sigma &= 0.67^\circ/\text{hr (from flight 905C)} \\ \text{Assume: } T &= 24 \text{ hr (mean time between false alarms)} \\ \text{Assume: } \Delta &= 30 \text{ sec (sample time)} \end{aligned} \quad (5)$$

Laboratory tests indicate that a failure threshold of 1.5 times the gyro standard deviation, σ_g , is appropriate, so

$$b = 1.5 \sigma_g \quad (6)$$

The gyro standard deviation is related to the parity standard deviation by

$$\sigma_g = \frac{1}{\sqrt{2}} \sigma \quad (7)$$

Thus, the detection logic can therefore presumably detect a gyro failure of

$$b_L = 0.71^\circ/\text{hr} \quad (8)$$

in level flight. Based on evaluation of the flight data from flight 905C, the failure threshold, b_L , for the level flight phase is estimated to be $0.75^\circ/\text{hr}$. From equation (2), the decision threshold for level flight is found to be

$$B_L = \ln \left[\frac{1}{2} \left(\frac{b_{Lp}}{\sigma} \right)^2 \frac{T}{\Delta} \right], \quad (9)$$

where b_{Lp} is the failure magnitude of the parity residual outputs:

$$b_{Lp} = \cos \alpha b_L = 0.64^\circ/\text{hr} \quad (10)$$

In equation (10), α is the half-angle between sensor axes,

$$\alpha = \frac{1}{2} \tan^{-1}(2) \cong 31^\circ 43' \quad (11)$$

Equations (5) and (10) are substituted into equation (9), and B_L is computed to be 7.17. The mean detection time in level flight, $\tau_L(T)$, is computed from equation (4) to be

$$\tau_L(T) = \left[2 \left(\frac{\sigma}{b_{Lp}} \right)^2 \left(B_L - 1.5 \right) \right] \Delta = 373 \text{ sec} \quad (12)$$

The resulting attitude error due to the detection time is calculated to be

$$\psi = \frac{1}{\sqrt{2}} b_L \tau_L(T) = 198 \text{ arcsec} \quad (13)$$

In summary, the future detection process for level flight can theoretically detect a gyro error magnitude of $0.75^\circ/\text{hr}$ with a resultant attitude error of 198 arcsec for a specified confidence of 24 hr between false alarms.

For turning flight, the parity residual standard deviation was computed from flight 905C's data to be

$$\sigma_T = 1.94^\circ/\text{hr} \quad (14)$$

If we assume that the turning flight duration is 10% of the total flight time, then an estimate of mean time between false alarms is

$$T_T = 10\% \times 24 \text{ hr} = 2.4 \text{ hr} \quad (15)$$

Using the same approach as previously, the failure threshold in turning flight is

$$b_T = 1.5 \times \frac{1}{\sqrt{2}} \times \sigma_T = 2.06^\circ/\text{hr} \quad (16)$$

When b_T is conservatively set to $2.5^\circ/\text{hr}$, the decision threshold, B_T , for turning flight is estimated by

$$B_T = \ln \left[\frac{1}{2} \left(b_{Tp}/\sigma_T \right)^2 T_T/\Delta \right] = 5.16 \quad (17)$$

Here, b_{Tp} is the failure threshold of the parity residual in turning flight, and is

$$b_{Tp} = \sigma_T \cos \alpha = 2.13^\circ/\text{hr} \quad (18)$$

Similarly, the mean detection time is

$$\tau_T(T) = \left[2 \left(\sigma_T/b_{Tp} \right)^2 \left(B_T - 1.5 \right) \right] \Delta = 182 \text{ sec}$$

The attitude error corresponding to the finite detection time is

$$\psi = \frac{1}{\sqrt{2}} b_T \tau_T(T) = 322 \text{ arcsec} \quad (20)$$

Thus, the failure detection process for the turning-flight phase can theoretically detect a gyro failure magnitude of $2.5^\circ/\text{hr}$ or greater, and may result in an attitude error of 322 arcsec for a confidence interval of 2.4 hr between false alarms.

To check the reasonableness of the theoretical values of the failure and decision thresholds, consider the decision function magnitude generated by a maximum error of $2.88^\circ/\text{hr}$ (flight 905C). Assume that the transient sensor failure occurred after a reset of the preceding sample ($\lambda_{n-1} = 0$).

$$\lambda_n = \lambda_{n-1} + \left(b_{Tp}/\sigma_T^2 \right) \left(y_n - b_T/2 \right) = 1.03 \quad (21)$$

A comparison of λ_n with the decision threshold B_T of 5.16 indicates that B_T represents a safety factor of five in preventing the error ($2.88^\circ/\text{hr}$) from generating a false alarm.

CONCLUSION

This appendix analyzes the hypothetical operation of SIRU's statistical FDICR algorithm for the flight test environment observed in flight test 905C. The flight test data were processed and compared with the laboratory test data. Observable gyro errors apparently increased by a factor of five in the flight test environment. It was concluded that the FDICR algorithm parameters should be modified if the process is to function properly in the flight test environment. The parameters of the failure threshold should be $0.75^\circ/\text{hr}$ and $2.5^\circ/\text{hr}$ for the level-flight and turning-flight phases, respectively. The decision thresholds for these phases should be 7.17 and 5.16, respectively. Attitude errors resulting from the detection delay would be 198 arcsec and 322 arcsec, respectively, based on the modified parameters.

A significant number of the flight-induced errors is known to be related to the treatment of sensor scale factor compensation, to an uncertainty in instrument misalignments and to the rigid sensor mounts used in the CV-340 aircraft. Proper corrective action could presumably reduce the observed errors by a factor of approximately 5, which would reduce the failure threshold for turning flight to $0.5^\circ/\text{hr}$.

PAGE INTENTIONALLY BLANK

APPENDIX F

SIRU FLIGHT TEST SYSTEM DESCRIPTION

SYSTEM MECHANIZATION

The flight test configuration of SIRU may be divided into four blocks or subsystems: the inertial sensor assembly, the dual computer assembly, the displays and tape transport, and the reference system (fig. F.1). The system is an experimental model and is not configured to be representative of production flight hardware.

The inertial reference unit consists of the instrument package, power supply assembly, instrument package heat exchangers, electronics assembly, and multiplexer. Redundancy concepts have been implemented in all of these assemblies. A complete description of the basic SIRU as operated in the laboratory is provided in documents listed later. Brief descriptions of these units are presented here.

The redundant instrument package (fig. F.2) is an assembly of six single-degree-of-freedom gyroscope modules and six linear accelerometer modules mounted on an alignment structure (Π -frame). Each module is pre-aligned and normalized and includes the instrument, its pulse torque-to-balance electronics, a temperature controller, a preamplifier, and the inertial instrument normalizing components.

The module outputs are in the form of an increment of angular motion, $\Delta\theta$, and velocity, ΔV , for the gyro and accelerometer module, respectively. These outputs are processed through the computational algorithms to obtain attitude and velocity and body angular rate and acceleration.

Geometric redundancy is achieved by using a nonorthogonal mounting configuration in which the instrument input axes are oriented to correspond to the array of normals to the faces of a dodecahedron.

The SIRU power system employs two identical power supplies (fig. F.3) each capable of producing all of the required power for the SIRU electronic assembly and multiplexer, connected to permit operation of the inertial system independently from either supply. Each supply has its own manual power sequencing, safety interlocking, and overvoltage protection. In the redundant configuration, each supply shares the total inertial system power requirements. The power system uses as a prime power source the 400-Hz, 3-phase, 205-Vac aircraft generator, with a 14-A-hr nickel cadmium battery as an emergency back-up source.

A finned liquid-to-air heat exchanger using forced cabin air flow was used in the flight test system. Two separate exchangers, pumps and fans were used, each of which alone is capable of providing an adequate cooling capability for the instrument package.

Redundant techniques were employed in the electronic mechanization to provide system output data flow that is free from any single-point failure mechanisms. Figure F.4 illustrates the basic features of the mechanization. Functional axes have been defined that correspond to each dodecahedron measurement axis. Each axis consists of a gyro and an accelerometer module supported by common power supplies. These power sources include: a 2-phase, 800-Hz gyro wheel power supply; a 9600-Hz supply for suspension and signal generator excitation; and a dc-axis supply. The dc-axis supply provides the modules' torque electronics with the required logic (5 V), amplifier (+ 10 V) voltage levels and a separate floating excitation (15 V) for each precision voltage reference (PVR). The per-axis implementation enables the isolation of any failure to a specific instrument axis, or at worst, to a functional axis. The functional axis concept was implemented both for ac and floating dc power.

The mechanization allows the incremental $\Delta\theta$ and ΔV outputs of each instrument module to be stored redundantly in an interface multiplexer. The multiplexer transmits data to the computer assembly on a dual bus. A serial data transmission format is used. The multiplexer includes provisions for digitizing analog data (voltages, etc.) for automatic monitoring, enabling more extensive fault localization.

Redundant dc power distribution to the functional axes is achieved by the use of dual dc power supplies. These supplies are designed so that each can independently support the total load of all functional axes. They are isolated from each other by diode networks to provide fail-safe operation.

The timing control pulses for the torque electronics and synchronization functions for the various power supplies are redundantly implemented. The oscillators used for these purposes are incorporated in a triply-redundant configuration, and frequency comparisons of the outputs are conducted by individual failure detectors.

Each gyro and accelerometer module includes its own temperature controller, preamplifier, torque control loop, etc. Scale factor stability and linearity performance on the order of 3 and 20 ppm, respectively, have been achieved with the present instrument control loop with a 1 rad/sec input limit. The gyro and accelerometer modules both use a standard, pulse-on-demand, ternary, torque-to-balance control loop.

The multiplexer (fig. F.5) is a dual-redundant assembly which provides buffering and transfer of the six axes of velocity and angle measurement data and includes special fault detection and test monitoring hardware.

The special hardware in the multiplexer is provided to augment and enhance the fault localization capabilities of the primary, real-time

monitoring provided in the basic SIRU software. The multiplexer hardware provisions include:

1. Warning status logic and appropriate software servicing signals for the operator (pilot) should any of the system's dual or triple redundant axes fail.
2. The ability to isolate an existing fault to a replaceable functional module. The multiplexer incorporates a limit-test sequencer that scans approximately 136 points and continually updates a display indicating the functional status of each point.
3. A high rate, analog/digital, diagnostic readout for detailed troubleshooting and performance monitoring. The multiplexer hardware incorporates an A/D that can be moded to monitor individual supplies, etc. at a high rate (40/sec) and with good resolution.

The computers are mechanized to run in a prime/backup mode. The prime data is used as the valid system output unless the prime channel shows a failure or the test engineer (pilot) forces a switchover. Each computer runs an identical software program, and the two computers are loosely synchronized at the start of each inertial data processing cycle and each data output event.

Data output is acquired by the computers from the multiplexer and the airborne reference system, processed, and transferred to the redundancy management hardware. Self-test programs are run in the background and the results transmitted along with the data for configuration of the prime computer status.

Redundancy management of the two computers is handled by dual transfer boxes (T boxes), dual receivers, and an arbiter (fig. F.1)

The T box is the heart of the redundancy mechanization. It includes the computer self-test feature, "night watchman," and an I/O wraparound to ensure that data received by the T box are identical to the data sent by the computer. It provides the capability for the two computers to compare data and to notify the operator if the data comparison indicates a disagreement. The T box initiates a serial transfer of data to the receiver from the computer as self- and cross-opinion test results. Parity is generated on this serial word, and an echo check is performed on the transmission.

The receiver consists of the shift register to accept the incoming data from the T box. It checks the parity of the transmission, returns the data for echo check, and records the result of the echo test. It also detects the "word watch" which is a code word sent out by the computers at specified intervals. If the code word does not appear on schedule, a failure is indicated. The destination address is decoded in the receiver and parallel data directed to the display, arbiter, or tape transport.

The arbiter receives all of the redundancy and self-check information from the two receivers, buffers this information, and makes the choice of remaining with the prime computer or switching to the backup computer. In addition to determining prime/backup computers, the arbiter controls a panel of lights indicating the nature of any computer failures including disagreement of the two computers. The arbiter does not remove either computer from operation in the flight test system.

Two displays provide a continuous, real-time, monitoring capability for all data output by the dual computers. Navigation and aircraft body information is normally displayed, but any information output by the computers can be displayed by operator intervention.

Each panel can be manually switched to display the output of computer A, computer B, or the designated prime. In addition to the self-scan panel, there is an LED display of gyro- and accelerometer-failure status, computer self- and cross-opinion, and identification of prime computer and electronics failure.

The digital flight recorder serves the dual purposes of loading the computer operating programs and, during tests, recording all computer outputs for post flight analysis.

A simple keyboard is provided to allow loading of programs from the tape transport and to permit the test engineer, by altering instrument compensation loads, to introduce a variety of gyro and accelerometer failures at designated times during the flight test sequence.

SOFTWARE DESCRIPTION

The basic software flow developed to operate the redundant instrument assemblage is shown in figure F.6. Briefly, the raw instrument data is received and compensation for static and dynamic instrument-loop errors applied. The corrected incremental body motion and velocity information is processed by the failure isolation equations and, if no failure is detected, is processed by the appropriate least square matrix, which outputs the reference triad solution. If a failure is detected and isolated, the failure state is entered into the adaptive matrix generator which reorganizes the matrix processor. Failure detection and isolation of up to two out of six of both instrument types can be effected without significant errors, and a third failure of either instrument type can be detected. Isolation of a third failure for many types of faults can also be effected (e.g., if the third-fault degradation is larger than a previously identified failure). The matrix processor uses no known bad data, and the triad body incremental solution is processed to yield the inertial attitude and velocity.

A local level navigator has been programmed with the necessary altitude damping and Coriolis compensation.

Two types of failure detection and isolation (FDI) algorithms have been implemented in the software. One, referred to as the Total Squared Error (TSE) algorithm (fig. F.7) operates on the compensated instrument data to estimate the difference, E_A , between what one instrument axis actually reads, A , and what that measurement is estimated to be, \hat{A} , on the basis of the other instrument axis measurements. The dodecahedron array shown in the figure yields a symmetrical, conical array that allows simple comparisons of data to achieve this solution. A fault is known to exist (detected) when the sum of the squares of all the individual errors (TSE) exceeds a preselected threshold. The fault is isolated (localized to a specific measurement axis) by means of a fault isolation ratio test, R . The thresholds used for TSE and R are primarily based upon the quantization level of the raw data and the system environment noise.

The second type of FDI (statistical FDICR) algorithm is based on a statistical technique using sequential probability ratio testing. The statistical technique operates at a lower iteration rate than the TSE algorithm. It uses the output of a set of 15 "parity" (scalar) equations that equals zero.

The redundancy management structure using the TSE algorithm is summarized in figure F.8. The statistical FDICR algorithm has been integrated into this structure to implement the recalibration loop and its more sensitive detection and isolation capabilities.

The self-alignment algorithm computationally initializes the system reference orientation in the preflight phase. The algorithm uses sensor data to establish a reference frame corresponding to the local vertical attitude and a local North. The system mechanical reference axes (body orientation) are then displayed with respect to the inertial coordinate reference frame. The self-alignment algorithm operates in two phases. In the initial phase, coarse alignment, level orientation is established using the indicated accelerometer data, and the horizontal earth rate vector is roughly determined by computing the change in the gravity vector in an inertial coordinate frame. The coarse alignment phase for an azimuth range of $\pm 90^\circ$ achieves an accuracy of better than 1° in about 5 min. The second phase, fine alignment, computationally implements conventional gyrocompassing concepts. In this phase, azimuth is precisely determined to better than 1 mrad in about 15 min.

Several other software routines have been implemented in the SIRU flight configuration. They include: a flight line, single position, self-calibration sequence, a self-alignment algorithm, and a local vertical navigation algorithm. These routines and their operational theory are briefly reviewed below.

The single position, aided calibration algorithm uses azimuth information from external optics plus latitude knowledge to compute the component of earth's rate to be expected on each gyro and the component of gravity on each accelerometer for a level system (Z_b -axis vertical). Data are filtered to attenuate any vibration effects, and the lumped bias error of each gyro

and accelerometer is printed on the teletype every 2 min. Each 2 min set of data is processed with the previous 2-min sets to yield running average bias errors and data variances (over 2-min samples) for each instrument. If the lumped bias errors are stable for 20 min or more, the appropriate compensation values for the gyros are corrected prior to the start of the alignment process.

An additional software package is available to determine the g-sensitive drift coefficients on each of the six gyros. This procedure (five-position gyro calibration) is a superset of the single-position, aided calibration, and requires five distinct test orientations of the inertial reference unit. A five-dimensional matrix solution is performed in the computer after the data have been acquired, and the five coefficients (bias, three acceleration-sensitive and one acceleration-squared-sensitive drifts) are typed out for future use.

Data handling and redundancy management of the two computers are handled by a combination software-hardware implementation.

The computers run identical programs and are loosely synchronized by the SIRU clock. The basic SIRU software is run at 20 iterations/sec for the flight test, and the data are transferred to the T boxes for eventual transfer to the displays and tape transport at the following rates:

1. 20 updates/sec: body acceleration, body rate, raw instrument data.
2. 1 update/sec: navigation data, quaternion attitude, reference system data.
3. 1 update/3.8 sec: BITE status.
4. 1 update/2 min: statistical failure detection and hard fail TSE failure detection data.

Each computer outputs, in addition to the system data, status information on its own health and an opinion of the other computer's health at a rate of 20 times per sec. Self-opinion is based on internal CPU tests and memory check-sum tests. Cross-opinion is based on a comparison with the other computer's output. The computer also performs a wraparound test on its output to the T box and is required to reset a flag in the T box within a specified time ("night watchman") or the T box will report the computer bad.

Failure checks on the computers and transmission electronics are a parity check, an echo check, a wordwatch and a time test.

Digital representations of over 100 analog functions are delivered sequentially to the computer during system operation. The computer performs a check on each parameter to determine if the magnitude of the latest data falls outside of a range determined by the maximum and minimum values of all previous data.

SYSTEM HARDWARE

Configuration and Mounting

Inertial system pallet- The inertial system pallet (fig. F.9) contains all those assemblies directly associated with the support of the redundant instrument package. These consist of the instrument package, its mounting and test fixture, the electronics assembly, the multiplexer, the heat exchanger assembly, the dual power supplies (A and B), the power distribution box, the NiCd battery, and the basic pallet. The complete assembly weighs 265 kg (608 lb) and requires approximately 1500 VA of 3-phase 400-Hz power.

Mounted on the test fixture is the porro prism which is used to accurately determine the location, in azimuth, of the system's X axis with respect to true north. The porro prism is located at an angle of 35° 36' 2.75" from the system's Y axis and at a height above the deck which permits optical sighting to it from a ground based theodolite. The porro prism's angular position has been calibrated with respect to the precision optical cube which is mounted on the underside of the inertial package and provides the reference coordinates for the system.

The computer console (fig. F.10) contains the equipment associated with the processing of the inertial data. Figure F.11 is a diagram showing the computer console power and signal cabling.

Thermal control- The basic flight test thermal design requirements were to remove approximately 125 W from the π frame and approximately 75 W from the electronics assembly in an aircraft ambient air temperature range from 40° to 95° F at altitudes from sea level to 2438 m (8000 ft).

The π frame thermal control implementation for the flight test system is shown schematically in figure F.12. It consists of a liquid-to-air heat exchanger through which a 37% ethylene glycol/water mixture, with inhibitor, is pumped from the π frame heat exchanger (a solid-to-liquid heat exchanger) attached to the π frame. Three-phase, 400-Hz fans circulate ambient air through the liquid-to-air heat exchangers while 3-phase, 400-Hz pumps circulate the liquid coolant between the solid-to-liquid and the liquid-to-air heat exchangers. To provide redundancy, the two liquid-to-air heat exchangers are connected in series in the liquid loop. Each has its own fan which is electrically failure-isolated by fuses and switches. The exchanger capacity is such that, following a fan failure, one heat exchanger alone can continue to produce satisfactory system operation. Two liquid pumps are connected in parallel with appropriate check valves so that one pump failure will not interfere with the operation of the other. The pumps are electrically failure-isolated by fuses and switches. Adequate flow is provided by a single pump. An electrical schematic of the cooling system is shown in figure F.13.

Multiplexer- Three types of data are monitored in the SIRU multiplexer assembly: inertial, analog, and status. All data are transferred to the computer. The analog and status data are also available on a digital panel meter and an LED display housed in the diagnostic module of the multiplexer. Both analog and status data are selected for display by addressing a three-digit thumbwheel switch.

Inertial data consist of pulses denoting gyro angle delta and accelerometer velocity delta. The gyro data include float position information (interpolator). The interpolator data represent a measure of residual input angle stored in the gyro float. Interpolators have not been implemented for the accelerometers.

Analog data (fig. F.14) consist of axis parameters of voltage, current, temperature (16 from each axis A through F) and system voltage parameters (9 from each of two redundant power supplies). There are a total of 104 analog parameters.

Status data are of three types: on/off line, in/out of limits, and fail. There are three oscillator and two scaler parameters which identify the oscillator and scaler that are on line. Each of the analog data is checked for in/out of specification by comparison with upper and lower limits stored in a ROM. There are seven parameters denoting failure; three oscillator, two scaler, two power supply, the electronic assembly temperature, and coolant status.

Data handling and redundancy management- Data enter the redundancy management system through the interface electronics. SIRU data are stored in a RAM. A priority interrupt request notifies the computers that fresh data are ready. At every SIRU update, all peripherals are checked to identify the presence of any new inputs. The peripheral inputs are routed directly to the computer input.

Computer data are output in parallel form and stored in a section of the system interface electronics called the T Box. Here, the stored data are checked for transmission errors and a cross comparison of data is made between the dual systems. From the T Box, data are transmitted serially to the display, arbiter and magnetic tape via the receiver. An echo check is performed on this transmission. Data coupling for all subsystems employs optical isolators to minimize errors due to noise.

SIRU data are serially multiplexed to the computers from the inertial assembly in groups of eight words at each 25 msec interval. It takes about 80 μ sec to transmit one 8-word package (see fig. F.15).

The eight-word package is made up of six gyro words and two status words, or six accelerometer words and two status words. The gyro and accelerometer data alternate, one after the other.

There are eight peripherals interfaced with the SIRU system (fig. F.16). Readings from each peripheral is under program control and is normally checked every 25 msec (every SIRU data input), i.e., if new data are ready, they are read in a maximum of 25 msec.

Some of the peripherals (DME) may have more than one input at a single service. In this case, the device is serviced until all data have been read.

The time code generator is updated every 2 sec. The altitude and altitude rate devices update every second.

SYSTEM SOFTWARE

The ground program consists of an overlay of two independent programs: the optically aided calibration and the compensation loadmaking program. Their common link is the current set of compensation values stored in the computer's base sector. Both programs use one computer and a teletype.

The loadmaking section of the ground program is used to change the instrument compensation values when sizable deviations are observed or when a new instrument is mounted in the system.

The manual input to the computers is initiated from a 16-element keyboard. Approximately 20 functions were defined and processing subroutines were created for each. These functions allow the operator to initialize the computer variables, to enter alignment or navigate modes, to observe and change the contents of any locations in core memory, and to insert various bias errors (or corrections) for any gyro or accelerometer.

Output software for the flight program was developed to write data on 9-track magnetic tape and to display various data formats on a character display panel. Eight distinct output formats were created for magnetic tape output, each of which is identified by a codeword in the first two data outputs. Permanent storage is allocated for each of the formats; flags are set as required to signal a format dump to magnetic tape. These flags are checked every 25 msec to determine which (if any) data to write on tape.

The display panel operates under control of keyboard commands to display any of six sets of data (navigation variables, fail detection variables, parity equation residuals, DME/Loran/Time Code data, system status bytes, body data).

The two SIRU computers write data into a 1024-byte magnetic tape buffer in an interleaved fashion over the period of the test. Each computer file is then processed to extract a variety of variables, most of which are paired with computer time once per second. These variables include latitude and longitude, the quaternion (attitude), inertial velocity, DME data and altimeter data; intermediate information such as instrument failure status, squared errors, and gyro parity equation residuals.

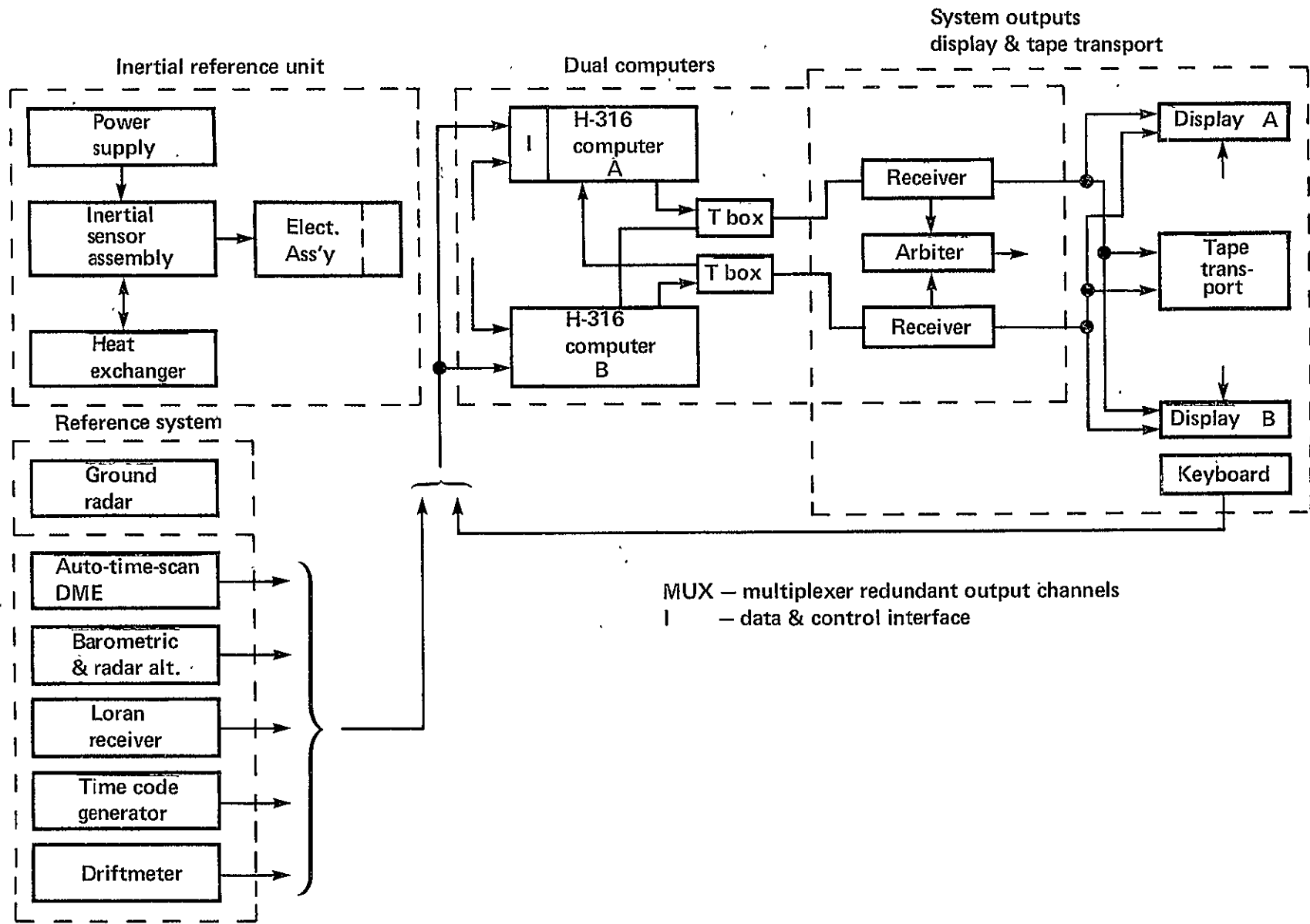
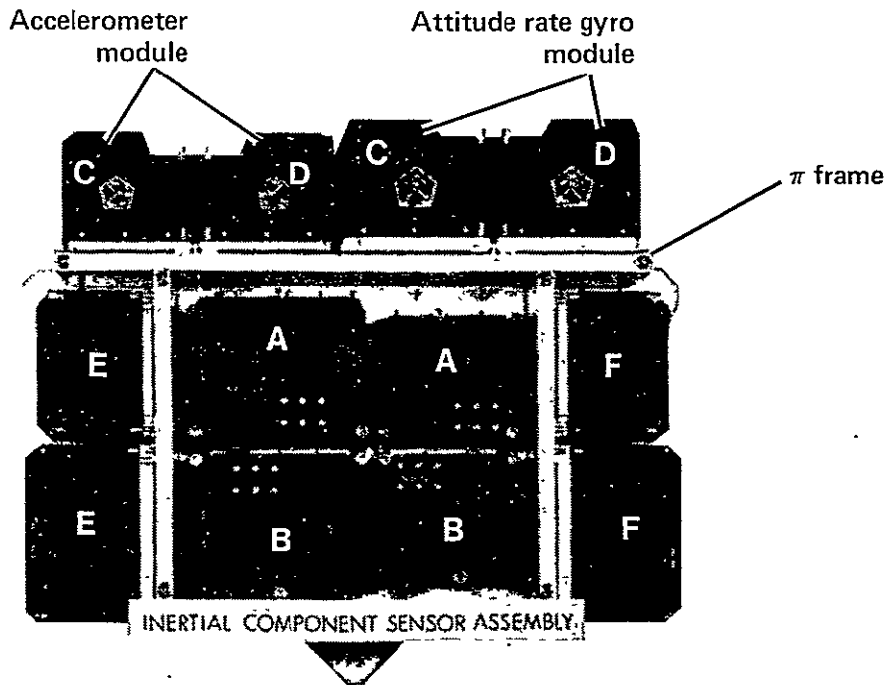
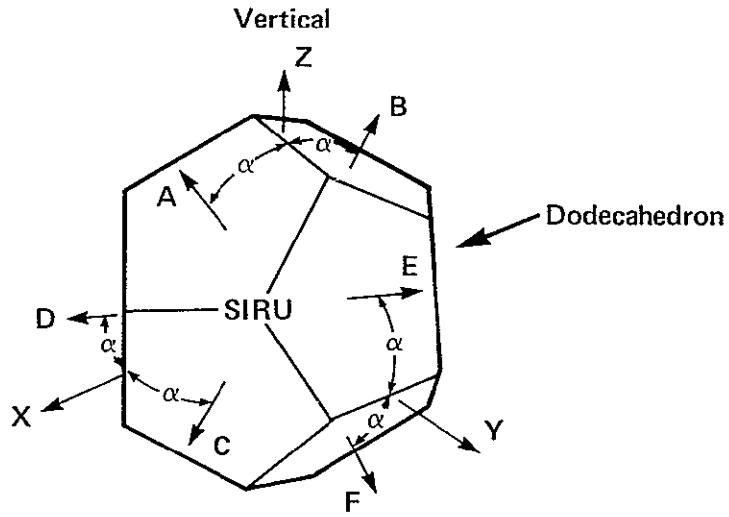


Figure F.1.- SIRU flight system block diagram.



SIRU
strapdown inertial reference unit

Figure F.2.- SIRU instrument package.

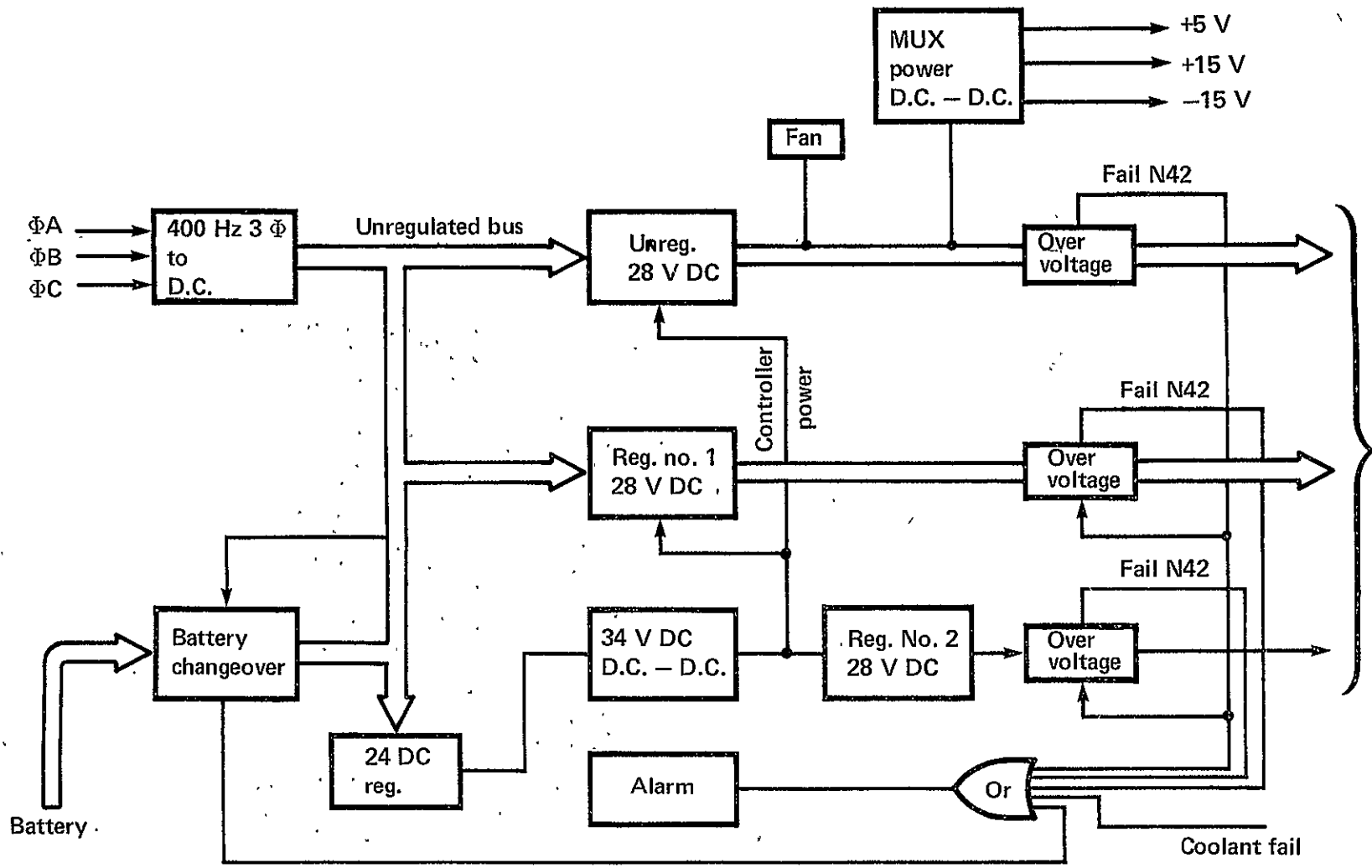


Figure F.3.- SIRU power unit (2 per system).

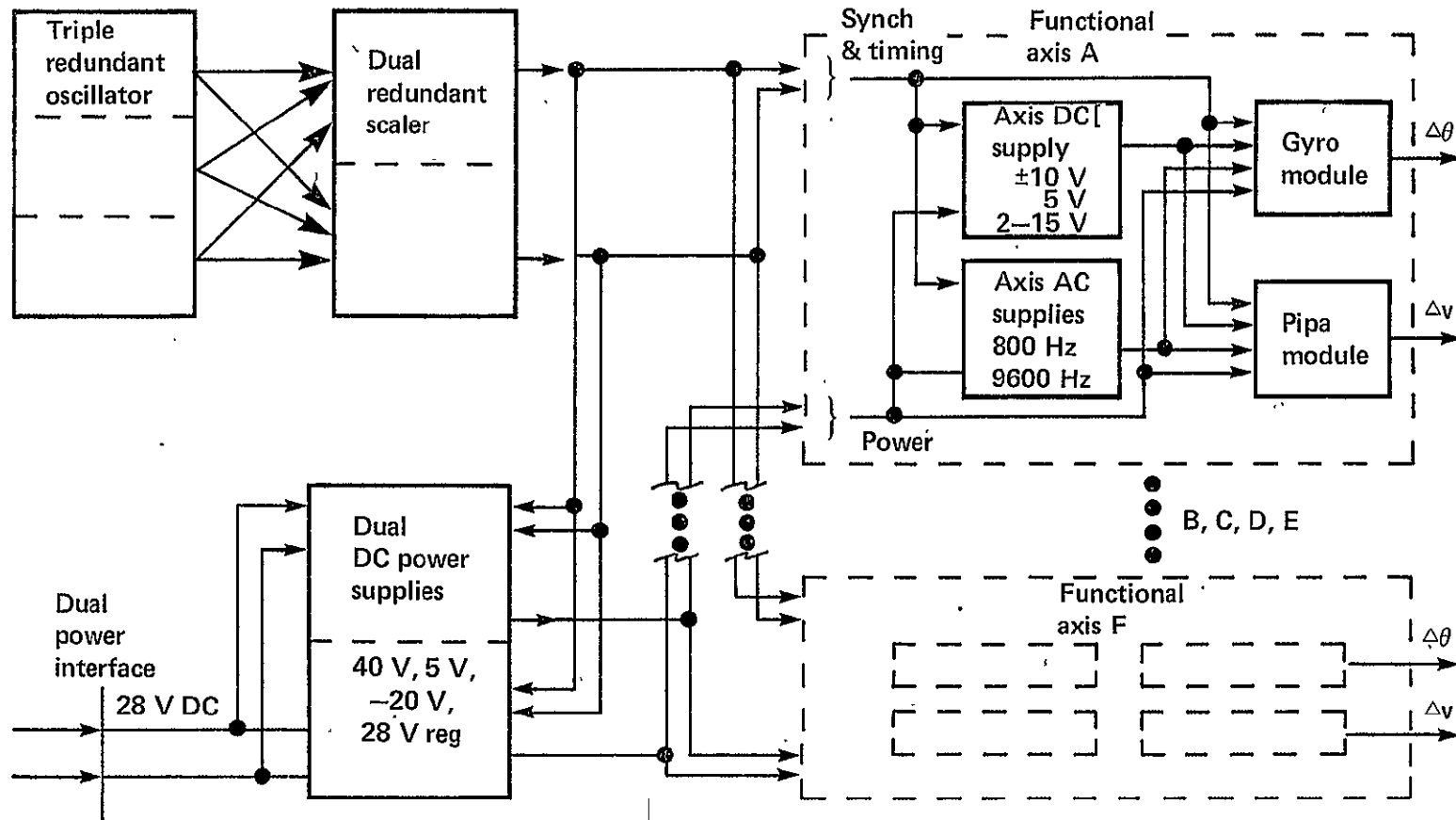


Figure F.4.- Block diagram of SIRU system.

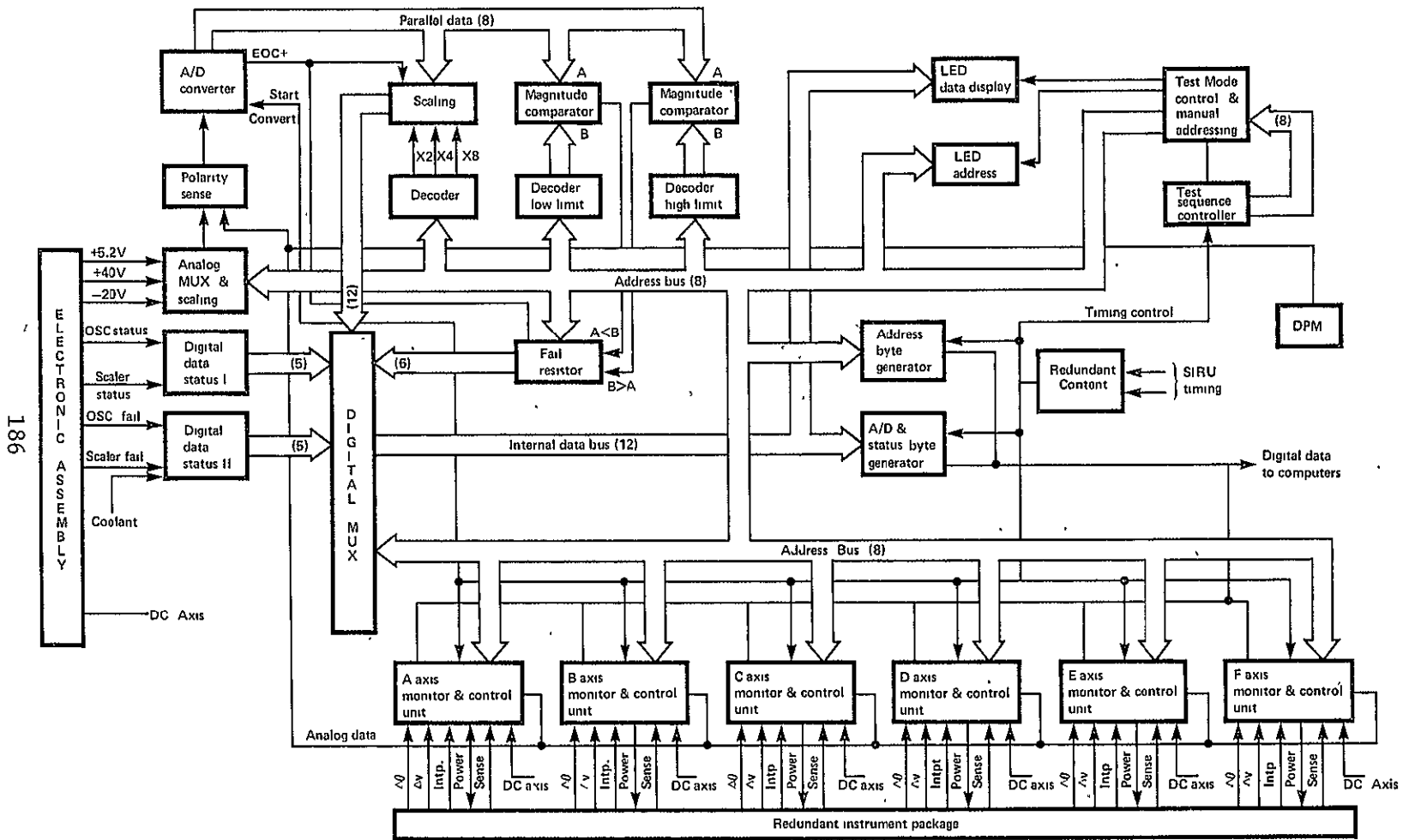
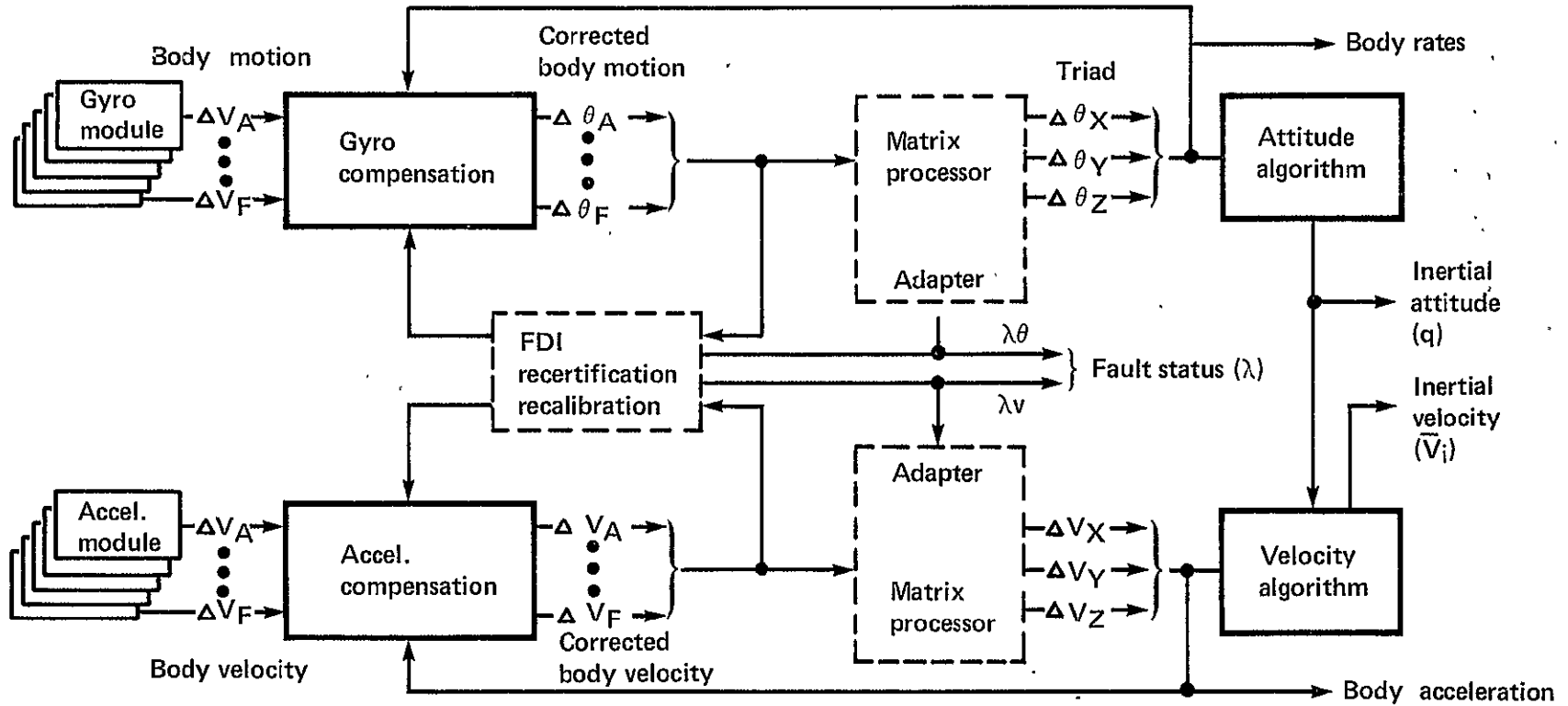


Figure F.5.- SIRU multiplexer schematic.

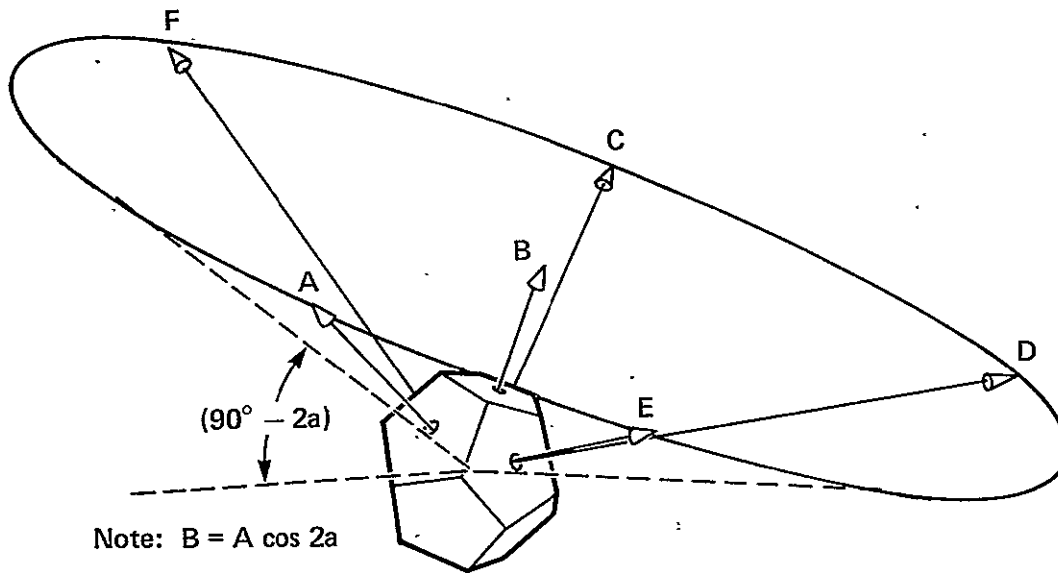
ORIGINAL PAGE IS
OF POOR QUALITY



———— Strapdown processing
 - - - - Redundancy management

Figure F.6.- Basic software flow diagram.

ORIGINAL PAGE IS
 OF POOR QUALITY



BASIC TSE – FAULT DETECTION & ISOLATION

CONICAL REPRESENTATION OF DODECAHEDRON

- Individual Meas. Axis Error Estimates
 (\hat{E}_j) difference between actual meas. and what other meas. say actual should be.
 (Body-Frame – Data Accumulation)
- Fault Detection (TSE)
 Total Square Error exceeds an acceptable threshold sum of each estimated error squared $(\hat{E}_j)^2$
- Fault Isolation – R
 Ratio of individual $(\hat{E}_j)^2$ to the TSE exceeds preselected level – (δ)
 $R_0 > 1^{\text{st}} \text{ Fail}$
 $R_1 > 2^{\text{nd}} \text{ Fail}$

Figure F.7.- Basic TSE – fault detection and isolation.

ACCUMULATE "LATEST" DATA T* MINUTES DEEP

- $\Delta\theta$ & ΔV registers accumulate T minutes of data, discard old data T/n min. segments
- new increment prior to each algorithm iteration Δt (*T/n selected on basis of desired FDI resolution)

FDI TEST PRIOR TO EACH ALGORITHM ITERATION

- Accumulation – Max Resolution of "Soft" Fails
- Test at Δt – Limits Max error propagation

FIRST FAIL ISOLATE → 2nd FAIL SEARCH & CONTINUE 1st FAIL TEST

- 2nd Fail Search does not use already faulted meas. axis; 1st Fail continues using all data
 - If 2nd Fail is original, 1st fail order changes – "Worst" Fail always 1st Fail
 - RECERTIFICATION for "Healed" Fails, transients (latch repetitive transients)

2nd FAIL ISOLATED → 3rd FAIL SEARCH

- 3rd Fail Alarm → Remember 2nd Fail – (reset its accumulator)
- Do 2nd Fail TSE, if 3rd Fail $>$ orig. 2nd Fail it will isolate as new 2nd fail
- If can't isolate, continue alarm (accept. BITE for reorganization)

MATRIX PROCESSOR REORGANIZED TO STOP PROCESSING " FAULT ISOLATED AXES" PRIOR TO Δt

- "PASS NO KNOWN BAD DATA" transient free output – multiple "Hard and Soft" Fails
- Minimum Geometric Performance Degradation as Fault Axes are Removed

Figure F.8.- Basic TSE - redundancy management structure summary.

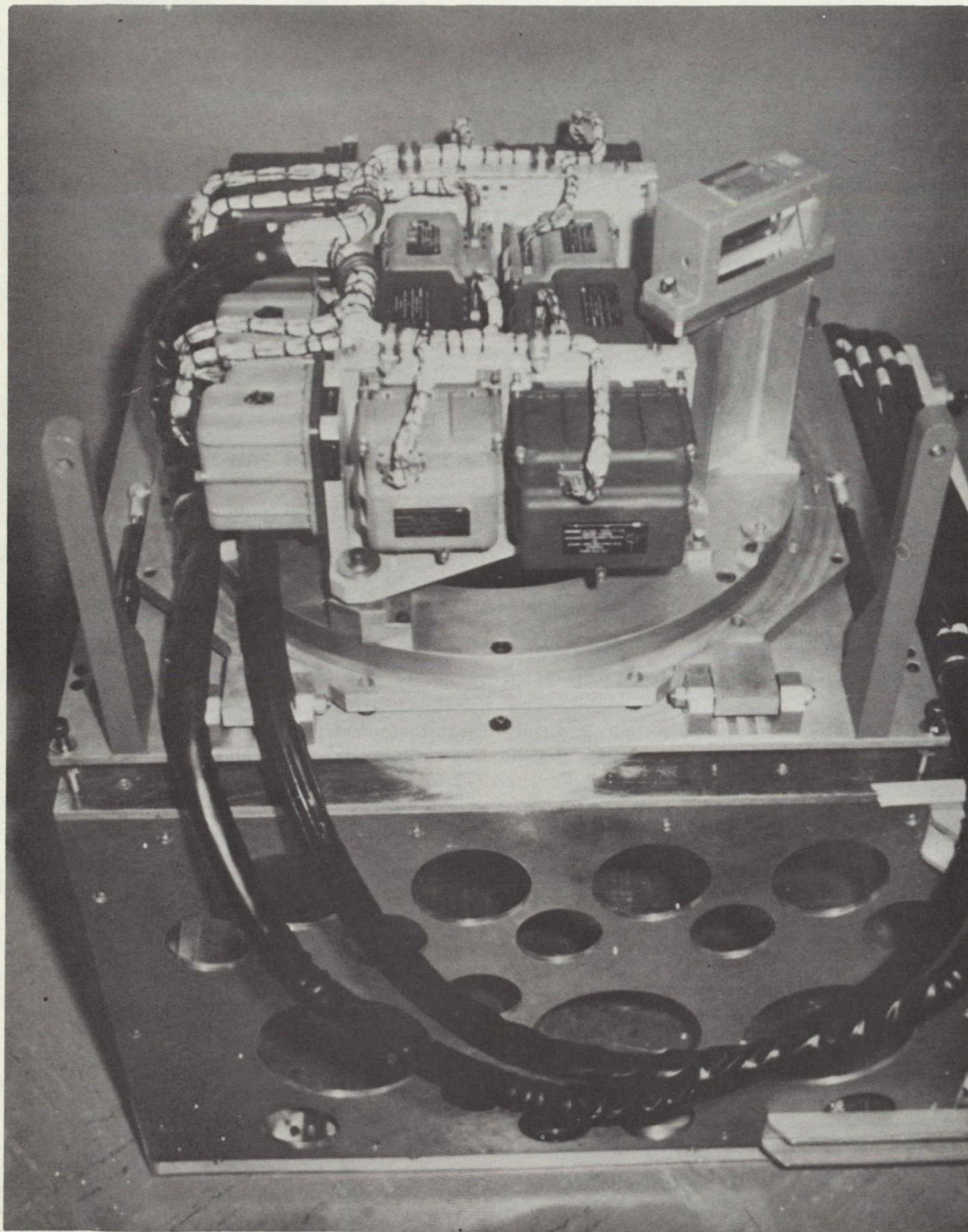


Figure F.9.- SIRU inertial system pallet.

ORIGINAL PAGE IS
OF POOR QUALITY

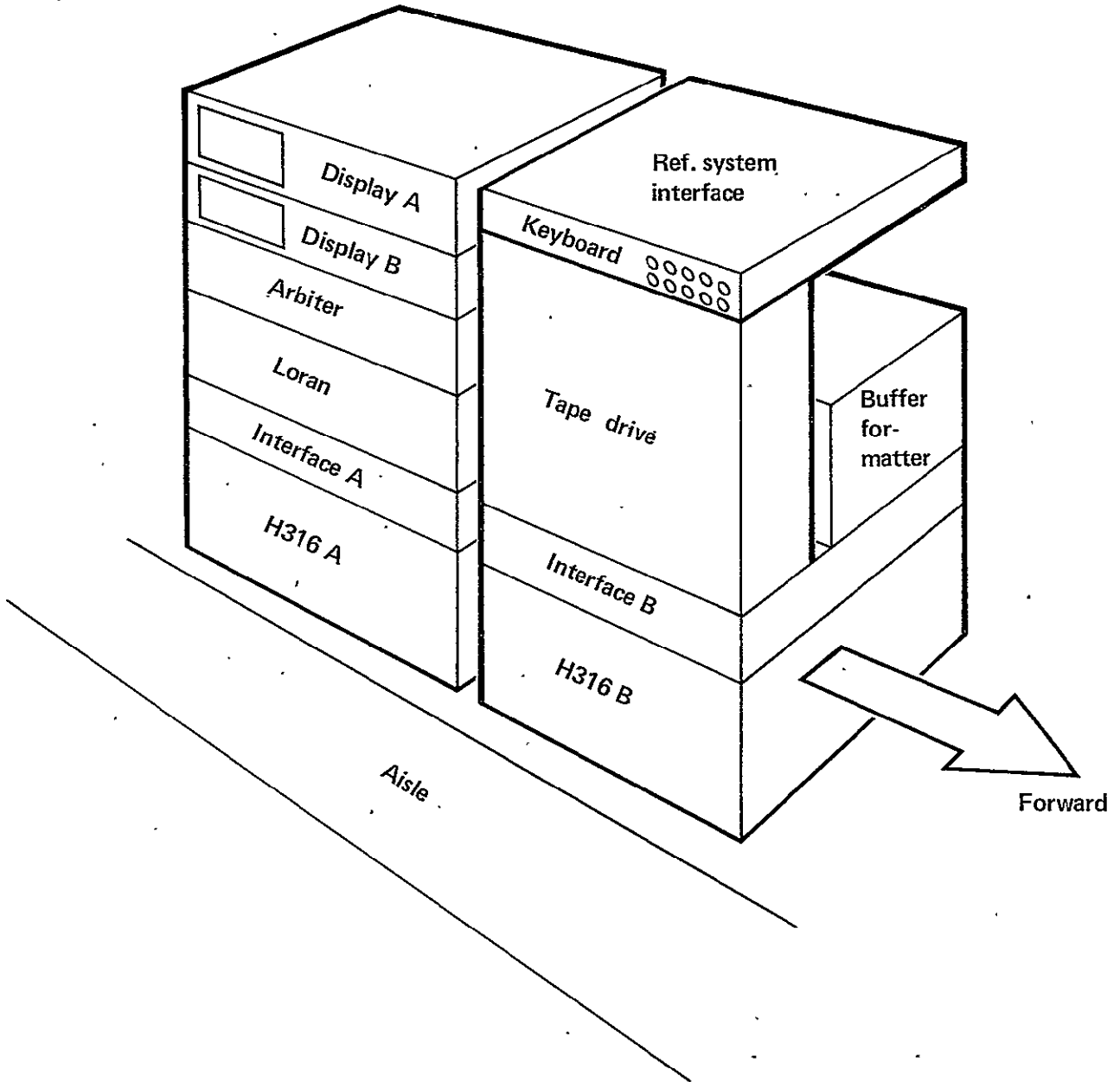
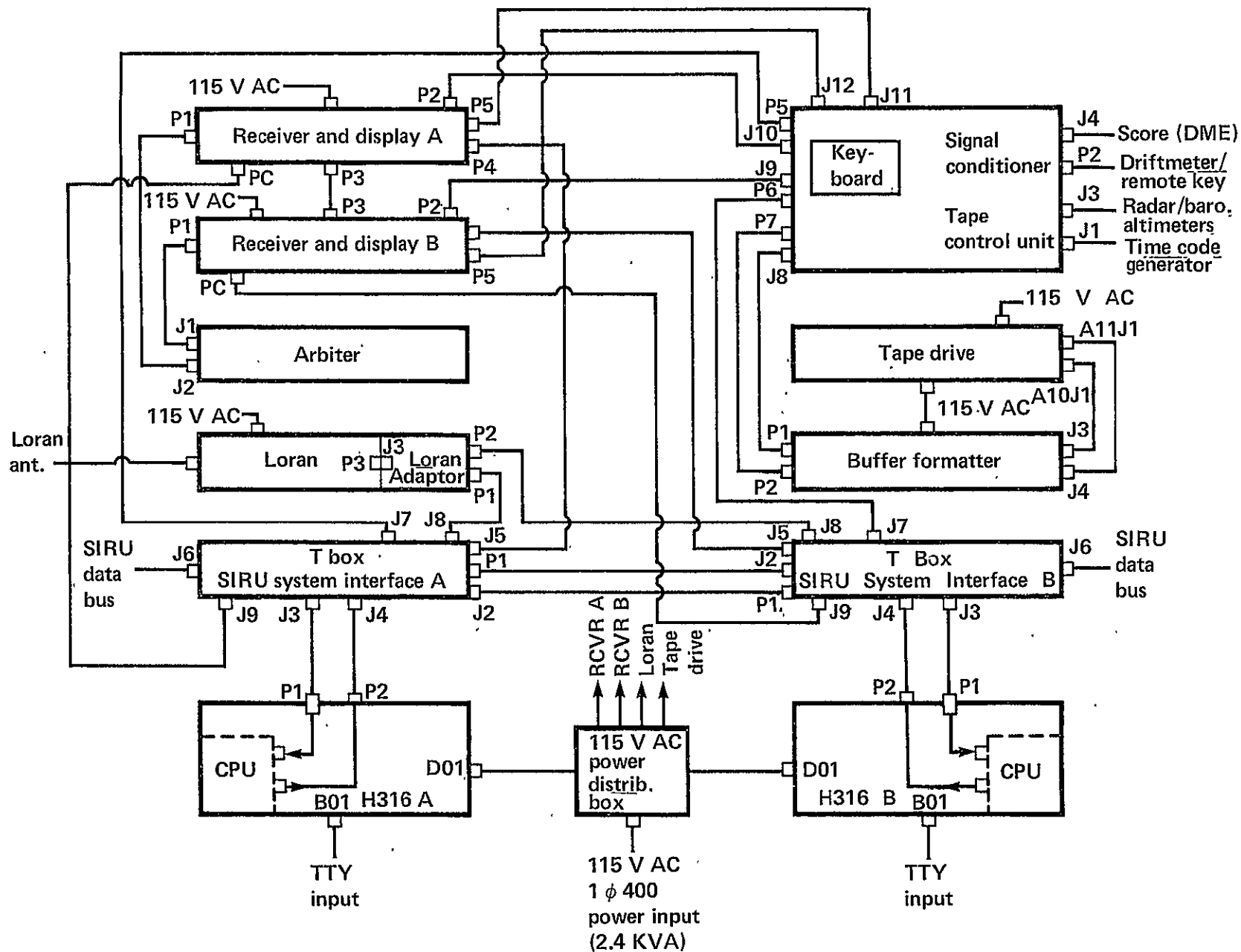


Figure F.10.- Computer control console.

192



ORIGINAL PAGE IS
OF POOR QUALITY

Figure F.11.- Computer console cabling.

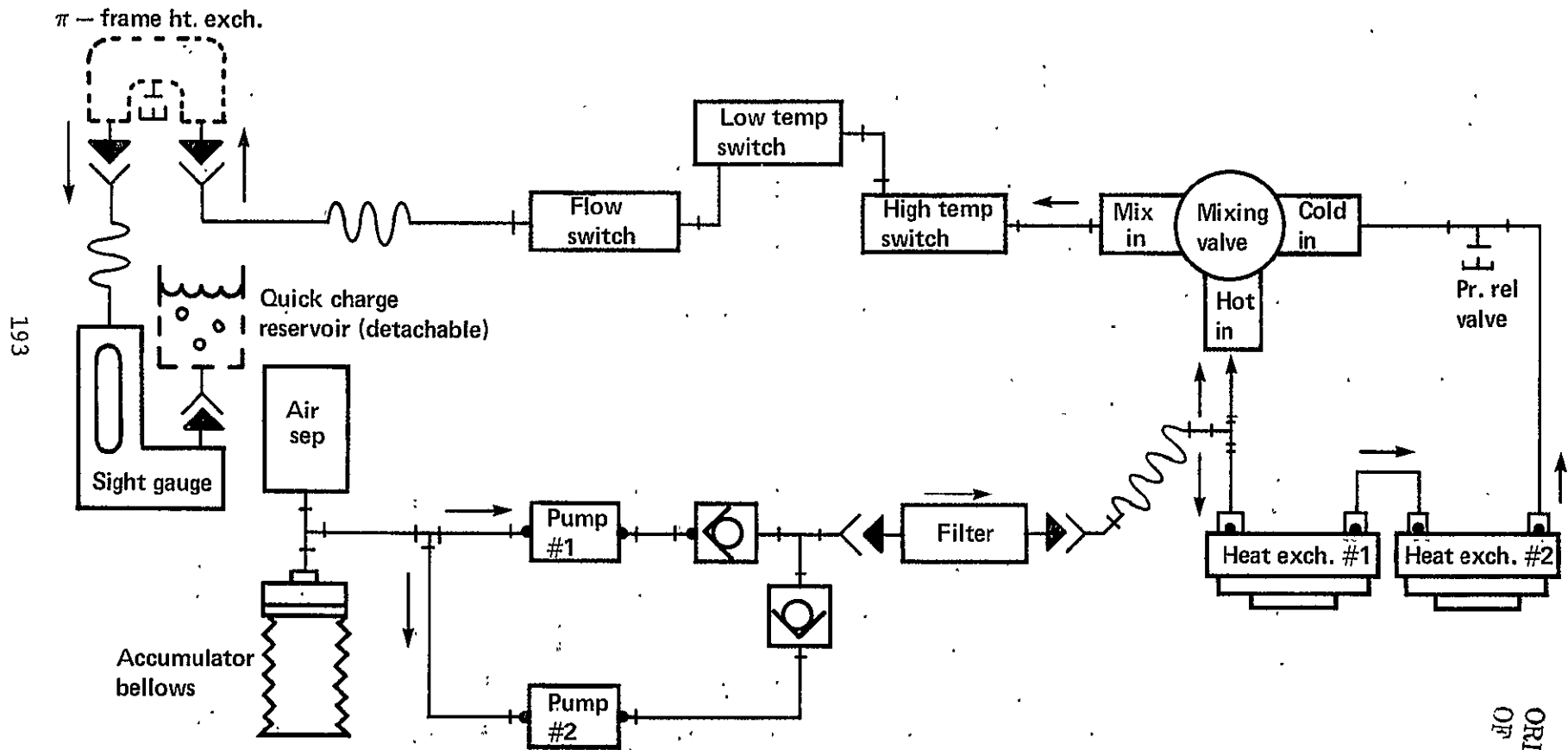


Figure F.12.- SIRU cooling assembly schematic.

ORIGINAL PAGE IS
OF POOR QUALITY

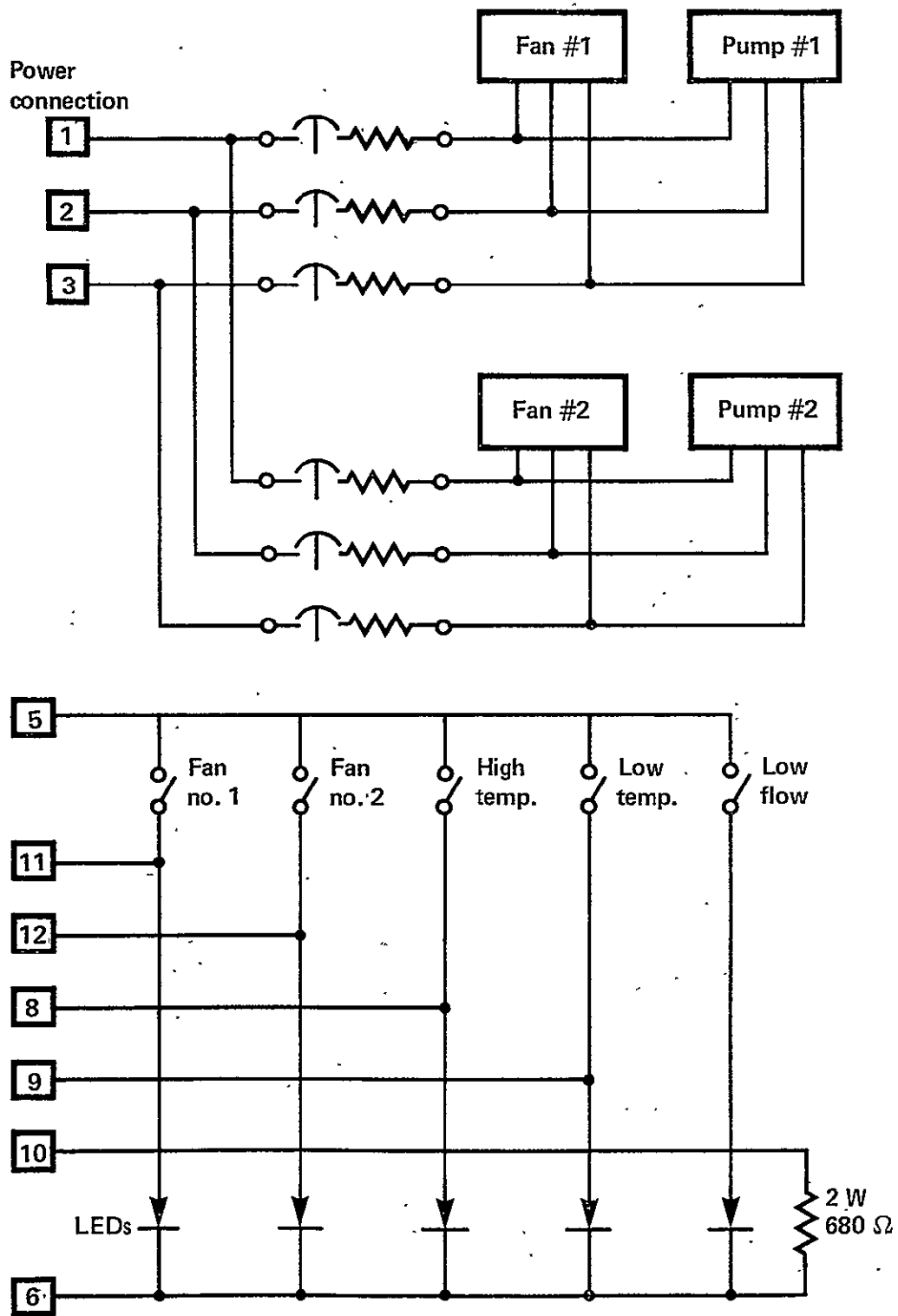


Figure F.13.- SIRU cooling assembly electrical schematic.

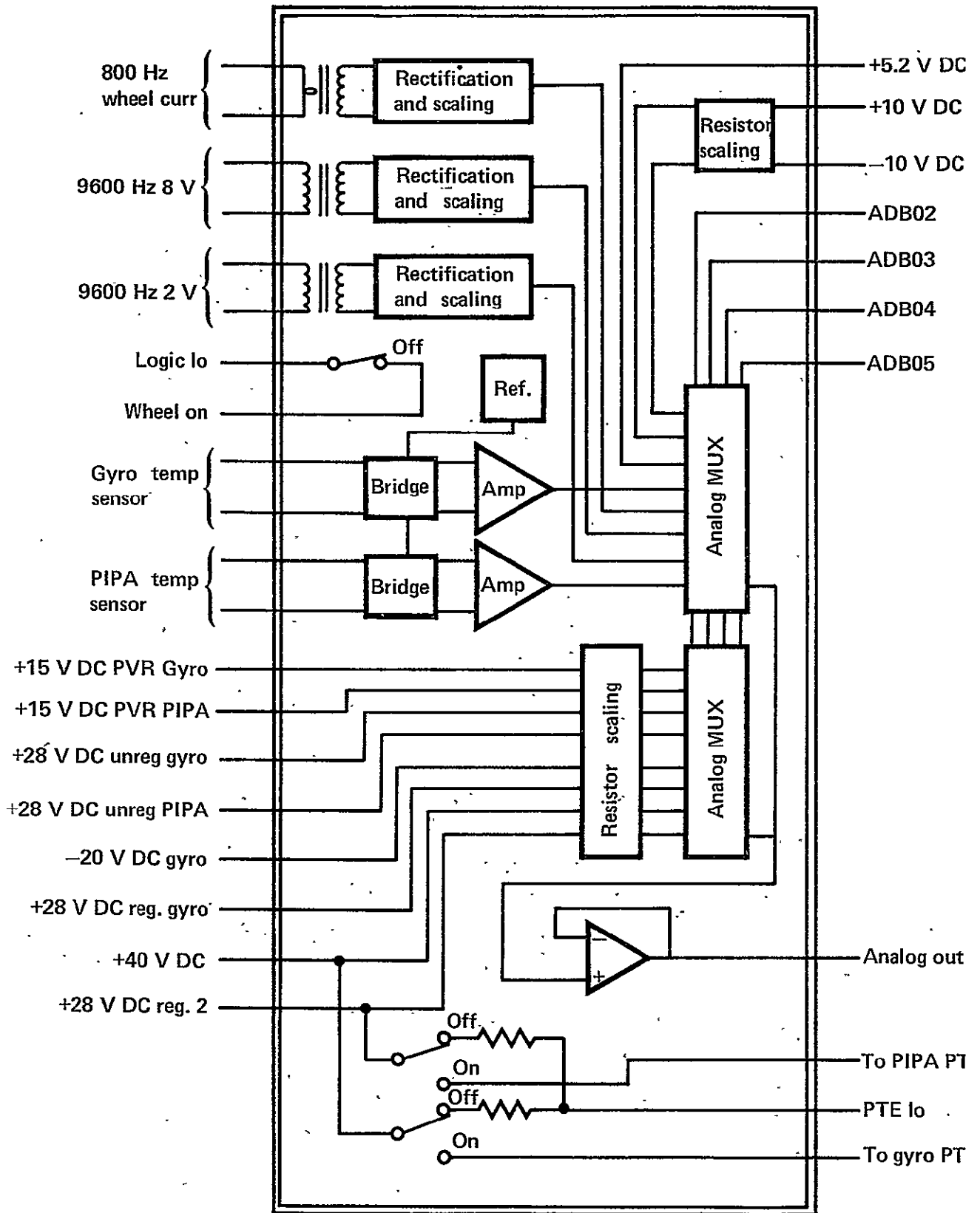


Figure F.14.- SIRU analog signals.

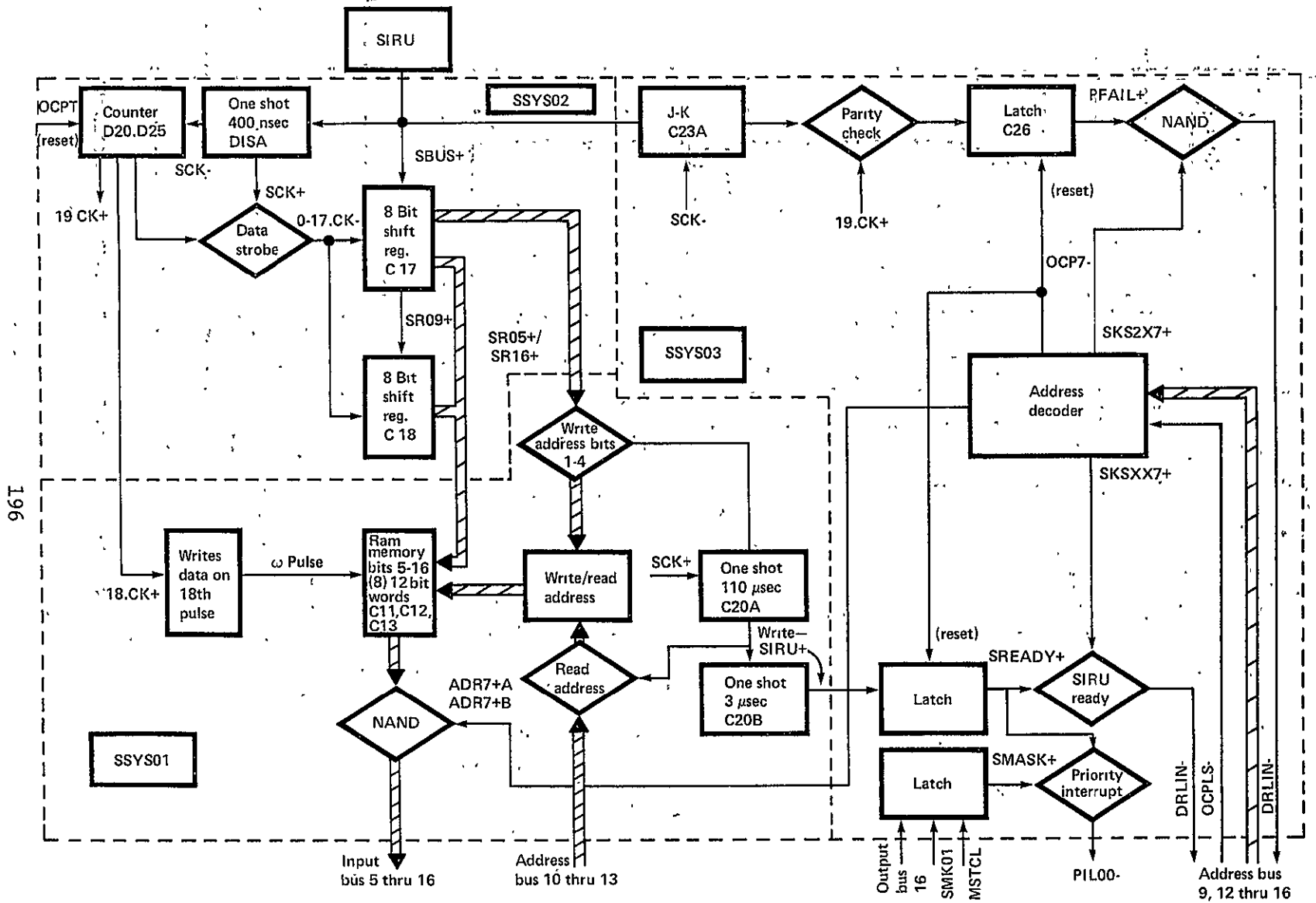
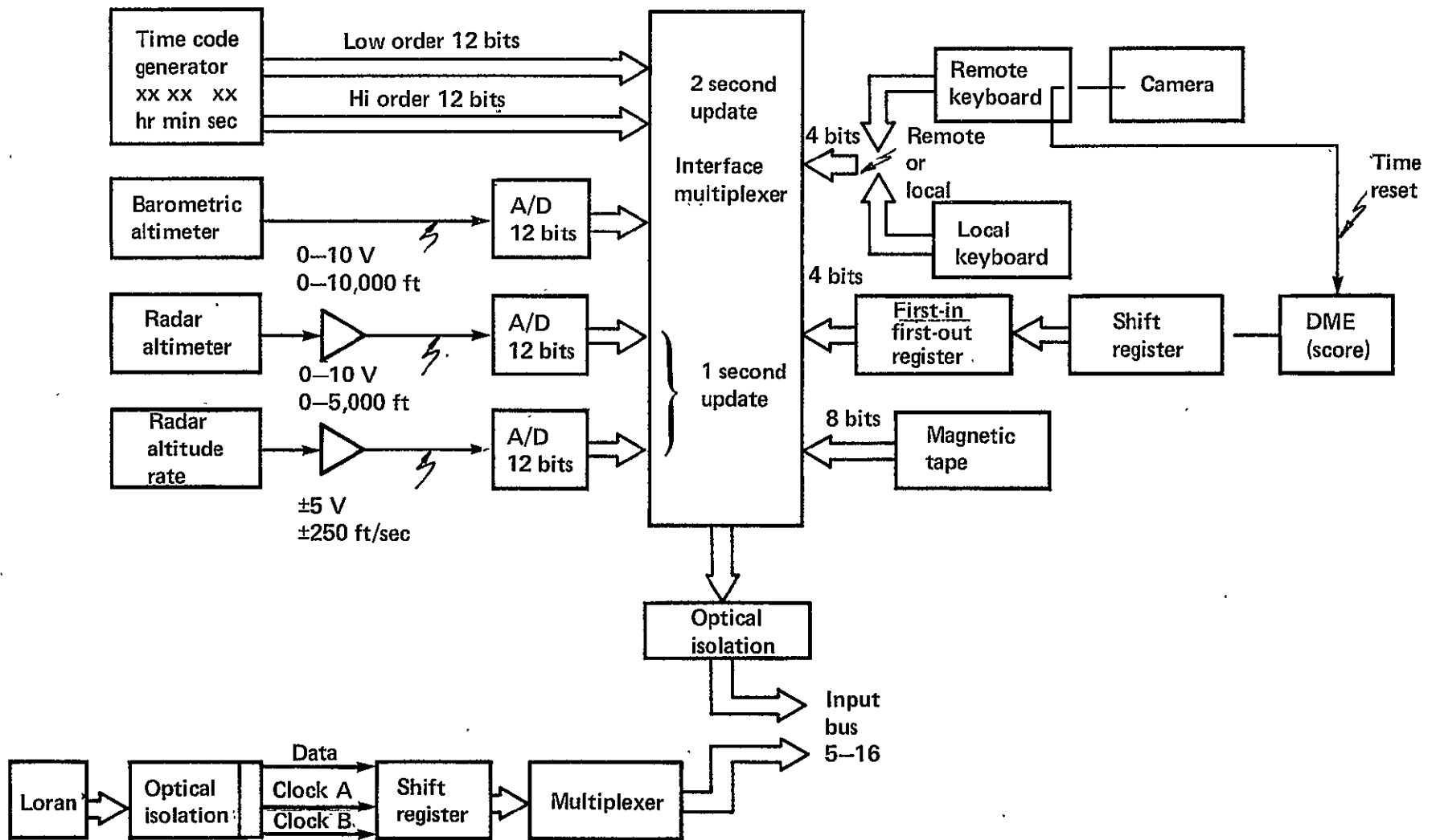


Figure F.15.- SIRU data input block diagram.

C-3



197

Figure F.16.- Peripheral data input.

PAGE INTENTIONALLY BLANK

APPENDIX G

SIRU INERTIAL SENSORS

16 Permanent-Magnet-Pulsed-Integrating
Pendulous Accelerometer (16PM PIP)

The 16 PM PIP accelerometer is a single-degree-of-freedom integrating specific force receiver. Figure G.1 is a mechanical line schematic and table G.1 presents a survey of operational and control parameters. The PIP accelerometer consists of a cylindrical body (float) that is suspended within a cylindrical case by a dense, highly viscous fluid. The fluid also provides rotational motion damping. In addition to the fluid buoyant support, the float is supported and centered radially and axially by a microsyn (variable reluctance transducer) at each end of the case.

The float has freedom of rotation about its longitudinal axis (Output Axis) and the float mass that is offset from the Output Axis provides specific force sensitivity along an Input Axis. Thus, specific force inputs rotate the float. The float rotation is sensed by the signal generator (SG), a linear angle-to-voltage generator located at one end of the instrument case. When the SG output voltage reaches a given threshold value, a discriminator detects the polarity of the SG signal and generates a torque command that switches a controlled current pulse of fixed amplitude and duration into the torque generator winding. The torque generator (TG) is a linear current-torque transducer, located at the opposite end of the case. The polarity of torquing is set to oppose the sensed input torque.

The float acts as a torque-summing member and the torques acting on the float (neglecting uncertainty torques) can be expressed as:

$$I_{OA} \frac{d^2\theta}{dt^2} + C \frac{d\theta}{dt} + m l a_{in} \pm M_{(tg)} = 0$$

$$I_{OA} \frac{d^2\theta}{dt^2} = \text{the torque due to inertia of the float}$$

$$I_{OA} = \text{moment of inertia of the float about OA}$$

$$\theta = \text{angle of rotation of the float about OA}$$

$$C \frac{d\theta}{dt} = \text{the viscous damping torque about OA}$$

The indicated velocity is the time integral of the average indicated acceleration over the update interval. This quantity includes the acceleration sensed along the input axis and the addition of various error sources characteristic of the accelerometer.

TABLE G.1.- 16 PM PIP PARAMETER SURVEY

	Nominal value	Symbol
Pendulosity	1 g-cm	ml(p)
Output axis moment of inertia	24 g-cm/sec ²	I _{OA}
Damping coefficient	14 × 10 ⁴ dyne-cm/rad-sec	C
Float time constant	170 μsec	t _f
Pendulous ref. axis moment of inertia	35 $\frac{\text{g-cm}}{\text{sec}^2}$	I _{pra}
Anisoinertia coefficient	1 $\frac{\text{cm/sec}^2}{\text{rad/sec}^2}$	$\frac{I_{IA} - I_{pra}}{ml}$
Torquer sensitivity	265 $\frac{\text{dyne-cm}}{\text{ma}}$	S _{TG}
Torquer time constant	27 μsec	t
Torquer temp. sensitivity	<10 ppm/° C	
Signal generator sensitivity	20 mV/mrad	S _{SG}
Suspension reaction torque	<0.2 dyne-cm	
Elastic restraint	<0.01 dyne-cm/m	
Operating temperature	130° F	
Excitation SG and suspension	4 V, 9600 Hz, 100 ma	end housing

18 Integrating Inertial Gyro Mod B (18 Mod B)

The 18 IRIG Mod B gyro is a single-degree-of-freedom gyroscope that was developed at the MIT CS Draper Laboratory. The basic features of the 18 IRIG Mod B gyro are its reduced size, gas bearing wheel package, and permanent magnet torquer. The 18 IRIG Mod B design is specifically designed for strap-down environment applications. The torquer, for example, is compatible with input rates up to 1 rad/sec. Similarly, the magnetic suspension design is capable of withstanding radial side loading for rates in excess of 1 rad/sec.

The 18 IRIG Mod B gyro (fig. G.2) has a gas-bearing wheel that rotates at 24,000 rpm and develops an angular momentum of 150,000 g-cm²/sec. The wheel is driven by a 4-pole, 800-Hz, 2-phase synchronous hysteresis motor. The wheel bearing consists of a stabilized journal pressurized by outboard thrust plates. The wheel and motor structures are mounted in a hermetically sealed cylindrical float and is pressurized with one atmosphere of neon gas. The float is surrounded by a high density damping fluid for fluid buoyant support and rotational motion damping. In addition to the fluid buoyant support, a 8-pole magnetic microsyn suspension is available at both ends of the case for support and centering of the float within the gyro case.

At one end of the case is a signal generator (a 12-pole multiple-E-connected microsyn) whose output magnitude is proportional to the angular position of the float about the output axis. At the other end of the case is the permanent-magnet torque generator consisting of an Alnico V permanent magnet with 8 poles, an armco iron return path, and 8 torquing coils each having 144 turns.

Table G.2 presents a survey of operational and control parameters for the 18 IRIG Mod B gyro, and figure G.3 displays a functional block diagram of the gyro.

The equation of motion for an ideal single-degree-of-freedom gyro is given by

$$I_{OA} \ddot{A}_{OA} + C \dot{A}_{OA} + KA_{OA} = H W_{IA} + M_{tg} + U_T$$

where

- I_{OA} = moment of inertia of the float about its output axis (g-cm²)
- A_{OA} = float-to-case angle about the output axis (rad)
- C = float damping coefficient about output axis (dyne-cm/rad/sec)
- K = elastic spring constant about the output axis (dyne-cm/rad)
- H = wheel angular momentum (g-cm²/sec)
- W_{IA} = angular rate of the case about the input axis (rad/sec)
- M_{tg} = commanded torque of the torque generator (dyne-cm)
- U_T = uncertainty torque acting on the gyro float about the output axis (dyne-cm)

TABLE G.2.- 18 IRIG MOD B NOMINAL PARAMETERS AND OPERATIONAL FEATURES

Gyro constants	Units	Symbol
Angular momentum	$0.15 \times 10^6 \frac{\text{g-cm}^2}{\text{sec}}$	H
Output axis damping coefficient	$\sim 400,000^*$ dyne-cm-sec	C_{OA}
Output axis inertia	225 g-cm ²	I_{OA}
Float time constant	$\sim 550^*$ μsec	$t_f = \frac{I_{OA}}{C_{OA}}$
Transfer function	7.6^* mV/mrad	$\left(\frac{H}{C_{OA}} S_{SG} \right)$
Torquer time constant	55 μsec	$t_{tg} = \frac{L}{R}$
Anisoinertia coefficient	1×10^{-4} rad/(rad/sec) ²	$\frac{I_{SA} - I_{IA}}{H}$

For the condition of no torque commands ($M_{tg} = 0$), a constant input rate will cause a constant torque about the gyro-float output axis. The resultant output axis float rotation corresponding to the torque is expressed as:

$$A_{OA} = \frac{H}{C} \int W_{IA} dt$$

Since the float output angle, A_{OA} , is proportional to the integral of input angular rate, W_{IA} , the gyro is called an integrating gyro. When the gyro is being pulse-torqued, the scale factor is defined as the angular motion about the gyro input axis that yields the same output axis rotation as one torque pulse.

The scale factor is expressed in equation (4), under steady state conditions ($M_{tg} = HW_{IA}$) where M_{tg} is a time invariant torquing level and t_s is the duration of torquing.

$$SF = \frac{M_{tg} t_s}{H}$$

The scale factor is used to determine the input axis angular displacement (A_{IA}) by scaling the accumulated positive (N^+) and negative (N^-) torque pulses.

$$A_{IA} = \frac{t_s}{H} \sum_{n=1}^{t_t/t_c} \left(M_{tg}^+ N^+(n) - M_{tg}^- N^-(n) \right)$$

where M_{tg}^+ - commanded torque (dyne-cm) for positive torque pulses

M_{tg}^- - commanded torque (dyne-cm) for negative torque pulses

t_c - interrogation period (208 msec)

t_t - test period

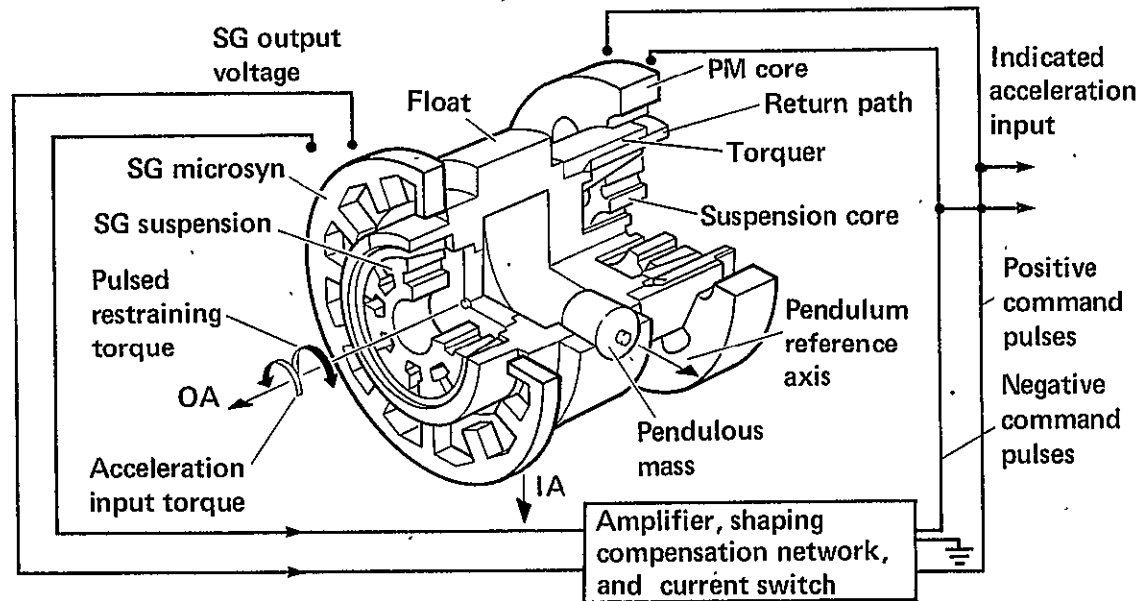


Figure G.1.- Line Schematic of the 16 PM PIP.

ORIGINAL PAGE IS
OF POOR QUALITY

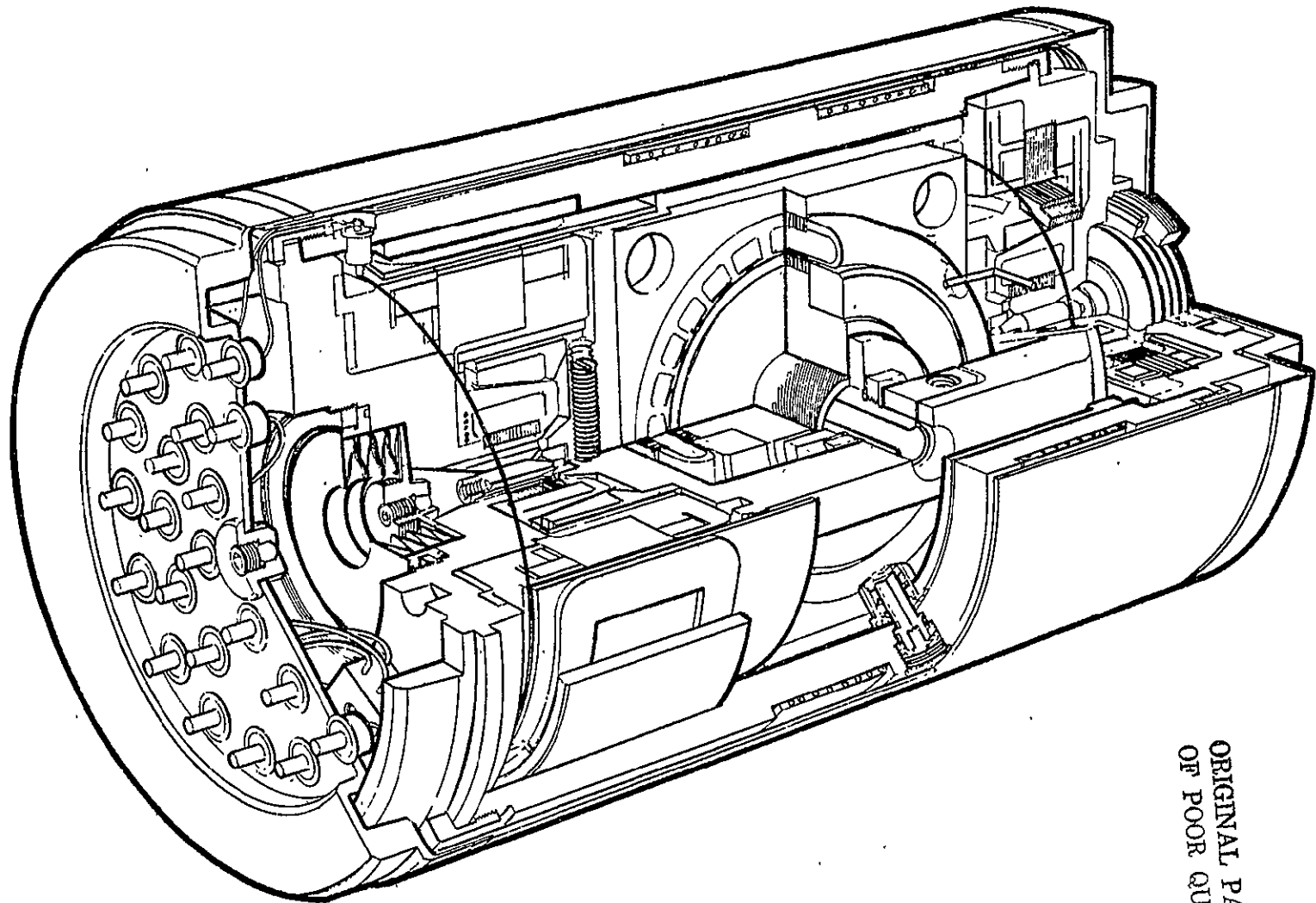


Figure G.2.- 18 IRIG Mod B cutaway view.

ORIGINAL PAGE IS
OF POOR QUALITY

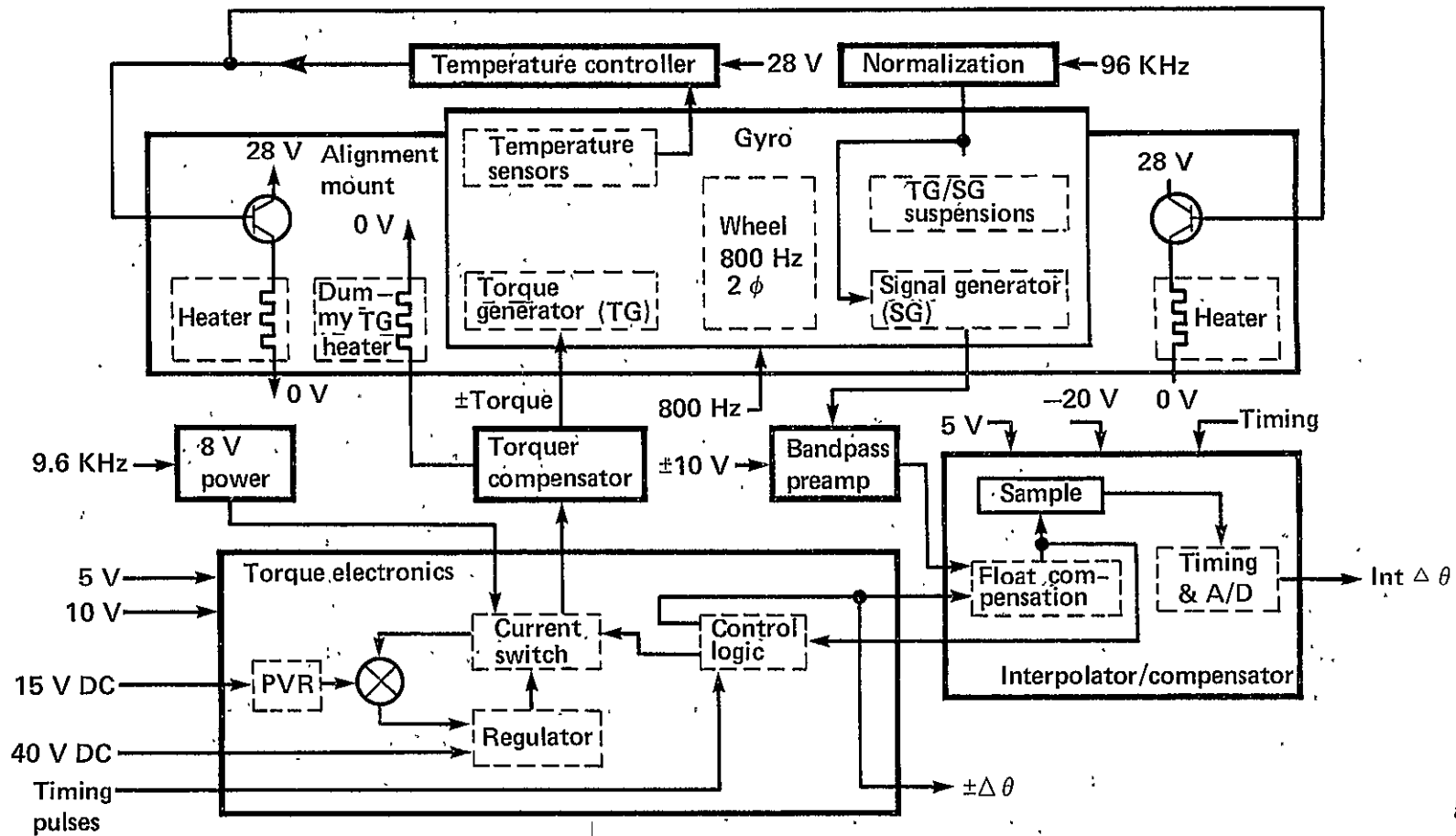


Figure G.3.- Gyro Module Functional Diagram.

ORIGINAL PAGE IS
OF POOR QUALITY

ORIGINAL PAGE IS
OF POOR QUALITY

1. Report No. NASA TM-73,224	2. Government Accession No.	3. Recipient's Catalog No.	
4. Title and Subtitle FLIGHT TEST RESULTS OF THE STRAPDOWN HEXAD INERTIAL REFERENCE UNIT (SIRU) VOLUME III: APPENDICES A-G		5. Report Date	
		6. Performing Organization Code	
7. Author(s) Ronald J. Hraby and William S. Bjorkman*		8. Performing Organization Report No. A-6974	
		10. Work Unit No. 513-53-05	
9. Performing Organization Name and Address NASA Ames Research Center Moffett Field, Calif. 94035		11. Contract or Grant No.	
		13. Type of Report and Period Covered Technical Memorandum	
12. Sponsoring Agency Name and Address National Aeronautics and Space Administration Washington, D.C. 20546		14. Sponsoring Agency Code	
		15. Supplementary Notes *Senior Analyst, Analytical Mechanics Associates, Inc., Mountain View, Calif. 94040.	
16. Abstract Results of flight tests of the Strapdown Inertial Reference Unit (SIRU) navigation system are presented. The fault-tolerant SIRU navigation system features a redundant inertial sensor unit and dual computers. System software provides for detection and isolation of inertial sensor failures and continued operation in the event of failures. Flight test results include assessments of the system's navigational performance and fault tolerance. This, the third of the three volumes, contains 7 appendixes which describe selected facets of the flight tests in detail: A. Flight Test Plans and Ground Track Plots B. Navigation Residual Plots C. Effects of Approximations in Navigation Algorithms D. Vibration Spectrum of the CV-340 Aircraft E. Modification of the Statistical FDICR Algorithm Parameters for the Flight Environment F. SIRU Flight Test System Description G. SIRU Inertial Sensors			
17. Key Words (Suggested by Author(s)) Strapdown inertial navigation Redundancy management, fault-tolerance Aircraft navigation		18. Distribution Statement Unlimited STAR Category - 04	
19. Security Classif. (of this report) Unclassified	20. Security Classif. (of this page) Unclassified	21. No. of Pages 207	22. Price* \$7.75